INVESTIGATIONS INTO THE ROLE OF ZINC AND ZINC TRANSPORTERS IN THE PATHOGENESIS OF TYPE 2 DIABETES IN db/db MICE

By

Mariea Dencey Bosco

Submitted to the Faculty of
Health Sciences School of Medicine in partial fulfilment
of the requirements for the degree of
Doctor of Philosophy

University of Adelaide

2015

TABLE OF CONTENTS

iv

List of Figures

List of Tables

Abstract

Zn is critical for the synthesis, storage and release of insulin and abnormalities in Zn and Zn transporters occur in type 1 and 2 diabetes. However, the mechanism by which Zn is regulated in islet cells is still poorly understood. The major goal of this thesis was to investigate the role of Zn and Zn transporters in the pathogenesis of normal and type two diabetic pancreatic islets, using the type 2 db/db mouse model. There is limited information available on the physiological role of Zn and Zn transporters in these mice. The following hypotheses were tested. 1) There is an early loss of Zn in the development of type 2 diabetes which contributes to the transition to established diabetes; 2) The loss of Zn causes a block in insulin maturation resulting in impaired glucose responsiveness, hyperglycemia and decline in beta cell function; 3) This loss of Zn is due to alterations in Zn transporter proteins and metallothionein at the gene and protein level. Specifically changes in the organelle Zn transporters ZnT7 and ZnT8 result in the block in insulin maturation, while dysregulation of the inflammation related plasma membrane Zn transporter protein ZIP14 contributes to inflammation that results in further beta cell dysfunction. The major aims of the project were to determine whether in early and late diabetes there are changes in 1) total and labile Zn and metallothionein, 2) Zn transporter gene expression; and 3) Zn transporter proteins. Whole pancreata from the db/db mice and age matched controls at various ages were used to investigate Zn, metallothionein protein, gene expression and subcellular distribution of Zn transporters and Zn related proteins. Immunofluorescence, immunoperoxidase and western blotting were used to investigate the Zn transporter protein expression and distribution. The major findings in this study were in early diabetes 1) loss of Zn occurred in the labile islet beta cells Zn pools without decrease in systemic Zn ; 2) There were no changes at the gene level of Zn transporters ZnT1-10 and ZIP1-14 or metallothionein; 3)There was a significant increase in islet ZnT7 protein with a golgi like appearance; 4) ZnT8 protein was downregulated in islet beta cells but not alpha cells; 5) ZIP4 was expressed almost exclusively in the somatostatin producing delta cells; 6) ZIP14 staining was signficantly increased and coincided with islet macrophages. Changes in ZnT7, ZnT8 and ZIP14 expression may be factors leading to the loss of islet beta granule Zn. ZIP4 may be the major influx transporter for Zn in delta cells, ZnT8 is the transporter regulating Zn in insulin secretory granules and ZIP14 may be a novel marker of macrophage infiltration in diabetic islets. There are

two potential clinical implications. The first is in understanding better the early events in development of type 2 diabetes, how these are influenced by Zn status and whether Zn supplements have a role to play in slowing down the transition from pre-diabetes to established diabetes. The second is a better understanding of islet Zn homeostasis with potential benefits for outcomes of islet transplantation.

It is the branch that bears the fruit,

That feels the knife,

To prune it for larger growth,

A fuller life

Though every budding twig be loped

And every grace

Of swaying tendril, springing leaf,

Be lost a space

O thou whose life of joy seems left,

Of beauty shorn;

Whose aspirations lie in dust,

All bruised and torn

Rejoice tho each desire, each dream

Each hope of thine

Shall fall and fade it is the land

Of love divine

That holds the knife that cuts and breaks

With tenderest touch,

That thou, whose life has borne,

Some fruit

Mayst now bear much

Annie Johnson Flint

Declaration

I, Mariea Dencey Bosco certify that this work contains no material which has been accepted for the award of any other degree or diploma in any university or other tertiary institution and to the best of my knowledge and belief, contains no material previously published or written by another person, except where due reference has been made in the text.

I give consent to this copy of my thesis, when deposited in the University Library, being made available for loan and photocopying, subject to the provisions of the copright Act 1968.

I also give permission for the digital version of my thesis to be made available on the web, via the University's digital research repository, the library catalogue, the Australasian Digital Theses Program (ADTP) also through web search engines, unless permission has been granted by the University to restrict access for a period of time.

………………….………………………

Mariea Dencey Bosco
Date:

Acknowledgements

I would like to thank the Department of Medicine of Medicine, the University of Adelaide for providing me with the resources for my PhD candidature. I would also like to thank the following people for their endless support, knowledge and friendship.

To Dr Peter Zalewski and Professor Patrick Toby Coates who took me under their wings and provided me with constant support, insightful advice and friendship in the past four years. Your belief and support has made it worthwhile and it has been a privilege and an inspiration to be working beside two wonderful people. I can say that two of you had one of the biggest impact on the person whom I am today.

Dr Peter: thank you so much for your support and encouragement through out these years. Thank you for helping and sitting through the harrowing months of write up. Thank you for being a great teacher and mentor and showing me the passionate side of science and teaching me that perservence and hard work not only brings you a long way in the career but also builds character. Thank you also for financially supporting me through the time when my stipend ran out and you were very generous in providing reagents when the critical time came I wish you all the best for your future.

Professor Toby Coates: thank you so much for accepting me as your PhD student and supporting me financially throughout these four years. Thank you for being my mentor. I would like to say that I would not of achieved the things that I did during my PhD without your trust and belief in me. You gave the opportunity to learn about myself and pushed me during the critical times when I needed it. You enabled me to go overseas to conferences and labs to learn about how the research is conducted. Thank you so much for your time and effort that you had put into my PhD.

Sue Lester: thank you for your support and constant encouragement through the past years. Thank you for being my mentor, you have made an impact on the person whom I am today.

Peter Coyle and Allan Rofe: thank you for your time and encouragement in the zinc studies. Thank you for letting me use your facility and resources to conduct my research.

Daisy Mohandasundram: thank you for being my friend and support through the years that you were my supervisor. Thank you for investing time and money (small grant that was obtained from The Hospital Research Foundation). I wish you all the best for your future.

Chris Drogemuller: thank you for your time and effort through the years of my PhD. Your technical input and intellectual input in my PhD was substantial and made a big impact in my studies. All the best for your future.

To the Centre for Clinical and Laboratory Science and lab members, thank you for being so welcoming and supportive since the time I started my PhD.

My loving family: thank you so much for your love and support over the years. Without all of you there this would not be possible. Thank you for being there through my tears and happiness and putting up with me. I would like to thank my Grandma for her constant prayers throughout my years and also my family in India for their prayers and encouragement

Praveen my darling husband: thank you for your encouragement through this time when I needed to complete my thesis. I am so lucky to get a husband like you.

"Obstacles don't have to stop you. If you run into a wall, don't turn around and give up. Figure out how to climb it, go through it, or work around it."

- Michael Jordan

"Success is not the key to happiness. Happiness is the key to success. If you love what you are doing, you will be successful."

- Herman Cain

Abbreviations used in this thesis

AAS	Atomic Absorption Spectrometry
Ca2+	Calcium
DNA	Deoxyribonucleic acid
ER	Endoplasmic Reticulum
FBS	Foetal bovine serum
FITC	Fluorescein isothiocyanate
GK	Goto Kakizaki rats
GLMS	Gaussian generalised linear models
GLP-1	Glucagon like peptide 1
GLUT2	Glucose transporter 2
IL-1β	Interleukin 1 beta
IL-6	Interleukin 6
MIN6	Mouse Insulinoma cell line
mM	milli Molar
MRE	Metal response element
mRNA	Messenger RNA
MT	Metallothionein
MTF-1	Metal transcription factor 1
nM	nano Molar
Ob	Obese gene
^{o}C	Degrees Celsius
PBS	Phosphate buffered saline
PKC	Protein kinase C
pM	pico Molar
RER	Rough endoplasmic reticulum
RIN	Rat Insulinoma Cell line
RT	Reverse transcriptase
SEM	Standard error of mean
SNP	Single nucleotide polymorphism
TLDA	Taqman low density array cards
TNF-α	Tumour necrosis factor alpha
TPEN,	N,N',N'-tetrakis-(2-pyridyl-methyl) ethylenediamine
TS-Q	6-Methoxy-(8-p-toluenesulfonamido)quinoline
UV	Ultraviolet
ZINPYR-1	4′,5′-Bis[bis(2-pyridylmethyl)aminomethyl]-2′,7′-dichlorofluorescein
ZIP14	Zinc transporter SLC39A14
ZIP4	Zinc transporter SLC39A4

ZIP5	Zinc transporter SLC39A5
Zn	Zinc
ZnT7	Zinc transporter SLC30A7
ZnT8	Zinc transporter SLC30A8
μL	micro Liter
μM	micro Molar

Publications and Awards Arising from Thesis

Peer-Reviewed Publications

Review: Rev Diabet Stud. 2010 Winter;7(4):263-74. doi: 10.1900/RDS.2010.7.263. Epub 2011 Feb 10.Zinc and zinc transporter regulation in pancreatic islets and the potential role of zinc in islet transplantation.Bosco MD, Mohanasundaram DM, Drogemuller CJ, Lang CJ, Zalewski PD, Coates PT.

Zinc and Zinc Transporters in Macrophages and Their Roles in Efferocytosis in COPD. Hamon R, Homan CC, Tran HB, Mukaro VR, Lester SE, Roscioli E, Bosco MD, Murgia CM, Ackland ML, Jersmann HP, Lang C, Zalewski PD, Hodge SJ.
PLoS One. 2014 Oct 28;9(10):e110056. doi: 10.1371/journal.pone.0110056. eCollection 2014.

Book Chapter: Zinc transporters expression in the pancreas; Islet of Langerhans
Mariea Dencey Bosco, Chris Drogemuller, Peter Zalewski and Patrick Toby Coates, Islets of Langerhans, DOI 10.1007/978-94-007-6686-0_42, # Springer Science+Business Media Dordrecht 2014, 511

Conference Proceedings

International Pancreas Islet Transplant Association 2013: Rapid fire-Oral Presentation: Published abstracts in Transplantation September 27, 2013 - Volume 96 - Supplement 6S pp: S1-S163

Post translational change in the regulation of Zinc and Zinc transporters in a Type 2 Diabetic db/db mice pancreatic islets.

Mariea D Bosco, Daisy M Mohandasundram, Chris Drogemullar, Peter Zalewski, Toby P Coates

Differential Regulation of Zinc Transporters and Metal Binding proteins in human Type 1 and Type 2 Diabetes.

Daisy Mohanasundaram, <u>Mariea Bosco</u>, Peter Zalewski, Chris Drogemullar, Tom Loudovaris, Tom Kay, Toby Coates

TSANZ ANNUAL SCIENTIFIC MEETING 2011: Mini Oral

Down regulation of Zinc transporter ZIP14 and ZnT8 in native pancreatic islets of type 2 diabetic db/db mice

<u>Bosco Mariea Dencey</u>, Zalewski Peter, Mohanasundram Daisy, Coates PTH.

Alteration of Zinc and Differential expression of Zinc transporters in Diabetic pancreatic islets.

Mohanasundram Daisy, Drogemullar Chris, <u>Bosco Mariea</u>, Zalewski Peter, Coates Toby.

ASMR Adelaide: Poster presentation

Down regulation of Zinc transporter ZIP14 and ZnT8 in native pancreatic islets of type 2 diabetic db/db mice

<u>Bosco Mariea Dencey</u>, Zalewski Peter, Mohanasundram Daisy, Coates PTH.

International Diabetes Federation 2011: Dubai, Oral presentation

Down regulation of zinc transporters ZIP14 and ZnT8 in pancreatic islets of type 2 diabetic db/db mice

<u>Bosco Mariea Dencey</u>, P. Zalewski, D. Mohanasandrum, P.T.H. Coates.

Alteration in the regulation of zinc and zinc transporters can contribute to beta cell dysfunction in type 2 diabetic pancreatic islets

Mohanasundram Daisy, Drogemullar Chris, <u>Bosco Mariea</u>, Zalewski Peter, Coates Toby.

Research Day 2011: Adelaide, Poster:

Down regulation of Zinc Transporters ZIP14 and ZnT8 levels in pancreatic islets of type 2 diabetic db/db mice.

Bosco MD, Mohanasundram D, Lester S, Zalewski P, Mee C, Drogemuller C, Miliner C, Coates P.T.H.

Australian Society for Immunology Annual Scientific 2011

Meeting- Adelaide-Australia: Poster presentation

Down regulation of zinc transporter 8 in type 1 diabetic pancreatic islet

Mohanasundram Daisy, Drogemullar Chris, Bosco Mariea, Zalewski Peter, Coates Toby.

Association of type 2 diabetes with significant reduction of zinc level in db/db mice liver

M.D. Bosco, P. Zalewski, D. Mohanasandrum, P.T.H. Coates.

International Pancreas Islet Transplant Association 2011: Poster Presentation

Role of zinc and zinc transporters in diabetic pancreatic islets

D. Mohanasundaram, C. Drogemullar, M. Bosco, C. Lang, P. Zalewski, T. Coates

Zn in Biology International Conference 2012: Melbourne, poster

Age related reduction in zinc concentration in type 2 diabetic db/db murine livers

Bosco, D Mohanasundaram, P Zalewski, C Cowley, A Rofe, PTH Coates.

Zinc transporter analysis in human type 1 and type 2 diabetic pancreatic islets

D. Mohanasundaram, C. Drogemuller, T.Loudovaris, L.Mariana, M.Bosco, C. Lang, P. Zalweski, T. Coates

ASMR 2012 Adelaide: Oral presentation

Regulation of Metallothionein and zinc in liver and pancreas in type 2 diabetic db/db mice

<u>Mariea Bosco</u>, Daisy Mohanasundram, Peter Zalewski, Patrick Toby H Coates

TSANZ Annual Scientific Meeting 2012: Canberra, Mini Oral
Zinc regulation in liver and pancreas in type 2 diabetic db/db mice

<u>Bosco Mariea</u>, Mohanasundram Daisy, Zalewski Peter, Drogemuller, Coyle Peter, ROFE Allan, Coates Toby.

Australian Diabetes Society 2012: Gold Coast, Poster Presentation

Leptin deficient type 2 diabetic db/db mice have altered zinc and zinc transporter metabolism.
<u>Mariea D Bosco</u>, Daisy M Mohandasundram, Chris Drogumullar, Peter Zalewski, Carina Cowley, Peter Coyle, Allan M Rofe, Toby P Coates

Research Day, Basil Hetzel Institute 2012: Adelaide, Poster presentation (mini oral)
Zinc and Zinc transporter ZnT8 regulation altered in prediabetic db/db mice

<u>Bosco Md</u>, Mohanasundram D, Zalewski P,Rofe A, Coyle P, Drogemuller C, Coates PTH.

The Australian Health and Medical Research Congress 2012: Oral /Poster presentation
Alteration of zinc and zinc transporter metabolism in a type diabetic db/db mice model
<u>Mariea D Bosco</u>, Daisy M Mohandasundram, Chris Drogumullar, Peter Zalewski, Carina Cowley, Peter Coyle, Allan M Rofe, Toby P Coates

TSANZ 2013: Oral Presentation
Loss of Zinc and alteration of Zinc transporters in db/db mice panceratic islets in early type 2 diabetes.
<u>Bosco Mariea</u>, Mohanasundram Daisy, Zalewski Peter, Drogemuller C, Coyle Peter, Rofe Allan, Coates PTH.

ASMR 2013: Oral Presentation

Early changes in zinc and zinc transporters in a type 2 diabetic db/db mice pancreatic islets.

Mariea Bosco, Daisy Mohansaundram, Chris Drogemuller, Peter Zalewski, Peter Coyle, Allan Rofe, Patrick Toby H Coates.

Australain Diabetes Society :Poster

Inflammation induced ZIP14 transporter upregulated in pancreatic islets of type 2 diabetic db/db mice

Mariea Bosco, Daisy Mohanasundaram Chris Drogemuller, Peter Zalewski, Peter Coyle, Allan Rofe, Patrick Toby H Coates

Australian Diabetes Islet Study Group: Poster

Islet specific reduction of zinc and alteration of zinc transporters in panceratic islets of a type 2 diabetic db/db mice model

Bosco Mariea, Mohanasundram Daisy, Zalewski Peter, Drogemuller C, Coyle Peter, Rofe Allan, Coates PTH.

International Zinc Biology Conference 2014 Asilomar Camp Grounds California

Role of Zn and Zn transporters in the pathogenesis of type 2 diabetes in db/db mice

Mariea D. Bosco, Daisy Mohanasundaram,Claire F. Jessup, Claudine S. Bonder, Darling Rojas-Canales, Chris Drogemuller, Tom Loudovaris, Tom W.H. Kay, Susan E. Lester, Shane Grey, Peter D. Zalewski and Patrick. T Coates

TSANZ and Amgen 2013 Young Investigator Book Prize $500, 2013

IPITA-TTS Young Investigator Travel 2013 for best Abstract $1100, 2013

Discipline of Medicine Travel Grant $800, 2012

TSANZ Travel grant $2500, 2013

Robinson Institute Travel Grant $1800, 2013

Walter and Duncan Trust Travel Grant $1500, 2013

Freemasons Trevor Prescott Scolarship $5000, 2014

International Zinc Biology Conference Book prize and Poster award

CHAPTER 1 Literature review

1.1 Introduction

The major aim of the studies reported in this thesis was to investigate the role of zinc (Zn) and two families of Zn transporter proteins in the pathogenesis of type 2 diabetes, and changes in pancreatic islets. This chapter begins with a brief review of the burden, pathogenesis and risk factors of type 2 diabetes and how the body controls the blood glucose levels. Next, there is a description of the relevant islet cells and tissues, including the structure of the exocrine and endocrine pancreas, islet vasculature, inflammation and macrophages in normal and diabetic islets. Then there is a description of the biology of the alpha, beta and delta cells. The second section describes the role of leptin and leptin receptor signalling in pancreatic islet function and abnormalities in type 2 diabetes. There is a description of some relevant animal models of obesity and type 2 diabetes, with a focus on the leptin receptor mutant db/db mouse model, as well as some commonly used insulin secreting beta cell lines. The third section describes the general role of Zn in the body and, more specifically, in insulin synthesis and storage in the pancreatic islet beta cells. The concept is introduced of fixed and labile Zn pools and their detection by atomic absorption spectrometry and Zn fluorophores such as Zinquin and ZINPYR-1, The fourth section discusses the two major families of Zn transporters (ZIPs and ZnTs) in the body and the pancreatic islets and their implications for type 2 diabetes, as well as Zn binding proteins such as metallothioneins and TRPM3 which are also known to be involved in Zn homeostasis. New insights into the regulation of these transporters are also described. Finally, the Hypotheses and Aims are presented.

1.2 Type 2 diabetes

Organs such as the brain, liver and pancreas need a constant supply of energy in order to function. Glucose is an important source of energy for the body and is involved in many pathways in cells, both anabolic (e.g. amino acid synthesis) and catabolic (e.g. oxidation to pyruvate and eventually to CO_2). When the body is deficient in glucose this leads to seizures, unconsciousness and eventually death. However, when blood glucose is in sustained excess this leads to development of diabetes, and complications of the heart, vasculature, nerves and kidney. Blood glucose homeostasis is maintained by many factors such as diet, hormone regulation, glucose uptake in peripheral tissues and liver glucose production (Figure 1.1). Amongst the hormones that maintain the blood glucose levels are leptin, insulin, glucagon and the incretins GLP-1 and GIP. They have positive and negative roles in controlling blood sugar levels[1].

1.2.1   Burden of type 2 diabetes

There are two types of diabetes mellitus. Type 1 results from autoimmune destruction of the pancreatic β cells, and type 2 results from insulin resistance and subsequently decreased ability of the pancreatic β cells to make insulin leading to β cell dysfunction, hyperglycaemia and secondary microvascular and macrovascular complications[2]. Type 2 is the most common form, affecting 85-90% of all people with diabetes. While it usually affects older adults, the disease is increasingly more prevalent in younger adults and children[3]. Type 2 diabetes results from an interaction of many factors such as genetic predisposition, lifestyle, environment and obesity[4]. Figure 1.2 depicts the normal progression and development of the disease. Usually, in healthy subjects, the insulin secretion is low and postprandial and fasting glucose are low. In type 2 diabetes, insulin resistance increases over time thereby leading to increased insulin secretion and increased postprandial and fasting glucose levels in the blood. The development of obesity is an important factor preceding the development of insulin resistance[1]. Prediabetes is defined as impaired fasting glucose and impaired glucose tolerance. Impaired fasting glucose is a condition in which blood glucose levels are higher than normal but not high enough to be diagnosed as type 2 diabetes. Impaired glucose tolerance is impaired clearance of glucose after a bolus of glucose or consumption of

3

oral glucose. People who have this early stage of the disease often do not realise that they have this condition[5]. Normal people have fasting blood glucose levels ~100mg/dl (5.6 mmol/L) and prediabetic individuals have blood glucose levels of 110 to 125 mg/dl (6.1 to 7.0 mmol/L).

A

B
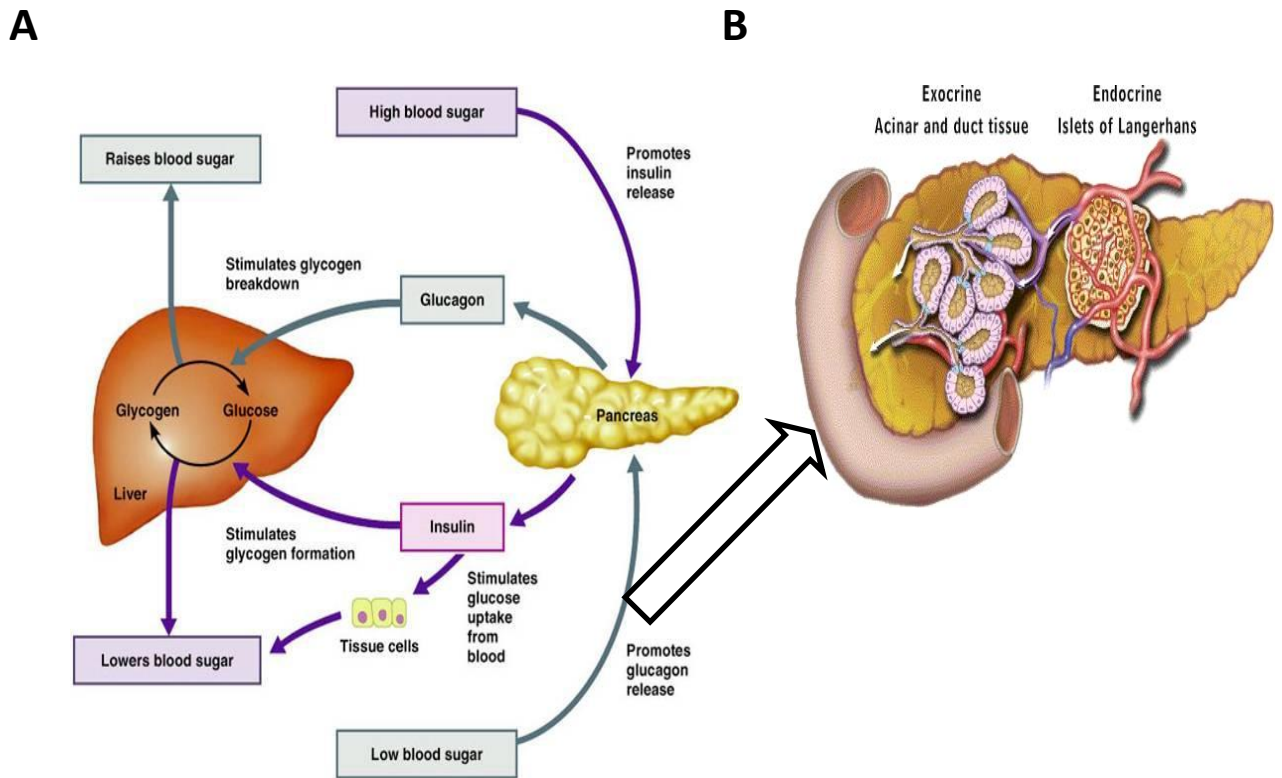
Figure 1.1 Regulation of blood glucose homeostasis in blood

The pancreas is an important organ which controls glucose homeostasis. (A) The pancreas is made up of two types of organs, exocrine (acinar and duct tissue) and endocrine (islets of Langerhans). The acinar tissue is involved in the digestion of food (secretion of pancreatic digestive enzymes). (B) The pancreatic islets are involved in releasing hormones that regulate blood glucose levels. The pancreas is innervated by the parasympathetic and sympathetic nervous systems, and the release of hormones is controlled in part by the hypothalamus but the major control is through the blood glucose levels. When the blood glucose levels are high, the pancreatic beta cells release insulin and this stimulates glucose transporter 2 (GLUT2) in peripheral tissues to take up glucose. Insulin also stimulates gluconeogenesis in the liver (glycogen formation), further lowering the blood glucose levels. When the blood glucose levels fall, the pancreatic alpha cells secrete glucagon, breaking down glycogen in the liver and raising

5

the blood glucose levels. (Figure modified from website http://physiology-11.wikispaces.com/02+Homeostasis, originally derived from Human Physiology, 11th edition)

1.2.2 Pathogenesis of type 2 diabetes

There are five stages of the progression of type 2 diabetes proposed by Gordon Weir and Susan Bonner-Weir[6]. **Stage 1** is called the compensation stage. The pancreatic islets increase in size (hypertrophy) to compensate for the insulin resistance and the beta cells have a lower set point for glucose stimulated insulin secretion and make more insulin than normal (hyperinsulinemia). **Stage 2** is called stable adaptation. It occurs when blood glucose rises above 6-7 mmol/L. At this stage the progression of diabetes can be treated with anti-diabetic drugs such as GLP-1 and changes in diet and lifestyle can slow the progression or even reverse it to normal. At this stage there is a loss of first phase insulin secretion in response to glucose. This is accompanied by changes in gene and protein expression in beta cells[7]. At this stage antioxidant and proapoptotic genes are also activated by high glucose levels and a subset of beta cells undergoes dedifferentiation to alpha and delta cells and this further increases hyperglucagonemia and can contribute to disease severity. Beta cell dedifferentiation to other cell types may due to glucotoxicity[8], local inflammation such as macrophage infiltration and release of cytokines IL-6, IL-1β and TNF-α[9]. Endoplasmic reticulum (ER) stress is also thought to be a major mechanism of beta cell dysfunction. ER stress is caused by multiple factors such as lipotoxicity, glucotoxicity and islet cell amyloid deposition. ER is a site where proteins are synthesised and folded into their correct tertiary structure. It is also involved in cholesterol biosynthesis and storage of calcium and Zn. ER stress is defined as "an imbalance between the protein folding capacity of the ER and the protein load, resulting in the accumulation of misfolded protein"[10,11]. Lipotoxicity is reported to cause ER stress by the action of saturated free fatty acids but the mechanism of how they act and cause stress is not yet elucidated. Fatty acids have been reported to inhibit proinsulin synthesis and maturation[12]. Glucotoxicity is another factor that causes ER stress, by accumulation of reactive oxygen species (ROS). Increase in ROS also leads to decreased proinsulin synthesis by decreasing mRNA expression of transcription factors such as pancreatic and duodenal homeobox 1 and MaFa. Finally islet cell amyloid deposition also causes ER stress, through deposition of hyaline in beta cells which are insoluble fibrous protein aggregates. However, the exact mechanism by which amyloid deposition leads to ER stress and eventually beta cell death by apoptosis is not known[13]. **Stage 3**: In this phase of the disease there is a further decline in beta cells and increase in insulin resistance. Proinsulin gene expression is increased to compensate for the

decline of mature insulin. **Stage 4** is the stable stage decompensation. At this stage up to 50% of the beta cells in human pancreatic islets are lost. Anti-diabetic drugs are not able to work to reverse hyperglycaemia. Increase in dedifferentiation of beta cells to alpha, delta and PP cells is also seen in this stage. Apoptosis can promote amyloid deposits and fibrosis of islets, as well as being a consequence of them. **Stage 5** represents severe loss of beta cells and ketosis where insulin is now required for survival. This is normally seen in type 1 diabetic patients but is less common in type 2 diabetes.

1.2.3   Risk factors for diabetes

Most patients with type 2 diabetes are obese, and the global epidemic of obesity largely explains the dramatic increase in the incidence and prevalence of type 2 diabetes over the past 20 years. The risk of type 2 diabetes in obesity is determined by the location of where the body fat is located. Abdominal fat is associated most with increased risk of type 2 diabetes. In a recent survey 2011-2012, 70% of adult males and 56% of females were overweight or obese (Australian Bureau of Statistics). The progression to diabetes from obesity is dependent on a number of factors including insulin resistance, inflammation, mitochondrial dysfunction and ER stress[14].

Not all obese individuals develop type 2 diabetes, due in part to a genetic predisposition for diabetes[4]. There are a number of genes involved in increasing the risk of type 2 diabetes. These include peroxisome proliferator activated receptor gamma gene (*PPAR*), *KCNJ11*, *calpain-10 gene (CAPN10)*, *hepatocyte nuclear factor 4 A gene (HNF4A)* and transcription factor 7 like 2 gene (*TCF7L2*). Relevant to this thesis, the gene for Zn transporter SLC30A8 (ZnT8) has recently been added to this list (discussed later in this chapter).Other risk factors include physical inactivity, diet, smoking and alcohol consumption[15].
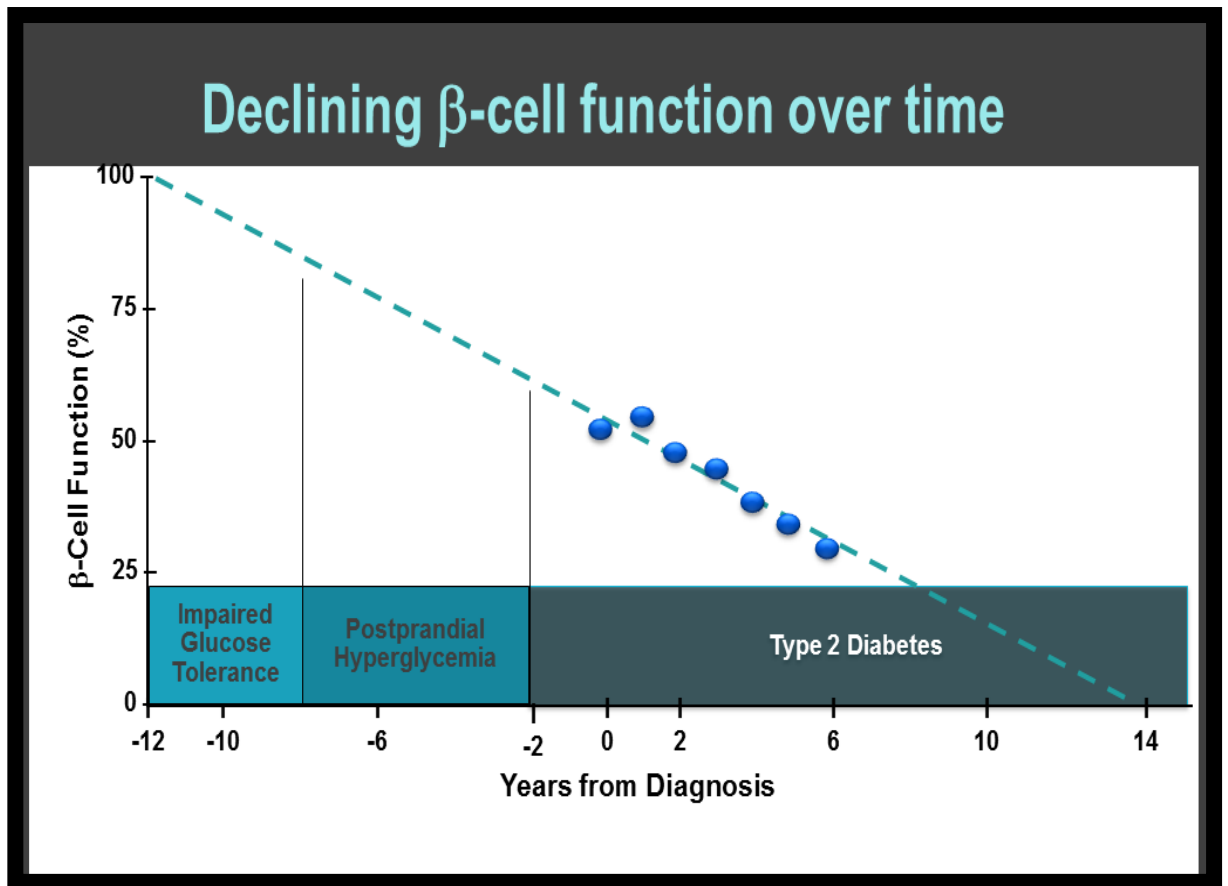
Figure 1.2 Declining beta cell function over time

The figure shows the stages in years from diagnosis of type 2 diabetes (X axis). Impaired glucose tolerance represents pre-diabetes, postprandial hyperglycaemia is early diabetes and type 2 diabetes is the established diabetes. The Y axis shows % Beta cell function. Beta cell dysfunction occurs early and, by the time of diagnosis, approximately 50% of the function is lost[16]

1.3 Pancreas: endocrine and exocrine

The pancreas is an elongated organ, located in the abdominal cavity, which has a major role in maintaining glucose levels in the blood. It is divided into three regions: the head, body and the tail. Figure 1.1 B shows the endocrine tissue which comprises 1-2% of the volume of the pancreas and is composed of the islets of Langerhans which are scattered in the exocrine tissue (acinar cells). The islets are more dense in the pancreatic body and tail region than in the head in both humans and rodents[17,18].

1.3.1 Acini

The acini are rounded structures consisting of acinar and ductal cells. The acinar tissue contains pyramidal epithelial cells which synthesise and release digestive enzymes such as carboxypeptidase and lipases. The digestive enzymes are stored within granules at the apical region of the acinar cell, and the enzymes are secreted into the lumen under the control of hormones and neurotransmitters. The digestive enzymes are secreted into the acinus and released into the interlobular ducts which drain into the major pancreatic duct[19].

1.3.2 The Islets of Langerhans

The islet of Langerhans is composed of five major cell types: - alpha cells which produce glucagon, beta cells which produce insulin, delta cells which produce somatostatin, PP cells which produce pancreatic polypeptide and epsilon cells which produces ghrelin (figure 1.3). Insulin, glucagon and somatostatin will be described in more detail as they are relevant for these studies. Within pancreatic islets, the composition and distribution of the endocrine cell types differs between species. For example, in humans, the pancreatic islet cells comprise 1% of the total pancreas. Of these, beta cells comprise 60%, alpha cells 30% and the remainder are delta and PP cells [20] Mouse islets have a greater proportion of beta cells compared to human islets ~77% and fewer alpha cells <20%[20] . However, these compositions can vary from islet to islet. In humans and primates, the endocrine cells are randomly distributed throughout the islet. However, in the mouse and rat, beta cells are predominantly located in the inner core of the islet and are surrounded by a mantle of alpha, delta and PP cells[20](Figure 1.3).

Despite obvious differences in size, humans and mice have similarly sized islets as islet function depends upon an optimal islet size. The number of islets is related to the size of the animal as this facilitates adequate glucose homeostasis. Insulin secreted by the beta cell has an inhibitory effect on glucagon secretion in alpha cells and vice versa. In addition, somatostatin, whose release from the delta cells is stimulated by hyperglycemia, has an inhibitory effect on hormone release by both alpha and beta cells. Hauge-Evans et al proposed that "locally released delta cell somatostatin exerts a tonic inhibitory influence on insulin and glucagon secretion[21,22].

Mantle

Central Core

■ **Insulin**

■ **Glucagon**

■ **Somatostatin**
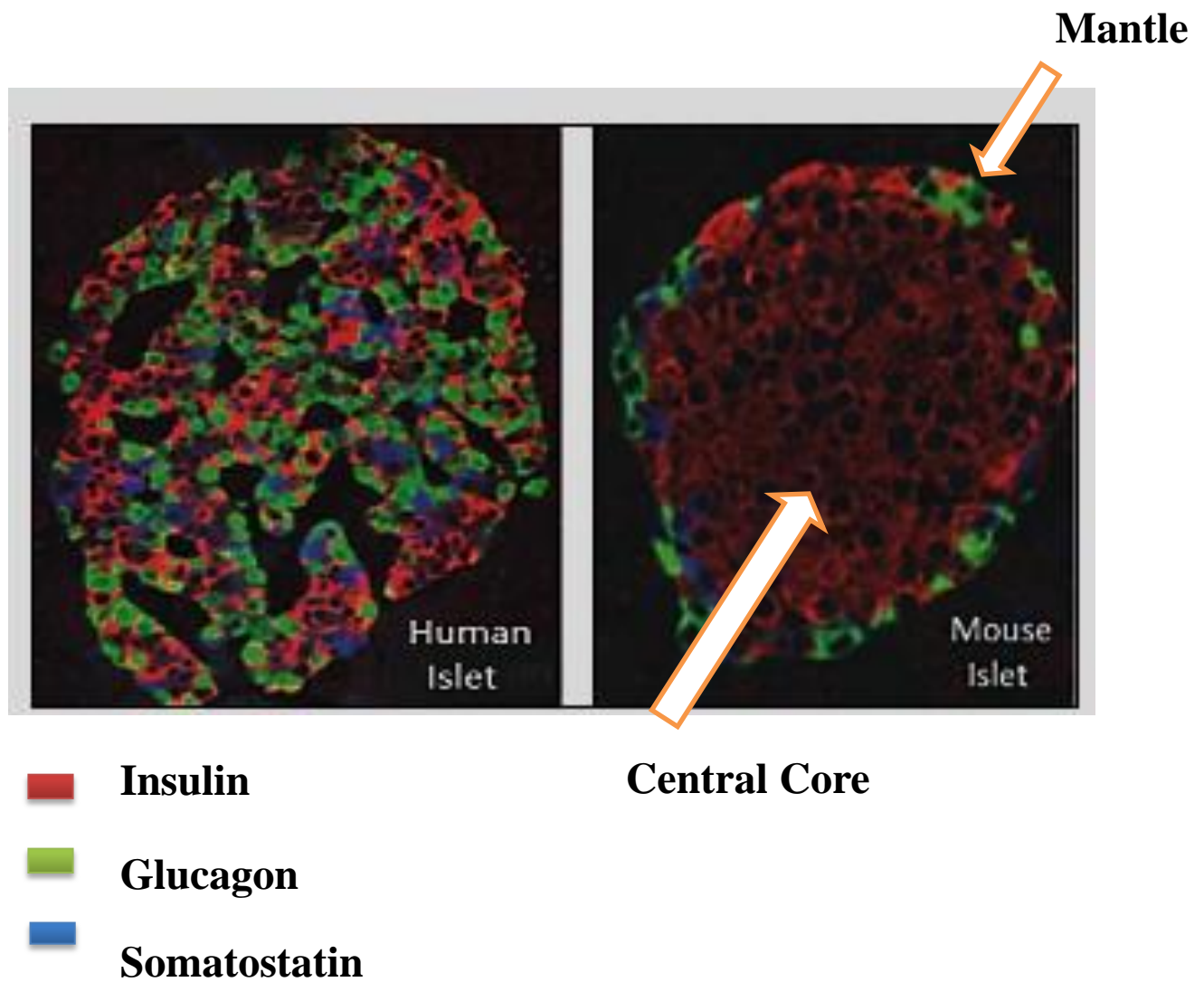
Figure 1.3 The unique architecture of human and mouse pancreatic islets

The figure shows the architecture of a pancreatic islet from human (left panel) and mouse (right panel). The pancreatic islet is composed of five major types of cells that have a regulatory role in controlling blood glucose homeostasis. They are the insulin producing beta cells (red), glucagon producing alpha cells (green), somatostatin producing delta cells (blue), polypeptide producing PP cells (not shown in figure) and epsilon cells which produces ghrelin an appetite regulating hormone (not shown in figure). In the human islet, the pancreatic islet cells are dispersed throughout the islet, whereas, in the mouse islet, there is a mantle composed of alpha, delta and PP cells and a central core composed of beta cells. The pancreatic islet cells produce hormones that have paracrine roles where insulin inhibits the secretion of glucagon and *vice versa*. Somatostatin controls the secretion of both insulin and glucagon. Figure adapted from Cabrera et al[20]

1.3.3   Islet vasculature

Islets are well-vascularized and their blood supply has been likened to that of a glomerulus, with between one and five arterioles per islet which branch into capillaries forming a spherical network. In close proximity to the capillaries, islet cells are both well-nourished and subject to hormonal signals. In the mouse, with its well-defined mantle of non-beta cells, the afferent arteriole (or arterioles, depending on the size of the islet) reach to the islet periphery and then divide into smaller vessels which supply non beta cells first[20,23]. Blood then flows to the beta cell region in the islet core, and leaves the islet through the venules (Figure 1.4). Islet perfusion is strongly influenced by the action of nerve endings in the islet including vasodilatory effects controlled by the vagus and sympathetic nerves. Islet blood flow is also regulated by glucose and ATP (which stimulate blood flow) and by insulin (which decreases blood flow)[23,24].

Studies with animal models of diabetes have indicated a close relationship between islet vascularisation and insulin secretion. For example, in Zucker fatty diabetic rats, islet vascularisation increases with increase in islet cell mass and, later, decreases as beta cell mass is lost. Increase in islet blood flow and blood pressure is also seen in ob/ob mice, non obese diabetic Goto Kakizaki rats (GK) and the Otsuka Long Evans Tokushima fatty rat model. A number of islet capillary changes were noted in adult db/db mice including loss of islet capillaries, increased capillary diameter and pericyte hypertrophy[25].
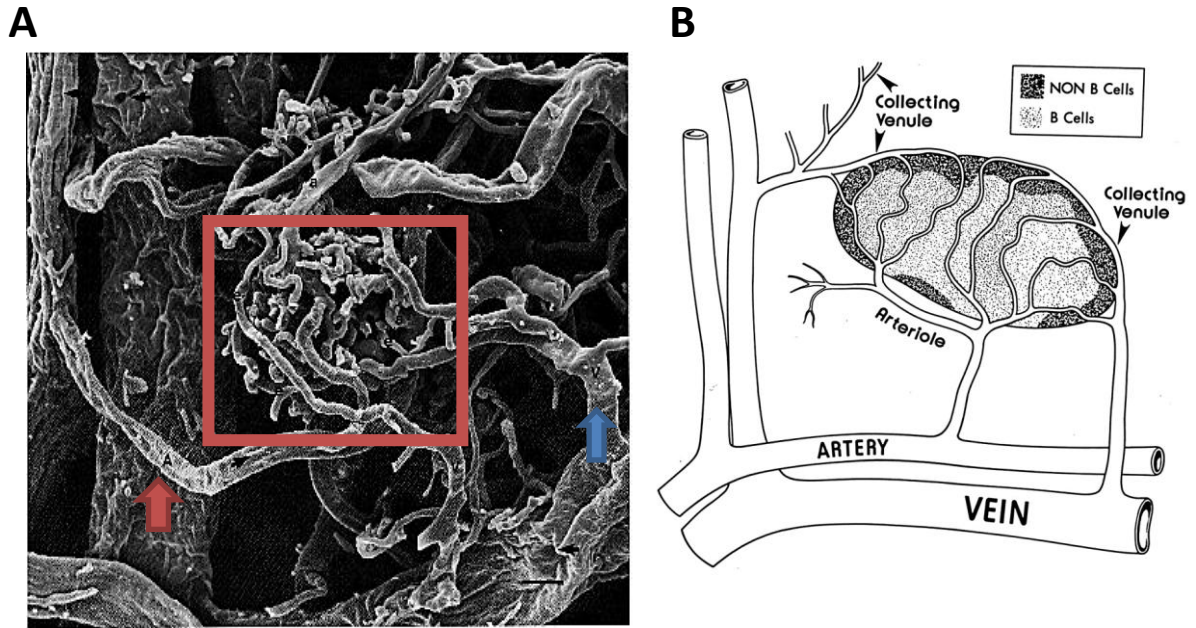
Figure 1.4 The microvasculature of mouse pancreatic islets

(A) This figure shows a scanning electron micrograph of the microvasculature of the pancreatic islet (red box), with a red arrow indicating the arteriole and blue arrow indicating the venule. (B) This figure shows a schematic diagram of the microvasculature of mouse islet. The arterioles enter the islet through a gap in the mantle cells and then directly enter the beta cell core where it branches out into numerous capillaries which, in turn, become collecting venules. Figure adapted from Bonner-Weir and Orci[26].

.

1.3.4　　Islet inflammation

Inflammation of islets is a major feature of type 1 diabetes but also occurs to a varying extent in type 2 diabetes. Islets from patients show immune cell infiltration, inflammatory cytokine production, and death of cells by apoptosis and fibrosis.

An important inflammatory cell that infiltrates the islets is the macrophage. Both vascular endothelial growth factor and inflammatory cytokines cause enhanced infiltration of islets by macrophages. Following infiltration, macrophages can produce more proinflammatory cytokines and amplify the process. As a consequence of elevated circulating glucose and fatty acids levels, ER stress in beta cells may also lead to inflammation and beta cell death[27].

1.3.5　　Macrophages

Tissue macrophages are derived from circulating blood monocytes and are important effector cells in both the innate and adaptive immune systems of the body, where they are involved in phagocytosis of bacteria, removal of apoptotic cells, cytokine production and other activities[28] Usually, macrophages comprise only a small percentage of the cells in a tissue but they are often increased during inflammation, infection and the immune response. In some organs, especially the liver and brain, they are normally present in much larger numbers (up to 20% of the cells) as Kuppfer cells[29] and microglia[30], respectively, where they have special roles such as removal of senescent red cells in the liver. A special type of tissue macrophage is the dendritic cell (DC), which is involved in presentation of antigen to T lymphocyte subsets as part of the initiation of an immune response[31].

Macrophages are recognized by their distinctive morphology, by their capacity to ingest particles or bacteria (phagocytosis) or dead cells (efferocytosis) and by the presence of specific cell surface markers such as CD68 and F480. Subsets of macrophages (M1 and M2) have been defined according to state of activation, cytokines produced and presence of surface markers[28]. Mouse CD68 is a heavily glycosylated and predominantly intracellular member of the lysosomal-associated membrane protein (LAMP) family and is rich in late endosomes of tissue macrophages. The function of

CD68 is not clear but it may be involved in cell-cell interaction or cell-ligand interactions[32].

Macrophages are involved in a number of roles concerning the vasculature such as angiogenesis[33], wound healing[34] and vascular remodelling[35] as well as pathological processes including atherosclerotic plaque development[36]. Macrophages are one of the main scavengers for low-density lipoprotein and continuous uptake of oxidized lipoproteins by macrophages in the arterial walls converts them into fat-rich foam cells, which are pro-thrombic and pro-inflammatory and contribute to vascular occlusion in atherosclerosis[37]. When mice lacking macrophage differentiating cytokine colony stimulating factor -1 (CSF1) were crossed with atherosclerosis-prone, apolipoprotein E null mice, there was decreased plaque formation. By contrast, treatment of hyperlipidaemic rabbits with CSF1 decreased atherosclerosis[38]. Overexpression of CSF1 in rabbit adipose tissue increased both the number of macrophages and the fat mass, while antibody to CSF1 decreased these. Administration of CSF1 to mice lacking functional CSF1 partially restored growth retardation and increased fat content[39,40].

Macrophages are increased in the adipose tissue of obese mice and humans. In part, this is due to the production of monomeric tartrate-resistant acid phosphatase by macrophages, which stimulates adipogenesis. It is believed that obesity drives a low level inflammatory state, which leads to insulin resistance, and that macrophages play a pivotal role in this since, in an animal model, removal of macrophages reversed inflammation and insulin resistance[28].

1.3.6   Macrophages in islets and diabetes

Macrophages play important roles during islet cell development and also inflammation in diabetes. The macrophages are required for proper enlargement of beta cell mass during embryonic development and after birth. However, the precise mechanism of how macrophages are involved in beta cell growth is not clear[41]. In diabetes, the macrophage may have a critical role in local inflammation leading to beta cell dysfunction and apoptosis. In rodent models, C57BL6J mice fed with high fat diet, db/db mice and GK rats showed increased numbers of M1 macrophages but no change in the number of M2 macrophages within the islets[42,43]. A recent study by Cucak et al also confirmed these

results. M1 macrophages (CD68+F4/80-) were increased in the db/db mice islets compared to the M2 macrophages (CD68+f4/80+)[44]. Whether the proinflammatory M1 macrophages play specific roles in diabetes-related events such as beta cell dedifferentiation needs to be determined.

1.3.7 Macrophages and iron metabolism

Macrophages are also important in the homeostasis of iron, the most abundant mineral in the body[45,46]. While the major focus of this thesis is on Zn, there are chemical and biological similarities between iron and Zn and some Zn transporters also transport iron (see later). Therefore, disturbances in iron metabolism and deposition may also influence Zn-dependent pathways in the islet and contribute to beta cell dysfunction and death in type 2 diabetes. Macrophages and iron will be reviewed briefly here. The relationship between macrophages and Zn will be discussed in a later section.

Iron is an essential component of oxygen-binding proteins, hemoglobin, in blood and myoglobin in muscle tissue, as well as proteins involved in energy metabolism and in tissue damage via iron-catalysed oxyradical production. Low levels of iron in the circulation may lead to anemia and hypoxia while excess iron promotes the generation of ROS. Iron levels in the body are mainly regulated at the level of dietary uptake in the small intestine. Iron-rich foods include lentils, red meat, liver and grains[47]. Hereditary hemochromatosis comprises a group of genetic disorders characterized by abnormal iron absorption and iron deposition in vital organs with toxic effects[48,49]. Excessive uptake of iron into the pancreas can result in type 2 diabetes mellitus.

Several proteins regulate iron uptake and distribution. Hepcidin, a 25-amino acid anti-microbial peptide in plasma and urine[50,51] is also found in the small intestine, liver and pancreas. The liver is a major producer of hepcidin. In the intestine, hepcidin acts to suppress iron uptake[48,49,52]. Because of their role in clearance of red cells, macrophages contain abundant iron. They release iron via the surface membrane iron efflux protein ferroportin[53]. By suppressing iron release from macrophages, hepcidin also controls iron levels[54]. When hepcidin levels are high, such as in inflammation, circulating iron levels can drop because iron is trapped inside macrophages.

In the pancreas, hepcidin is present in the insulin-containing granules of beta cells and

its levels in these cells are regulated by iron[55]. It has been proposed that regulation of iron metabolism may also be an important function of beta cells that explains previous findings on iron and glucose metabolism, including a positive correlation between body iron stores and serum insulin and blood glucose concentrations[45,56,57].

1.4 Beta cells and Insulin

Discussion on the role of Zn in insulin synthesis and storage is presented in section 1.14

1.4.1 Transcription of insulin

Insulin was discovered by Banting and Best in the early 1920s as a factor in pancreatic extracts that was able to prolong the life of dogs that were rendered diabetic following removal of their pancreas. Insulin obtained its name from the Latin word *insula*, meaning island. It is derived by proteolysis from a 11.5 kda precursor polypeptide known as preproinsulin[59]. Preproinsulin is transcribed from the *INS* gene on the short arm of chromosome 11 (11p15.5) in humans. Mutations in the INS gene that block cleavage of proinsulin or binding of the A chain of insulin to the B chain result in a genetic disorder in infants called permanent neonatal diabetes mellitus[60]. Mice express two nonallelic genes of insulin:- Insulin 2 is the murine homologue of the human insulin gene and is located on mouse chromosome 7 while Insulin 1 on mouse chromosome 19 may have arisen by a gene duplication event[61] Transcription is regulated by a number of transcription factor-binding elements in the promoter region of the gene. These include regulatory sequences for Pdx1, NeuroD and MafA. Other elements negatively regulate transcription of the INS gene. Intervening sequences are then excised, the 5' terminus is capped by 7-methyl, guanosine and the 3' terminus is polyadenylated. One form of post-transcriptional regulation involves stability of this mature preproinsulin mRNA[61].

1.4.2 Post translational maturation

Following translation, the preproinsulin is targeted to the rough endoplasmic reticulum (RER) via a 24-residue, hydrophobic signal sequence that binds to a receptor in the RER membrane[62]. This sequence is then removed by a peptidase at the luminal side of the membrane and the cleaved polypeptide (now referred to as proinsulin) enters the

lumen and is folded within the cisternae of the RER into the native tertiary conformation with the help of 3 disulfide bonds. Next, proinsulin is moved to the trans-Golgi network and incorporated into immature granules (condensing vacuoles or early secretory granules). Here, further proteolytic processing occurs mediated by two endopeptidases known as prohormone convertase PC1/3 and PC2, and by the exoprotease carboxypeptidase E. In the process, three polypeptide chains are formed. These are the A and B chains of insulin that recombine via disulphide bonding to form mature insulin and a separate sequence known as C-peptide (which was formerly the intervening sequence between B and A in proinsulin). Finally, mature secretory granules containing insulin are formed[63](Figure 1.5).

1.4.3   Regulation of insulin secretion:

The beta cell senses blood glucose levels and responds with enhanced insulin release. Unlike many receptor-mediated signalling events in cells, glucose-mediated signalling of insulin secretion in the beta cell requires the intracellular metabolism of the signalling molecule, glucose. Glucose is internalized via the glucose transporter GLUT2[64].Within the cytosol of the beta cell, glucose is converted to pyruvate via glycolysis, forming ATP and NADH.The latter is used by the mitochondrial electron transport chain to produce more ATP. Pyruvate is also metabolized by the mitochondrial TCA cycle to generate further NADH and additional ATP[65].

There are two phases to glucose action. Firstly, glucose modestly stimulates (~ 2-fold), the transcription of the preproinsulin gene but, more importantly, it greatly enhances (10- to 20-fold) the translation of preproinsulin mRNA through an increase in the activity of the translation machinery and changes at the level of the structure of the mRNA[66]. It has been proposed that there is cooperatively between the preproinsulin mRNA 5'- and 3'-UTRs for the specific translational control of glucose-induced proinsulin bio- synthesis. In addition, glucose stimulates the synthesis of proteins which comprise the secretory granule[67]. Glucose is a positive effector of biosynthesis and is the primary regulator of insulin biosynthesis and secretion of other hormones. This is, in part, mediated by an increase in cAMP levels and activation of protein kinase A to phosphorylate key target proteins.

In response to glucose and other signalling molecules, the secretory granules fuse with the plasma membrane of the beta cell, releasing insulin, Zn and C-peptide. The increase in the cytosolic ratio of ATP to ADP causes a rise in intracellular cytosolic Ca2+ concentration which is essential for insulin exocytosis. This is mediated by closure of ATP-sensitive K^+-channels, depolarizing the plasma membrane and thereby opening voltage- sensitive L-type Ca^{2+}-channels, that result in influx of extracellular Ca^{2+} [68]. Free fatty acids, formed as a consequence of pyruvate metabolism to oxaloacetate as a step in replenishing TCA cycle metabolites, is also thought to be an important requirement for glucose- induced insulin secretion and may act via protein kinase C dependent phosphorylation, or protein acylation, of proteins involved in the exocytosis pathway[69-72].

1.4.4 Function

Insulin is transported in the bloodstream and binds to its specific receptor in the plasma membrane of cells in target tissues where it regulates glucose homeostasis. Control of blood glucose levels is also regulated by glycogenolysis (breakdown of liver glycogen to glucose) and gluconeogenesis (synthesis of glucose from amino acids and glycerol)[73]. Binding of insulin to its receptor triggers an intracellular signalling cascade. As a result, glucose uptake is rapidly increased via translocation of the GLUT4 glucose transporter to the plasma membrane[74,75]. Insulin also promotes storage of glucose as glycogen, in muscle and liver, via activation of glycogen synthase[76] and storage as fat, in liver and adipose tissue, via increased lipogenesis[77]. In addition, insulin blocks gluconeogenesis[78] and lipolysis (which releases fatty acids from triglycerides stored in adipose tissue and muscle[79]). Therefore, in diabetes, when insulin levels are low and/or when insulin function is impaired, there is increase in circulating sugars and lipids.

1.4.5 Insulin and diabetes

Insulin resistance in liver, skeletal muscle and other organs or tissues is an early event in diabetes and is further worsened by the chronic exposure of these to hyperglycaemia. An early response to insulin resistance is hyperplasia and hypertrophy of islets allowing increased insulin release and hyperinsulinemia. With time, however, beta cell function

fails, beta cell mass may decrease, insulin output is decreased and blood sugars rise to high levels[80-82]. Obese non-diabetic subjects have an increase in their relative beta cell number, whereas obese diabetic subjects have significant decrease in the beta cell number (both compared to non diabetic lean subjects).This indicates that obese individuals are able to compensate for the increase in blood sugar by increasing their mass of beta cells, whereas in the diabetic individuals the beta cell mass decreases due to the beta cells not being able to compensate for the hyperglycamia[80].

While the insulin protein regulation has been extensively studied and established, the regulation of insulin at the gene level is still controversial. More studies are needed to identify the role of gene expression of insulin in diabetes.

A

Pre-proinsulin
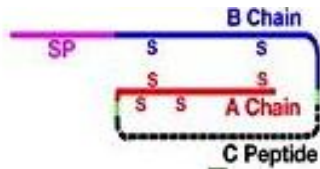
Proinsulin
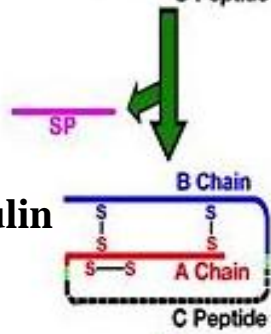
Insulin
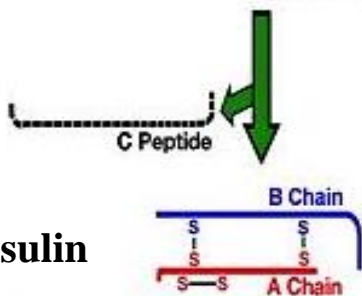
B
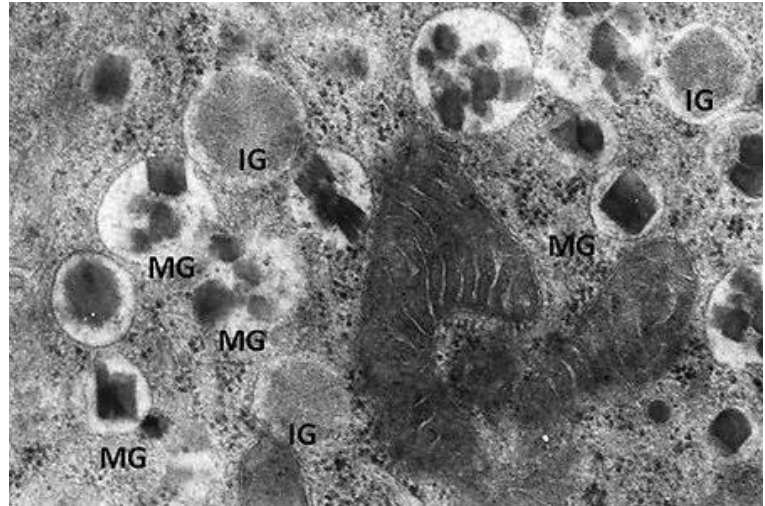
Figure 1.5 Conversion of pre-proinsulin to mature insulin

A) This shows the two stages of proteolytic processing of 1) pre-proinsulin to proinsulin in the ER, with removal of signal peptide sequence (SP) and 2) proinsulin to mature insulin in the secretory granules, with removal of C-peptide sequence. Figure modified from website (http://sitemaker.umich.edu/liu.lab/home)

B) This shows an electron micrograph of immature granules (IG) containing proinsulin and the mature granules (MG) with a dense core containing mature insulin. This figure was adapted from Masini et al[83].

1.5 Alpha cells and Glucagon:

In 1923, a year after the discovery of insulin, Kimball and Murlin identified a hormone that contaminated impure insulin preparations and was present in pancreatic extracts that had the opposite effect to insulin, that is increasing blood sugars[84]. It was named glucagon and the hormone was purified as a 29 amino acid peptide hormone[85] and shown to be secreted by the alpha cells of the pancreatic islets[86]. By their opposing actions, insulin and glucagon tightly regulate glucose homeostasis[87].

1.5.1   Preproglucagon gene transcription

The glucagon gene is more widely expressed than insulin, being not only expressed in the α-cells of the endocrine pancreas, but also heavily expressed in various regions of the brain, such as the hypothalamus as well as in intestinal L cells[88].

1.5.2   Proteolytic processing to form glucagon

Similar to insulin, the glucagon gene product is an inactive precursor polypeptide of 180 amino acids (preproglucagon) that requires further proteolytic processing and maturation to become the active hormone. Preproglucagon also contains the amino acid sequences for three other hormones known as glucagon-like peptide-1 (GLP-1), glucagon-like peptide-2 (GLP-2) and glicentin-related polypeptide (GRPP)[89,90].Preproglucagon is first converted to proglucagon by removal of a 20 amino acid leader sequence. It is then cleaved at several points by prohormone convertases that differ between glucagon-expressing cells. Within the alpha cells, glucagon is the major product of the cleavages whereas in intestinal L cells, GLP-1, GLP-2 and glicentin are major products[90,91]. Prohormone convertase (PC2) is important for processing to glucagon in alpha cells. PC2 knockout mice had marked hyperplasia of α-cells with proglucagon-containing granules[92,93] (Figure 1.6).

1.5.3   Glucagon function

Inadequate glucagon results in hypoglycaemia. Glucose suppresses glucagon secretion while arginine and other amino acids produced during protein turnover stimulate glucagon secretion[94]. Overall glucagon signalling promotes glycogenolysis.

Glucagon exerts its effect on cells via its membrane receptor which, when bound by glucagon, leads to activation of G proteins Gs alpha and Gq[95]. Activation of Gs alpha causes activation of adenalyate cyclase and therefore a rise in intracellular cAMP which, in turn, activates protein kinase A; activation of Gq triggers a second major signalling pathway mediated via phospholipase C, inositol 1, 4, 5-triphosphate, release of intracellular calcium from ER and diacylglycerol-mediated activation of protein kinase C. Activation of glycogen phosphorylase results in phosphorylation of glycogen and glycogen breakdown[96].

1.5.4 Glucagon and diabetes

Normally after a meal, insulin is released and has an inhibitory effect on glucagon release. Therefore glucagon levels fall after the meal. In people with type 2 diabetes there is a delay in insulin response and therefore glucagon levels are not immediately depressed. Due to the abnormality of insulin and glucagon secretion in type 2 diabetic patients they are unable to clear the glucose ingested i.e. glucose tolerance is impaired. In type 2 diabetes in mice, the alpha cell number increases and they are no longer present in the mantle of the islet but also the inner core of the islet. The mechanism of how and why these cell numbers increase in diabetes are yet to be determined[97].

1.5.5 Alpha cell hyperplasia in diabetes

Alpha cell hyperplasia is observed in conditions such as insulin deficiency and hyperglycaemia and in rodent animal models of streptozotocin induced diabetes (NOD-SCID), diet induced obesity and type 2 diabetic models. Hyperglucagonemia is common in both type 1 and 2 diabetes[98], where glucagon is released and stimulates glucogoneolysis in the liver thereby leading to elevation of blood glucose level in the blood in both pancreatic islets of animals and humans. In type 1 and 2 diabetes, there is an increase in alpha cells while beta cells decrease[99,100]. Alpha cells may increase in diabetes due to dedifferentiation of beta cells back to their stem cell progenitors (which express Neurogenin3, Oct4, Nanog, and L-Myc) and thence into alpha cells[101].
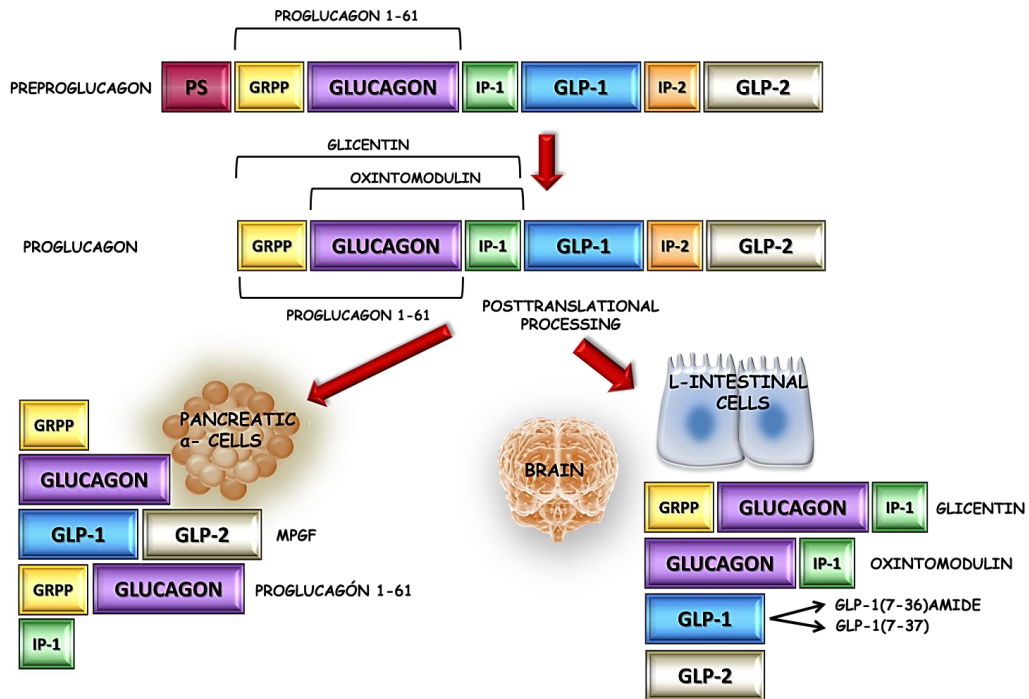
Figure 1.6 Conversion of preproglucagon to glucagon

The figure shows the stages of proteolytic cleavage for of preproglucagon processing and maturation to become the active hormone. Preproglucagon also contains the amino acid sequences for other hormones known as glucagon-like peptide-1 (GLP-1), glucagon-like peptide-2 (GLP-2), glicentin-related polypeptide (GRPP) and intermediate peptide 1 and 2 (IP1 and IP2). Preproglucagon is first converted to proglucagon by removal of a 20 amino acid leader sequence. Within the alpha cells, glucagon is the major product of the cleavages whereas in intestinal L cells GLP-1, GLP-2 and glicentin are major products. Figure adapted from Veronica et al[102].

1.6 Delta cells and Somatostatin

Somatostatin is a peptide hormone produced by delta cells (D cells) of the islets. It was initially found in the extracts of the hypothalamus where it was found to inhibit the release of growth hormone[103]. There are two forms of somatostatin that are derived by proteolytic cleavage of preprosomatostain, a single 116 amino acid polypeptide[104], forming 14 and 28 amino acid compounds. The 14 amino acid isoform of somatostatin is expressed highly in the hypothalamus and the pancreatic islets while the other isoform is expressed abundantly in the intestine. The D cells are located next to the alpha and beta cells and play an important inhibitory role in insulin and glucagon secretion. D cells are not only expressed in the pancreatic islets but they also are found in the gastrointestinal system[105]. They are located in the gut mucosa in the gastric fundus atrium and duodenum. The delta cell regulates the secretion of various gastrointestinal hormones including gastrin. Somatostatin is released into the circulation by delta cells and controls gastrointestinal motility and blood flow[106]. Somatostatin receptors are expressed on both alpha and beta islet cells where somatostatin binds to its receptors, thereby activating cyclic AMP, altering calcium transport into cells and inhibiting hormone secretion[107,108](Figure 1.7).

Somatostatin plays an important role in the regulation of cancer growth[109]; however its role in diabetes is not well understood. It was reported that delta cells in the early diabetes db/db mice pancreatic islets increase and in late diabetes delta cells decrease[110]. Delta cells in the periphery of the islets translocate into the central core of the islet in diabetes[110-112].

1.7 PP cells and Pancreatic Polypeptide:

The other endocrine cell in the islet is the PP cell which makes pancreatic polypeptide hormone, a 36-amino acid peptide. This hormone is also involved in regulation of other islet hormones and has been suggested to function as a feedback inhibitor of pancreatic secretion after a meal[113].
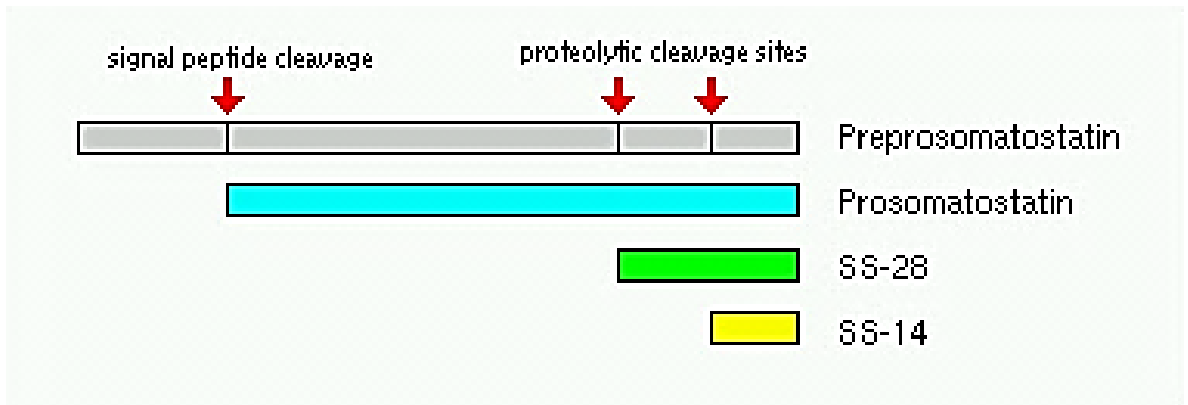
Figure 1.7 Conversion of preprosomatostatin to somatostatin

The figure shows that somatostatin is derived by proteolytic cleavage of preprosomatostatin, forming 14 and 28 amino acid compounds. The subtype 14 of somatostatin is expressed highly in the hypothalamus and the pancreatiic islets while the 28 isoform is expressed abundantly in the intestine.

Figure adapted from website:

http://www.vivo.colostate.edu/hbooks/pathphys/endocrine/otherendo/somatostatin.html

1.8 Leptin and leptin receptor

Leptin is a 16kDa neuroendocrine hormone which is produced by adipose tissue and secreted into the blood stream. It suppresses food intake and increases energy expenditure and its circulating levels are proportional to the amount of adipose tissue in the animal. Mutations in the obese (ob) gene cause leptin deficiency leading to obesity in animals and humans. Supplementation of leptin has been shown to reduce weight gain[114,115].

Leptin binds to the leptin receptor (Ob-R) in the hypothalamus, which in turn acts as an efferent feedback to maintain homeostasis[116,117]. Ob-R is member of the cytokine class 1 family [118]. The gene codes for five isoforms Ob-Ra, Ob-Rb, Ob-Rc, Ob-Rd and Ob-Re[119] (Figure 1.8 A). The Ob-Rb isoform is expressed highly in the hypothalamus and is involved in signal transduction. Leptin acts on the leptin receptors in neurons which activates the JAK /STAT signalling pathway (Figure 1.8 B). Leptin is also involved in the insulin receptor pathway involving phosphatidylinositol 3 kinases (PI3-K).

1.8.1   Leptin and pancreatic islet function

Leptin significantly reduces insulin release from pancreatic beta cells under physiological conditions. It suppresses insulin secretion in beta cells by affecting ATP sensitive potassium channels through PI3K dependent activation of PDEB and glucose transport into beta cells[120]. Leptin has also been shown to suppress pre-proinsulin mRNA expression in response to high glucose concentrations. Leptin also inhibits glucagon secretion from pancreatic alpha cells[121]. These findings suggest that leptin may modulate glucose homeostasis by inhibiting insulin and glucagon release from the pancreatic   islets.

1.9 Animal models of obesity and type 2 diabetes

To investigate pathogenic mechanisms in type 2 diabetes, various animal models of obesity, type 2 diabetes and insulin resistance have been used. Rodent models include spontaneously diabetic rodents, artificially induced diabetic rodents and transgenic or knockout diabetic rodents. Spontaneous rodent models are most often used because they best mimic features of type 2 diabetes, obesity and insulin resistance in humans. These include the ob/ob and db/db mice as well as the Zucker rat.

1.9.1 The ob/ob mouse model

In 1950 Ingalls and colleagues from the Jackson laboratory first described the ob/ob mouse. The ob/ob mutation arose spontaneously in a colony of mice and resulted in hyperplasia and obesity at an early age[122]. These mice have a point mutation in the leptin gene, which makes them deficient in leptin. The size of the pancreatic islets are also increased and they have marked hypertrophy and hyperplasia of the pancreatic islets, due to increase in both number and size of the alpha and beta cells[123,124]. Hyperplasia of these islet cells is accompanied by increased circulating levels of glucagon and insulin, respectively[125,126]. Insulin levels in their blood are increased by 3 weeks of age [127] and peak at 25-30 ng/ml by 6-8 months of age[126,128]. These mice do not go on to develop diabetes and this is thought to be due to the successful compensatory increase in beta cells[129].

1.9.2 Zucker Diabetic Fatty Rat

The most commonly used rat diabetic model, the Zucker diabetic fatty rat, develops both obesity and diabetes, when on a high fat and carbohydrate diet [130]. It has a single base point mutation in the leptin receptor gene resulting in an amino acid change (glutamine to proline at amino acid 279) altering the extracellular domain and the dimerization of this receptor. This impairs leptin signalling leading to early obesity, hyperphagia (increased appetite) and reduced thermogenesis (body heat production)[131]. In these rats, hyperglycaemia occurs at 7-9 weeks of age and is accompanied by obesity and insulin resistance.

1.9.3   db/db mouse

Diabetic db/db mice arose as a spontaneous autosomal recessive mutation in a colony of mice at Jackson Laboratory[132,133]. Like the Zucker diabetic rat, the db/db mouse lacks a functional leptin receptor and develops both obesity and diabetes. Consistent with impaired leptin signalling due to leptin receptor mutation, exogenous administration of leptin to db/db mice was ineffective in altering food intake and weight gain.

The db/db mouse has an autosomal recessive mutation in the leptin receptor gene on chromosome 4 which renders them leptin receptor deficient. This $G \rightarrow T$ point mutation results in alternative splicing of the receptor coding region and the addition of a 106bp insert containing a premature termination signal resulting in a truncated leptin receptor lacking the cytoplasmic region[119,134]. Heterozygotes with one mutant copy of the leptin receptor are phenotypically normal, at least with respect to body weight and blood concentrations of glucose and lipids[135].

As discussed by Belke and Severson (2012)[135], there are at least two experimental advantages of the db/db mouse model. Firstly, the natural progression of the diabetes, with initial insulin resistance followed by an impairment of insulin secretion, is very similar to the pathogenesis of type 2 diabetes in humans. Secondly, hyperphagia and insulin resistance occur as early at 2 weeks of age, quickly followed by compensatory responses of hyperinsulinemia, beta-cell hyperplasia and islet hypertrophy. Later, when beta cell compensation can no longer match peripheral and hepatic insulin resistance, the onset of hyperglycemia occurs. The db/db mice develop obesity at the age of 3 to 4 weeks. They become hyperglycaemic at the age of 4 to 8 weeks and their diabetes is established at 10 weeks. This is followed by rapidly decreasing insulin levels as beta-cells apoptose[136,137].

Interestingly, the severity of the db phenotype is influenced by the genetic background. On the most commonly used background C57BL/KsJ the diabetes is severe and accompanied by extensive beta-cell necrosis. However, on the C57BL/6J background, there is severe insulin resistance, less severe hyperglycaemia and beta-cell hyperplasia. The db/db mice that were used in this thesis were B6.BKS (D)-*Lepr*^{db}/J. The disease phenotype of these mice was of intermediate severity and will be discussed further in

chapter 3. Like the ob/ob mice, the pancreas of these mice is heavier compared to littermates and there is hypertrophy and hyperplasia of the pancreatic islets. However, while ob/ob mice have a beta cell compensatory response that protects them from diabetes, the db/db mice have decreased beta cell compensation leading to beta cell dysfunction and finally failure[139].
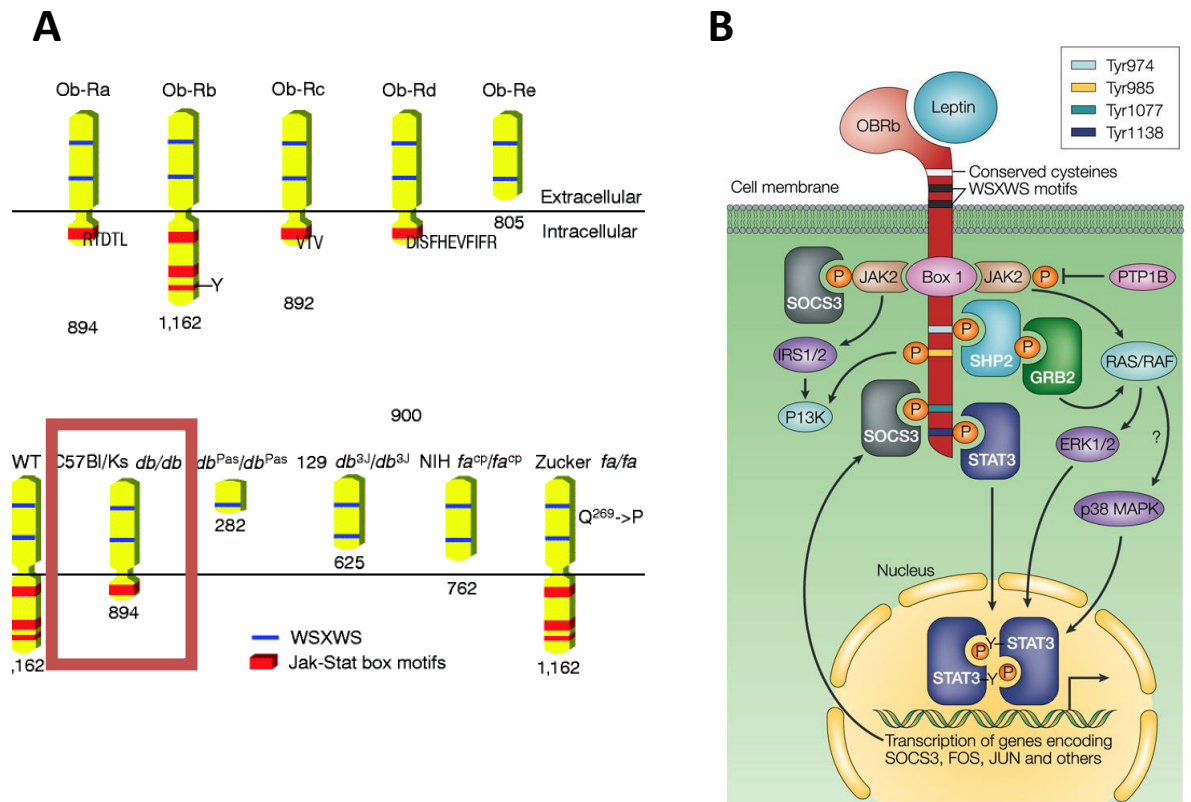
Figure 1.8 Leptin receptor isoforms and signal pathway

The figure shows the five isoforms of the leptin receptor that are found in the mouse (upper panel in A). Mutation in the leptin receptor results in a truncated derivative which lacks the intracellular tail and leads to obesity and diabetes in db/db mice (red box, lower panel). Figure adapted from Friedman and Halaas[140]. (B) The figure shows the signalling pathway resulting from leptin binding to the leptin receptor isoform Ob-Rb. Ob-Rb contains protein motifs that are involved in the JAK-STAT signalling pathway altering gene expression. After binding of leptin to Ob-Rb receptor, a number of signalling pathways are turned on, including STAT3 which becomes phosphorylated and activated and translocates to the nucleus to modify gene expression. Figure adapted from Cava et al[141].

1.10   *Insulin-secreting beta cell lines*

Beta cell lines are tools for islet cell research as they are helpful in answering important biological questions on the physiology and pathology of beta cells. They are also important in understanding the pathogenesis of diabetes and the development of new therapies[142]. Isolated islets have many disadvantages compared to beta cell lines as they are vulnerable to hypoxia [143] and they are separated from the vasculature[26], connexins and intergrins as well as nerves. The loss of these connections leads to increased insulin, glucagon and somatostatin release and eventually to islet cell death[142].

The commonly used insulin secreting cell lines are rat insulinoma cell line (RIN), Human Insulinoma cell line (INS-1) and mouse insulinoma cells (MIN6). MIN6 cells are mouse insulinoma cells derived from a pancreas B cell tumour in a C57BL6/J mouse transgenic for a human insulin promoter - SV40 T-antigen hybrid gene. They grow as a three dimensional aggregate. MIN6 cells are considered to be an appropriate model for studying the mechanism of glucose-stimulated insulin secretion in pancreatic beta cells as they have properties similar to those of isolated mouse islets. However, they secrete not only insulin but also glucagon and somatostatin (to enable them to grow and survive). Another beta cell line (RIN rat insulinoma cells) also secretes insulin, glucagon and somatostatin, although the latter two hormones were only made in small amounts[144]. MIN6 cells are glucose responsive at early passages and lose this over an extended period of time[145-147].

1.11   Zinc (Zn)

Zn is the second most abundant essential mineral that is found in all cells of the body. A constant dietary intake of Zn is essential. A total of 2-3g of Zn is distributed in all organs, tissues, fluids and secretions in the human body[148](Figure 1.9) Zn is important for the function of many hundreds of enzymes, metalloproteins and transcription factors[149,150]. It plays an important role in metabolic processes including carbohydrate, lipid, protein and nucleic acid synthesis and degradation. Zn ions are hydrophilic and do not cross cell membranes by passive diffusion; uptake by cells is mediated by special membrane transporter proteins[151].

1.11.1   Zn is important in public health

The essential requirement of Zn for higher plants and animals has been known for more than 70 years. Zn deficiency, in humans, was discovered about 50 years ago, when it was recognized that young men in rural villages of Iran and Egypt were stunted in growth and had immature sexual development[152]. They also had hepatosplenomegaly and anaemia which was attributed to iron deficiency. However the cause of growth stunting and delayed sexual maturation was found to be due to insufficient intake of Zn and could be reversed by Zn supplements. Since then Zn deficiency has been reported to affect children of many countries. Other groups at particular risk are pregnant women, the elderly and the chronically sick[153].

1.11.2   Zn toxicity and intake from the diet

Zn in high concentrations is toxic to cells. Zn in the body is regulated through intestinal uptake, faecal excretion, and renal reabsorption via Zn transporters present in the kidney. The dietary intake of Zn is estimated at approximately 10-15mg/day[154]. Zn is absorbed across the small intestine by the action of a combination of Zn transporter proteins at the luminal surface of the duodenum and jejunum, as well as other Zn transporters at the serosal surface that export the newly absorbed Zn into the portal blood system[155]. Zn is then carried by albumin to the liver and eventually other organs where it is incorporated into metalloenzymes[156]. The main cause of human Zn deficiency is consumption of diets that are low in readily absorbable (bioavailable) Zn.

Red meat is an excellent dietary source of bioavailable Zn since about 25% of Zn in red meat is retained by individuals with normal Zn status. Other sources of Zn are seafood, dairy foods, cereals, and nuts[157]. Phytates (e.g in unleavened bread and rice) and dietary fibre chelate Zn and inhibit its absorption[158]. Diets which are low in animal protein and rich in phytate contribute to the high incidence of Zn deficiency in many developing countries[159]. Secondary causes of Zn deficiency are illnesses that impair food intake or intestinal absorption as well as conditions that lead to excessive losses of Zn from the body (e.g. in the urine in many patients with type 2 diabetes. A number of diseases are associated with Zn deficiency including diabetes[160].
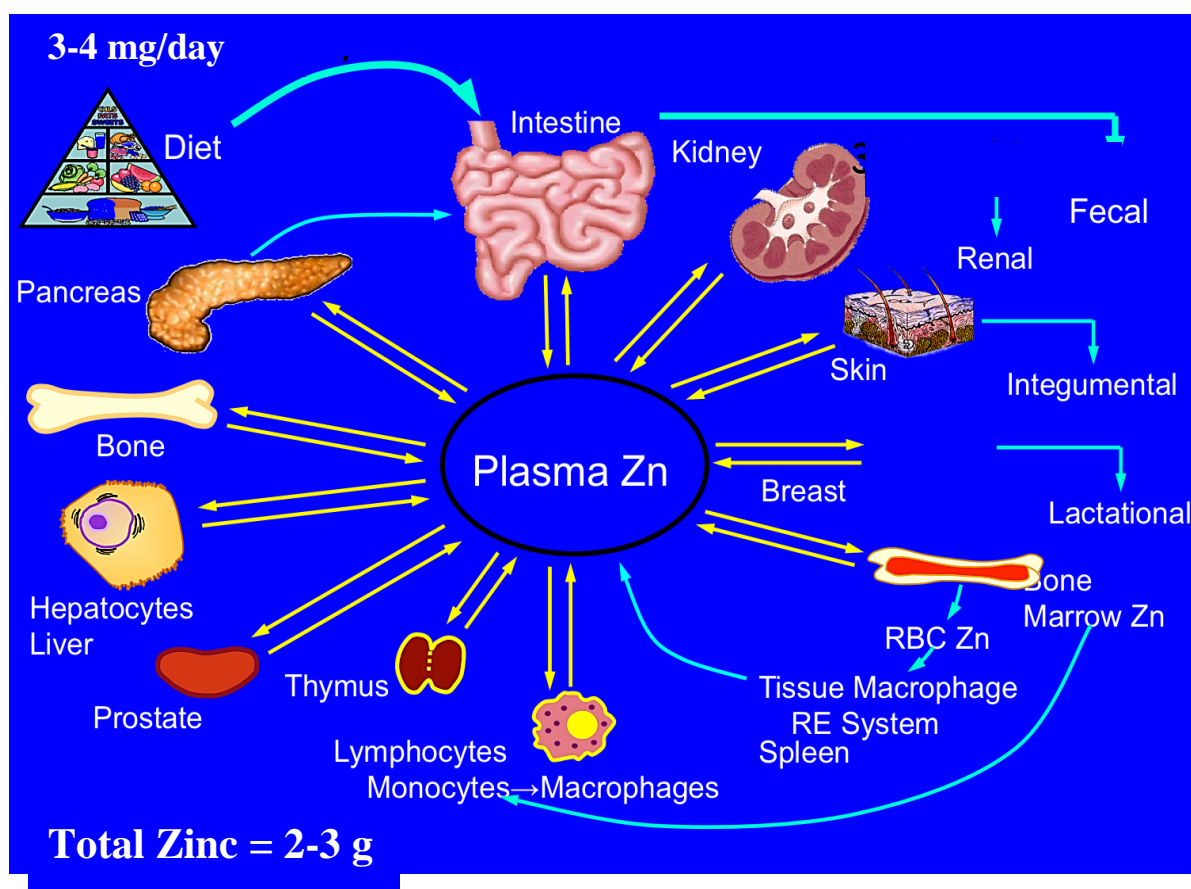
Figure 1.9 Zn homeostasis in the body

The human body contains 2-3 g of Zn which is obtained from the diet and absorbed through the small intestine (3-4 mg/day). Some of the Zn enters the plasma and is distributed non-uniformly throughout all organs, secretions, fluids and tissues. The excess Zn is excreted out through urine (via the kidneys). Some Zn is lost via the pancreatic secretion into the small intestine. Figure kindly provided by Dr Chiara Murgia (unpublished).

1.12   Two distinct pools of Zn

Zn is incorporated into all types of cells and once internalised is taken up by intracellular organelles[161]. At the cellular level Zn is regulated by membrane Zn transporters and by the cytosolic metal-binding protein metallothionein[162,163]. In the body, Zn exists in two main states: approximately 90% of Zn is in a tightly bound form (fixed Zn) in metalloenzymes and Zn finger proteins involved in housekeeping functions, in cellular metabolism and gene expression and relatively unaffected in Zn deficiency[164] while a more loosely bound form (labile or exchangeable Zn) participates in intracellular Zn fluxes, secretion, cytoprotection and signal transduction and is readily depleted during Zn deficiency. Some organs and tissues such as the hippocampus[165], testis[166], prostate[167], secretory glands[168], pancreatic islet cells[169] and mast cells[170] contain very high levels of intracellular labile Zn. In mammalian cells, it is estimated that free (ionic) Zn is in the pM range but labile Zn can reach mM concentrations when sequestered in organelles such as the secretory granules[171,172].

1.12.1   Measurement of tightly bound Zn pools

The tightly bound Zn is often measured by atomic absorption spectrometry (AAS) and related techniques such as ICP-MS. In these methods, there is digestion and destruction of the tissue which involves wet ashing with nitric acid and hydrochloric acid and subsequent conversion into a dry powder. AAS detects absorption of certain wavelengths of light that are specific to each element and correspond to the energies needed to promote electrons from one energy level to another, higher, energy level[173].

1.12.2   Labile Zn and ZINPYR-1

A major advance in Zn biology was the identification of novel fluorophores to visualize and measure tissue and cell Zn without using techniques that destroy the tissue. These fluorophores also preferentially detect the labile Zn pools since much of the fixed Zn buried within protein structures is not available for binding[174]. One of the first real-time Zn flurophores developed was Zinquin[175,176], a UV excitable probe. Subsequently a number of other Zn flurophores were developed with various improvements, including excitation with FITC-like wavelengths that are less prone to UV-induced photo bleaching and less toxic. One such fluorophore that is now used widely is ZINPYR-1,

in which the Zn binding ligand is a di-2-picolylamine moiety[177] (Figure 1.10). ZINPYR-1 has an excitation maximum at 515nm in the absence of Zn which shifts to 507nm when ZINPYR-1 is complexed with Zn and, at the same time, the quantum yield increases more than two fold. ZINPYR-1 is relatively specific for Zn although, like some other Zn fluorophores, it also reacts with cadmium and manganese ions[178].

1   **2**   **3**
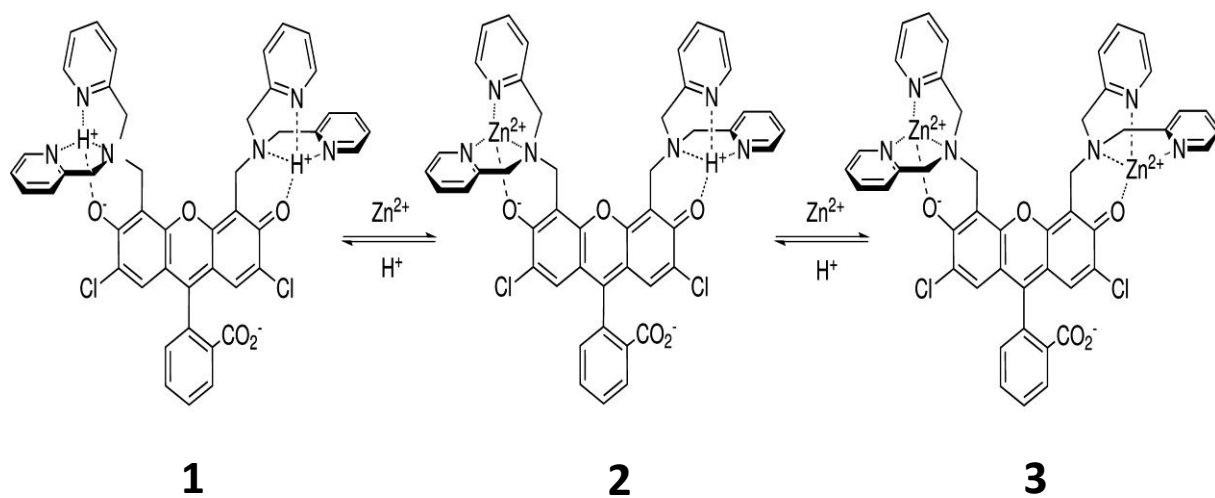
Figure 1.10 ZINPYR-1 Structure

Zn free ZINPYR-1 (1) binds Zn in two stages to form the 1:1 complex (2) and 2:1 complex (3), with loss of protons. Zn ions bind to the two di-2-picolylamine groups to form the fluorescent compound. Figure adapted from Kowalczyk et al[179].

1.13   The many roles of Zn in the body:

Zn plays an important role in synthesis of insulin and other pancreatic islet hormones, as is described in a later section. Some of its other roles in the body are summarized here.

1.13.1   Zn and intestine function

Zn is known to play an important role in the physiological function of the gastrointestinal tract[155] such as maintaining epithelial structural integrity. Zn deficiency is often accompanied by diarrhoea and gut lesions as in Crohn's disease and the hereditary Zn deficiency disease known as acrodermatitis enterophaica[180]. Zn helps to maintain intestinal tight junctions and, in support of this, oral Zn supplements reduced (by 50%) gut leakiness in experimental colitis[181,182].

1.13.2   Zn as a neurotransmitter and survival factor in the brain

Another important role of Zn is in neurotransmission[183]. Stimulation of the mossy fibre pathway in the hippocampus results in the release and of Zn into the synaptic cleft where it is taken up by neighbouring post-synaptic cells through gated ion channels and plays an important role in modulation of synaptic signalling[184]. In neurons, exocytotic stimuli induce Zn release into the surrounding milieu Zn may also help to maintain neuronal viability by preventing apoptosis[185]. This anti-apoptotic property of labile Zn ions has been seen in many other cells and tissues of the body[186].

1.13.3   Zn and lung infection and inflammation

Another property of Zn is its anti-oxidant and anti-inflammatory action. Zn is a cytoprotectant in the respiratory tract tissue against toxins and inflammatory mediators[187,188]. Zn supplementation has been shown to decrease the severity and incidence of respiratory infections in young children from developing countries[189]. It has been reported that there was a 45% decrease in the incidence and prevalence of acute lower respiratory infection in children of 6 to 35 months of age receiving 10mg of supplemental Zn daily[189]. Numerous studies have suggested that significant decreases in

the intake of dietary antioxidants may be an important contributing factor to the increasing incidence of asthma[190-192].

1.13.4 Zn and skin

Zn is rich in cells and extracellular matrix of the epidermis, where it is involved in cytoprotection, epidermal mitosis and wound healing[193]. Zn deficiency often leads to pathological skin changes such as in acrodermatitis enteropathica[194].

1.13.5 Zn and mammary gland

Zinc is essential for the newborn infant and is provided in breast milk; the mammary gland secretes 0.5-1mg of Zn/ day[195]. Early neonatal death associated with low milk Zn levels occurs in lethal milk (lm) mutation in mice[196]. Dysregulation of this process in infants causes growth retardation, impaired immune function and increased susceptibility to infection[197].

1.13.6 Zn and bone:

Zn is required for the growth, development and maintenance of healthy bones. A reduction in Zn in the long bones (e.g. femur) contributes to growth retardation in Zn deficient infants while Zn supplementation in children can restore normal growth and maturation[198-201].

1.13.7 Zn, macrophages and immunity

Zn homeostasis is crucial for the normal immune response and, especially, the development of cell-mediated immunity. Zn deficiency primarily affects the T cells, due to atrophy of the thymus and apoptosis of T cells[202]. resulting in a decreased number of T helper cells, a reduction of the absolute number of splenocytes, decreased response to T-cell- dependent and T-cell-independent antigens, production of IgG and generation of cytotoxic killer cells to allogenic tumor cells[203,204]. Zn deficiency also inhibits the proliferation and/or function of B cells, macrophages, neutrophils, dendritic cells and natural killer cells[205]. Amongst the actions of Zn ions on the immune system

are effects on thymocyte, dendritic cell and monocytoid differentiation, T helper cell function and phagocytosis[206]. Initial studies on phagocytosis described inhibitory effects of high micromolar (pharmacological) concentrations of Zn ions on monocyte/macrophage functions, including phagocytosis of yeast particles[207]. Inhibition by Zn was shown to be dependent also on Mg and to be reversible following washing away the Zn. Later studies showed impairment of phagocytosis in Zn deficient mice[208]. In the latter study, the effects of suboptimal levels of Zn on the ability of murine macrophages to phagocytose Trypanosoma cruzi were studied. The percentage of mouse peritoneal macrophages with associated parasites, the number of parasites per 100 macrophages and the intracellular killing of parasites were significantly lower for macrophages from moderately and severely deficient mice compared to control fed mice; pretreatment of the macrophages from Zn-deficient mice with Zn for 30 min completely restored both their capacity to take up and kill the parasites. The effect was specific to Zn and not other metals[209]. Another study showed that Zn stimulated phagocytic capacity of canine monocytes by increasing TNF-α production[210].

A series of studies from the laboratory of Joshi and colleagues have suggested links between lung injury, impaired phagocytosis and Zn deficiency. In rats, stresses to the lung caused by alcohol[211] or virus resulted in significant decreases in alveolar macrophage (AM) GM-CSF receptor expression and phagocytosis of bacteria. These were accompanied by a significant decline in lung Zn concentrations. The authors proposed that the decline in Zn caused the defects in phagocytosis since the membrane-permeable Zn chelator Zn chelator, N,N,N',N'-tetrakis-(2-pyridyl-methyl) ethylenediamine (TPEN) impaired AM phagocytosis of bacteria *in vitro* while Zn supplements prevented both the decline in lung Zn and the impairment of phagocytosis *in vivo and in vitro*. Alcohol-fed rats had a 5-fold decrease in capacity to clear inoculated Klebsiella pneumonia from their lungs and this impairment of bacterial clearance, as well as increased oxidative stress in the lung, could be prevented by dietary Zn supplementation. The conclusion was that Zn is required to maintain AM bacterial phagocytosis, and that pulmonary Zn deficiency could be one of the mechanisms by which chronic HIV-1 infection and alcohol abuse impair immune function and predispose to pneumonia and other lung infections[211].

1.13.8 *Zn in the liver*

Although the body does not store Zn, like it does iron, the liver can act as a reservoir for Zn. In the acute phase response, as occurs in infection, trauma and inflammation, there is a transient shift of blood (plasma) Zn to the liver, mediated by cytokines (especially IL-6), corticosteroid hormones, subsequent up-regulation of Zn transporter protein ZIP14 in the membranes of hepatocytes and up-regulation of cytosolic metallothioneins (see Section 1.15.8). Zn is temporarily held in the hepatocytes as a complex with metallothionein[156]. The function of this shift of Zn to liver is still not properly understood but it may include cytoprotection of hepatocytes and removal of Zn from invading bacteria, thereby suppressing their growth. As in mammals and other eukaryotes, bacterial DNA polymerase and other nucleic acid-synthesizing enzymes are highly dependent on Zn[212].

1.14   Zn function in pancreatic islets and during *diabetes*

1.14.1 *Zn in the pancreatic islets*

Beta cells contain high concentrations of Zn and this metal is essential for insulin production; less is known about the other pancreatic islet cellular constituents. In the beta cell, labile Zn is critical for insulin maturation, synthesis and secretion. Labile Zn is concentrated in the insulin-containing granules, reaching mM concentrations[213].

1.14.2 *Zn and insulin synthesis and storage*

Zn acts in two stages in the insulin pathway of beta cells.

In the first Zn-dependent step, trimers of proinsulin monomers become held together by a Zn ion coordinated to the imidazaole groups of histidines in the B chain (B5 and two His B10 side chains at each Zn binding site. Two trimers associate to form the proinsulin hexamer. Therefore, each hexamer contains two Zn ions[214,215]. It is thought that the Zn-mediated formation of the proinsulin hexamer protects some portions of the polypeptide chain from proteolytic cleavage by burial within the subunit interfaces of a soluble hexamer, while leaving the C-peptide segment of proinsulin exposed on the hexamer surface to the action of the trypsin- and carboxypeptidase-like processing enzymes.

Secondly, within the mature secretory granules of the beta cell, crystallization of insulin is triggered by a large excess of Zn ions. It is thought that each crystal contains at least 12 Zn ions per hexamer. This crystallization is critical for storage of insulin in the beta cell and the additional Zn ions are provided by a pool of labile Zn ions in the granule, the uptake of which is under the control of granule membrane Zn transporter ZnT8 (described in a subsequent section of the thesis). It is estimated that granules contain > 3mM labile Zn ions, which is amongst the highest concentration of Zn ions in the body. Dysregulation of the zinc transporter ZnT8 results in a loss of granule Zn and impairment of insulin storage and release (see later)[216].

1.14.3   *Zn and other islet cells*

During glucose stimulation, Zn and insulin are co-secreted into the extracellular space where, the insulin structure (hexamers) breaks up into monomers of insulin and Zn ions are released. Whether the released Zn ions are reabsorbed by beta cells is not clear but they have been shown to exert an inhibitory action on glucagon secretion by neighbouring alpha cells[217]. Alpha cells also contain Zn but at lower levels than beta cells, and Zn is most likely involved in the maturation, synthesis and secretion of glucagon, although this is not yet proven[218].

1.15   *Zn binding proteins and Zn tranporters*

Free or labile Zn is toxic to cells in high concentrations. Therefore, it is tightly regulated. Labile intracellular Zn in cells and tissues is regulated by three classes of proteins: i) membrane zinc transporter proteins belonging to the SLC39a (ZIP) and SLC30a (ZnT) families, ii) certain metal binding proteins, especially metallothioneins, which act as Zn buffers[219] and iii) Zn-permeable membrane channels such as transient receptor potential cation channel.

1.15.1   **Zn transporter family** *SLC39a (ZIP)*

The ZIP transporters were first identified in yeast and plants. There are 14 members of the ZIP family reported to date (summarized in Table 1). It should be pointed out that some members of the family are included based on sequence similarity and actual Zn

44

transporting function has yet to be confirmed. Some ZIP transporters are ubiquitously expressed, whereas others are specific to certain tissues.

ZIP transporters are membrane proteins which mostly contain eight transmembrane domains with the N and C terminus on the cytoplasmic side of the membrane (Fig 1.11.). On the cytoplasmic side is a histidine-rich loop which is thought to be a major Zn-binding region, since Zn binds to the N in histidine (in addition to the S in cysteine)[220]. ZIP transporters act to *increase* cytosolic Zn, by either transporting Zn from the extracellular space or by releasing Zn ions into the cytosol from organelles where it is sequestered, such as ER and Golgi. The ZIPs may function either at the cell/tissue level in the various organ systems of the body or in the small intestine where they regulate absorption of Zn from the diet (e.g. ZIP4, see below). Some ZIP transporters (e.g. ZIP8 and ZIP14) not only transport Zn, but can also transport other metal ions such as iron and cadmium[221]. Both transcriptional and post translational expression of some of these proteins may be regulated by factors such as Zn availability, cytokines and hormones, thereby altering cytosolic Zn concentrations. Dysregulation of ZIP transporters have been associated with various diseases, including cancer[222].
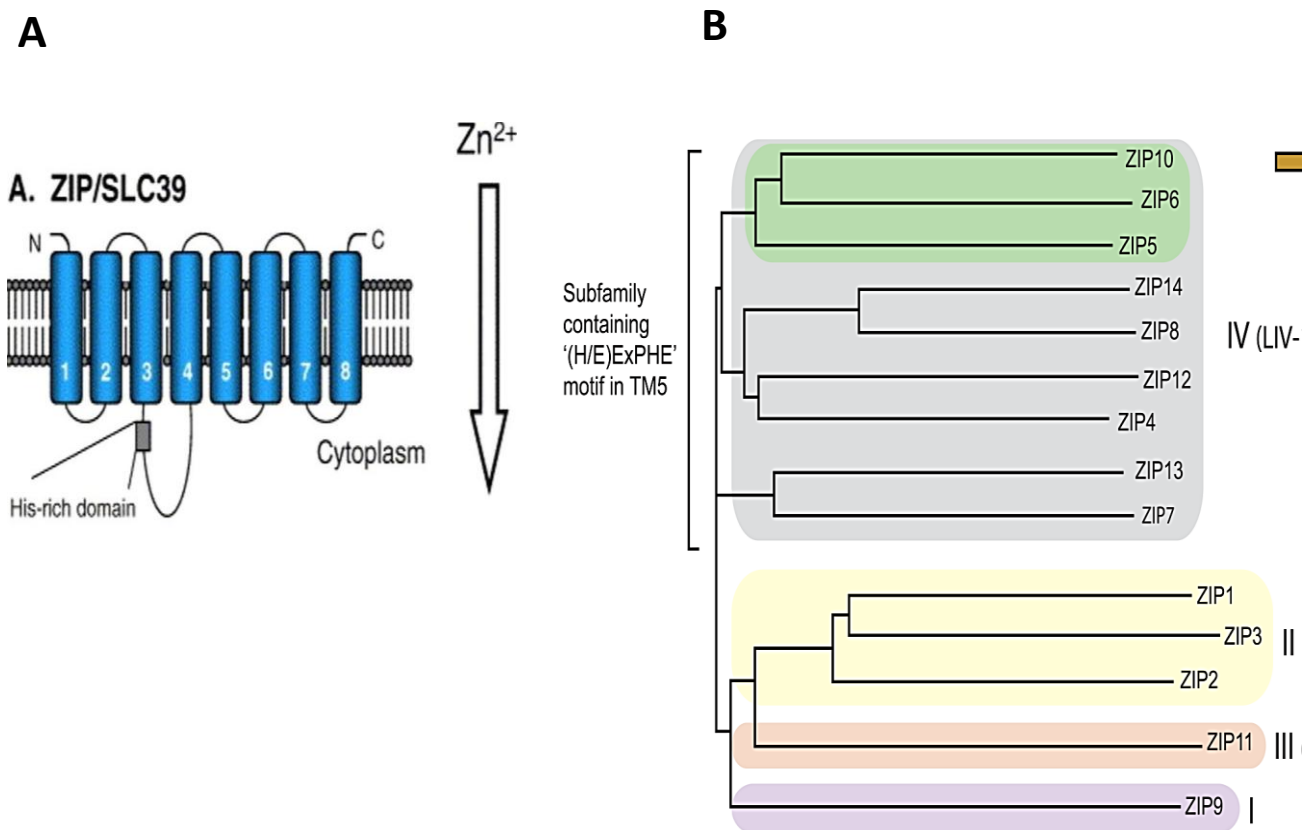
Figure 1.11 ZIP protein structure and phylogeny of Zn transporters

This figure shows (A) ZIP transporter protein containing eight transmembrane domains and the putative Zn-binding Histidine-rich domain (also potential metalloproteinase motif) which is usually found between transmembrane domains 3 and 4 on the cytoplasmic side. ZIP proteins are involved in transporting Zn from the extracellular fluid or organelles such as endoplasmic reticulum and Golgi into the cytoplasm[223]. (B) Phylogenetic tree of ZIP transporters, showing four subsets of ZIPs based on evolutionary relationships: ZIP9 (I), ZIP 1, 2 and 3 (II), ZIP11(III) and remaining ZIPs (IV) also known as LIV[224]. Figure was adapted from Schmitt-Ulms G et al

In the following paragraphs, two members of the ZIP family are discussed in more detail. These are ZIP4 and ZIP14 because they emerged in my studies to be of special interest in islet function and diabetes.

1.15.2   ZIP4

Mouse ZIP4 is located on chromosome 15 and human ZIP4 is on chromosome 1. Figure 1.12 A shows sequence similarities and conserved motifs between human and mouse ZIP4 protein in a region around a putative metalloprotease cleavage site (PALV) that is thought to be cleaved prior to endocytosis resulting in removal of the extracellular amino-terminal ectodomain. Figure 1.12 B shows that ZIP4 protein contains 8 transmembrane domains with N and C terminus located on the extracellular side. ZIP4 is a major intestinal Zn transporter involved in absorption of Zn. Normally, in the small intestine, ZIP4 is expressed in low levels[225,226]. ZIP4 is regulated by transcriptional and posttranscriptional mechanisms[227,228]. During Zn deficiency, ZIP4 message and protein are upregulated due to increase in the stability of the mRNA and protein[229]. Mutation of ZIP4 is responsible for causing Zn deficiency in the human genetic disorder acrodermatitis enteropathica. Children with this disease have lesions of the skin, and gastrointestinal tract, which can be reversed in Zn supplementation[230]. ZIP4 is also up-regulated in pancreatic tumours, where it may act to increase Zn required for growth and suppression of apoptosis[231].

A   mouse; 287 MAVYGLSEEAGVSPQAWAQLTPALVQQQLSGACSPYPTI 325
human; 277 MAAYGLSEQAGVTPEAWAQLSPALLQQQLSGACTSQSRP 315
** ***** *** * ***** *** *******

B
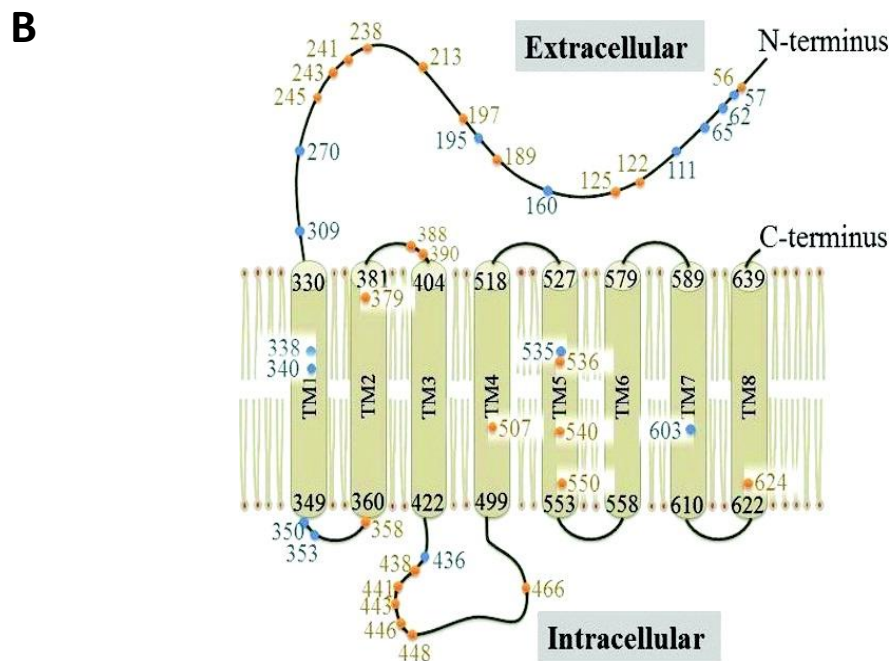
Figure 1.12 Structure of human and mouse ZIP4

The figure shows human and mouse ZIP4. (A) Alignment of the amino acid sequences of human and mouse ZIP4 in the region of the ectodomain near the predicted start of the first transmembrane domain showing the conservation of amino acids encompassing the potential metalloproteinase motif (PALV). Conserved amino acids are indicated by an asterisk. Figure from Kambe et al[232]. (B) ZIP4 Zn transporter has eight transmembrane (TM) domains with its N and C terminus in the extracellular fluid of the cell. The Zn binding domain is thought to be in the histidine rich loop between TM3 and TM4. Mutations of ZIP4 result in the autosomal recessive disease *acrodermatitis enteropathica*, leading to growth retardation, behavioral and neurological disturbances and diarrhea (all associated with severe systemic Zn deficiency). The coloured numbers

in the sequence of ZIP4 represent known mutations. Figure adapted from Antala et al[233].

1.15.3   ZIP14

The mouse ZIP14 gene is located on chromosome 14[234,235]. ZIP14 protein has 8 transmembrane regions containing a histidine rich region and the N and C termini, both of which are located in the extracellular space of the cell. ZIP14 is expressed in the plasma membrane of cells as a glycosylated protein where it is involved in the cellular uptake of Zn from the extracellular space (Figure 1.13). ZIP14 is strongly expressed in the liver, small intestine, pancreas, adipose tissue and kidney[236]. Both human and mouse ZIP14 exist as two isoforms of 489 amino acids formed by alternative splicing (diagonal shading indicates variable region of the isoforms). The significance of these isoforms is unclear but one study has shown a relationship to colorectal cancer[235]. Six single-nucleotide polymorphisms have been reported in the coding sequence of human Zip14 including two in the histidine-rich loop which might affect Zn binding and transport[237].

ZIP14 works through the G protein coupled receptor (GPCR). Knockdown of ZIP14 leads to decrease in cyclic adenosine monophosphate activity (cAMP) and increase in phosphodiesterase activity[238] ZIP14 protein is involved in growth of bones, liver growth and adipogenesis[239]. Like nutritionally Zn deficient mice, ZIP14 knockout mice have stunted growth[238].

Two properties of ZIP14, which are particularly relevant to macrophages, involve iron transport and inflammation. ZIP14 not only transports Zn but also iron (Fe), cadmium and manganese[240]. It may therefore be involved, along with divalent metal-ion transporter-1 (DMT-1), in normal iron uptake and homeostasis. It may also be a factor in iron overload toxicity in the liver, pancreas and the heart (primary sites for iron storage). During iron overload, the liver undergoes fibrosis, cirrhosis and liver cancer and in the pancreas it leads to beta cell apoptosis and diabetes[241]. Zip14 is expressed in membranes of hepatocytes and mediates uptake of non-transferin bound iron[242]. ZIP14 was significantly upregulated in the pancreas in iron overloaded rats[243]. and ZIP14 protein expression is known to be altered in hemochromatosis in type 2 diabetes. Liver macrophages (kuffer cells) release iron into the plasma maintaining iron homeostasis in the liver[244]. During inflammation, the release of iron is reduced. It is also known that

ZIP14 is expressed highly in the liver and, in animals treated with LPS, turpentine and IL-6[245]. ZIP14 is up-regulated in hepatocytes as part of the acute phase response and there are subsequent shifts of plasma iron and Zn to hepatocytes creating a state of hypoferemia and hypozincaemia[234,240,246-248].
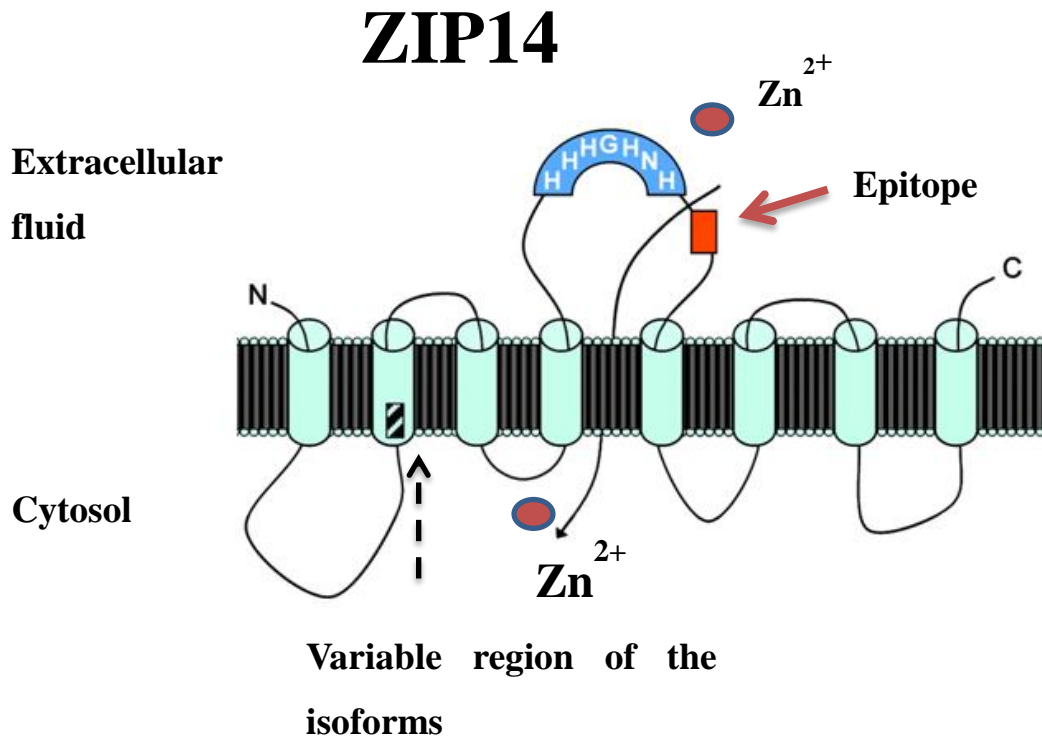
ZIP14

Figure 1.13 Structure of mouse ZIP14

The figure shows that ZIP14 has eight transmembrane domains, with, facing into the extracellular fluid of the cell, the N and C terminus and the histidine rich region. Note that this domain is on the cytoplasmic side in some other ZIPs (e.g. ZIP4). Both human and mouse ZIP14 exist as two isoforms of 489 amino acids formed by alternative splicing (diagonal shading indicates variable region of the isoforms). Figure adapted from Liuzzi et al

1.15.4   Zn transporter family *SLC30a (ZnT)*

ZnT Zn transporters have six transmembrane domains with N and C termini at the cytoplasmic side of the cell membrane. At least one ZnT transporters (ZnT1) transports Zn from cytoplasm across the plasma membrane to the extracellular space of the cell[249]. Other ZnTs (ZnT2-8) are expressed on membranes surrounding cytoplasmic organelles (e.g. Golgi) and sequester Zn from the cytosol into the organelles[250]. They may also transport other metals such as cobalt, cadmium, nickel, copper and mercuric ions[251]. Clues to the mechanism by which these transporters transport metal ions has come from studies with the Ecoli Zn transporter (ZnT-like) YiiP[252]. The x ray structure of YiiP was reported by Lu et al[253]. It was shown that this transporter is a homodimer, held together in a parallel orientation with four Zn ions at the interface of the cytoplasmic domains. The overall structure appears Y- shaped[253]. Later, Coudray et al investigated the molecular dynamics of YiiP transporter within a lipid bilayer using purified YiiP[252]. In the presence of Zn, there was a conformational change which involves the pivoting of the six transmembrane helixes from outward facing state to an inward facing state (Figure 1.14). This conformational change is thought to mediate membrane transfer of Zn.

Table 1.1 Lists the properties of ZIP type transporters

Transporter	Specificity	Localization in cells	Function	Transcriptional Regulation	Post-transcriptional	Disease Associations	Presence in Pancreas	Refs
ZIP1	Zn	Plasma membrane and intracellular vesicles	Active major transport of zinc into cells eg prostate cells	Cadmium induced up-regulation of ZIP1	Zip1 is ubiquitylated *in vivo*	In many prostate cancers SLC39A1 is silenced causing prostate cancer cells to be low in zinc. Neurodegeneration	Not in the pancreatic islets	Costello LC, Franklin RB 2006 Duffner Beattie 2006 Guo 2012 254
ZIP2	Zn, Fe	Plasma membrane	May be important in contact inhibition of normal epithelial cells Zinc uptake may be mediated by a Zn^{2+}-HCO_3^- symport mechanism.	Induced by Zinc and inhibited by Cu^{2+}, Co^{2+} and Mn^{2+} ions and not inhibited by Fe^{2+}.	Unknown	Loss of its expression may play a role in tumorigenesis		Zhang & Knutson 2012

ZIP3	Zn and other metals	Plasma membrane and lysosomes	Acts as a zinc-influx transporter	Up-regulated by Zn deficiency	No evidence but exists as a phosphoprotein	Neurodegeneration Glutamate excitoxicity	Expressed in the pancreatic islets not yet confirmed (pregnant mice).	Duffner Beattie 2006 Qian ey al 2011
ZIP4	Zn	Plasma membrane and lysosomes

Apical membrane of the intestine | Major dietary zinc transporter in the intestine | ZIP4 mRNA level increase in zinc deficient mice
ZIP4 mRNA is low in zinc replete conditions | Induced by zinc deficiency in Hepa cells and rapidly degraded in response to added zinc. | Mutated in acrodermatitis enteropathica

Pancreatic cancer and liver cancer | Expressed in the pancreas | Antala & Dempski 2012 Weaver BP 2007 Geiser 2012 |
| ZIP5 | Zn | Basolateral surface of enterocytes and plasma membrane | Cellular response to zinc starvation and role in polarised cells by carrying out serosal to mucosal zinc | | Translation is zinc-responsive. During zinc deficiency, Zip5 mRNA remains associated with polysomes, while the protein is internalized and degraded
Capable of being glycosylated but | Basolateral membrane of pancreatic acinar cells | | Weaver BP 2007 Wang et al 2004 Duffner Beattie 2004 |

56

			transport		function unknown		
ZIP6	Zn	Plasma membrane ER	Neuronal differentiation		Phosphoprotein and glycoprotein	Neuroblastoma, pancreatic cancer, prostate cancer and breast cancer	Marat 2008
ZIP7	Zn, Mn	Vesicles, ER and Golgi			Protein kinase CK2 dependant phosphorylation of ZIP7 leads to release of Zn2+ from intracellular stores, activation of tyrosine kinases and phosphorylation of AKT and ERK 1 and 2.	Breast cancer		Taylor 2012
ZIP8	Zn, Cd, Mn	Plasma membrane ,mitochondria and lysosomes	Multiple organogenesis and haematopoiesis in utero is critical in zinc-mediated cytoprotection in lung epithelia		phosphoprotein	Breast cancer, inflammation, Sepsis, Cadmium induced testicular necrosis and renal proximal tubule damage		Knoell 2012 Wang et al 2007
ZIP9	Zn	Trans-golgi			Glycoprotein			Thomas 2014

ZIP10	Zn	Plasma membrane	Zinc uptake across rat renal brush border membrane		Glycoprotein and phosphoprotein	Breast cancer		P. Kaler , R. Prasad 2007
ZIP11	Zn			Evidence at transcript level	unknown			Martin et al 2013
ZIP12	Zn				Glycoprotein	Mutation in chromosome 10p increases susceptibility to Schizophrenia		Dean Brian 2009
ZIP13	Zn	Golgi and intracellular vesicles			homo-dimerization	The Ehlers-Danlos syndrome (EDS) is a group of genetic disorders affecting connective tissues.		Fukada 2008 Bin 2011
ZIP14	Zn, Fe, Cd and Mn	Plasma membrane	Possible regulation of ZnT8 and ZIP10 shown by ZIP14 knockout study	IL-6, TNF-α, LPS	Glycosylation pH dependant iron transport	Colorectal cancer, Asthma and inflammation		Zhang & Knutson 2012 Liuzzi 2005 Tolunay Beker Aydemir 2012

Table 1.2: Lists the properties of ZnT type transporters

Transporter	Specificity	Localization in cells	Function	Transcriptional Regulation	Post-translational	Disease Associations	Presence in Pancreas	Refs
ZnT1	Cd and Zn	Plasma membrane	Zinc efflux and intestinal serosal zinc transport to portal blood supply	mRNA upregulated by zinc supplements and glucocorticoids	Glycosylation	Embryonic lethal	Expressed in the pancreas and pancreatic islet	Robert J Cousins 1998
ZnT2	Zn	Endosomal lysosomal/secretory vesicle, mitochondria and plasma membrane	ZnT2 plays a major role in Zn secretion from the mammary gland into milk	Stat5 and glucocorticoid receptor and MTF-1 and Zinc upregulates ZnT2	Glycosylation	Lactating women with a mutation in the gene secrete ~75% less Zn into their milk	Expressed in the pancreas	Guo et al 2010 Seo et al 2010 Shannon L Kelleher et al 2003
ZnT3	Zn	Synaptic vesicles	Accumulation of zinc in synaptic vesicles and role in olfactory response	Regulated by glucose and zinc in beta cell line	Phosphorylation	Seizures, learning deficit, memory loss Alzheimer's Dementia	Low expression in pancreas	Smidt 2009 Zheng W 2010
ZnT4	Zn	Secretory vesicles, plasma membrane and cytoplasm	Transports zinc to apical region of airways Secretion of zinc into breast milk and gut differentiation	Regulated by zinc supplements	Unknown	Lethal milk and Asthma		Chaira Murgia 2011 Huang 1997

ZnT5	Zn	Secretory vesicles, Golgi and plasma membrane	Transports zinc into Golgi and immature insulin vesicles Incorporation of zinc into alkaline phosphatase	Upregulated by Zn depletion	Phosphorylation	Bone abnormalities and heart failure	Expressed in beta cells	Fukunaka A 2011 Sheline et al 2012 Devergnas et al 2004
ZnT6	Zn	Secretory vesicles and trans golgi	Imports zinc into the trans golgi network incorporates zinc into alkaline phosphatase		Phosphorylation Glycosylation	Alzheimer's disease	Expressed in the pancreas	Beyer N 2012 Huang 2002
ZnT7	Zn	Secretory vesicles and Golgi	Imports zinc into the trans golgi and also incorporates zinc into alkaline phosphatase	Upregulated by Zn depletion	Phosphorylation Glycosylation	Prostate cancer, diet induced diabetes	Expressed in the pancreas	Huang et al 2010 Suzuki 2005 Catherine P. Kirschke 2003 Devergnas et al 2004
ZnT8	Zn	Secretory granule	Incorporates zinc into mature granules of insulin		Methylation and phosphorylation	Type 1 (autoantigens)and type 2 (SNP) Diabetes	Expressed in the pancreas	Lemaire 2009 Chiara Murgia et al 2009

								Wijesekara -2010
ZnT9	Zn	Nucleus and cytoplasm	Plays a role in the p160 coactivator signalling pathway and in the transcriptional activation of Wnt responsive genes		Unknown	Not known		Sim 1999
ZnT10	Zn	Unknown	Zinc efflux Foetal development		Unknown	Not known		Cousins 2009
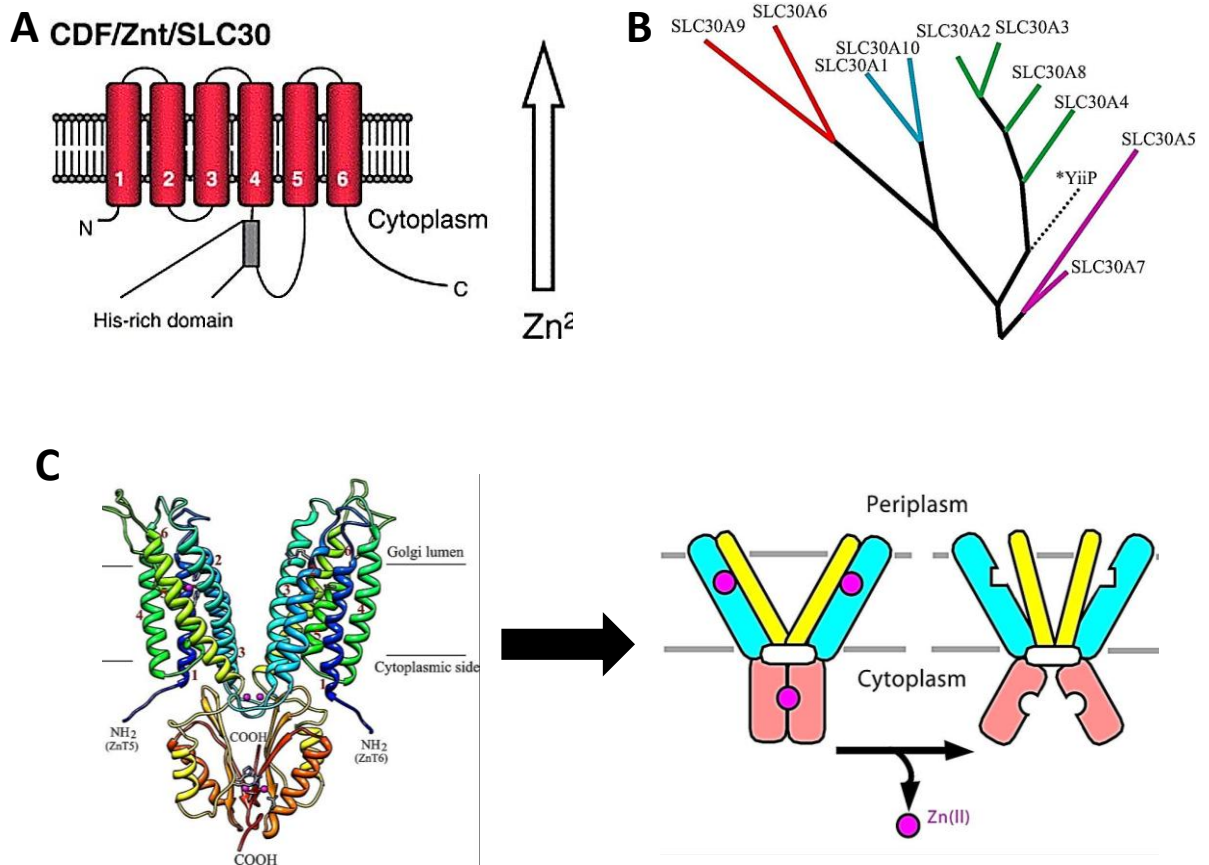
Figure 1.14 ZnT protein structure, phylogeny and the YiiP transporter mechanism

The figure shows (A) SLC30A (ZnT) transporters containing six transmembrane domains. ZnT transporters are involved in transporting Zn from the cytoplasm either into organelles or outside the cell. They have their N and C terminus and a histidine rich loop domain in the cytoplasm of the cell. Figure adapted from Krane et al[223]. (B) Phylogenic tree of ZnT family members which shows close relationships between the islet relevant ZnT8 transporter and ZnT2, 3 and 4. Figure adapted from Huang et al[255] as well as the bacterial Zn transporter YiiP. Figure adapted from Lu et al[256]. (C) YiiP transporter is the only Zn transporter member of which the mechanism is now partially elucidated of how Zn ions are transported and may serve as a model of Zn transport by the mammalian ZnT transporters. In the presence of Zn, there is a conformational change which involves the pivoting of the six transmembrane helixes such that the Zn transport sites are expressed on the periplasmic side of the membrane (between bacterial cell wall and plasma membrane) with an outward facing state when saturated with Zn, enabling the removal of Zn from the cytoplasm. Figure adapted from website https://www.bnl.gov/newsroom/news.php?a=11005

1.15.5 ZnT7

The ZnT7 gene is located on chromosome 1 in humans and chromosome 3 in mice. It encodes a 42kDa membrane protein that is abundant in the mouse nervous system and the small interstine[257,258]. It is also expressed in many other tissues and localizes to the Golgi apparatus where it likely mediates uptake of cytoplasmic Zn into the Golgi apparatus for incorporation of Zn into newly synthesised Zn metalloproteins. ZnT7 KO mice had systemic Zn deficiency and associated symptoms such as growth retardation that could not be corrected by Zn supplements[258]. ZnT7 KO mice also showed decreased adiposity associated with low circulating leptin levels[258]. They were also more susceptible to high fat diet induced postprandial hyperglycemia, glucose intolerance and insulin resistance. Huang and colleagues reported that ZnT7 protein is expressed predominantly in pancreatic islet beta cells of mice; overexpression of ZnT7 in beta cells increased the total insulin content (mRNA and protein) as well as a 2-fold increase in basal insulin secretion confirming an important role for Zn in insulin synthesis and secretion. As the insulin promoter contains a metal responsive element, it was suggested that ZnT7 and Zn may be acting via this site[259].

1.15.6 ZnT8

The Zn transporter ZnT8 is involved in the pathogenesis of type 1 and 2 diabetes[260-266]. ZnT8 is located in the membrane of the insulin secretory vesicles. It is the most abundantly expressed ZnT (gene or protein) in the pancreatic islets. Chimienti and colleagues were the first to report that overexpression of ZnT8 in beta cells increased insulin content and also increased insulin secretion in response to glucose[267]. When ZnT8 was knocked down, this capacity was reduced. After investigating the role of ZnT8 in cell lines, studies investigated the role of ZnT8 by global knockout in mice. ZnT8 knockout mice had fewer dense core vesicles in insulin producing beta cells and impaired glucose homeostasis[268]. Knockdown of ZnT8 in beta cells may decrease the availability of Zn into the insulin vesicles to form insulin hexamers and crystals. Knockdown of ZnT8 in alpha cells, did not affect the insulin content or glucose metabolism[268]

ZnT8 is also a major target of humoral autoimmunity in Type 1 diabetes[263,269-271]. Achenbach and colleagues[263] were first to report humoral autoimmune responses against ZnT8 in a large cohort of children with a first-degree family history of Type 1 diabetes. They also reported that the COOH terminal in the ZnT8A was an epitope for Type 1 diabetes rather than the NH2-terminal of this protein[270]. ZnT8A-COOH-positive children who were homozygous for the ZnT8A8 SNP rs13266634 progressed faster to diabetes than those who were heterozygous[263]. Another study investigated two major isoforms of ZnT8, ZnT8-Arginine (ZnT8R) and ZnT8-Tryptophan (ZnT8W) on Type 1 diabetes patient cohorts with different age distributions at onset. Most of the Type 1 diabetic patients tested positive for ZnT8Ab to both isoforms; however, ZnT8 autoantibiody titres were significantly higher in the younger age group[272].

In Type 2 diabetes, genetic polymorphisms for ZnT8 influence the level of expression and function of the protein[273,274]. Population studies revealed a strong association with type 2 diabetes of a nonsynonymous SNP RS13266634[264],arg325Trp (C>T) variant in ZnTA8[275-277]. The C allele variant was suggested to be the risk allele for type 2 diabetes[278-282] . Other studies[267] also reported that variations in ZnTA8 may affect Zn accumulation in insulin granules and hence influence insulin stability and insulin trafficking. The R325W mutation in ZnTA8 is associated with Type 2 diabetes as well as decreased first phase insulin secretion in non-diabetic subjects bearing at least one copy of the risk allele[283,284].

The handling of immunosuppressive drugs necessary for islet transplantation is also influenced by ZnT8 polymorphisms. The calcineurin inhibitor cyclosporine (CsA) did not suppress glucose-stimulated insulin secretion in islets when ZnT8 W325 variant was expressed in insulinoma cells, whereas cells expressing ZnT8 R325 were suppressed by these drugs. This indicates that the structure of the ZnT8 variant W325 is important for the protection against post transplant diabetes[261]. Kang and colleagues[285] reported that a polymorphism in ZnTA8 confers resistance against postransplantation diabetes mellitus in renal transplant recipients. In addition Kim and colleagues[261] reported that the ZnT8 R325 expressed in the insulinoma1E cells variant showed, reduced insulin content and secretion when treated with cyclosporine A (CsA). When

ZnT8 variant W325 expression was treated with CsA, the insulin content and secretion were not affected. This indicates that by altering ZnT8 structure such as in the W325 variant, there is protection of cells from immunosuppressive drug toxicity. Studies in islet transplantation have not yet been performed to examine the effect of these polymorphisms on islet function post transplant and would require extensive multi-centre collaborative effort.

1.15.7   *ZnT7 versus ZnT8*

The differences in the cellular localization between ZnT7 and ZnT8 suggest that the two Zn transporters may play different roles in the regulation of insulin metabolism in the beta cell. Some evidence to support this concept has come from two separate overexpression studies in two different cell lines. Chimienti et al overexpressed ZnT8 in INS-1E cells[267], while Huang et al overexpressed ZnT7 in RIN5Mf beta cells[259].ZnT7 overexpression in beta cells did not increase total cell zinc (as measured by atomic absorption spectrometry) whereas overexpression of ZnT8 increased total cell Zn in both Zn supplemented and non supplemented conditions. In line with the above, ZnT7 overexpression in beta cells significantly increased total cellular insulin content and the basal insulin secretion while overexpression of ZnT8 in beta cells showed no effects on cellular insulin content and the basal insulin secretion. Furthermore, ZnT7 overexpression did not augment glucose induced insulin secretion whereas ZnT8 overexpression enhanced glucose induced insulin secretion. The authors proposed that ZnT7 is involved in regulation of insulin biosynthesis while ZnT8 plays a role in regulation of insulin maturation/storage in the beta cell. However, this needs to be confirmed in a single cell line because there may be differences between the two beta cell lines including such things as glucose responsiveness. The relative role of ZnT7 and ZnT8 in insulin synthesis and storage is discussed further in chapter 7.
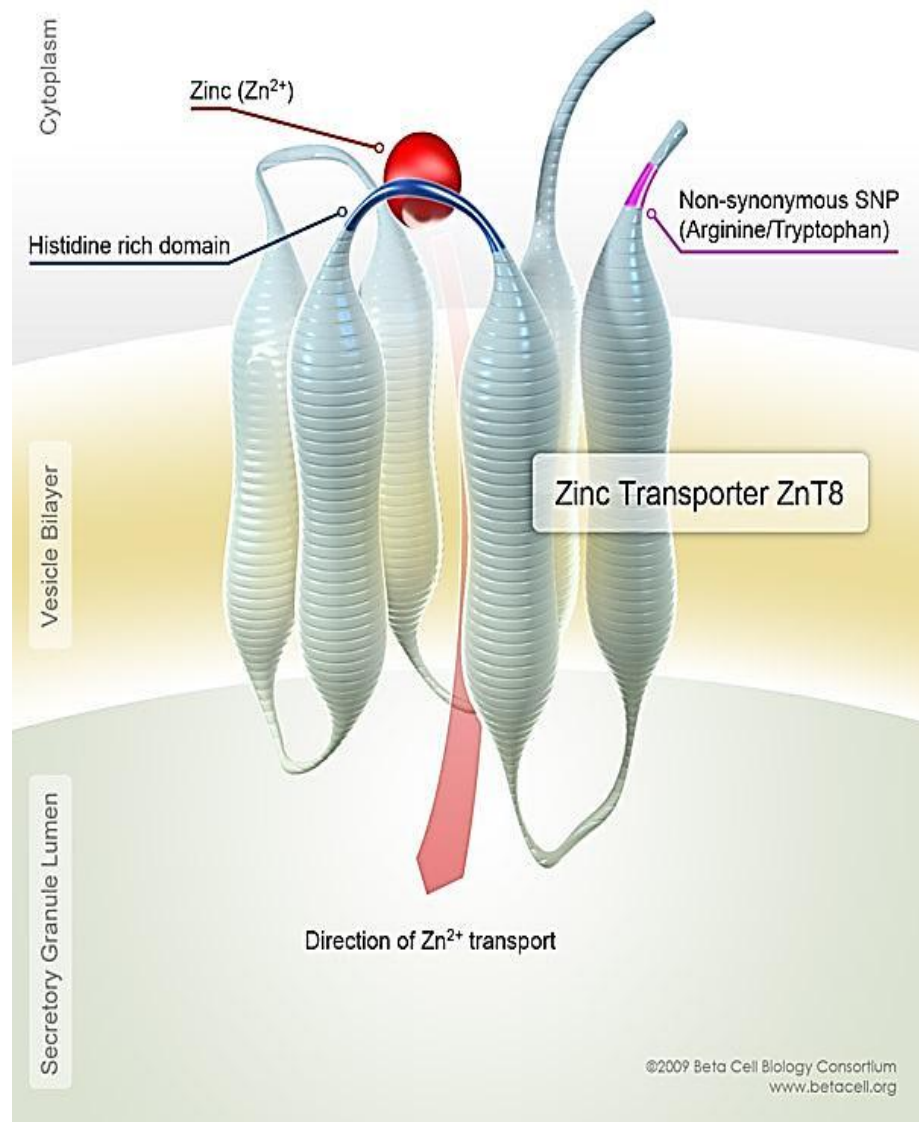
Figure 1.15 Structure of the secretory granule membrane Zn transporter ZnT8

ZnT8 has six transmembrane domains and a putative Zn binding domain containing a histidine rich loop between domains 4 and 5 in the cytoplasm of the cell. The figure also shows the non-synonomous single nucleotide polymorphism (SNP) at amino acid 325 which changes arginine to tryptophan. This is associated with increased risk of type 1 and 2 diabetes. Figure adapted from website

http://www.betacell.org/content/articleview/article_id/234/page/2/glossary/0/.

1.15.8   Metallothioneins

Metallothioneins are cysteine rich proteins of low molecular weight 6 to 10 kDa in size, which play an important role in Zn homeostasis[286]. Metallothionein proteins were first discovered as cadmium- binding proteins derived from horse kidney[287]. In mammals, 4 subtypes are found (MT1-4); MT1-2 isoforms are ubiquitously expressed in many cell types, MT-3 is expressed highly in the brain and in the male reproductive organs and MT-4 is expressed in the stratified tissues[288]. MT1 and 2 are known to be inducible by glucocorticoids, cytokines, reactive oxygen species and metal ions such as cadmium and Zn whereas MT3 and MT4 are not induced by these compounds[289]. Metallothioneins are soluble cytosolic proteins that both transport Zn intracellularly, including from cytoplasm to nucleus as well as buffering cytosolic Zn, as free Zn is toxic to cells. Transportation of Zn into the nucleus is known to be important in controlling transcription of many genes and also cell differentiation. Zn-metallothionein complex is also an antioxidant, which scavenges reactive oxygen species such as nitric oxide, superoxide and hydroxyl radicals[286].

1.15.9   Metallothionein in islets

Immunocytochemical staining shows that the expression of metallothionein corresponds to the levels of labile Zn (anti-metallothionein antibody) in the pancreatic islets of humans[290]. Metallothionein is involved in the zinc homeostasis and metabolism in pancreatic islets. Metallothionein may also modulate pancreatic hormone secretion but this is not proven. Metallothionein subtypes MT1 and MT2 are abundant in the pancreatic islets[291]. In rodent pancreatic beta cell line (MIN6), MT2 expression is higher than MT1 expression[292]. There was significant reduction of both MT1 and MT2 when beta cells were treated with high glucose. Transgenic mice (overexpression of metallothionein) had significantly reduced hyperglycaemia and also decreased islet cell death in response to treatment with STZ compared to control mice treated with STZ[293]. Thus, metallothionein may play a protective role in islet cell function, protecting them from beta cell death as well as an important role in storing Zn.

1.15.10 *TRPM3 and other Zn channels*

Transient receptor potential channels (TRPM) are cation influx channels, involved in vital roles in the body including metal homeostasis and tumorigenesis[294]. TPRM3 has six transmembrane domains including a pore domain between the fifth and six transmembrane segments with both amino and carboxy termini located at the cytosolic side. It has been proposed that, in depolarizing conditions, TPRM3 is one of the major channels transporting both calcium and Zn into the beta cells. Insulin secretion occurs during depolarisation of beta cells when the blood glucose levels are elevated in the plasma. Depolarisation occurs in the nerve ending in the beta cells where TPRM3 channels are activated leading to the activation of voltage gated calcium channels leading to further influx of both calcium and Zn through these channels[295,296].

PDLIM7 is a scaffolding protein containing PDZ and LIM domains. Hogstrand et al[297] (unpublished), found that ZnT8 interacts with PDLIM7. If confirmed, this would be an exciting finding, linking a membrane Zn transporter with a protein involved in in cellular migration, signal transduction, differentiation, heart development and oncogenesis. It would also be interesting from the point of view of how Zn is incorporated into insulin within the granules as well as for diabetes, if mutations or SNPs occur within the PDLIM7 gene.

1.16 *Transcriptional and post translational regulation of Zn transporters in the body and the pancreas*

Although incompletely understood, regulation of Zn transporters is complex and acts through various mechanisms including transcriptional and post-transcriptional. The posttranscriptional can include translational stability, phosphorylation, ubiquitination and trafficking between the plasma membrane and intracellular organelles such as mitochondria and Golgi apparatus. The following paragraph describes some of these mechanisms for each of the transporters. There may be species differences of some of these regulations and functions of the transporters which need further investigations.

1.16.1   ZnT1 and ZnT2

A major mechanism for the regulation of ZnT1 and ZnT2 involves transcriptional control via metal transcription factor 1 (MTF-1). Zn binds to MTF1 thereby activating the metal response elements (MREs) 5'-TGCRCNC-'3, these proteins increase or decrease the production of proteins according to Zn availability, regulating intracellular Zn[298-300]. Another mechanism for the control of ZnT1 and ZnT2 is via Zn dependent trafficking between plasma membrane and ER. ZnT1 is mainly found in the plasma membrane and involved in efflux of excess Zn out of the cell but trafficks to the ER depending on cellular Zn levels M[301]. ZnT2 behaves in the opposite manner since it is mainly found on the intracellular vesicles and accumulates high concentrations of Zn in the endosomal compartment. It is also involved in the uptake of Zn in the mitochondria[302]. Murgia et al have shown Zn and ZnT4 to move from the trans-Golgi network and cytoplasmic vesicles to the plasma membrane depending on concentrations of Zn in rat kidney cells[303]. Huang et al have shown similar movements of ZnT6[304].

1.16.2   ZnT5 and ZnT7

ZnT5 and ZnT7 are expressed in the Golgi and immature vesicles and mediate the uptake of Zn into these compartments. One function of ZnT5 is to regulate the translocation of protein kinase C to the plasma membrane as part of the mechanism by which NF-Kb leads to cytokine production in mast cells. The mRNA expression of ZnT5 and ZnT7 was shown to be induced by Zn deficiency in Hela cells to maintain adequate levels of Zn in the Golgi in vesicles[306].

1.16.3   ZIP1 and ZIP3

ZIP1 localises to vesicles or plasma membrane under the influence of Zn concentration[307]. In human prostate cancer cells, ZIP1 was regulated by testosterone and prolactin to increase intracellular Zn for growth[308]. In mouse kidney cells, under Zn deficient conditions ZIP1 and ZIP3 were localised to the plasma membrane, whereas when Zn levels were normal they were found in intracellular organelles and regulated post-translationally[309].

1.16.4   ZIP4

ZIP4 is controlled at both transcriptional and post-translational levels. Firstly, Zn deficiency increased transcription of mouse ZIP4 mRNA via transcriptional stimulation of MTF-1 and MRE[310-312]. Secondly, under the conditions of Zn excess, there was decreased stability of ZIP4 mRNA and ZIP4 protein. The latter was subject to ubiquitination and degradation by proteasome and lysosomes[311,313]. In addition, mouse ZIP4 has been shown to traffic between cytoplasmic vesicles in the perinuclear region and plasma membrane according to intracellular availability. Thus Zn depletion by TPEN in HEK293 cells resulted in movement of ZIP4 to the plasma membrane in order to bring more Zn into the cells[314].

1.16.5   ZIP5

ZIP5 is interesting because it is regulated at the translational level. In Zn deficiency, ZIP5 mRNA remains bound to polysomes and not translated; this has been known as a translational stall mechanism[311]. In addition to the translational regulation, the trafficking of ZIP5 to the basolateral membranes is also regulated by the levels of Zn.

1.16.6   ZIP6

ZIP6 is involved in the STAT3 signalling pathway. STAT3 activates ZIP6 to increase cytosolic Zn leading to translocation of Zn finger transcription factor Snail to the nucleus. The authors hypothesised that via Zn transporters intracellular Zn affects the activation status of key intracellular signalling molecules, such as Snail[315]. ZIP6 is regulated at the transcriptional level in response to oestrogen levels[316].

1.16.7   ZIP8 and ZIP14

ZIP8 and ZIP14 are related both phylogenetically (figure 1.11) and by their involvement with inflammation. ZIP8 is upregulated by TNF-α in lung epithelial cells while ZIP14 is upregulated by IL-6, TNF-α and LPS in hepatocytes and macrophages[221,245,317,318]. In response to hormones released from pituitary gland and liver, ZIP14 increases intracellular Zn which inhibits phosphodiesterase and thereby facilitates G protein-coupled receptor (*GPCR*) signalling in growth and endocrine function.

1.16.8   ZIP13

ZIP13 has been recently shown to be important in the nuclear translocation of Smads in signalling via the (BMP/TGF-β) pathway, although little is known about how ZIP13 is regulated (Figure 1.16).
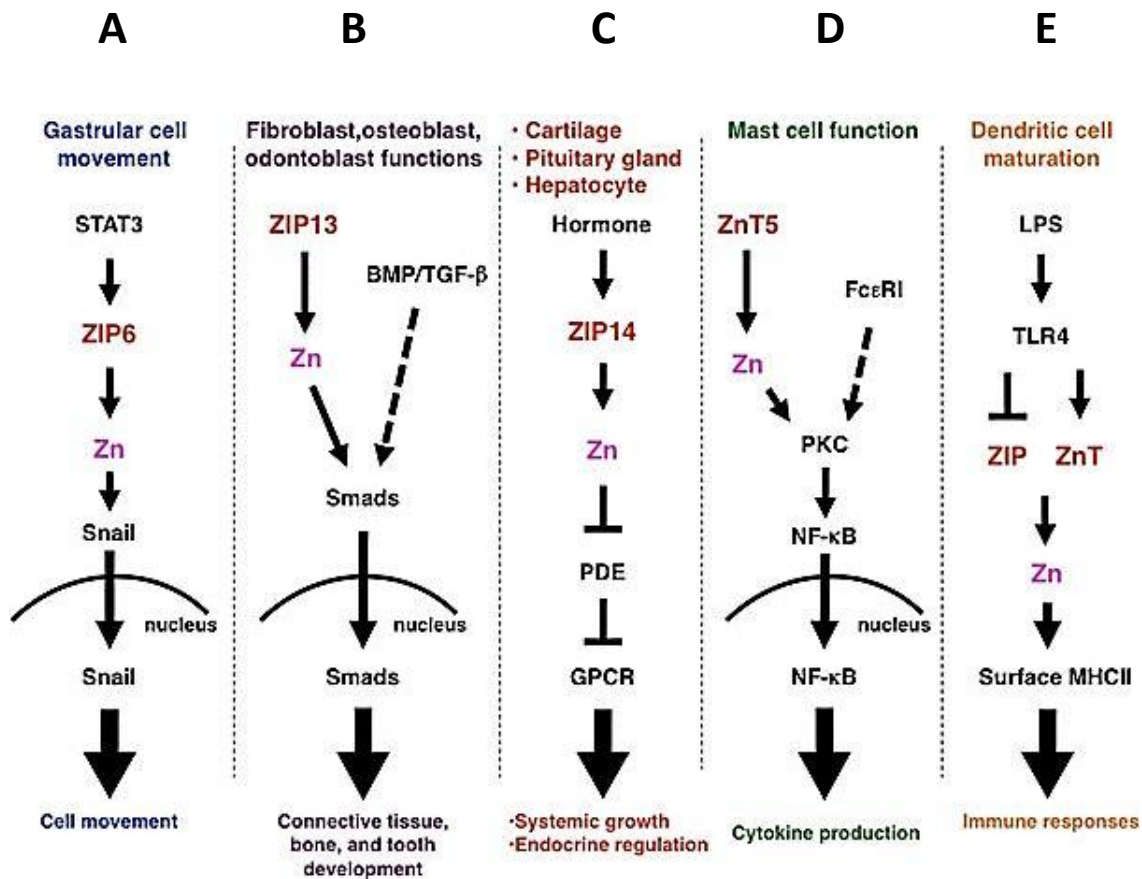
Figure 1.16 Zn transporter regulation and their role in intracellular signalling

The figure shows roles of various Zn transporters in intracellular signalling (A) ZIP6 is transcriptionally induced by STAT3 and is activated by N-terminal cleavage resulting in plasma membrane translocation and Zn influx that, in turn, leads to Snail movement to the nucleus and transcriptional repression of E-cadherin causing cell rounding and detachment[319] (B) ZIP13 results in Zn influx which interacts with the bone morphogenic protein (BMP) and transforming growth factor beta pathways that cause nuclear translocation of Smads and gene expression that mediates connective tissue, bone and tooth development[320] (C) ZIP14 mediates Zn influx and inhibition of phosphodiesterase (PDE) and G coupled protein receptor (GPCR) involved in systemic growth and endocrine regulation[238] (D) ZnT5 acts on the Fc epsilon receptor controlled protein kinase C (PKC) pathway that modulates NF kappa beta nuclear translocation, gene expression and downstream cytokine production in mast cells[321] and (E) ZIP inhibition and ZnT stimulation induced by lipopolysaccharide (via toll-like receptor TLR4) involved in dendritic cell maturation[305,322].

1.17   Thesis hypotheses and specific aims:

The major goal of this thesis was to investigate the role of Zn and Zn transporters in the pathogenesis of normal and type 2 diabetic pancreatic islets, using the db/db mouse model. There is limited information available on the physiological role of Zn and Zn transporters in these mice.

The following hypotheses are proposed.

1) There is an early loss of Zn in the development of type 2 diabetes which contributes to the transition to established diabetes;

2) The loss of Zn causes a block in insulin maturation resulting in impaired glucose responsiveness, hyperglycemia and decline in beta cell function;

3) This loss of Zn is due to alterations in Zn transporter proteins and metallothionein at the gene and protein level. Specifically changes in the organelle Zn transporters ZnT7 and ZnT8 result in the block in insulin maturation, while dysregulation of the inflammation related plasma membrane Zn transporter protein ZIP14 contributes to inflammation that results in further beta cell dysfunction.

The overall Aim of the study was to determine whether there are changes in pancreatic Zn and Zn transporters in a mouse model of type 2 diabetes at early, medium and late stages of diabetes:

Aim 1: To examine the development of diabetes in these mice from 4 to 18 wk of age and to confirm the diabetic status of the db/db mice by a number of parameters including hyperinsulinemia, hyperglycemia and impaired glucose tolerance

Aim 2: To determine whether there are changes in the total and labile Zn pools and metallothionein content of the pancreatic islets.

Aim 3: To determine whether the Zn transporters are altered at the gene level.

Aim 4: To determine whether the Zn transporters are altered at the protein level (expression, islet cell specificity and subcellular distribution).

CHAPTER 2 Materials and Methods

2.1 Animals

2.1.1 db/db mice:

Male mutant inbred mice homozygous for the diabetes spontaneous mutation (Lepr^{db}) and known as B6.BKS(D)-Leprdb/J strain (originally derived from Jackson Labs), were purchased from Animal Resource Centre Perth (ARC). The background strain was C57BL/6J as routinely recommended as controls for the B6.BKS(D)-Leprdb/J strain. Mice were purchased at three ages: 4-5 weeks (designated in this thesis as 4 wk, early diabetes), 10-11 weeks (designated 10 wk, established diabetes) and 14-15 or 17-18 weeks (designated 14wk or 18wk, respectively, chronic diabetes).

Blood glucose measurements were provided for each mouse by ARC Perth and were later confirmed in this study. Upon arrival they were housed in separate plastic cages according to their age. Before culling, the 4 wk mice were allowed to settle for 3 days to overcome any stress from air freight. The 14 and 18 wk animals were purchased at the age of 8 weeks and were housed till they reached the ages of 14 and 18 weeks. During this period, the mice were maintained in the (pathogen free) animal house at 22°C and subject to a 14h light / 10 h dark cycle and had access to food and water *ad libitum*.

The Animal Care and Ethics Committees of the Institute of Medical and Veterinary Science (IMVS) (project no 141a10) and the University of Adelaide (project code M-2010-166A) approved all animal related protocols. All animal procedures conformed to the guidelines of the National Health and Medical Research Council of Australia.

2.1.2 Harvest of db/db mice organs:

Control and db/db mice were weighed and then anaesthetized (isoflurane) and blood was collected from the heart using a 30 gauge needle. Up to 0.7ml of blood was drawn and injected into a 0.8ml LH Lithium Heparin tube (Mini spin, Greiner Bio-One, Arlington Heights, United States) which was immediately centrifuged at 8000 x g for

10 minutes to obtain the plasma and stored in -80 degree Celsius. Animals were then euthanized by CO_2 aspiration and cervical dislocation.

2.1.3   Glucose testing and intraperitioneal glucose tolerance test

Blood glucose was determined by tail vein bleeding and a drop of blood was placed in a glucose electrode and analysed using a glucometer (Optium Xceed, Victoria, Australia). Urine was collected from mice in metabolic cages and urine glucose was measured using urine glucose strips (Clinisticks, UK). Glycosuria was indicated by a colour change from yellow to dark green (at concentrations of glucose greater that 55mmol/L).

For glucose tolerance tests, animals were fasted overnight and then a dose of glucose (2 g/kg body weight) was administered *via* an intraperitoneal injection at. Blood samples were collected from a small cut at the tip of the tail at 0, 15, 30, 60, 90 and 120, 240 and 360 min after the glucose load.

2.2 Molecular techniques:

2.2.1   Laser capture microdissection:

For microdissection, pancreas tissues were rapidly excised, embedded in Optimal cutting temperature medium (OCT) and frozen slowly with isopentane and then in liquid nitrogen before being stored at -80°C until use. Whilst still frozen, tissues embedded in OCT were cut into 4 serial sections with a thickness of 15μm and sections were mounted onto poly-L-lysine (POL)-coated membrane slides and immediately fixed in 100% Ethanol (EtOH) for 10 mins at room temperature. The slides were treated with 100% EtOH for 30 sec and were immediately dehydrated and stained with sequential additions of 95% EtOH, 75% EtOH, 70% EtOH, 4% cresyl violet in 70% EtOH, 70% EtOH, 95% EtOH, 100% rinsed twice for 30 seconds each. The membrane slides were then stored at -80°C in air tight tubes containing silica gel. The slide was loaded onto the stage of the Leica AS LMD (North Ryde, Australia) system. The islets from the pancreas tissue were microdissected onto a cap (0.2ml microfuge tube) containing 20μL RLT buffer and were stored at -80°C ready for RNA extraction. Islets were extracted using RNA aqueous micro kit (Ambion, Mulgrave Victoria, Australia).

77

2.2.2   *RNA extraction:*

All tissues were rapidly excised, embedded in OCT and frozen slowly with isopentane and then in liquid nitrogen before storage at -80°C until use. The frozen tissue was placed in the cryostat and 15 shavings (10uM) of pancreas of each sample were collected in 800μl Trizol and then continuously pipetted until the tissue was fully homogenised. Tubes were then vortexed and stored at $-80°$C until assayed. The samples were then thawed and centrifuged at 12,000g for 10 mins at 4°C. 100μl of chloroform was added to the sample and vortexed. The sample was then incubated for 2 mins at room temperature. The samples were centrifuged at 12,000g for 15 min at 4°C. The upper aqueous phase layer containing the RNA was transferred to a tube containing an equal volume of 70% ethanol. If the sample volume exceeded 200μL, then successive aliquots were centrifuged in the same RNeasy spin column and the flow through was discarded with each centrifugation. The sample was then centrifuged for 15s at 8000 g and the flow through was discarded. If the volume exceeded 700 μl, successive aliquots of the sample were centrifuged in the same RNeasy spin column and the flow-through was discarded after each centrifugation. 350 μl of Buffer RW1 was then added to the RNeasy spin column and centrifuged for 15 s at 8000 g. 80 μl of Dnase 1 mixture (70 μl of RDD buffer and 10 μl of Dnase 1), RNase free DNase set, (Qiagen, Cadstone, Victoria, Australia) was added to the membrane of the spin column for 10 min at room temperature. 350 μl of Buffer RW1 was then added to the RNeasy spin column and centrifuged for 15 s at 8000 x g to wash the spin column membrane. 500 μl of Buffer RPE was added to the RNeasy spin column and centrifuged for 15 s at 8000 x g to wash the spin column membrane. 500 μl of Buffer RPE was then added to the RNeasy spin column and centrifuged for 2 min at 8000 x g to wash the spin column membrane. The RNeasy spin column was placed in a new 1.5 ml collection tube and 30μl of RNase-free water was added directly to the spin column membrane and centrifuged for 1 min at 8000 x g to elute the RNA. This step was repeated to obtain a higher yield of RNA (RNA easy mini kit protocol, Qiagen, Chadstone Centre, Victoria, Australia).

2.2.3   *RNA quantification*

RNA was quantified using Experion RNA StdSens kit (Biorad, Galdesville, New South Wales, Australia). The experion chip loader was washed with 800μL of experion cleaner for 2 min and washed with 800μL of Diethylpyrocarbonate (DEPC) treated water twice. 1μL of RNA and RNA ladder (Biorad, Galdesville, New South Wales, Australia) were denatured for 2 min at 55°C and then kept on ice for 5 min. The experion chip was primed using 9μL of gel stain (1μL of experion stain and 65μL of filtered gel). Then another 9μL of gel stain was added to the chip. 1μL of the denatured RNA and 5μL of loading buffer were added to the chip. The experion chip was then added to the experion machine (Automated Electrophoresis System, Biorad, 100–240 V) and the RNA quality and quantity were analysed. RNA above 5 (yellow) and able to show the 18S and 28S band, was considered to be of good RNA quality for quantitative real time PCR analysis.

2.2.4   *Reverse transcription PCR of RNA samples:*

Reverse transcription PCR was used to generate cDNA from RNA extractions using an Omniscript reverse transcription kit (Qiagen, Chadstone centre, Victoria, Australia) According to suppliers protocol, Oligo-DT's, 10X buffer RT, dNTP mix and RNase free water were thawed on ice. 2μg of RNA was transferred to a tube with master mix (2μL of 10x buffer RT, 2μL of dNTP (5mM), 2μL of OligodT primer (Cat no 79105), and 1μL Omniscript Reverse Transcriptase and RNase free water was added to make the reaction volume up to 20μL (refer to Table 2.1). Each of the components was mixed briefly by vortexing and centrifuging for 5 seconds. Tubes were then incubated at 37°C in a heating block for 1hr to allow the reverse transcription of RNA and the generation of cDNA.

Table 2.1 Reaction mix for the RT PCR

Component	Volume/reaction	Final concentration
10x buffer RT	2μL	1x
dNTP Mix (5mM each dNTP)	2μL	0.5mM each dNTP
Oligo-dT primer (10μM)	2μL	1μM
Omniscript Reverse Transcriptase	1μL	10 units (per 20μL reaction)
RNase free water	Variable	4 units (per 20μL reaction)
Template RNA	Variable	Up to 2μg (per 20μL reaction)
Total volume	20μL	0

2.2.5   *Preamplification of cDNA targets:*

The preamplification step of the samples was performed using the taqman PreAMP master mix protocol (part number 4384557, Applied Biosystems, Mulgrave, Victoria, Australia.). 31 taqman assays were embedded in a 386 well plate with 8 ports where the samples are loaded. The pooled taqman assays were then diluted using 500μL of 1x TE buffer to make up final volume to 1ml. Subsequently, 12.5μL pool assay mix (0.2X) with 12.5μL neat cDNA sample and 25μL of the Taqman Preamp Master mix (2X) were mixed to make the final volume of 50μL (refer to Table 2.2). The reactions were incubated in an Applied Biosystems 7300 thermocycler for 10 mins at 95°C followed by 10 cycles of 95°C for 15 seconds and 60°C for 4 mins and then it was held at 4°C (refer to table 2.3) and stored at -20°C.

Table 2.2 Preamplication reaction mix

Component	Volume (μL/Reaction)	Final Concentration
TaqmanPreAmp Master mix (2X)	25.0μL	1X
Pooled assay mix (0.2)	12.5μL	0.05 x (each assay)
1-250ng cDNA sample +nuclease free water	12.5μL	0.02-5.0 ng/μL
Total	50μL	-

Table 2.3 Preamplification PCR

	Enzyme Activation	Preamplification PCR	
	HOLD	Cycle (10 cycles)	
		Denature	Anneal/ Extend
Temperature	95°C	95°C	60°C
Time	10 min	15 secs	4 mins

2.2.6   Low density microfluidic cards

2.2.6.1   Preparing the samples for the PCR:

The cDNA samples were removed from the -20°C freezer and placed on ice and allowed to thaw. The samples were briefly vortexed and centrifuged. 50μL of the preamplified sample, 30μL of the 1x TE buffer (Ambion, Mulgrave, Victoria, Australia) and 80μL of the Taqman gene expression master mix (2X) were prepared. The Taqman low density array cards were stored at 4°C. Before using them, they were allowed to thaw for 15 min. 160μL of the samples were loaded into the reservoir ports of the low density Taqman array cards (Applied Biosystems, Mulgrave, Victoria, Australia).

2.2.6.2   Centrifuging the Taqman array cards:

After the reservoirs were loaded with the cDNA samples, the array cards were then centrifuged to distribute the cDNA samples to the reaction wells. The taqman cards were placed in the Sorvall/Heraeus buckets in the centrifuge and balanced using blank arrays. The taqman array cards were then centrifuged twice for 1 min to ensure complete distribution of the sample. The Taqman card was removed from the centrifuge bucket and was examined to determine whether the filling of the cards was complete and was checked further to ensure the samples in the reservoirs remained uniform and consistent. The taqman array card was placed on to the sealer and was lined up to the rear to the pin groves and foil side up of the sealer (as per manufacturer's instructions). After sealing, the fill reservoirs were then trimmed and were run on the 7900 HT instrument (Applied Biosystems, Mulgrave, Victoria, Australia). The low density array custom made taqman array cards were shipped with the information of Taqman gene expression assays on a CD. The sample TLDA setup file was imported into the software. The Taqman array cards were run on the machine.

2.2.7   Mercodia Mouse Insulin ELISA:

The kit was taken out from 4°C and allowed to come to room temperature. 25 µL of Calibrators 0,1,2,3,4 and 5 and serum samples from both wildtype and db/db mice were added to the wells of the monoclonal insulin antibody coated 96 well plates. 100µL of enzyme conjugate 1x was added to each of the wells. The plate was placed in the plate shaker (700-900 rpm), for one hr at room temperature. The plate was then washed with 1x buffer solution and emptied and this step was repeated 5 times. 200µL of substrate TMB was added to each well and was incubated for 15 min at room temperature. Finally 50µL of stop solution was added to each well and plate was placed on a plate shaker for 5 min to ensure mixing. The insulin Elisa plate was read using a microplate reader (Biorad, Galdesville, New South Wales, Australia), at 450nm optical density and the insulin concentration was calculated.

2.2.8   Bioplex 3-plex cytokine assay:

Serum cytokines were measured by Bioplex as per the manufacturer's instructions (BioRad, Gladesville, New South Wales, Australia). Samples were analysed in duplicate using a Bioplex Pro mouse Cytokine 3 plex magnetic bead array. All wash steps were performed using the Bioplex II Wash Station. Plate data was collected using a Bioplex 200 suspension array system and analysed using the Bioplex Manager 5 Software (BioRad, Galdesville, New South Wales, Australia).

2.2.9   Western Blot:

2.2.9.1   Protein quantification:

Protein was quantified using a Pierce BSA protein quantitation (Thermoscientific, Rockford, Illinois USA). The 60µL of standard was diluted 1:10 to give a concentration of 200µg/ml. Dilutions from the substock tube was diluted to 1,2,3,4 and 5 µg. Blank (0 µg), samples and standards were added to the 96 well plate as triplicates. 50 parts of reagent A and 1 part of reagent B were mixed and 200µL of this mixture was added to the 96 well plate. The plate was covered with foil and incubated for 30 min in a 37°C incubator. The plate was cooled down to room temperature for 20 min and the optical density was read at 570nm on ELISA reader (Biorad, Gladesville, New South Wales,

Australia). The data was imported to the excel sheet and the concentration was calculated using the standard curve.

2.2.9.2   Preparation of samples for western blot:

Samples were thawed and then were prepared for loading by boiling for 5 min at 100°C. Samples were placed on ice until loaded on the gel. More details are provided in chapter 7.

2.3 Cell Culture:

2.3.1   Preservation and storage of cell lines:

We obtained MIN6 cells from Dr. Ross Laybutt (Garvan Institute of Medical Research who obtained them from Dr Miyazaki)[147] and cells were maintained in Dulbecco's modified Eagle's medium (DMEM) containing 25 mM glucose, supplemented with 10% fetal calf serum, 2 mM L-glutamine, 25 mM Hepes, and 285 μM 2-mercaptoethanol (Life technologies, Mulgrave, Victoria, Australia). MIN6 cells presented in this study were at passages 30–40 (low passage, LP). Min6 cells were detached from the flask using trypsin (Life technologies, Mulgrave, Victoria, Australia) and the number of cells was counted in a hemocytometer. The remaining culture was centrifuged for 5 min. The aliquots of the cells were transferred into labelled cryovials (Thermoscientific, Rockford, Illinois USA). The cryovials were placed inside a Mr Frosty (Thermoscientific, Rockford, Illinois USA) filled with isopropyl alcohol and placed at -80°C overnight. Following this, frozen cells were transferred to the vapour phase of a liquid nitrogen storage vessel.

2.3.2   Recovery of frozen cell lines:

Frozen MIN6 cells were thawed rapidly by first removing them from liquid nitrogen or -80°C storage. The cells were transferred immediately to a 37°C water bath (Ratek, Boronia, Victoria, Australia) until the contents were completely thawed. The cells were then transferred to a 25ml polypropylene tube (Sarstedt, Newton, USA) containing 9 ml of growth medium. The cells were centrifuged for 5 min at 400g. The supernatant was aspirated and the cell pellet was resuspended in 5ml growth medium and was added to a

25 cm^2 flask. The cells were cultured in a 37°C humidified incubator (Hirschmann, Louisville, Kentucky, USA) with 5% CO_2 overnight or until the cells became adherent to the tissue culture plastic. After 3 days, the cells were then washed with 8 ml of warm 1xPBS (Thermoscientific, Rockford, Illinois USA) to remove any non-adherent cells and cell debris. Following this, fresh growth medium was added to the cells. The flask was then incubated at 37°C in 5% CO_2 until the cells reached 80% confluence.

2.3.3   Cell quantification:

MIN6 cells were detached from their flasks using 1 ml of trypsin. The cells were resuspended in 4 ml of growth medium. 10μL of this medium with cells was removed and added to 90μL of trypan blue (1 in 10 dilution) and mixed gently by pipetting. 10μl of the cell suspension was added to both sides of a clean haemocytometer containing a coverslip. The cell suspension was viewed under a light microscope using x100 magnification. The total number of cells was determined by counting four corner squares of the haemocytometer. The cell concentration per ml and the total number of viable cells were determined.

2.3.4   Glucose-stimulated insulin secretion in vitro.

1 x 10^6 MIN6 cells were cultured in 6 well plates with DMEM medium (25mM glucose) for 3 days. The cells were then transferred into a low glucose medium (3mM) for 1 hr to get them out of high glucose and this was repeated three times. The cells were then stimulated with 3, 16 or 25 mM glucose for 1 hr. The supernatants were collected and assayed for insulin using an ELISA kit (Crystal Chem, Downers Grove, IL, United States). The optical density was read at 450 and 650 nm and the values were obtained for each of the samples and were read using a microplate reader (Biorad, Galdesville, New South Wales, Australia).

2.4 Zn related measurements

2.4.1 Tissue collection and processing for Zn analysis for plasma, liver and pancreas:

Liver and pancreas were removed from groups of db/db or wildtype mice (6-8 mice) at ages 4, 10 and 14 weeks. Livers were added to 4 volumes (optimised method in the lab) of 10mM TRIS-HCL buffer (10mM, pH 8.2) while pancreas was added to nine volumes. The liver and pancreas were homogenised using a Potter-Elvehjem homogeniser ensuring that the organs were completely squeezed past the pestle five times. The homogenates were transferred to 1.5ml eppendorf tubes. Borex tubes (75x12mm in size) were numbered and weighed as (W1). 500µL of the organ homogenates were transferred into the tubes and reweighed (W2). The borex tubes with the samples were then placed in a heating block (Ratek, Boronia, Victoria, Australia) at $80^{o}C$ overnight. The tubes were cooled and weighed the next day as (W3). 1ml of Aristar 69% nitric acid (Merck, New Jersey, USA) was added to each tube and tubes were placed in the heating block at $50^{o}C$ for 15 minutes until the samples were dissolved. Tubes were then vortexed and heated to $100^{o}C$ to allow nitrogen dioxide to boil off and the solution to go clear yellow; then the temperature was raised to $150^{o}C$ to evaporate the samples to dryness. 1.5 ml of hydrochloric acid was added and the tubes were vortexed and placed at $50^{o}C$ in the heating block.

Appropriate number of 10ml tubes for samples, calibrators and quality control (Seronorm) were labelled and 150µL of sample, calibrator and quality control were diluted with 1ml of working diluent using a Hamilton diluter. The flame atomic spectrometer was set up for Zn analysis and samples and standards were read.

2.4.2 Tissue collection and processing for metallothionein (MT) assay by cadmium haemoglobin affinity assay (for liver and pancreas):

The livers were diluted at (1:5) and pancreas (1:10) with TRIS HCL Buffer. The tissue was homogenised using the Potter-Elvehjem Homogeniser and was squeezed past the pestle five time and was always kept cold. The homogenised tissue was transferred into a 1.5ml eppendorf tubes and was labelled. The samples were heat treated for 2 min and

then cooled in ice cool water for 2 min. The samples were centrifuged for 2 min at 14,000 g and the supernatant was transferred into a new 1.5ml eppendorf tube.

Aliquots of homogenised liver and pancreas were transferred into 1.5ml eppendorf tubes and heat treated by placing into boiling water before cooling in ice water. The samples were centrifuged for 3 min at 14,000 g. Supernatant was transferred into a new tube and stored at -80°C until metallothionein (MT) analysis. The supernatant and quality control were thawed and centrifuged for 1 min at 13,000 g. 40μl of supernatant and quality control were diluted and vortexed with 960μl TRIS buffer (pH 7.4). 200μl of the samples were transferred to a new eppendorf tube containing 200μl of radioactively labelled cadmium (0.5 MBq, New England Nuclear, Sydney). The samples were incubated for 15 min. 100μl of haemoglobin was added to the samples was added to remove any unbound cadmium and the samples were heat treated for 2 min and then placed on ice cold water before centrifugation (13,000 g). This process was repeated twice. 400μl of the clear supernatant from the samples was transferred into Borex tubes for MT analysis. The MT concentration in the supernatant was determined using a gamma counter (Parkard Auto Gamma 5650).

2.4.3   Zinpyr-1 staining for labile islet Zn:

Zinpyr-1 (Mellitech, Grenoble France) was diluted in PBS to a final concentration of 1μM and added to 5 micron tissue cryosections for 20 min at 37°C. Slides were then washed with PBS and a drop of DAKO fluorescence mounting medium (Cat no S302380-2, DAKO, North Sydney, New South Whales, Australia) was added. Slides were mounted with a coverslip and viewed by fluorescence microscopy within an hour. Images were captured on a Zeiss Apoptome microscope. ZINPYR-1 staining quantification was done by using FIGI image J software. Firstly the length of the scale bar was calculated to get the distance in pixels. The scale was set by adding the calculated length from the scale bar, known distance such as 100μM, pixel ratio set to 1 and the unit of length set to microns. The colour image was then split to 3 grey channels (red, green and blue). This was done by clicking image, colour and then split channels. The green channel (GFP) was then chosen to be analysed. The image was set to a threshold, leaving the background as red. Islets were circled and were added to a region

of interest manager window (ROI), where it was set a number to be analysed. Then the area of interest was added to the ROI window and the area and mean grey values were recorded.

2.4.4 *Immunofluorescence staining for ZnT7, ZnT8, ZIP4, ZIP5, ZIP14 and glucagon*

Tissues from WT (C57BL6J) and db/db mice at 4, 10 and 18 weeks of age were embedded in OCT medium and frozen. Sections, 5µm, were cut using a cryotome then fixed in cold acetone for 10 min. The sections were blocked in a humidified chamber for 60 min with serum from the secondary antibody host animal. Sections were incubated with rabbit polyclonal Anti-Slc30a7 (1:150; Cat no. HPA018034; Sigma Aldrich, USA), Rabbit polyclonal Anti Rat ZnT8 (1:100; Cat no. RZ8; Mellitech, Grenoble Cedex, France) rabbit polyclonal rabbit polyclonal Anti-ZIP4 (1:100; Cat no. PA5-210669; Thermoscientific, Rockford, Illinois USA) or rabbit polycolonal Anti-ZIP5 (1:150; Cat no. PA5-21070; Thermoscientific, Rockford, Illinois USA) and rabbit polycolonaL Anti-ZIP14 (1:150; Cat no. PA5-21077; Thermoscientific, Rockford, Illinois USA) and mouse monoclonal Anti-glucagon (K79Bb10) (1:50; Cat no. ab10988; Abcam, Melbourne, Victoria, Australia) overnight at 4°C. Excess primary antibody was removed by washing the slides with 1x PBS and incubated for 60 min with goat anti-rabbit Alexa488IgG(1:400; Cat no. 54533A Invitrogen, Mulgrave, Victoria, Australia) conjugate and rabbit anti-mouse Alexa594 conjugate IgG1γ (1:400;Cat no. 940829; Invitrogen, Mulgrave, Victoria, Australia). Sections were washed with PBS, nuclei were counter stained with DAPI (4', 6-diamidino-2-phenylindole; 1:1000) and mounted with fluorescent mounting medium (DAKO; Cat no. E7023-500ML). The images were captured in Axio vision fluorescence microscope.

The images were captured in Axio vision fluorescence microscope. The images were converted to JPEGS. ZIP4 and ZIP14 staining quantification was done by using FIGI image J software. Firstly the length of the scale bar was calculated to get the distance in pixels. The scale was set by adding the calculated length from the scale bar, known distance such as 100µM, pixel ratio set to 1 and the unit of length set to microns. The colour image was then split to 3 grey channels (red, green and blue). This was done by

clicking image, colour and then split channels. The green channel (GFP) was then chosen to be analysed. The image was set to a threshold, leaving the background as red. Islets were circled and were added to a region of interest manager window (ROI), where it was set a number to be analysed. Then measure was selected in the ROI window and the area, integrated density values were inserted into the excel sheet and analysed.

2.4.5   *Immunoperoxidase assay:*

Tissue sections (4 μm) were cut, mounted on Superfrost Plus coated slides, labelled and then placed on a fully automated immunohistochemistry (IHC) staining Ventana Benchmark XT (Roche Diagnostics, Roche Diagnostics, Castle Hill New South Wales Australia) instrument. The section was then washed in reaction buffer followed by addition of Cell Conditioning 1 (CC1) solution Roche Diagnostics, Castle Hill New South Wales Australia) for 30 min. CC1 was removed, washed, and the primary polyclonal Rabbit Anti-Glucagon at dilution 1/800 (Dako, Carpinteria, California, USA) added for 28 min whilst the slide was heated to 37°C. Visualisation was of the staining was using *ultra*View DAB detection kit (Roche Diagnostics, Castle Hill New South Wales Australia) in accordance with the manufacturer's standard procedures followed by counterstaining with haematoxylin 11(Roche Diagnostics). The same procedure was used for Polyclonal Guinea Pig Anti-Swine Insulin (Dako, Carpinteria, CA) at 1/100 and ZIP4 (Thermo Scientific Rockford, USA) at 1/400, ZIP 14 (Thermo Scientific Rockford, USA) at 1/1600 CD68 1/1500 (Dako, M0814 Clone KP1) and Polyclonal Rabbit Anti-human Somatostatin (Dako Carpinteria, California, USA) at 1/1600. Immunohistochemistry images were captured using a Nikon Eclipse 90i microscope (Nikon, Tokyo, Japan).

2.4.6   *Iron staining:*

Frozen section of normal human liver and chronic diabetic 18 weeks (db/db) mice and control (human liver) was washed with distilled water. Equal parts of ferrocyanide and hydrochloric acid was added to the slides and incubated for 10 min. The slides were then washed with distilled water for 5 min. A counterstain with filtered neutral red stain

was used to stain the nuclei and was incubated for 5 min. The slides were air dried, and dehydrated with absolute ethanol and then mounted with coverslip.

2.5 Statistical analysis:

Analysis was performed by an ANOVA approach, using likelihood ratio tests, as the datasets were not completely balanced. A two-factor interaction model (Group*Time) was estimated for each response. All data was log-transformed prior to analysis because of non-constant variance. The fitted "means" were estimated by back-transforming the fitted log-means, and therefore represent medians. Gaussian generalised linear models (GLMs) were used for datasets where there was a single observation for each mouse, and Gaussian generalised linear mixed models (GLMMs) were used for datasets where there were repeated observations on each individual (i.e. random effect = animal). Statistical analysis was performed using R software V 3.0.1[323].GLM models were estimated using base functions in R. GLMM (random effect models) were estimated using the lme4 library V1.0-5 [324].Type II Likelihood ratio ANOVA tables were generated by the Anova function in the car library V2.0-19[325].Planned comparisons, corrected for multiple comparisons, were performed between db/db and wildtype mice at each time point using the multcomp library V1.3-1[326]

CHAPTER 3 Sub classification of diabetic status of db/db mice

3.1 Introduction

Pancreatic islets are multicellular organs, which are composed of many cell types such as glucagon producing (alpha) cells, insulin producing (beta) cells, somatostatin producing (delta) cells and polypeptide producing PP cells. It is known that islet cell architecture differs between species, and that this regulates the blood glucose levels according to body size[327-329].

In contrast to human, primate and pig islets, mouse islets contain a mantle and an inner core of cells. The mantle is mainly composed of alpha, delta and PP cells and the inner core of the islets is composed of the beta cells. In humans, the alpha, delta and the PP cells are not located in the periphery of the islets, but are dispersed throughout the islets. It has been proposed that the structural architecture of the pancreatic islets in humans enables beta cells to respond to lower concentrations (e.g. 1mM) of glucose in the blood, because the beta cells are in close proximity to the afferent artery; by contrast, in the mouse, the afferent artery first has to pass through the layer of non-beta cells in the mantle[327,329]. The structural architecture and the cell to cell contact between the cells in the mantle are important for the regulation and secretion of insulin. It is also known that as the size of the islet increases, vascularisation increases to enable proper nutrient supply and regulation of function in non-beta cell types.

In diabetic rodent models, it is known that the islet volume is increased (hypertrophy) and the number of beta cells is increased (hyperplasia) in early diabetes, in order to compensate for the hyperglycaemia. The islet size and the number of the beta cells decrease in the late stage of diabetes[330,331]. Increase in the islet size leads to disorganisation of the islet cells in the diabetic rodent models especially the db/db mice. Alpha and delta cell number was shown to increase in the pancreatic islets of these mice[112]. This disorganisation, in turn, leads to a lack of cell to cell communication in the mantle of the islet and loss of a negative feedback loop, resulting in enhanced secretion of islet hormones[332]. Similarly, in human type 2 diabetic patients increased alpha cell mass was observed in pancreatic islets, however there was no change in delta

cell number[100]. In the db/db mouse pancreatic islets there is an increase in macrophage infiltration in the pancreatic islet in early diabetes and this was also noted in human diabetic pancreatic islets stained for the macrophage marker CD68[44,333,334]. All of these factors have been shown to contribute to the loss of beta cell mass and function in diabetes in both humans and rodents.

The reason why the db/db mice was chosen as a model of type 2 diabetes for the studies in this thesis is that it best reflects the natural history of type 2 diabetes in humans (e.g. similar phenotype of beta cell expansion in the development and progression of the diabetes). The spontaneously diabetic db/db mice beccone obese early in diabetes. They later develop severe diabetes leading to many secondary complications such as nephrophathy, neurophathy and cardiovascular complications and also weight loss (like some human subjects with diabetes)[335].There is a genetic component to the risk of diabetes. It has been established that mice with a C57BL6J background are more susceptible to diabetes than other strains of mice. For example, there was a 50% increase in fasting plasma glucose and increase in insulin after C57BL6J mice were fed a high fat and carbohydrate diet[336], while C57BL6J mice were the least tolerant to glucose of six other strains of mice tested[337]. Another factor that is involved in increased risk of diabetes is gender which is thought to be related to testosterone levels[338]. Male db/db mice have more severe diabetes compared to female mice. Male db/db mice develop hyperglycemia as early as 4-5 wk with the blood glucose ~16 mmol/L compared to female mice. Female mice were shown to have a lower incidence (~12%) of diabetes compared to males (50%).

This study has a particular emphasis on early diabetes, diabetes and chronic diabetes which has not been systematically examined for changes in Zn and Zn transporters before in the db/db mice. The most practical and economical approach for the db/db mouse experiments in my thesis was to purchase the db/db mice and age-matched controls from the Animal Resources Centre (ARC) in Western Australia. Male db/db mice were from a colony derived from B6.Cg-m +/+ Lepr[db] also known as B6.BKS(D)-Leprdb/J (originally derived from Jackson Labs). The control mice used was the

C57BL/6J strain[339]. Mice were purchased at three ages: - 4-5 wk (designated in this thesis as 4 wk, early diabetes), 10-11 wk (designated 10 wk, established diabetes) and 14-15 or 17-18 wk (designated 14wk or 18wk, respectively, chronic diabetes).

The aim of the experiments described in this chapter was to examine the development of diabetes in these mice from 4 to 18 wk of age and to confirm the diabetic status of the db/db mice by a number of parameters including hyperinsulinemia, hyperglycemia and impaired glucose tolerance.

It was hypothesised that:

- The db/db mice will show early changes (4 wk) characteristic of diabetes such as hyperglycemia, hyperinsulinemia, glycosuria and obesity unlike the age matched wildtype mice

- The db/db mice will show early changes in islet morphology and hormones unlike the age matched wildtype mice

3.2 Methods

Detailed methods are described in chapter 2

3.2.1   Tissue collection

Pancreata from 4, 10 and 18 week db/db mice and age matched wildtype mice were removed and were embedded in OCT medium and frozen using isopentane and liquid nitrogen. They were then stored at -80°C.

3.2.2   Glucose testing and intraperitioneal glucose tolerance test

Blood glucose was determined by tail vein bleeding and a drop of blood was placed in a glucose electrode and analysed using a glucometer (Optium, Abbott Diabetes Care, Victoria, Australia). For glucose tolerance tests, animals were fasted overnight and then a dose of glucose (2 g/kg body weight) was administered *via* an intraperitoneal injection at. Blood samples were collected from a small cut at the tip of the tail at 0, 15, 30, 60, 90 and 120, 240 and 360 min after the glucose load.

3.2.3   Histology and microscopy

The samples were serially sectioned into slices 5 μm thickness. Slides were deparaffinized, hydrated, treated with Haemotoxylin and Eosin, and covered with glass coverslips. Images were captured using Nikon Eclipse 90i microscope (Nikon, Tokyo, Japan).

3.2.4   Islet size

Islet size was measured in cryosections by capturing representative images using a Zeiss Apoptome microscope (Carl Zeiss GmbH, Goettingen, Germany). The islet perimeter was circled and measured using ImageJ software (FIJI). Islets from 4, 10 and 18 wk db/db mice and age-matched controls were used. The area was represented as pixel squared.

3.2.5   Plasma insulin

Plasma insulin was measured by ELISA (Mercodia Insulin ELISA kit). The optical density was measured at 450nm in a microplate reader (Biorad, Gladesville, New South Wales, Australia).

3.2.6   Statistics

Diabetes-related parameters were measured and the data log-normalized. Medians, fold-changes (relative to age-matched controls), confidence intervals and p values were determined using the R software. For most of the parameters, data are tabulated in Table 3.1.

3.3 Results

3.3.1   Confirmation of obesity in db/db mice

Body weight (g) was measured as an index of obesity in mice and is depicted in figure 3.1 and Table 3.1 for db/db and WT mice. Body weight of db/db mice was significantly increased compared to that of WT mice at 4 wk (1.3 fold, $p<0.005$), 10 wk (1.8 fold, $p<0.005$), 14 wk (2.0 fold, $p<0.05$) and 18 wk (1.6 fold, $p<0.005$). In the db/db mice, obesity was evident at 4 wk, peaked at 10 wk and was maintained thereafter.

3.3.2   Confirmation of hyperglycaemia in db/db mice

Blood glucose (mmol/L) was measured as an index of hyperglycemia in mice and is depicted in figure 3.2 and Table 3.1 for db/db and WT mice. Blood glucose of db/db mice was significantly increased at 4 wk (1.7 fold, $p<0.005$), 10 wk (3.0 fold, $p<0.005$), 14 wk (2.9 fold, $p<0.005$) and 18 wk (5.0 fold, $p<0.005$) compared with age matched WT mice. In the db/db mice, hyperglycemia was evident at 4 wk, and progressively increased till 18 wk. In WT mice, there was no significant age effect on blood glucose levels.

3.3.3   Confirmation of diabetic status of db/db mice by measuring urine glucose

To confirm glycosuria, spot urine sample glucose levels were measured using dip sticks. Glycosuria was indicated by a colour change from yellow to dark green (at concentrations of glucose greater that 55mmol/L). None of the WT mice at 4, 10 and 14 wk had a dipstick colour change whereas all of the db/db mice (at each age tested) had a dipstick colour change to dark green. There was insufficient urine from the mice to do a more precise analysis (Table 3.1).

3.3.4   Confirmation of diabetic status using interperitioneal glucose tolerance test in db/db mice

To measure the glucose tolerance and clearance, mice were fasted overnight. Blood was collected for a basal glucose level and then mice were given an intraperitoneal glucose

injection (2mg/kg body weight). Blood was collected at various time-points over the next few hrs.

The db/db mice, at each age, had significantly higher basal fasting blood glucose concentrations when compared to age matched controls (Fig 3.4). Panel A, B and C show the data for 4, 10 and 18 wk, respectively. The upper graph in each panel shows the smooth scatter plot. Each dot is the means of the group of mice. The shaded area is the upper and lower confidence intervals. The lower graph in each panel shows the area under the curve as a box plot for each individual mouse. There were significant differences in the area under the curve at 4, 10 and 18 wk for db/db compared to the age matched control. Clearance of glucose was rapid in 4 wk db/db mice, less so in 10 wk db/db mice and very slow in 18 wk db/db mice. This confirms the diabetic status of the mice.

3.3.5   *Confirmation of hyperinsulinemia in db/db mice*

Plasma insulin levels (µg/L) were measured as an index of hyper-insulinemia in mice and are depicted in figure 3.5 and Table 3.1 for db/db and age matched controls. The peak hyper-insulinemia occurred at 4 wk (9.5 fold increase, $p < 0.005$). The increases were less but still highly significant ($p < 0.005$) at 10 wk (5.2 fold) and at 18 wk (3.6 fold, $p < 0.005$). There was no significant age effect on plasma insulin levels in the WT mice.

3.3.6   *Confirmation of hypertrophy in db/db mice*

Islet area as an index of islet size in mice was measured using image J software. Between 18 and 67 islets were measured from 4 mice in each group. Typical images are shown in figure 3.6 and the quantitative data in figure 3.7 and Table 3.1. Peak increase in islet area in db/db mice occurred at 4 wk (4.9 fold, $p < 0.005$, figure 3.6 the left upper and lower panels). Islet hypertrophy was maintained at 10 wk (4.5 fold, $p < 0.005$, figure 3.6 middle panels) and at 18 wk (3.5 fold, $p < 0.005$, Figure 3.6 right panels). There was no significant age effect on islet size in the WT mice.

3.3.7   Islet hormone distribution in typical islets in 4 week old db/db mice

Figure 3.8 shows immunoperoxidase staining of serial pancreatic sections for insulin and glucagon, in WT mice at 4 wk (upper panels) and db/db mice (bottom panels) at 4 wk. In the WT mice, insulin staining in islets was dense and closely packed throughout the interior of the islet where beta cells are present. In the db/db mice (bottom panel) the insulin staining was patchy, more loosely packed and showing evidence of beta cell degranulation.

Glucagon in the WT mice was largely present in the periphery (or mantle) of the islet (Figure 3.8 upper panels) where the alpha cells are known to predominate. In the db/db mice however, the glucagon staining was more disorganized existing in the periphery and the inner core of the islets, even in early diabetes (Figure 3.8 lower panels). Somatostatin in the WT mice was present in the periphery of the islet (Figure 3.9 upper panels) where the delta cells are known to predominate. In the db/db mice however, the somatostatin staining was more disorganized and increased in expression in the inner core of the islets, even in early diabetes (Figure 3.9 lower panels).

3.3.8   Plasma cytokine levels in the db/db mice

Proinflammatory cytokines IL-6, TNF-α and IL1-β were measured in the plasma of db/db mice and age matched controls at 4, 10 and 18 wk, as a measure of systemic inflammation. There were no detectable levels of any of the cytokines in either the db/db or age matched controls, suggesting no systemic inflammation.
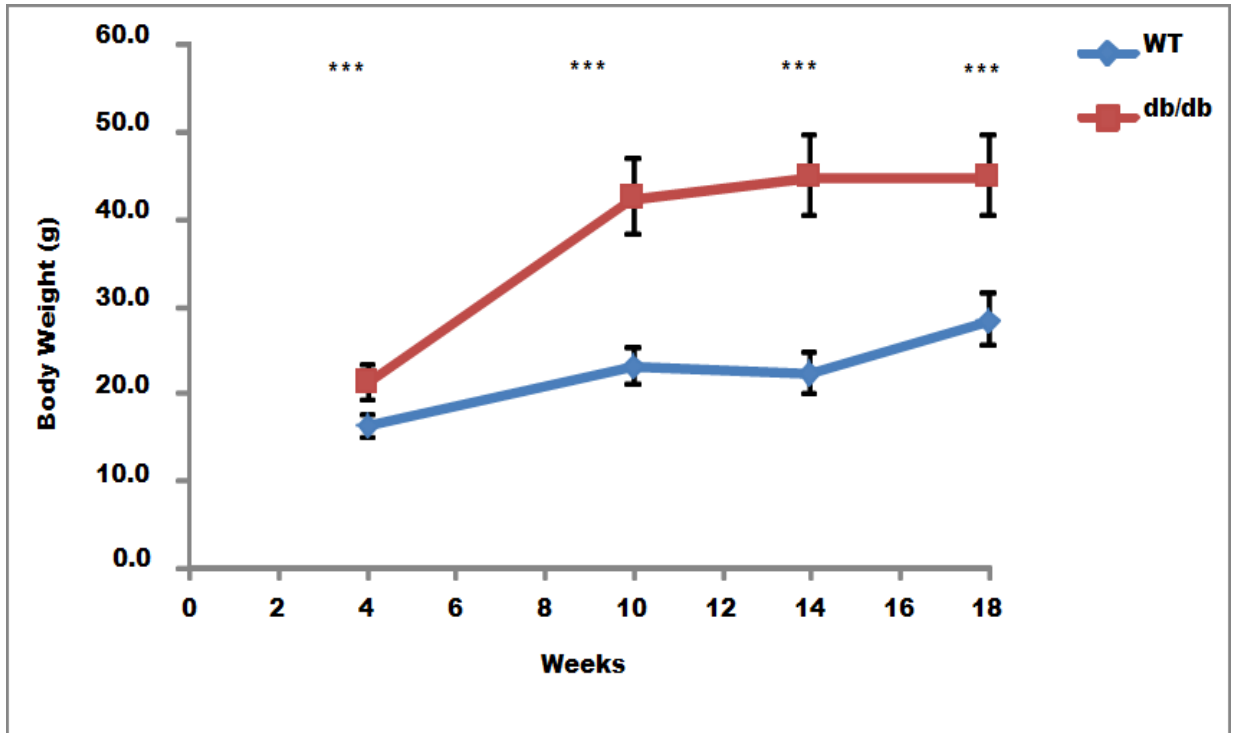
Figure 3.1 Confirmation of obesity in db/db mice

Figure shows that the db/db mice at 4 wk are significantly heavier compared to age matched controls but their peak body weight occurred at 10 wk of age. The X axis represents the wk (age of mice) and the Y axis represents the body weight (g). Wild type mice are shown as the blue lines and the db/db mice are shown as the red lines. The data is shown as medians and the range as confidence intervals. * (p<0.05), ** (p<0.005) and *** (p<0.0005). Statistical analysis was performed by type 2 ANOVA. 6-8 mice were used at each time point, and each point was a single body weight measurement.
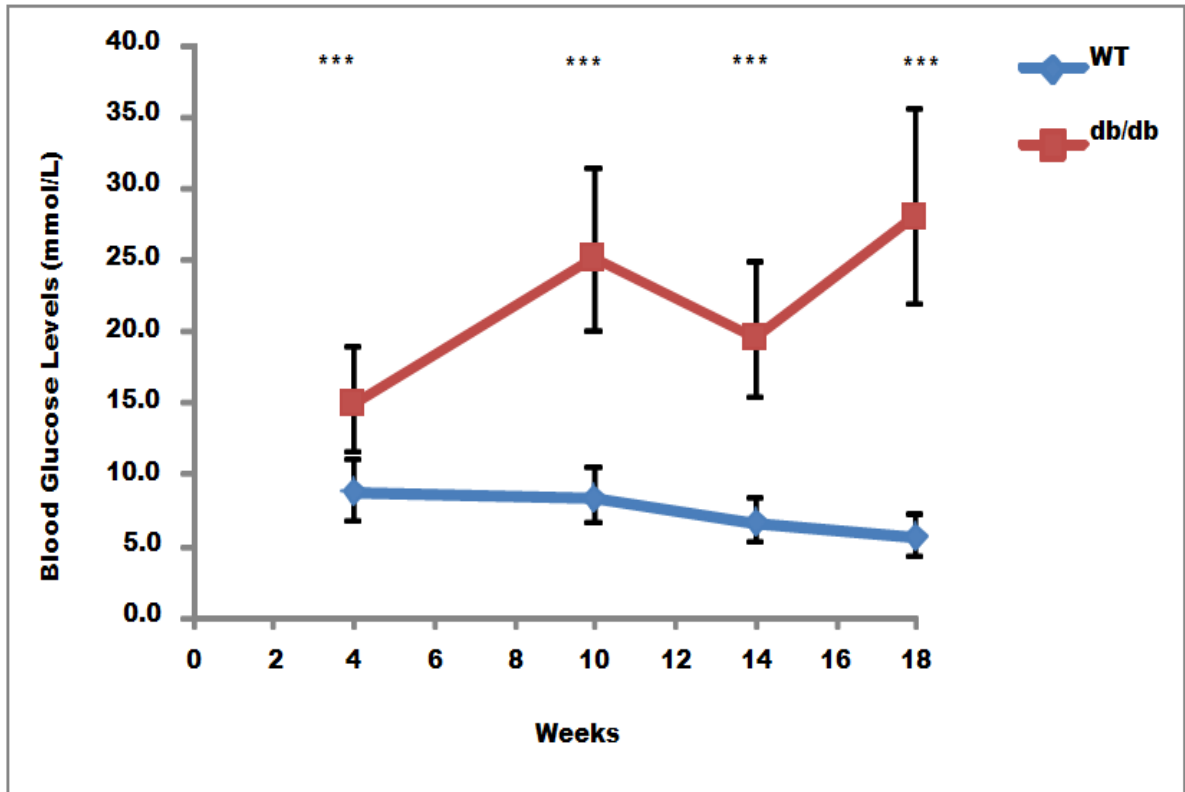
Figure 3.2 Confirmation of hyperglycaemia in db/db mice

Figure shows that as the db/db mice age the hyperglycaemia worsens. The X axis represents the wk (age of mice) and the Y axis represents the blood glucose levels (mmol/L). Wild type mice are shown as the blue lines and the db/db mice are shown as the red lines. The data is shown as medians and the range as confidence intervals. * (p<0.05), ** (p<0.005) and *** (p<0.0005). Statistical analysis was performed by type 2 ANOVA. 6-8 mice were used at each time point, and each point was a single glucose measurement.

Urine Glucose levels for prediabetic mice		
	Glucose Levels	Observation
WT1	Normal	Yellow
WT2	Normal	Yellow
WT3	Normal	Yellow
WT4	Normal	Yellow
WT5	Normal	Yellow
WT6	Normal	Yellow
WT7	Normal	Yellow
WT8	Normal	Yellow
Pre1	55 mmol/L	Dark green
Pre2	55 mmol/L	Dark green
Pre3	55 mmol/L	Dark green
Pre4	55 mmol/L	Dark green
Pre5	55 mmol/L	Dark green
Pre6	55 mmol/L	Dark green
Pre7	55 mmol/L	Dark green
Pre8	55 mmol/L	Dark green

Urine Glucose of Diabetic db/db mice		
	Glucose level	Observation
WT1	Normal	Yellow
WT2	Normal	Yellow
WT3	Normal	Yellow
WT4	Normal	Yellow
WT5	Normal	Yellow
WT6	Normal	Yellow
WT7	Normal	Yellow
WT8	Normal	Yellow
D1	55 mmol/L	Dark green
D2	55 mmol/L	Dark green
D3	55 mmol/L	Dark green
D4	55 mmol/L	Dark green
D5	55 mmol/L	Dark green
D6	55 mmol/L	Dark green

Urine Glucose levels for Chronic Diabetic Mice		
	Glucose Levels	Observation
WT1	Normal	Yellow
WT2	Normal	Yellow
WT3	Normal	Yellow
WT4	Normal	Yellow
WT5	Normal	Yellow
WT6	Normal	Yellow
WT7	Normal	Yellow
WT8	Normal	Yellow
CD1	55 mmol/L	Dark green
CD2	55 mmol/L	Dark green
CD3	55 mmol/L	Dark green
CD4	55 mmol/L	Dark green
CD5	55 mmol/L	Dark green
CD6	55 mmol/L	Dark green

Table 3.1 Confirmation of diabetic status of db/db mice by measuring urine glucose

Glucose urine strips were used to measure urine glucose in random urine samples in mice. The individual mice are in the left hand column. Wild type is (WT1-8), db/db (Pre1-8) is the 4 week diabetic mice. (D1-6) are the 10 week diabetic and (CD1-6) are the chronic diabetic. The yellow colour indicates the urine glucose level below 55mmol/L. and the dark green indicates greater than 55mmol/L.

Figure 3.3 Confirmation of diabetic status using intraperitioneal glucose tolerance test in db/db mice

In the following figures panel A, B and C shows that the db/db mice were significantly but mildly glucose intolerant as early as 4 wk of age and their condition worsened at 10 and 18 wk of age. Panel A, B and C show the data for 4, 10 and 18 wk, respectively. The upper graph in each panel shows the smooth scatter plot. Each dot is the mean of the group of mice. The shaded area is the upper and lower confidence intervals. The lower graph in each panel shows the area under the curve as a box plot for each individual mouse. The dot represents individual mice. The horizontal line in the box plot represents the median for the group of mice. The box height represents the interquartile range. The vertical line represents the non-outlier range. Statistical analysis was performed by Wilcoxen rank test and each point was a single mouse with single glucose measurement in the glucometer.

A
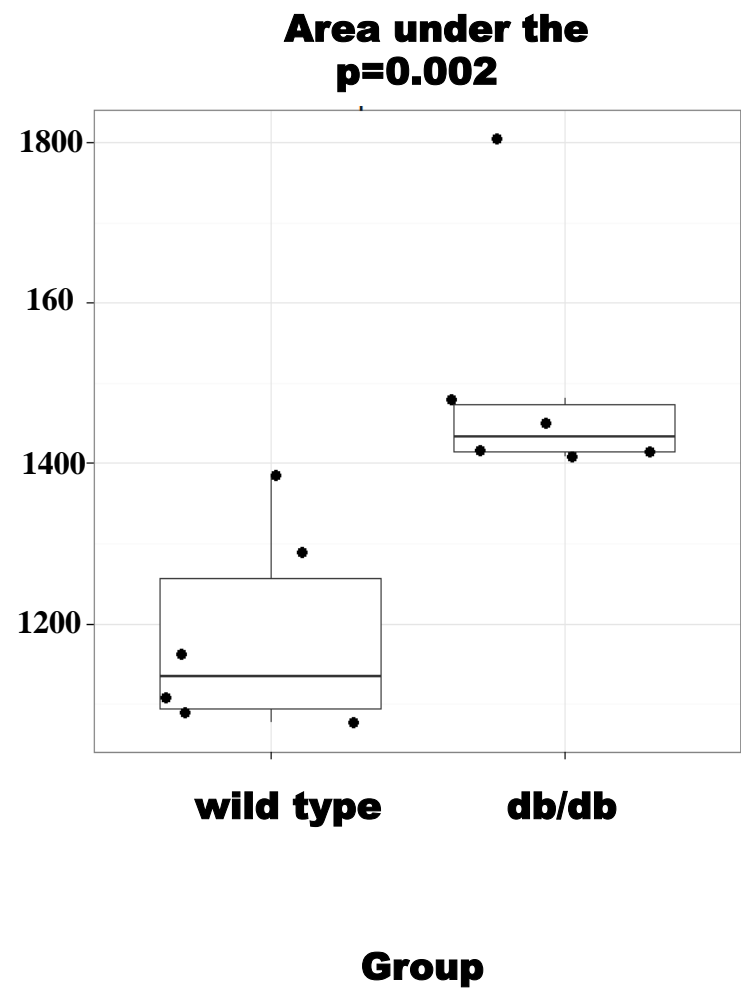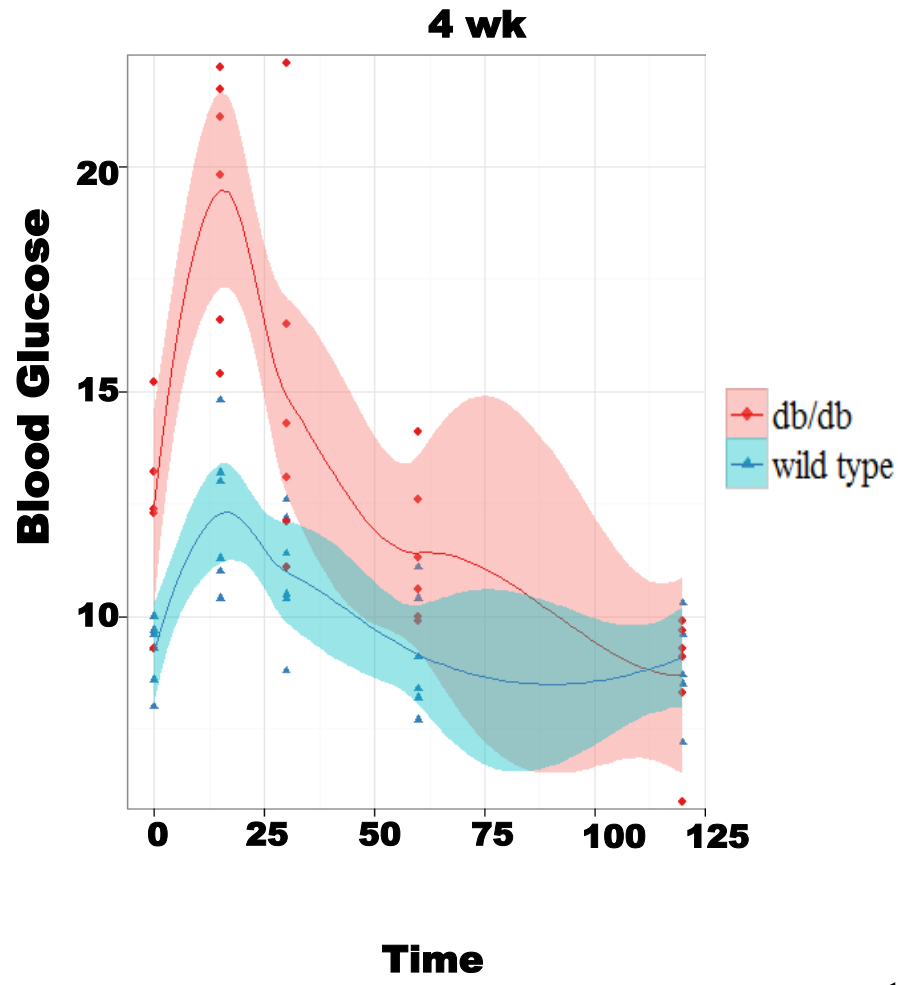
B
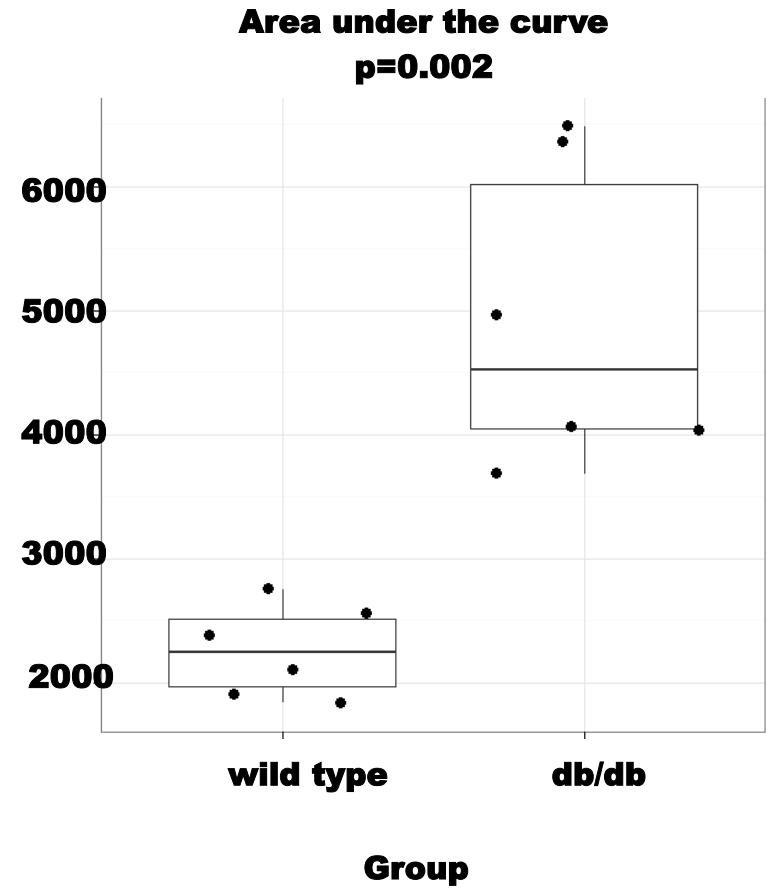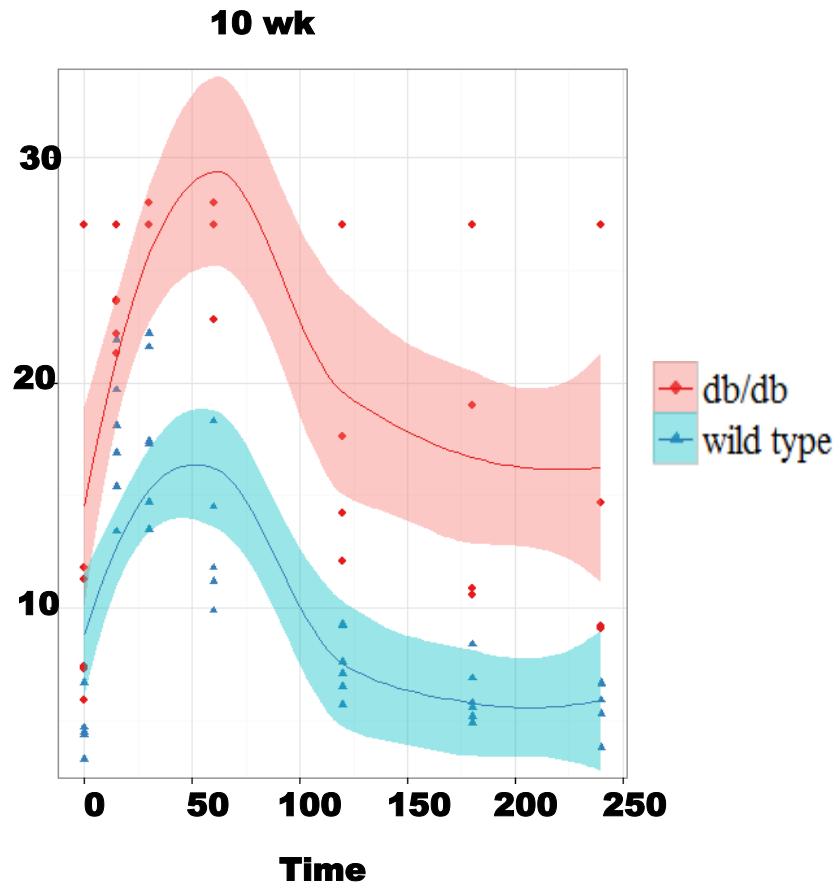
C
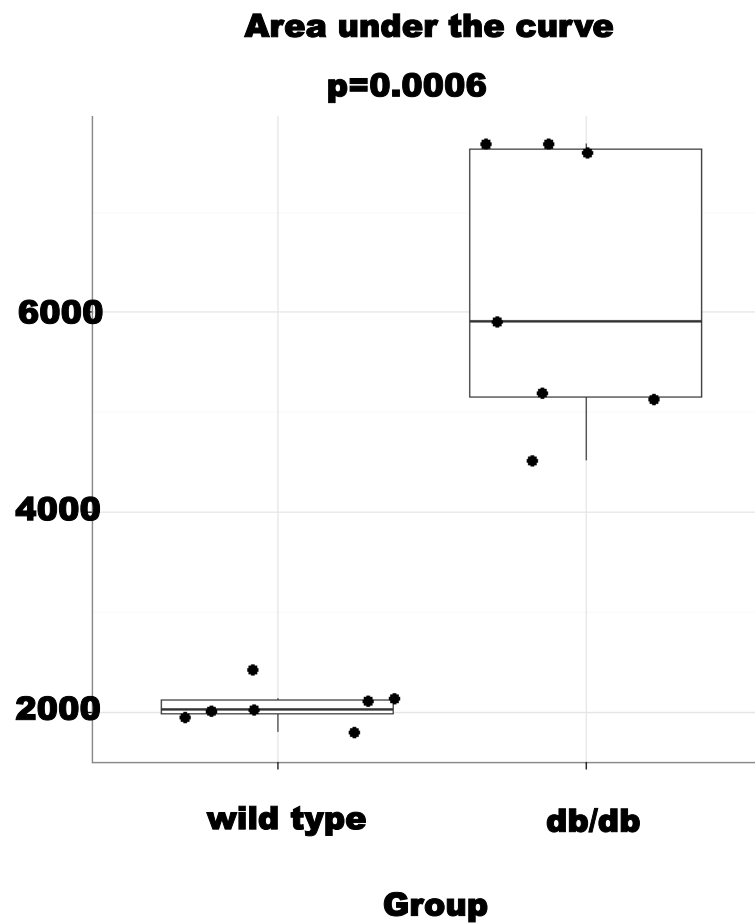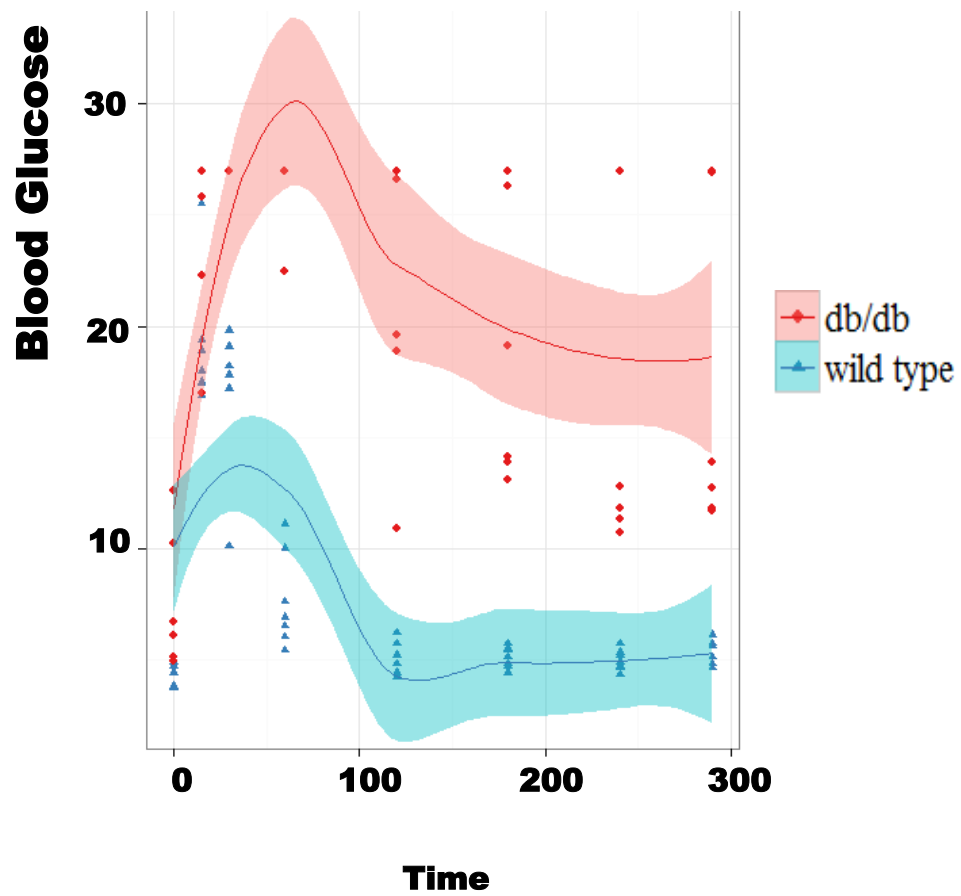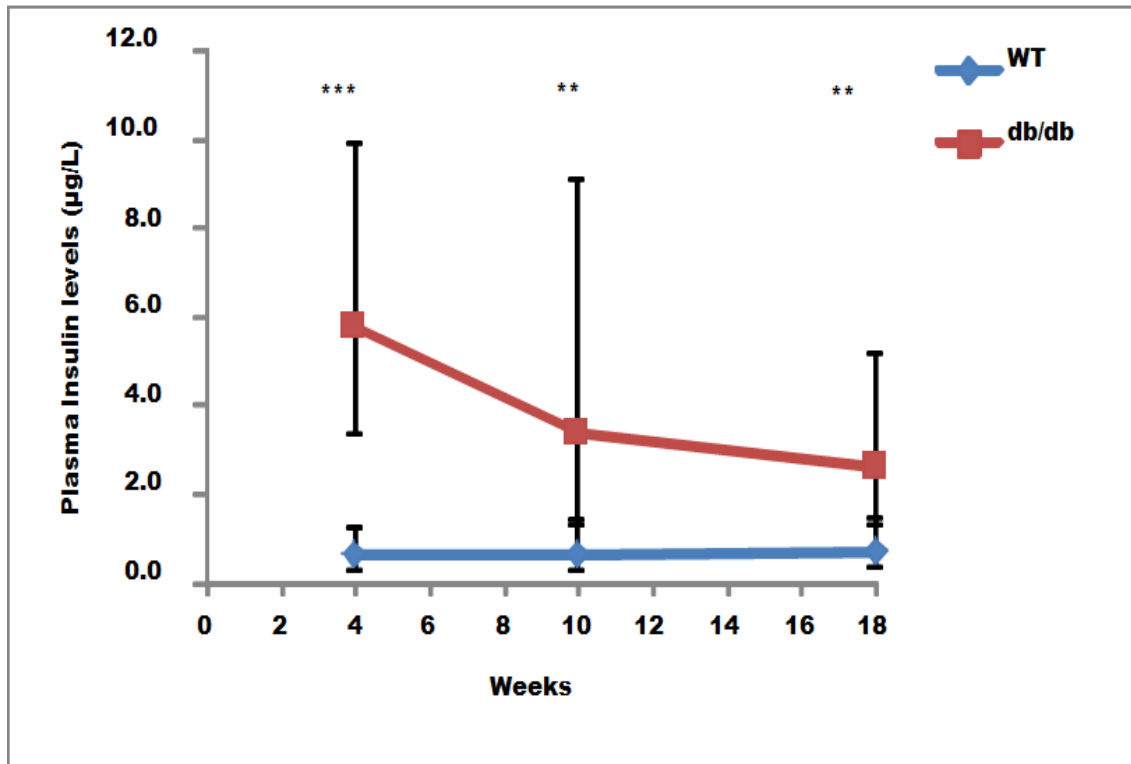
Figure 3.4 Confirmation of hyperinsulinemia in db/db mice

The db/db mice have hyperinsulinemia as early as 4 wk of age and their plasma insulin levels declines at 10 and 18 wk of age, although compared to controls they are still hyperinsulinemic. The X axis represents the wk (age of mice) and the Y axis represents the plasma insulin levels (μmol/L). Wild type mice are shown as the blue lines and the db/db mice are shown as the red lines. The data is shown as medians and the range as confidence intervals. * (p<0.05), ** (p<0.005) and *** (p<0.0005). Statistical analysis was performed by type 2 ANOVA. 6-8 mice were used at each time point, and each point was a triplicate measurement based on an Elisa assay.
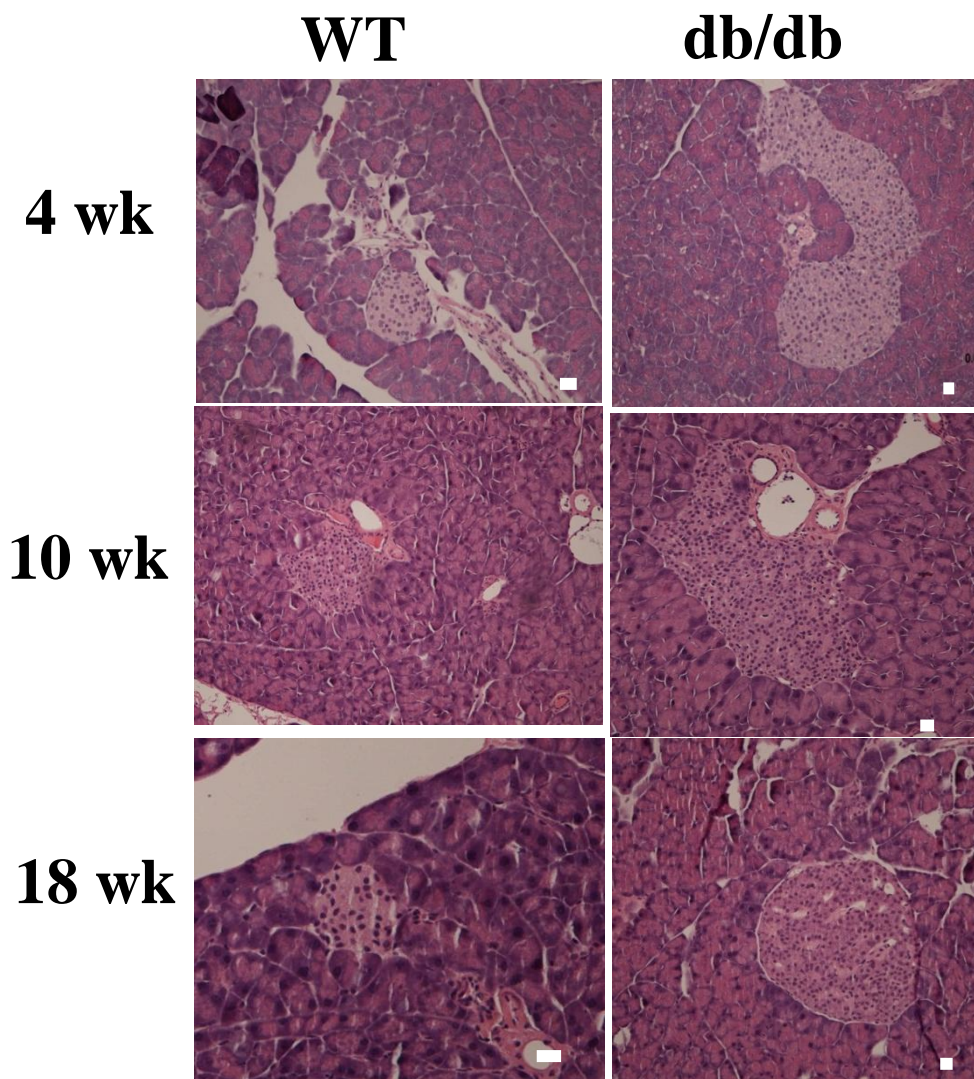
Figure 3.5 Morphology of typical islets in db/db mice

Typical islets surrounded by acinar tissue in H & E stained paraffin embedded sections of wild type mice (upper panel) and db/db mice (bottom panel) at 4 (left) , 10 (centre) and 18 (right) wk of age. The size of the islets in the db/db mice was larger than that of islets in the wild type. The diabetic islets also showed frequent dilated sinusoids seen as the gaps within the islets. There was no apparent inflammation around the diabetic islets.
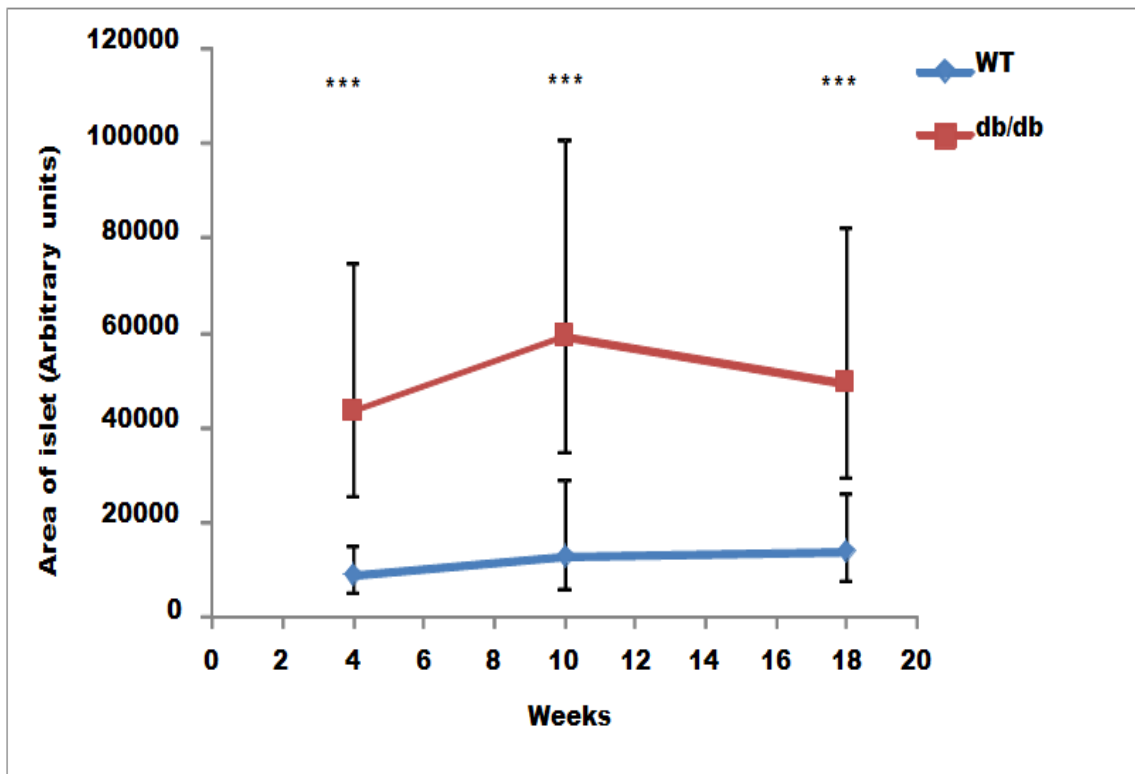
Figure 3.6 Confirmation of hypertrophy in db/db mice

The db/db mice have islet hypertrophy as early as 4 wk of age and this is maintained at 10 and 18 wk of age compared to controls. The X axis represents the wk (age of mice) and the Y axis represents the mean area of islet (arbitrary units). Wild type mice are shown as the blue lines and the db/db mice are shown as the red lines. At each time point, between 18 and 67 islets were measured by Image J (FIGI) from 4 mice.The data is shown as medians and the range as confidence intervals. * ($p<0.05$), ** ($p<0.005$) and *** ($p<0.0005$). Statistical analysis was performed by type 2 ANOVA.
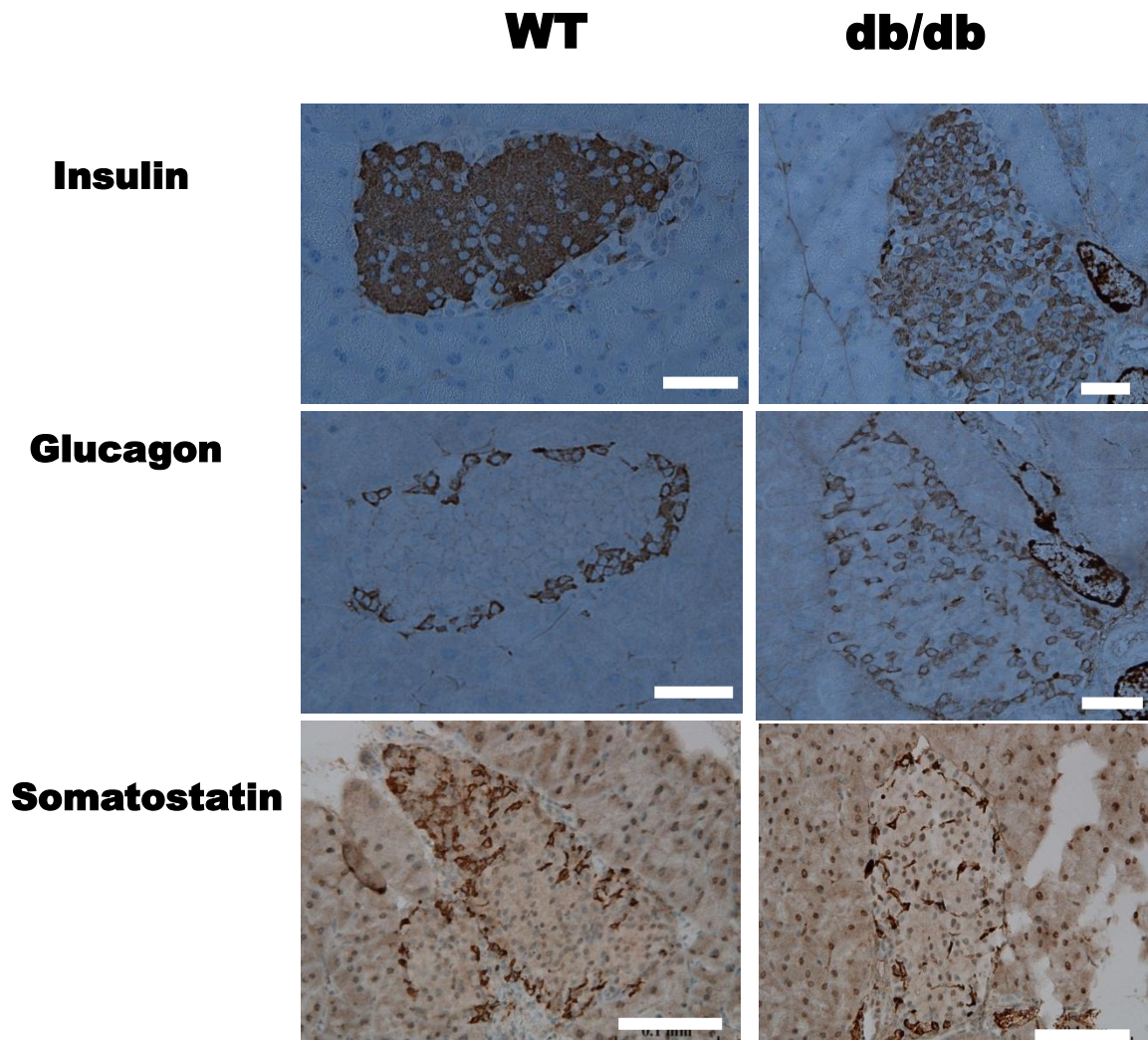
Figure 3.7 Islet hormone distribution in typical islets in 4 week old db/db mice

Typical islets stained for islet hormones in immunoperoxidase-labelled paraffin embedded sections of 4 week old WT mice (upper panel) and db/db mice (bottom panel). The hormones assayed were insulin (left), glucagon (centre) and somatostatin (right) for beta cells, alpha cells and delta cells, respectively. Insulin staining in the WT mice had dense immunoreactivity in the inner core of the islet, whereas in the db/db mice the immunoreactivity was less and in a more degranulated form. The glucagon staining was in the mantle of the islet of the WT mice, whereas in the db/db mice it was both in the mantle and the inner core of the islet. Somatostatin staining was mainly in the mantle of the islet in the WT mice, whereas in the db/db the staining was disorganised and distributed throughout the islet.

Table 3.2 Diabetes-related measurements in db/db model

Parameter	Wk	WT	db/db	Units	Fold-Change	Lower CI	Upper CI	n	P value
Body Weight	4	16.2	21.2	g	1.3	1.2	1.5	7-8	< 0.005
	10	23.3	42.8	g	1.8	1.6	2.1	6-8	< 0.005
	14	22.4	45.0	g	2.0	1.8	2.3	6-8	< 0.005
	18	28.4	45.0	g g	1.6	1.4	1.8	6	< 0.005
Blood Glucose[a]	4	8.9	15.2	mmol/L	1.7	1.3	2.3	6	< 0.005
	10	8.4	25.3	mmol/L	3.0	2.3	4.0	7	< 0.005
	14	6.8	20.2	mmol/L	2.9	2.2	4.0	6	< 0.005
	18	5.8	28.0	mmol/L	5.0	3.8	6.8	6-8	< 0.005
Plasma Insulin	4	0.66	6.2	µg/L	9.5	4.3	21.2	6-10	< 0.005
	10	0.69	4.0	µg/L	5.2	1.7	16.2	3-5	< 0.005
	18	0.8	4.0	µg/L	3.6	1.5	8.8	6	< 0.005
Islet Area	4	9917	3791	Square	4.9	2.5	9.6	4	< 0.005

				0	microns					
	10	10631	54586	Square microns	4.5	1.9	10.5	4	< 0.005
	18	10664	43776	Square microns	3.5	1.7	7.0	4	< 0.005
Plasma Cytokines	4	nd[b]	nd	NA[c]	NA	NA	NA	NA	NA
	10	nd	nd	NA	NA	NA	NA	NA	NA
	18	nd	nd	NA	NA	NA	NA	NA	NA

a Random blood glucose level (non-fasting)

b Not detected

c Not applicable

3.4 Discussion:

In this chapter we performed a through in vivo characterisation of db/db and wildtype mice at 4, 10, 14 and 18 wk of age. The primary observations made were that these mice midly hyperglycemic and glucose intolerant as early as 4 wks of age and their severity increases as age increases. The peak obesity occurs at 10 wks of age and they progressively become heavier. They have significantly larger islets at 4, 10 and 18 wks. Further, they had significantly high plasma insulin in the db/db mice. In addition, alpha and delta cells were increased and was expressed in the interior of the pancreatic islet. The control mice islets had high immunoreactivity for insulin which was densely packed within the beta cells. In contrast, the db/db mice islets showed evidence of degranulation in the large proportion of beta cells.

This animal model futher confirms the results from the db/db and other animal models of diabetes, showing hyperglycemia, obesity, islet hypertrophy and disorganised islet architecture[328,332,340]. In relation to the blood glucose in the db/db mice at 4, 10 and 18 wk of age, there was a significant increase in the blood glucose levels from 4 to 10 wk of age and was elevated at 18 wk of age. Similar trend in the body weight of the db/db mice was seen at these ages.

Islet hypertrophy (increased beta cell mass) has been observed in diabetes, obesity[341,342] and pregnancy[343] and has been reported in many studies. Changes in islet size and number occur during animal development, growth, aging, pregnancy and type 2 diabetes[344]. There are two major pathways that the islet growth and number increases; firstly the expansion of pre-existing endocrine cells, growth of new islets and finally differentiation of the pancreatic ductal epithelium and each of these factors are regulated in response to demand for example body weight and disease severity. The islet cell number is also regulated by changes in replication, apoptosis, atrophy, hypotrophy and neogenesis[345]. Garris et al reported that the ob/ob and db/db in the KsJ background mice have islet hypotrophy, beta cell degranulation and lipid deposition in both islets and acinar tissue. It was also noted that these events occur at an early age leading to islet atrophy and eventually leading to islet cell degeneration and is dependent on the severity of the disease in these mice[346,347]. In experiments described in

this chapter, it was seen that the islet cell size increased from 4 to 10 wk and then decreased at 18 wk in the db/db mice. This could be due to the increase number of beta cells at 4 weeks leading to a increase in islet size to increased demand (moderate high blood glucose) and in 18 weeks of age the islet cell size decreased indicating increased beta cell apoptosis. In support of these studies, Louise et al[348] reported that in young db/db mice, there was increased beta cell proliferation resulting in increased beta cell mass which was due to increased insulin demand (hyperglycemia). It was also seen that there was a subsequent decrease in beta cell mass in older animals 10 to 24 weeks which was characterized by decreased proliferation of beta cells and increase in apoptosis.

During islet cell expansion, not only beta cells undergo alteration during the disease progression, alpha and delta cells have also shown to be altered[332]. In this study there was more immunoreactivity for glucagon in the db/db mice indicative of the increased number of alpha cells. The distribution of the alpha cells in the db/db mice was more disorganized, including both mantle and the inner core of the islets whereas in the control mice the alpha cells were restricted to the periphery of the islet. Three mechanisms have been proposed for the disorganised islet architecture. Firstly, mantle alpha and delta cells undergo proliferation and spread to the interior[327,329,330,332]. Secondly, some beta cells may undergo reprogramming into alpha and delta cells[328]. Finally, there is beta cell loss due to apoptosis[349]. It was noted that there was decreased staining of the insulin producing beta cells indicating degranulation of insulin. These studies with glucagon and somatostatin in the db/db mice are in agreement with previous reports showing disorganisation of both the alpha and delta cells early in diabetes, with an increase in expression within the inner core of the pancreatic islet[110,112]. Somatostatin is an important regulator of islet function through its paracrine effects on various cell types[22,350]. The cell to cell interactions are critical for maintaining these paracrine effects and the disorganisation of the islets leads to disruption in the signalling and abrupt secretion of insulin and glucagon[112]. This chapter further confirms that the plasma insulin at the earlier age is significantly high at 4 wk of age in the db/db mice and decreases as the age increases and therefor indicate that they are insulin resistant at early age and the decline in insulin at 18 weeks correlates with

the decreased beta cell mass. Zn is an essential trace element which is involved in the formation of mature insulin (Zn-insulin crystals) and it is also known that it is rich in secretory granules of islet cells and released during secretion of insulin and possibly other islet hormones. In the next chapter the regulation of total and labile Zn, Zn binding protein metallothionein will be investigated in the early, moderate and late diabetic db/db mice group.

CHAPTER 4 Measurement of zinc and zinc-binding protein metallothionein in db/db mice liver, pancreas and pancreatic islets

4.1 Introduction

Zn is obtained from the diet and is absorbed in the small intestine and carried by the protein albumin through the circulation to liver, pancreas and other organs[351,352]. Insufficient Zn in the tissues, via decreased absorption of Zn or increased losses of Zn from the body, results in Zn deficiency. Growth, wound healing, immune function, cognition and many other functions in the body are impaired in Zn deficiency, which in severe conditions can be fatal[353,354] .

Recent developments in our understanding of type 2 diabetes have been heightened by the relevance of dysfunction in Zn signalling in this disease. Patients with poorly controlled diabetes mellitus have been reported to have decrease in Zn in the plasma/serum (hypozincaemia), decrease in Zn in the circulating leukocytes and enhanced loss of Zn through the urine (hyperzincuria)[355-359]. Whether abnormalities in Zn homeostasis are a consequence of the diabetic state or contribute to the pathogenesis is not known. In support of the latter, Zn deficiency is known to impair glucose-induced insulin secretion while Zn chelators induce beta cell death and diabetes in some species[360]. Zn supplementation has been shown to reduce the severity of the disease in some patients[355] while, in animal studies, both streptozotocin induced diabetic rats[361] and db/db mice[362] had lowering of blood glucose levels to normal levels following Zn administration (intra-peritoneal or oral Zn).

It has long been known that beta cells are very rich in Zn, that this metal plays an important role in the storage and release of insulin and that it is released along with insulin in response to glucose stimulation[266]. While Zn is required for multiple metalloenzymes within the acinar tissue, there are even higher amounts of Zn in the islets of the pancreas[363]. There are two forms of Zn in the pancreatic islets:- labile Zn and tightly-bound Zn. The latter is required for the function of many metalloenzymes and transcription factors and maintains the integrity of cell membranes. Zn metallothionein complex, present in the cytosol of the pancreatic islet cells, is involved in the scavenging hydroxyl radicals in vitro. Labile islet Zn is found in the insulin-containing secretory granules and involved in the synthesis, maturation and storage of insulin[250,363].

Very little is known about what happens to the intracellular levels of Zn in the pancreas or the pancreatic islets during the development of diabetes. Studies aimed at measuring changes in islet cell Zn in diabetes have been hampered due to the lack of sensitive techniques to visualise and measure the relevant pools of intracellular Zn. Atomic absorption spectrometry is routinely used to measure total cell or tissue Zn that is tightly bound by metalloenzymes and non-exchangeable Zn[150,364]. A colorimetric stain for Zn, dithizone, forms a red precipitate with Zn and this has been used to stain islet Zn[265,365]. However, dithizone is relatively insensitive and not suitable for quantification. Zalewski et al used a UV excitable intracellular Zn specific flurophore zinquin to fluorescently label free or loosely bound (labile) Zn in cells[186]. Ester groups are present as in the calcium flurophores so that following cleavage by intracellular esterases the probe will carry a negative charge and be trapped within the cell. Zinquin reveals the very high content of labile Zn in pancreatic islets and in particular in the insulin containing secretory granules[366]. This pool of Zn was substantially decreased in response to glucose in vitro[367]. A related compound 6-Methoxy-(8-p-toluenesulfonamido) quinoline (TS-Q) has also been used effectively to label Zn in islets[368] . These two fluorophores rely on UV excitation which is not ideal because of rapid bleaching of the fluorophore and potential artifacts due to autofluorescence of tissue. A range of other Zn fluorophores have now been developed, including 4′,5′-Bis[bis(2-pyridylmethyl)aminomethyl]-2′,7′-dichlorofluorescein (ZINPYR-1) which gives a more stable tissue fluorescence in the FITC wavelength range[369].

The aim this chapter is to report experiments which were designed to measure total and labile (granular and bound to metallothionein) in the liver and pancreas (pancreatic islets) of db/db mice in early and late diabetes. In these studies 3 methods were used i) atomic absorption spectrometry to measure the Zn in liver, pancreas and plasma, ii) cadmium haemoglobin affinity assay to measure the cytosolic Zn-metallothionein complex in the liver and pancreas and iii) ZINPYR-1 and image analysis to measure the labile Zn in the pancreatic islets at various stages during the development of type 2 diabetes in db/db male mice.

It was hypothesised that:

- The Zn in the db/db mice organs will be significantly lower as early as 4 weeks of age than the age matched controls

- The Zn in the pancreatic islets and not the acinar will be significantly decreased compared to age mathed controls.

4.2 Methods:

4.2.1 Tissue collection and processing for Zn analysis for plasma, liver and pancreas:

Liver and pancreas were removed from groups of db/db or wildtype mice (6-8 mice) at ages 4, 10 and 14 weeks. Livers were added to 4 volumes (optimised method in the lab) of 10mM TRIS-HCL buffer (10mM, pH 8.2) while pancreas was added to nine volumes. The liver and pancreas were homogenised using a Potter-Elvehjem homogeniser ensuring that the organs were completely squeezed past the pestle five times. The homogenates were transferred to 1.5ml eppendorf tubes. Borex tubes (75x12mm in size) were numbered and weighed as (W1). 500μL of the organ homogenates were transferred into the tubes and reweighed (W2). The borex tubes with the samples were then placed in a heating block (Ratek, Boronia, Victoria, Australia) at 80°C overnight. The tubes were cooled and weighed the next day as (W3). 1ml of Aristar 69% nitric acid (Merck, Darmstadt, Germany) was added to each tube and tubes were placed in the heating block at 50°C for 15 minutes until the samples were dissolved. Tubes were then vortexed and heated to 100°C to allow nitrogen dioxide to boil off and the solution to go clear yellow; then the temperature was raised to 150°C to evaporate the samples to dryness. 1.5 ml of 1M hydrochloric acid (Merck, Darmstadt, Germany) was added and the tubes were vortexed and placed at 50°C in the heating block. Appropriate number of 10ml tubes for samples, calibrators and quality control (Seronorm) (SERO, Stasjonsveien, Billingstad, Norway) were labelled and 150μL of sample, calibrator and quality control were diluted with 1ml of working diluent using a Hamilton diluter. Total Zn was measured by absorption at 214 nm in a PE 3030 Flame Atomic Absorption Spectrometer with a graphite furnace HGA 400 (Perkin Elmer).

4.2.2 Tissue collection and processing for metallothionein (MT) assay by cadmium haemoglobin affinity assay (for liver and pancreas):

The livers were diluted (1:5) and pancreas (1:10) with TRIS HCL Buffer. The tissue was homogenised using the Potter-Elvehjem Homogeniser and was squeezed past the pestle five time and was always kept cold. The homogenised tissue was transferred into a 1.5ml eppendorf tubes and was labelled. The samples were heat treated for 2 min and then cooled in ice cool water for 2 min. The samples were centrifuged for 2 min at 14,000 g and the supernatant was transferred into a new 1.5ml eppendorf tube.

Aliquots of homogenised liver and pancreas were transferred into 1.5ml eppendorf tubes and heat treated by placing into boiling water from 2 mins before cooling in ice water. The samples were centrifuged for 3 min at 14,000 g. Supernatant was transferred into a new tube and stored at -80°C until metallothionein (MT) analysis. The supernatant and quality control were thawed and centrifuged for 1 min at 13,000 g. 40μl of supernatant and quality control (sample of known concentration) were diluted and vortexed with 960μl TRIS buffer (pH 7.4). 200μl of the samples were transferred to a new eppendorf tube containing 200μl of radioactively labelled cadmium (0.5 MBq, New England Nuclear, Sydney). The samples were incubated for 15 min. 100μl of haemoglobin was added to the samples to remove any unbound cadmium and the samples were heat treated for 2 min and then placed on ice cold water before centrifugation (13,000 g). This process was repeated twice. 400μl of the clear supernatant from the samples was transferred into Borex tubes for MT analysis. The MT concentration in the supernatant was determined using a gamma counter (Parkard Auto Gamma 5650) (Waltham, Massachusetts, USA).

4.2.3 Zinpyr-1 staining for labile islet Zn:

ZINPYR-1(Mellitech, Grenoble Cedex, France) powder was solubilised with DMSO to make stock solution (5mM). ZINPYR-1 was diluted in PBS to a final concentration of 1μM and added to 5 micron tissue cryosections for 20 min at 37°C. Slides were then washed with PBS and a drop of DAKO fluorescence mounting medium (DAKO; Carpinteria, California, USA) was added. Slides were mounted with a coverslip and viewed by fluorescence microscopy within an hour. Images were captured on a Zeiss Apoptome microscope (Carl Zeiss GmbH, Goettingen, Germany). The images were

converted to JPEGS. Quantification of immunofluorescence was done by using FIGI image J software (NIH, Bethesda, Maryland, USA).

4.2.4   Statistics

Zn-related parameters were measured and the data log-normalized. Medians, fold-changes (relative to age-matched controls), confidence intervals and p values were determined using the R software. For most of the parameters, data are tabulated in Table 4.1.

4.3 Results

4.3.1   Systemic levels of Zn:

4.3.1.1   Zn levels in the liver

As the liver is one of the main reservoirs of Zn in the body, liver Zn was assessed in both control and db/db mice at 4, 10 and 14 wk. The liver Zn concentrations were calculated on dry weight basis and equal amount of homogenised tissue was added to each borex tube to adjust for the size of the livers. Data are shown in Figure form in Fig 4.1 and in Table 4.1

Liver Zn of db/db mice was not significantly increased at 4 wk (0.9 fold of control, p>0.05) or 10 wk (1.0 fold, p>0.05). However, at 14 wk there was a significant decrease in liver Zn (0.54 fold, p<0.005).

4.3.1.2   Metallothionein levels in the whole liver

Metallothionein levels in the liver were measured as metallothionein is an important Zn binding protein which is involved in liver Zn homeostasis. Data are shown in Figure form in Fig 4.2 and in Table 4.1. There was no significant difference in metallothionein between db/db and age matched control mice at 4, 10 or 14 wk.

4.3.1.3   Zn levels in the plasma:

Zn in the plasma was assessed as another measure of systemic changes in Zn in the body during the diabetes. Zn in the plasma was measured by atomic absorption

spectrometry and expressed as μmol/L. Data are shown in Figure form in Fig 4.3 and in Table 4.1

Overall, ANOVA showed that db/db mice plasma had significantly higher Zn concentration compared to controls. However there was no significance in the mean differences in db/db mice at each individual age (4,10 and 14 wk) compared to age matched controls.

4.3.1.4 *Zn levels in pancreas*

Total Zn in the pancreas was assessed to see whether pancreatic Zn levels decrease in the db/db mice model as previously reported[362,370]. Pancreas weight in db/db mice was calculated on the dry weight basis and equal amount of tissue homogenate was added to the reaction tube and expressed as nmol/g dry weight. Data are shown in Figure form in Fig 4.4 and in Table 4.1

ANOVA analysis of pancreatic Zn content showed differences due to both age and disease. With regards to disease, there were significant decreases in pancreas Zn at both 4wk (0.44 fold of control, $p < 0.005$) and at 10 wk (0.66 fold, $p < 0.005$). However, at 14 wk there was no significant decrease (0.78 fold, $p > 0.05$). Most of the decrease in Zn in the db/db mice occurred by 4 wk. There was also an age-effect. In the WT mice, there was a substantial drop in pancreatic Zn between 4 and 10 wk of age.

4.3.1.5 *Metallothionein levels in the whole pancreas*

Metallothionein is also involved in Zn homeostasis in the pancreas and therefore was measured in the whole pancreas of db/db and age matched controls at 4, 10 and 14 wk. Data are shown in Figure form in Fig 4.5 and in Table 4.1. There was no significant difference in metallothionein levels between the db/db and age matched controls at any of the age groups.

4.3.2 *Labile Zn in the pancreatic islets*

In section 4.2.2, a significant decrease in total pancreatic Zn was observed. However, as the pancreas is composed of both endocrine and exocrine tissue, this result provides no information on whether the loss was in endocrine or exocrine compartments. To address this, I used a Zn binding fluorophore ZINPYR-1 to investigate the distribution of labile Zn in the pancreatic islets and the effect of diabetes on these Zn pools. The pancreas was removed from mice at 4 and 18 wk. 5μM frozen pancreas sections were cut and attached to poly-lysine subbed slides. These were incubated with 1μM of ZINPYR-1 for 30 mins in a 37°C incubator. Slides were then washed, mounted and fluorescence images captured (see methods).

Figure 4.6 shows typical images of the distribution of labile Zn in islets from control and db/db mice at 4 and 18 wk. In control mice, ZINPYR-1 stained both acinar tissue and islets. However, islets stained much more intensely than acini. There was a heterogenous, granular-like labile Zn distribution in the control islets. In db/db mouse islets, the loss of the fluorescence was almost uniform throughout each islet although occasional cells remained brightly fluorescent (arrows in Fig 4.6). The loss of Zn in the db/db mice pancreas was in the islets rather than in the acinar tissue. Data are shown in Figure form in Fig 4.7 and in Table 4.1

As for total pancreatic Zn determined by AAS (section 4.2.2), there were both age and disease effects on ZINPYR-1 measured labile islet Zn. At 4 wk, in db/db mice, there was a significant decrease in pancreatic islet Zn (0.66 fold of control $p<0.05$). However, at 18 wk, there was no significant difference in the Zn levels between db/db and controls. The reason for the latter was that there was a substantial loss of islet Zn staining in the control mice between 4 and 18 wk of age. The loss of Zn at 4 weeks in the db/db mice indicates that Zn is important at the young age.

Table 4.1 Zinc-related measurements in db/db model

Zinc-related measurements in db/db model

Parameter	Wk	WT	Db/db	Units	Fold-Change	Lower CI	Upper CI	n	P value
Liver Zn	4	1904	1701	nmol/g	0.9	0.69	1.15	6-8	ns[b]
	10	1193	1193	nmol/g	1.0	0.78	1.29	6-8	ns
	14	1683	909	nmol/g	0.54	0.42	0.70	6-8	< 0.005
Liver MT	4	7	7.3	nmol/g	1.0	0.5	2.0		ns
	10	5.2	4.7	nmol/g	0.90	0.4	1.9		ns
	14	7.1	5.7	nmol/g	0.80	0.4	1.8		ns
Plasma Zn	4	9.8	12.7	µmol/L	1.3	0.9	1.9		ns
	10	8.7	11.3	µmol/L	1.3	0.8	2.9		ns
	14	9.7	12.2	µmol/L	1.3	0.8	2.1		ns
Pancreatic Zn	4	2295	1019	nmol/g	0.44	0.34	0.59	6-8	< 0.005
	10	1435	945	nmol/g	0.66	0.50	0.86	6-8	< 0.005
	14	1582	1227	nmol/g	0.78	0.59	1.02	6-8	ns

Pancreatic MT	4	33	35	nmol/g	1.1	0.5	2.3		ns
	10	28	24	nmol/g	0.8	0.4	1.7		ns
	14	34	23	nmol/g	0.7	0.3	1.4		ns
Islet Zn	4	110	73	afu[a]	0.66	0.43	1.01	6-8	< 0.05
	18	75	66	afu	0.87	0.58	1.29	6-8	ns

a Arbitrary fluorescence units
b Not significant
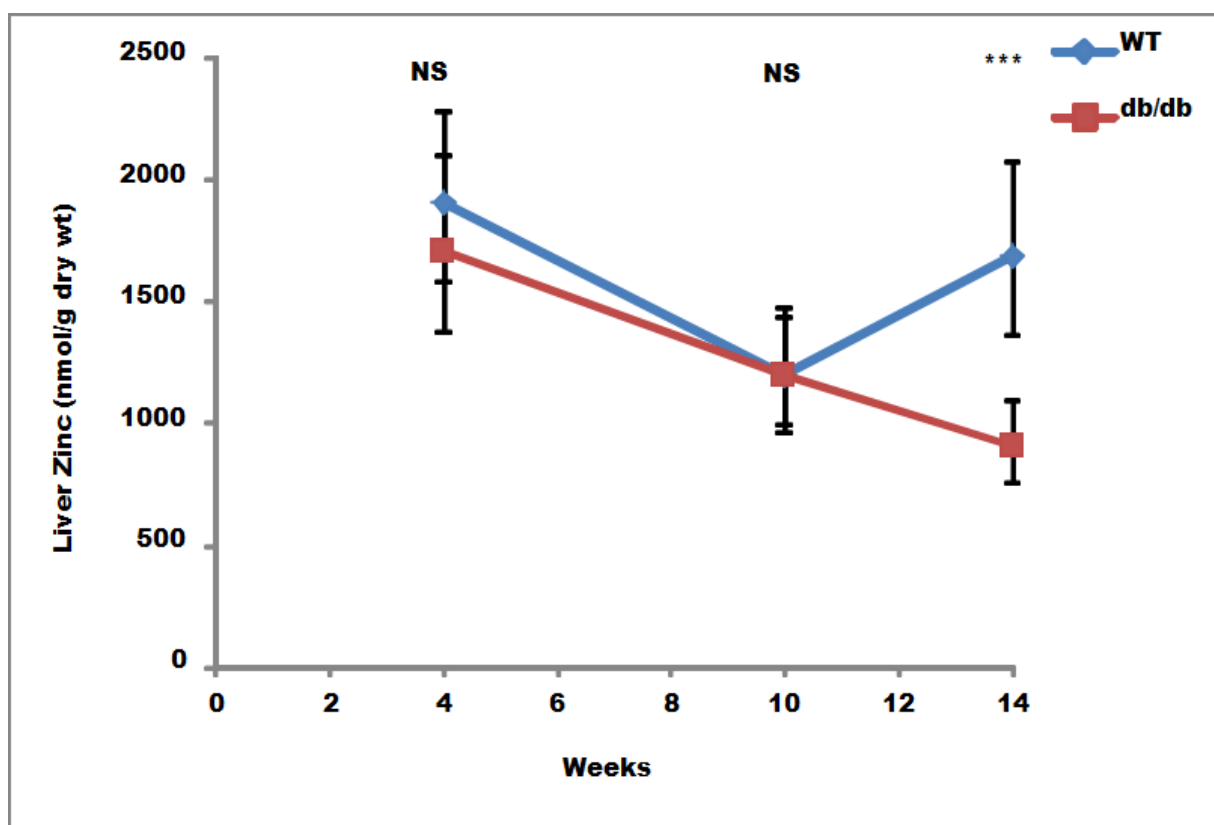
Figure 4.1 Effect of age and diabetes on liver Zn in db/db mice

Figure shows that the db/db mice did not have any significant differences in liver Zn at 4 and 10 weeks compared to age matched wild type mice. However a significant reduction was seen at 14 week of age. The X axis represents the weeks (age of mice) and the Y axis represents the liver Zn (nmol/g dry weight). Wild type mice are shown as the blue lines and the db/db mice are shown as the red lines. The data is shown as medians and the range as confidence intervals. * ($p<0.05$), ** ($p<0.005$) and *** ($p<0.0005$). Statistical analysis was performed by Type 2 ANOVA. 6-8 mice were used at each time point, and each point was a single Zn measurement.
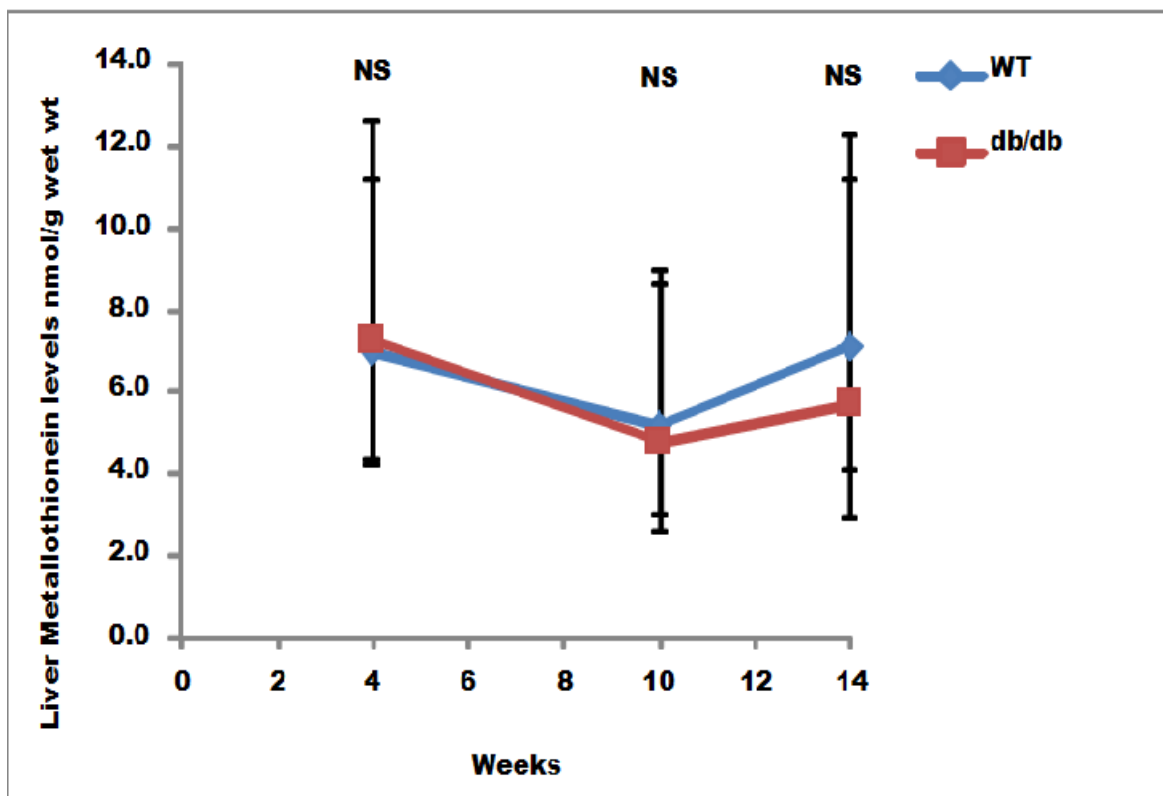
Figure 4.2 Effect of age and diabetes on liver metallothionein in db/db mice

Figure shows that the db/db mice did not have any changes in their liver metallothionein levels at any of the age groups compared to age matched wild type mice. The X axis indicates the age of mice (weeks) and the Y axis represents the liver metallothionein (nmol/g dry weight). Wild type mice are shown as the blue lines and the db/db mice are shown as the red lines. The data is expressed as medians and the range as confidence intervals. * ($p<0.05$), ** ($p<0.005$) and *** ($p<0.0005$). Statistical analysis was performed by type 2 ANOVA. 6-8 mice were used at each time point, and each point was a single a single Zn measurement.
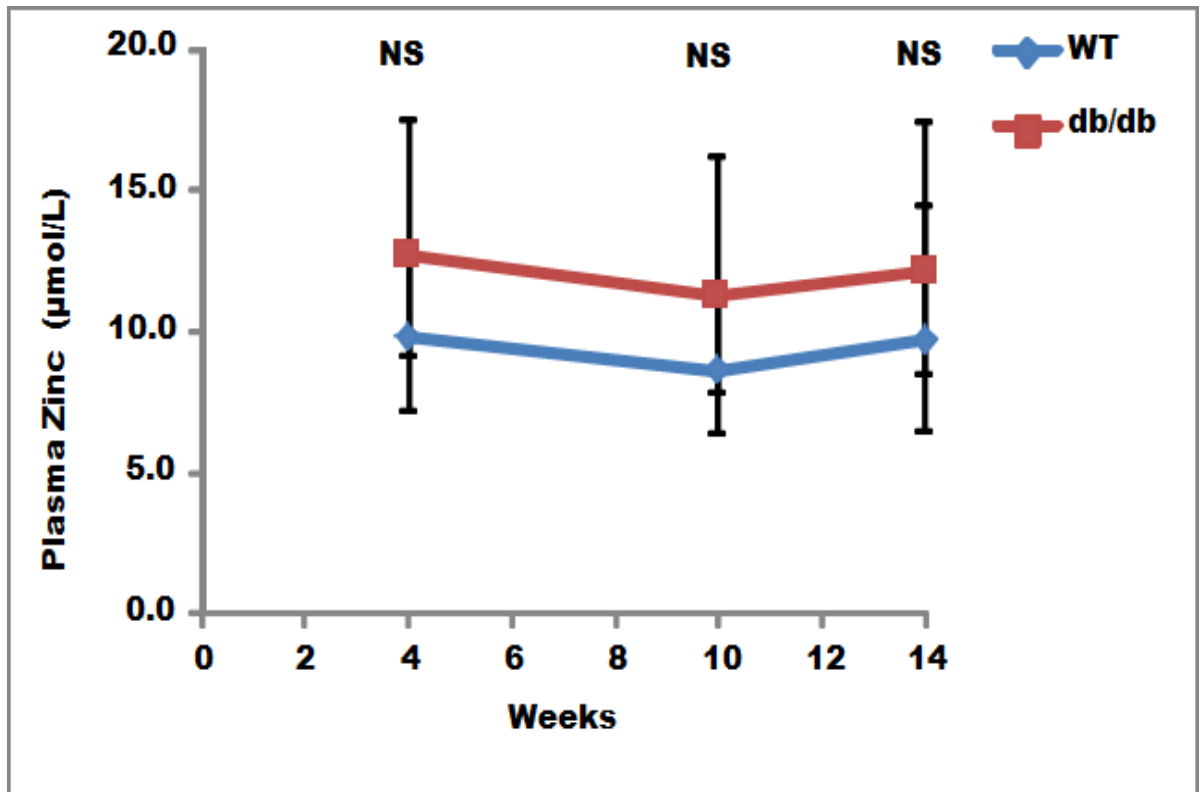
Figure 4.3 Effect of age and diabetes on plasma Zn in db/db mice

Figure shows that the db/db mice did not have any significant changes in plasma Zn compared to age matched wild type mice. The X axis represents the age of mice (weeks) and the Y axis represents the plasma Zn (nmol/g dry weight). Wild type mice are shown as the blue lines and the db/db mice are shown as the red lines. The data is expressed as medians and the range as confidence intervals. * (p<0.05), ** (p<0.005) and *** (p<0.0005). Statistical analysis was performed by type 2 ANOVA. 6-8 mice were used at each time point, and each point was a single Zn measurement.
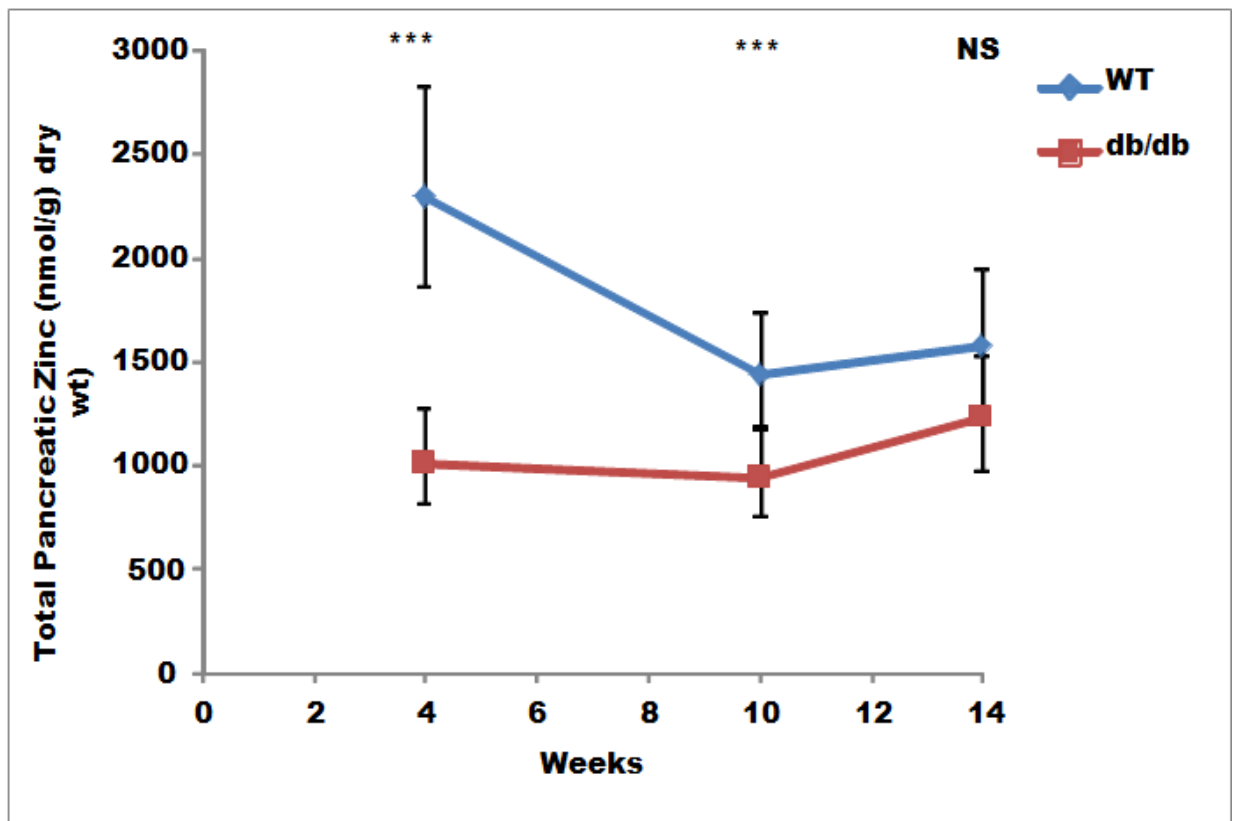
Figure 4.4 Effect of age and diabetes on pancreatic Zn in db/db mice

Figure shows that the db/db mice had a significant reduction in pancreatic Zn as early as 4 weeks of age. Pancreatic Zn was also reduced at 10 weeks compared to age matched wild type mice. The X axis represents the age of mice (weeks) and the Y axis represents the pancreas Zn (nmol/g dry weight). Wild type mice are shown as the blue lines and the db/db mice are shown as the red lines. The data is expressed as medians and the range as confidence intervals. * ($p<0.05$), ** ($p<0.005$) and *** ($p<0.0005$). Statistical analysis was performed by type 2 ANOVA. 6-8 mice were used at each time point, and each point was a single Zn measurement..
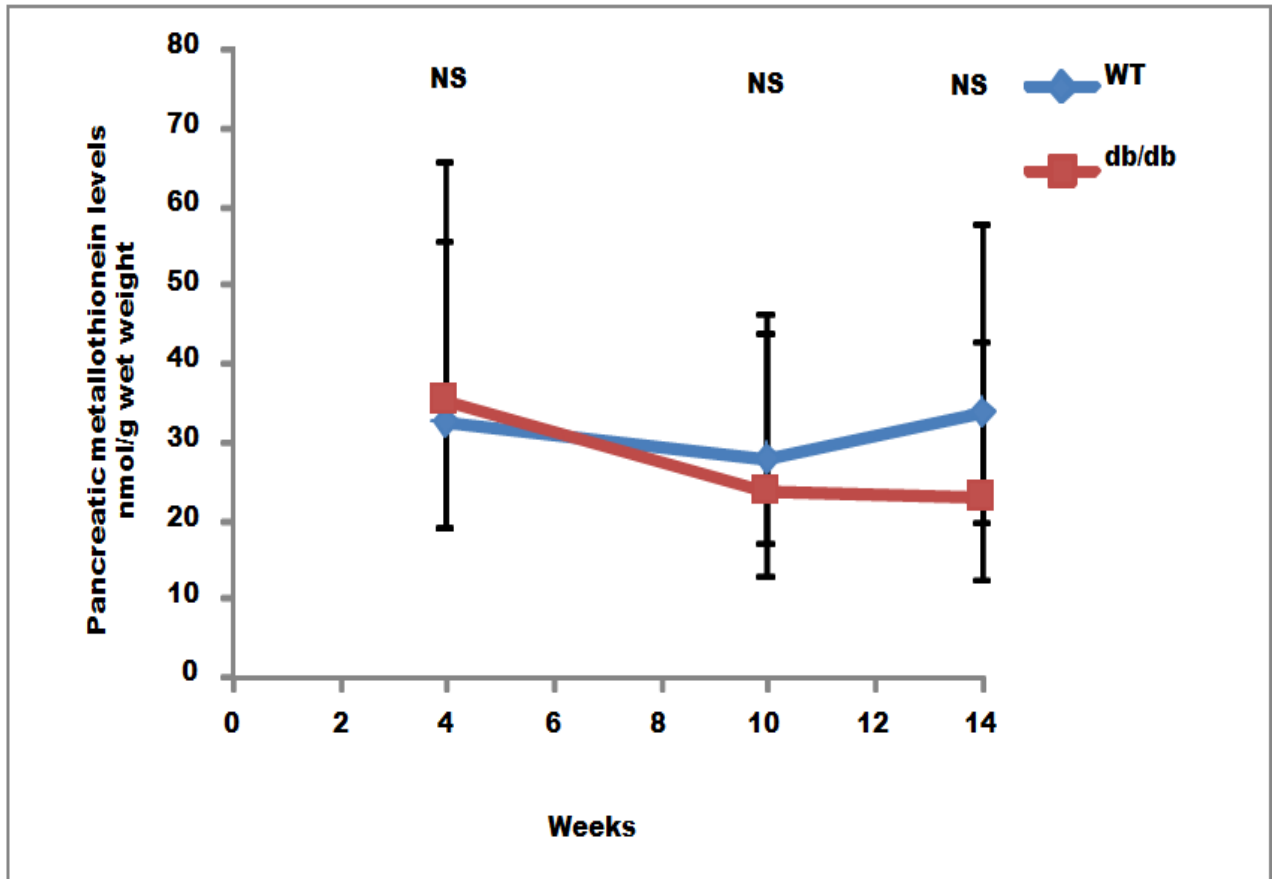
Figure 4.5 Effect of age and diabetes on pancreas metallothionein in db/db mice

Figure shows that the db/db mice did not have any changes in their pancreas metallothionein levels at any age compared to age matched wild type mice. The X axis represents the age of mice (weeks) and the Y axis represents the pancreas metallothionein (nmol/g dry weight). Wild type mice are shown as the blue lines and the db/db mice are shown as the red lines. The data is shown as medians and the range as confidence intervals.   * ($p<0.05$), ** ($p<0.005$) and *** ($p<0.0005$). Statistical analysis was performed by type 2 ANOVA. 6-8 mice were used at each time point, and each point was a single a single Zn measurement.
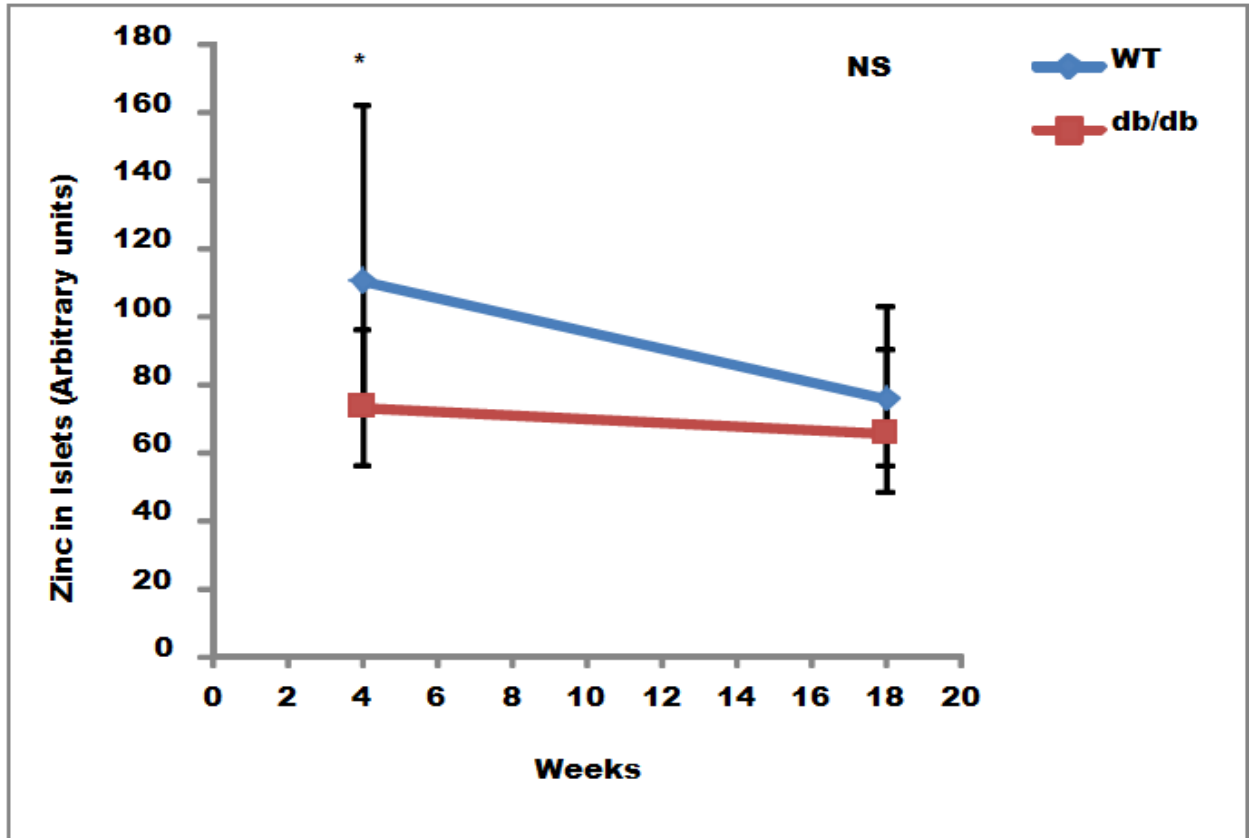
Figure 4.6 Effect of age and diabetes on pancreatic islet labile Zn in db/db mice

Figure shows that the db/db mice had a significant reduction in pancreatic islet labile Zn as early as 4 weeks of age compared to age matched wild type mice. The X axis represents the weeks (age of mice) and the Y axis represents the pancreas islet labile Zn in (arbitrary units). Wild type mice are shown as the blue lines and the db/db mice are shown as the red lines. The data is shown as medians and the range as confidence intervals. * ($p<0.05$), ** ($p<0.005$) and *** ($p<0.0005$). Statistical analysis was performed by type 2 ANOVA. 6-8 mice were used at each time point, and each point was a single Zn measurement.
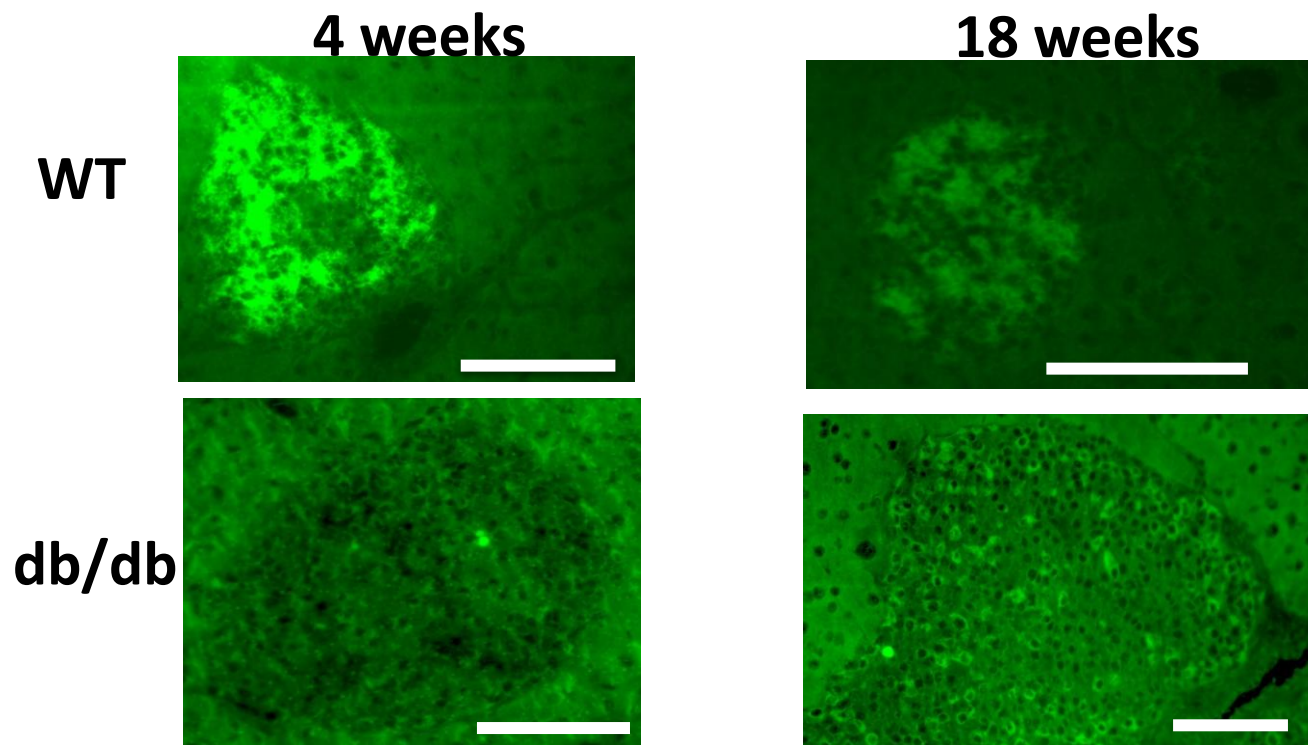
Figure 4.7 Islet Zn distribution in typical islets of 4 and 18 week old db/db mice

Figure shows typical islets stained with ZINPYR-1 for islet Zn in frozen sections of 4 and 18 week old wild type mice (upper panel) and db/db mice (bottom panel). The Zn staining was greater in the wild type mice at 4 and 18 weeks. In the db/db mice pancreatic islets had a reduction of Zn, mostly in the insulin producing beta cells. At 18 weeks, in db/db mice pancreatic islets, there was preservation of Zn in the non-beta cells, likely alpha and delta cells..

4.4 Discussion

Previous studies have not established whether the Zn loss in the pancreas during diabetes is a late event and therefore a consequence of diabetes or an early event that may be influencing the development of type 2 diabetes. Therefore, as described in chapter 4 of this thesis, both total Zn (measured by AAS) and labile Zn (visualized and measured by Zn fluorophore ZINPYR-1) were studied in db/db mice versus controls at three ages: 4 wk (early diabetes), 10 wk (diabetes) and 18 wk (chronic diabetes).

No systemic changes in Zn levels in the db/db mice.
Liver was included in this study as it is a reservoir for Zn and an indicator for systemic Zn levels in the body. At 4 and 10 wk in the db/db mice , there was no significant change in the liver Zn. However, there was significant reduction of Zn in the 14 wk db/db mice compared to controls. The db/db mice at 4, 10 and 14 wk showed a trend to decrease in Zn content. As it it has been reported that they have high fat content in their livers[371,372], this may be due to artifact related to fat content and this will be claified in future studies, there was no significant change in the liver Zn in the control mice with age.

Plasma zinc is another indicator of systemic Zn levels. At 4, 10 and 14 wk db/db mice, there were no significant changes in the plasma Zn levels compared to age matched wildtype (although the db/db mice group had significantly higher Zn than wildtype) suggesting that the systemic Zn levels are not altered. Therefore they are not Zn deficent at the whole body level, although they may be local changes in the Zn levels within the pancreas. There was no significant change in the control mice plasma Zn levels.

An important question is whether the loss of Zn in the diabetics islets is a consequence of a systemic zinc deficiency . If so, low dietary intake of Zn might be a factor in diabetes and zinc supplements could therefore prove useful as an aid to therapy. It is relevant here that zinc supplements have been shown by others to be beneficial in attenuating hyperglycemia in db/db mice [362]. Excessive loss of zinc from the body (e.g. via urine) could also be important. Mechanisms are in place in the body to move zinc from plasma to liver during the acute phase response in stress, trauma, infection and inflammation[373]. This has been shown, for example, to have adverse consequences for the foetus in maternal zinc deficiency [374].

135

Therefore, it was important to determine whether changes in systemic levels of zinc occur in db/db mice, especially during early diabetes when zinc loss in the pancreas and islets is already apparent. Three measures of systemic zinc used in this thesis were liver zinc, plasma zinc and liver metallothionein. It is not clear to what extent loss of pancreas and islet Zn in diabetes is due to local effects on Zn or due to systemic Zn changes. Both pancreas and liver have been considered to be reservoirs of Zn in the body. Plasma Zn is the major transport pool of Zn in the body. Plasma Zn and liver Zn were therefore measured in the db/db mice as indicators of systemic Zn levels. Neither changed significantly from early diabetes to chronic diabetes. Therefore, islet Zn loss is not accompanied by whole body changes in Zn.

Loss of Zn in the pancreas of db/db mice occurred early in diabetes and was maintained into late diabetes, compared to age matched controls

The next question to be addressed was to investigate the Zn levels in the whole pancreas by flame atomic absorption spectrometry. The major decrease in Zn is during early diabetes (4 wk) and at 10 and 14 wk the difference was still significant but less pronounced as there was a decrease in 10 and 14 wk Zn levels in the control mice. There is substantial evidence that tissue Zn is reduced during aging in multiple organ systems. This may explain why the difference in pancreatic Zn levels are less pronounced between control and diabetic mice at later ages.

Novel studies with ZINPYR-1 indicated that in the diabetic mice there was loss of labile zinc in the islet beta cells but not in the alpha cells

In 1984, Figlewicz et al [367] determined that there were three distinct pools using uptake of radioactive Zn 65 distribution. In rat pancreatic islets treated for 24 hour with high or low glucose there was reduction of islet zinc and insulin. They concluded that zinc in islets exists in secretory granules, extra granular pools and a poorly-defined metabolic labile islet compartment. A more recent study (Nicolson et al 2009)[265] showed there were two pools of beta cell Zn as Zn flurophore Zinquin labelled the secretory granules while another Zn fluorophore FluoZin-3 labelled cytosolic Zn. Zinquin has some disadvantages including its requirement for UV excitation and rapid quenching of fluorescence. Other fluorophores for Zn have since been developed. One of the best of these is ZINPYR-1 and this was chosen for

the experiments in this thesis. Like other Zn fluorophores there is preferential detection of labile Zn pools (since ZINPYR-1 is not able to compete for Zn in the tightly bound metalloprotein pools). To the best of my knowledge this is the first description of ZINPYR-1 in pancreatic islets.

Labile Zn detected using ZINPYR-1 in the islets of the control mice had a granular-like pattern which likely corresponds to the beta cell insulin-containing secretory vesicles. The staining was heterogeneous. Some islets were stained more brightly than others; this may indicate different levels of Zn in the granules due to the islets being in different phases of secretion. For example, an islet which has recently secreted insulin would be expected to have less Zn than one in resting phase.

Limited studies report the role and function of Zn in alpha cells and how this could influence the role and function of insulin. In 2001, Kristiansen et al reported zinc in the periphery of granules in alpha cells using electron microscopy following staining of Zn by autometallography (a process which allows ultrastructural monitoring of Zn in cells)[375]. Consistent with this, the peripheral alpha cells (identified by glucagon staining) also fluoresced strongly with ZINPYR-1, indicating they are also rich in labile Zn. Since large amounts of Zn are generally found in a variety of endocrine cell granules, this may indicate that Zn is contained within the glucagon-containing granules of the alpha cells. It is known that glucagon is unaltered in the pancreatic islets of db/db mice ([110,112,376] confirmed by many studies and also confirmed by the present study in chapter 3).

The islets in the early diabetic mice had substantial loss of ZINPYR-1 detectable Zn in the beta cells; however, the alpha cells retained their Zn. This observation could be correlated with the retention of glucagon staining in the early diabeteic islets. Not all beta cells of the islet showed a decrease in Zn. There were areas in which beta cells appeared to lose Zn first. This is consistent with the alpha cells progressively replacing the beta cells during the development of the type 2 diabetes. In the chronic diabetic mice, it could be seen that the Zn was still retained in the alpha cells and there was almost complete loss of Zn in the beta cells. An interesting question is whether ZINPYR-1 detects Zn complexed within the stored insulin-Zn crystals or whether it only fluoresces with granule Zn that has not yet incorporated

into the crystals. Isolating the db/db mice pancreatic islets and dissociating them into alpha, beta and delta cells and stain them individually could give us more clues on which cells still contain Zn in them.

These studies suggest that ZINPYR-1 will be a useful Zn fluorophore for islet cell Zn measurements. Zinquin appeared to confirm the loss of zinc in early diabetes, although the quality of staining precluded a rigorous quantitative study.

Zn is involved in making the proinsulin more soluble in solution and is involved in hexamerisation of proinsulin[377]. In low zinc concentrations it was reported that the mature insulin precipitates; however, proinsulin remains stable in the rough endoplasmic reticulum and transport to the Golgi apparatus where the process of conversion of the pro-insulin to the mature insulin occurs. In the 4 wk db/db mice (early diabetes), insulin was reduced compared to wildtype mice. Therefore the loss of Zn could be a factor in the precipitation and exhaustion of mature insulin in beta cells in early diabetes.

There was no change in protein levels of pancreas and liver metallothionein during the development of diabetes in the db/db mice

Metallothionein is a small, cysteine-rich cytosolic protein capable of binding large amounts of certain metal ions, including Zn. It is strongly up-regulated by these metal ions through a metal response element in the gene. Metallothionein has been proposed to play a role in preventing metal toxicity by buffering cytosolic metal ions so that free metal ions do not reach toxic concentrations. In addition to actions of metallothionein on Zn homeostasis within islets, liver metallothionein is also interesting since it is responsible for large shifts of Zn from plasma to liver during acute stress, trauma and other conditions. It was therefore of interest to study both pancreas and liver metallothioneins in the db/db mice.

There was no difference in pancreatic metallothionein levels between db/db and control mice. Therefore, changes in Zn levels during the diabetes are unlikely to be a consequence of changes in metallothionein levels in the beta cell cytosol; metallothionein may therefore not be a major player in the altered zinc homeostasis in db/db mice. The liver metallothionein did not change in the db/db mice at 4, 10 and 18 wk. This was consistent with the lack of

systemic changes in the Zn pools. If there was an increase in liver metallothionein, plasma Zn would be expected to fall.

These observations suggest that zinpyr-1 is an effective Zn flurophore that can detect Zn in vesicles and showed that Zn was reduced in the db/db mice pancreatic islets compared to WT. Zinc transporters are involved in regulating Zn influx an efflux in the cell and exhibit tissue specific expression in various according to requirement. However during zinc deficiency and excess, hormones and cytokines these Zn transporters regulated differentially transcriptionally and post-transcriptionally[311,312,378-381].

In the next chapter , the changes in the Zn transporters, Zn binding protein metallothionein, TRPM3 and PDLIM7 in the pancreas of 4 and 10 weeks db/db and age matched wildtype mice, will be discussed.

CHAPTER 5 mRNA regulation of Zn transporters in whole pancreas in db/db mice and age matched wildtype (C57BL6J)

5.1 Introduction

In the previous chapter it was shown that Zn was reduced in early diabetes in db/db mice in the pancreatic islets (Figure 4.7), specifically in the beta cells. It was also shown that the Zn binding protein metallothionein was not altered in the liver and pancreas of these mice (Figure 4.4 and 4.5). There is a need to elucidate which Zn transporter genes are expressed in normal pancreatic islets. A recent study[169] has quantified relative expression of ZIP and ZnT genes in isolated islets from normal mice and it showed a wide range of levels of expression. Of the ZIP transporters, ZIP1 and ZIP7 were very highly expressed, ZIP2, 3, 8, 9, 11, 13 and 14 were moderately expressed and ZIP4, 5,6,10 and 12 were lowly expressed[169]. In the ZnT transporters, ZnT5, 7 and 8 were highly expressed, ZnT1, 4,6 and 9 were moderately expressed and ZnT2, 3 and 10 were lowly expressed in islets isolated from normal mice[169]. The effect of diabetes on the expression profile of ZIP and ZnT genes in islets now needs to be determined. . A concurrent study done by Liu et al[382], investigated the critical Zn transporter ZnT8 which is involved in bringing Zn into the vesicles containing insulin and they found that the ZnT8 gene was downregulated in the pancreas and adipocyte tissue in db/db mice compared to the heterzygote controls. However, no studies are evident investigating the expression of Zn transporter genes in the db/db mice at different age groups or at different stages of disease.

In experiments described in this chapter, we aim to determine whether Zn transporters are altered at the gene level in diabetes. The null hypothesis is that Zn transporter gene expression is not altered in early diabetes. Whole pancreata from the db/db mice and age matched controls in 4 and 10 weeks were used to investigate the gene expression of Zn transporters in diabetes. I attempted to do laser capture microdissection of the pancreatic islets of the mice, however the quality and quantity of the RNA obtained was not sufficient to carry out these studies. It would have been best done on purified islets. However, the preliminary attempts of getting good quality and quantity RNA from laser captured isolated islets was not achieved (see Figure 5.1). Therefore, the next best approach was to use the frozen pancreatic shavings. The genes that were investigated were ZnT1-10, ZIP1-14, TRPM3 and PDLIM7, Zn binding proteins metallothionein 1 and 2, insulin and glucagon, and house keeping genes HPRT1 and 18S. The reasons for

choosing the panel of genes are as follows. The aim was to investigate all of the known ZnT and ZIP transporter genes. In addition, there is evidence that Zn ion channels such as TRPM3 and PDLIM7 are capable of transporting Zn into islet cells[383,384] and metallothioneins may also mediate Zn uptake. There have not been many studies looking at expression of insulin and glucagon genes in the db/db mouse model. Preliminary studies showed that HPRT1 and 18S had the most stable expression amongst samples with varying quality and disease state.

The number of samples and genes amongst different age groups and disease necessitated using a high thoughput system such as the recently introduced low density microfluidic Taqman fluidic cards. The major advantages of this assay are that it minimizes pipetting errors, sample volumes, sample variability (tight replicate values), reduces time and reagents used and multiple controls can be incorporated into the cards so for example they can be double normalized. Custom made plates embedded with the primers for these genes were purchased, samples were loaded in the plates and centrifuged and analysed in a 7900HT ABI system University of Adelaide[385-387]. The CT values were obtained and were expressed as fold differences.

In this chapter, relative expressions of ZIPs and ZnTs in the whole pancreata of the wildtype and db/db mice at two age groups 4 and 10 weeks are reported.

5.2 Methods

5.2.1 Laser Capture Microdissection

100 islets from each mouse were captured by laser capture microdissection. The RNA was extracted using the RNAqueous Kit and the RNA quality and quantity were determined using experion (Biorad). Details in chapter 2.

5.2.2 RNA extraction from whole pancreas shavings from wildtype and db/db mice

10 micron sections were cut in the cryostat, stored in trizol and were extracted using RNA easy mini kit. RNA was reverse transcribed using Omniscript reverse transcription kit. The cDNA was preamplified using a preamplfication master mix and pool of primers (Zn transporters, metal binding proteins and islet hormones) and was run on a PCR. The preamplified sample was then loaded into the low density microfluidic card.

5.2.3 Low density microfluidic cards

Custom made cards for Zn transporters Zn binding proteins and islet hormones insulin and glucagon were designed. Primers for ZnT 1-10, ZIP1-14, Metallothionein 1 and 2, TRPM3 and PDLIM7 were selected to be on the cards. The primers were in triplicates and two house keeping genes HPRT1 and 18S were included. Up to 4 samples were added to each plate where 2 wildtype and db/db mice were run on the plate. In total 6 mice per group were analysed. The cards run on an Applied Biosystems 7900 HT instrument.

5.3 Results:

5.3.1 Laser capture microdissection of control mouse islets:

Frozen sections of mouse pancreas were embedded onto Polyester membrane slides and the islets and acinar tissue were micro-dissected and captured in the tube caps filled with lysis buffer. Figure 5.1 (Left) shows before (upper panel) and after (lower panel) micro-dissection of a captured islet. Right panel shows the quality and quantity of the total RNA recovered. The RNA quality was poor in both mouse acinar and islet tissue as seen by the lack of two distinct bands for 18S and 28S in the experion chip. Instead there were multiple bands and also showed a red colour which indicates degraded RNA and this is tabulated in the lower table. Due to the lack of good quality and quantity of RNA obtained from laser captured islets, it was then necessary to use whole pancreas scrapings. Ideally for the messenger RNA studies isolated islets would be used. However, because of the design of the experiment the whole pancreas had to be used in several different assays and it would not have been possible to use the pancreas for isolated islets.

5.3.2 RNA extraction of control and db/db mouse pancreas scrapings.

The processing of the mouse pancreas is critical to obtain good quality RNA. If the sample in experion showed degradation and gave a red signal it was discarded from the experiments (Figure 5.2). It also contains the RNA of liver, intestine and kidney samples of mice and it shows that the technique is good but pancreas RNA is difficult to obtain. The average quality of the pancreas samples was yellow and suboptimal. Because of this and low expression levels of certain genes I included a preamplification step by using the cDNA and the pool of primers of the genes that are going to be investigated, TaqMan® PreAmp Master Mix and RNAase free water. Figure 5.3 shows the difference between unamplified cDNA and amplified cDNA. Most of the samples in the unamplified were giving CT values greater than 28 cycles, whereas nearly all of the amplified cDNA gave CT values less than 28 cycles.

5.3.3 *Low density microfluidic taqman card assay of gene expression in control and diabetic mice.*

Preamplified cDNA , taqman master mix and RNAase free water were loaded into the ports of the taqman cards with the embedded primers in them. The card contained 32 genes including two housekeeping genes which were 18S and HPRT1. 18S was an endogenous control and HPRT1 was chosen of several house keeping genes that also included beta actin, GAPDH, B2M and Cyclophilin, because it was the most stable across samples (figure 5.4). The cards were then spun down in the centrifuge and were analyzed using the RT-PCR machine. The results are shown in Table 5.1 comparing 4 and 10 week control and diabetic mice for 32 genes in triplicates. Only two significant changes were observed (highlighted in red) and both of these changes involved lowly expressed genes ZnT3 and ZIP12 and were not significant across all the age groups. In addition, there was greater than expected variability between triplicates in the lowly expressing genes which may be the reason why significance was hard to find.

A

B

| Lanes | 1 | 2 | 3 | 4 |

6000
4000
3000
2000
1500
1000
500
200
50

C

Well ID	Sample Name	RNA Area	RNA Concentration (ng/µl)	Ratio [28S/18S]	RQI	RQI Classification	RQI Alert
L	Ladder	115.73	160				
1	Sample 1	9.61	13.28	0.92	3.1	Red	
2	Sample 2	5.28	7.3	1.7	N/A		RNA conc. too low
3	Sample 3	6.12	8.47	3.69	N/A		RNA conc. too low
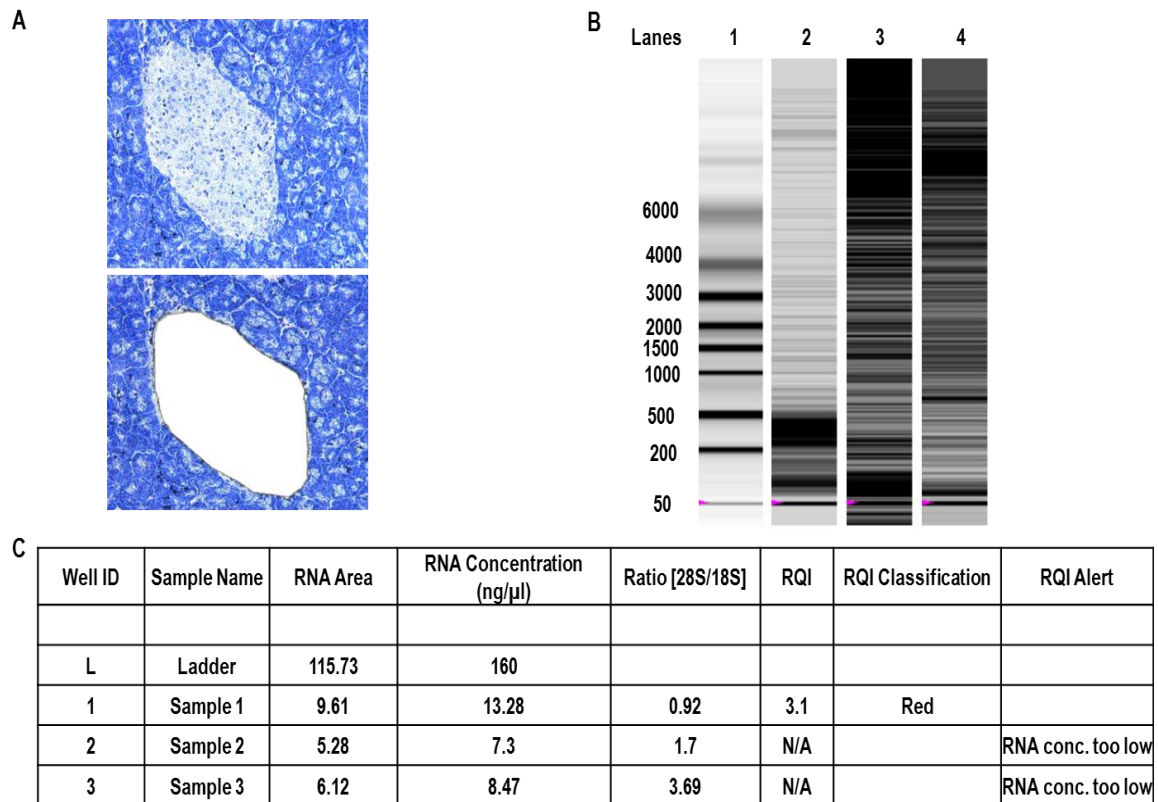
Figure 5.1 Laser capture microdissection of mouse islets and RNA quantification

Figure 5.1 (A) shows before (upper panel) and after (lower panel) micro-dissection of a captured islet. (B) shows the quality and quantity of the total RNA recovered.(C) The RNA quality was poor in both mouse acinar and islet tissue as seen by the lack of two distinct bands for 18S and 28S in the experion chip assay. 100 islets were collected.
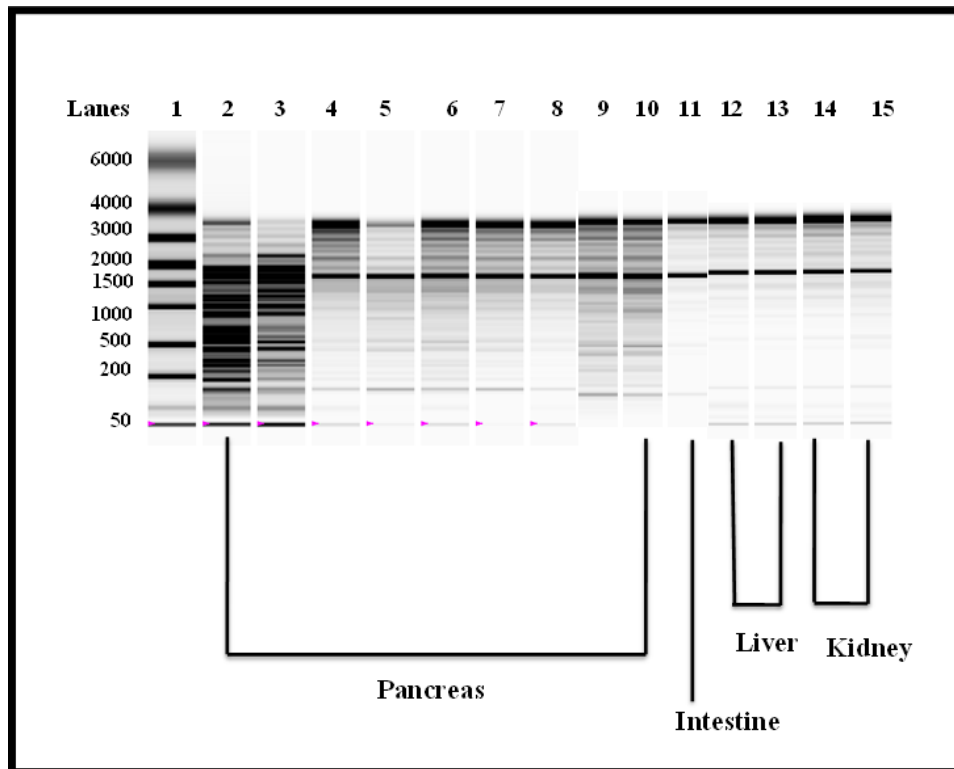
Figure 5.2 RNA extraction of control and db/db mouse pancreas scrapings

Lane 1) RNA ladder; Lane 2 to 8) pancreas samples 9) intestine; 10 and 11) liver; 12 and 13) kidney samples. The samples in lane 2 and 3 showed degradation and gave a red signal; this was discarded from the experiments. It also contains the RNA of liver, intestine and kidney samples of mice and it shows that the technique is good (lane 9-13) giving a green signal. Good quality RNA was difficult to obtain for the pancreas (yellow signal).
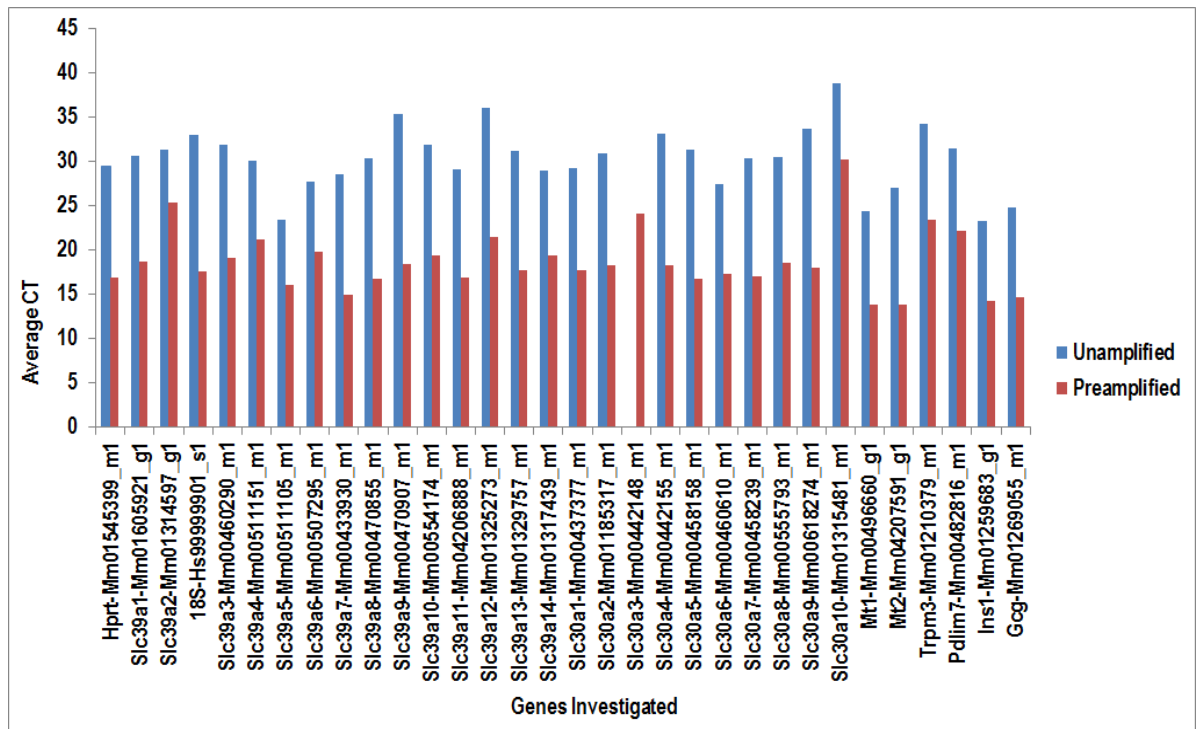
Figure 5.3 Housekeeping gene stability in varying sample quality

Figure shows line graph of the expression levels of 6 control genes HPRT1 (blue), B2M (red), Cyclophilin PP1A(green), 18S(pink) ,beta actin ACTB (black) and GAPDH(grey) determined in 5 pancreatic tissue scrapings from both control and db/db mice with varying RNA quality. HPRT1 was chosen as a control gene as it was the most stable among samples. X axes represent the samples and Y axes represents the average CT obtained from each of the house keeping genes.
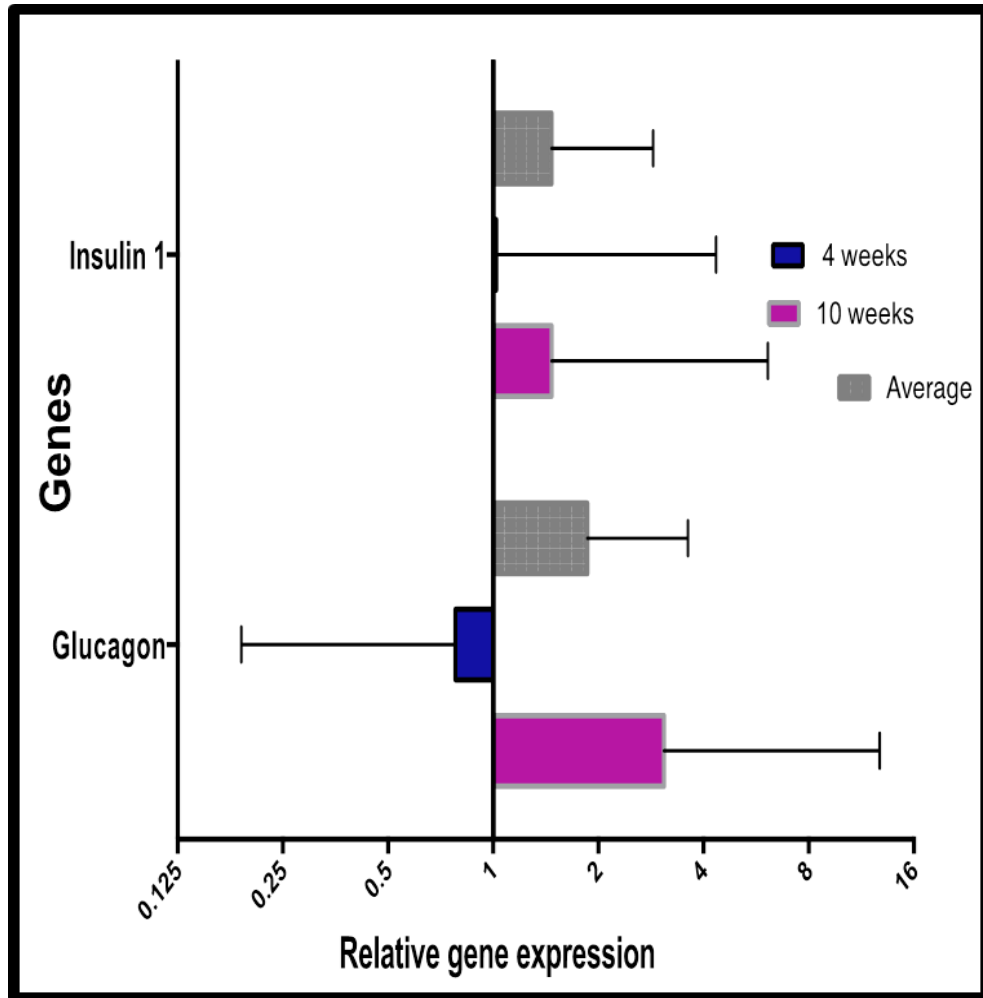
Figure 5.4 Islet hormone mRNA expression in db/db mice at 4 and 10 weeks of age.

RNA was isolated from control and db/db mice at 4 and 10 weeks of age. The cDNA was preamplified with insulin and glucagon genes (Taqman probes) and were loaded into a Taqman low density microfluidic cards containing these taqman genes, HPRT1 and 18S rRNA used as endogenous controls. n=6 mice were included in both the control and disease group. The blue in the figure represents db/db mice at 4 weeks, the pink bar graphs represents the db/db mice at 10 weeks and the grey bars represent the average over time in the genes in db/db mice. Data is presented as mean fold change (±95 Cl) compared to control (non-diabetic). *p<0.05, **p<0.01, ***p<0.001, NS, p>0.05.
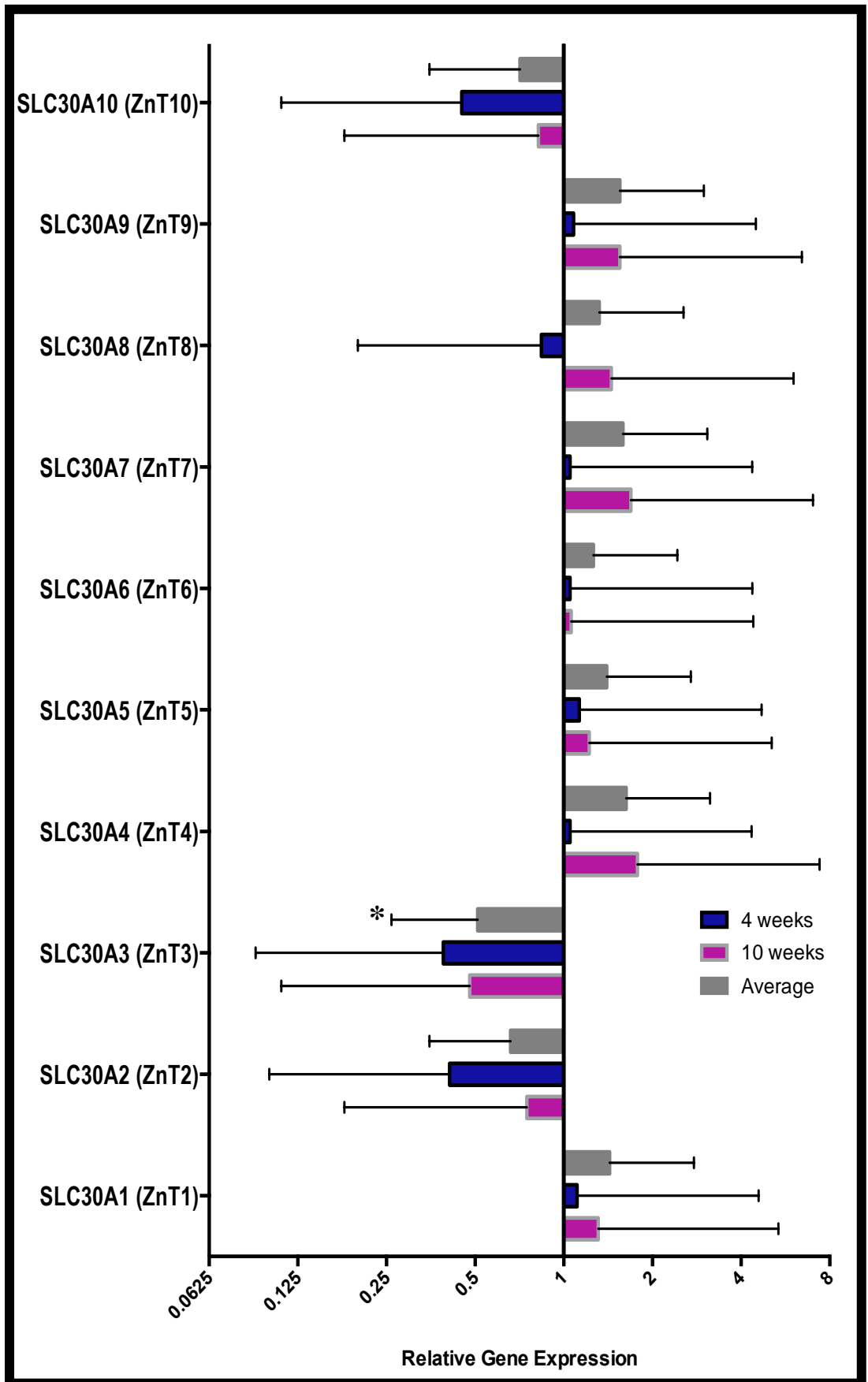
Figure 5.5 Zn transporters ZnT1-10 mRNA expression in db/db mice at 4 and 10 weeks of age and db/db mice.

RNA was isolated from control and db/db mice at 4 and 10 weeks of age. The cDNA was preamplified with Zn transporter genes ZnT 1-10 (Taqman probes) and were loaded into a Taqman low density microfluidic cards containing these Taqman genes, HPRT1 and 18S rRNA used as endogenous controls. n=6 mice were included in both the control and disease group. The blue in the figure represents db/db mice at 4 weeks, the pink bar graphs represents the db/db mice at 10 weeks and the grey bars represent the average over time in the genes in db/db mice. Data is presented as mean fold change ($\pm$95 Cl) compared to control (non-diabetic). *$p<0.05$, **$p<0.01$, ***$p<0.001$, NS, $p>0.05$.

Relative Gene Expression

Legend: 4 weeks (blue), 10 weeks (magenta), Average (gray)

Genes listed top to bottom: SLC39A14 (ZIP14), SLC39A13 (ZIP13), SLC39A12 (ZIP12) **, SLC39A11 (ZIP11), SLC39A10 (ZIP10), SLC39A9 (ZIP9), SLC39A8 (ZIP8), SLC39A7 (ZIP7), SLC39A6 (ZIP6), SLC39A5 (ZIP5), SLC39A4 (ZIP4), SLC39A3 (ZIP3), SLC39A2 (ZIP2), SLC39A1 (ZIP1)

X-axis values: 0.0625, 0.125, 0.25, 0.5, 1, 2, 4, 8, 16
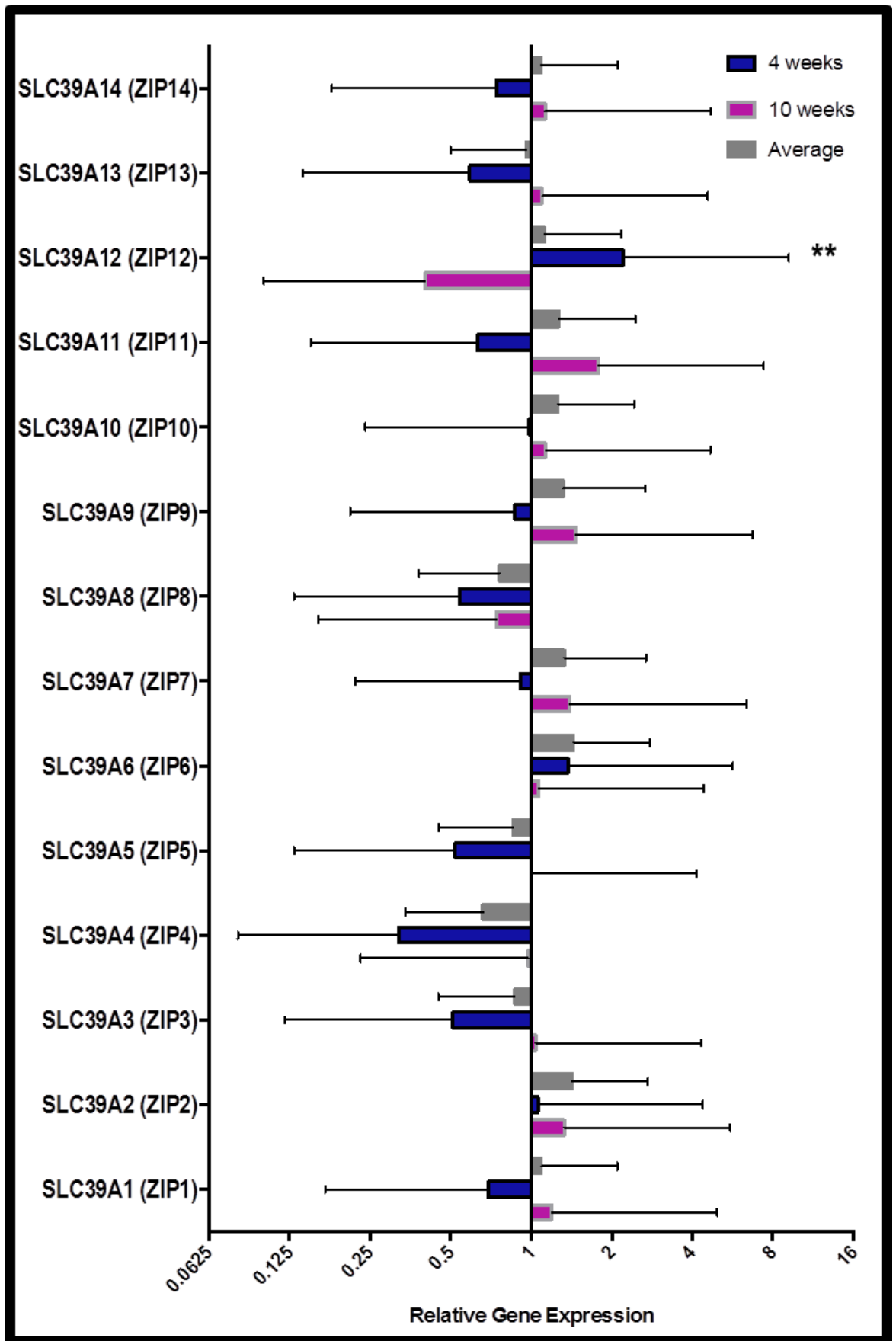
Figure 5.6 Zn transporters ZIP 1-14 mRNA expression in db/db mice at 4 and 10 weeks of age and db/db mice.

RNA was isolated from control and db/db mice at 4 and 10 weeks of age. The cDNA was preamplified with Zn transporter genes ZIP 1-14 (Taqman probes) and were loaded into a Taqman low density microfluidic cards containing these Taqman genes, HPRT1 and 18S rRNA used as endogenous controls. n=6 mice were included in both the control and disease group. The blue in the figure represents db/db mice at 4 weeks, the pink bar graphs represents the db/db mice at 10 weeks and the grey bars represent the average over time in the genes in db/db mice. Data is presented as mean fold change ($\pm$95 Cl) compared to control (non-diabetic). *p<0.05, **p<0.01, ***p<0.001, NS, p>0.05.
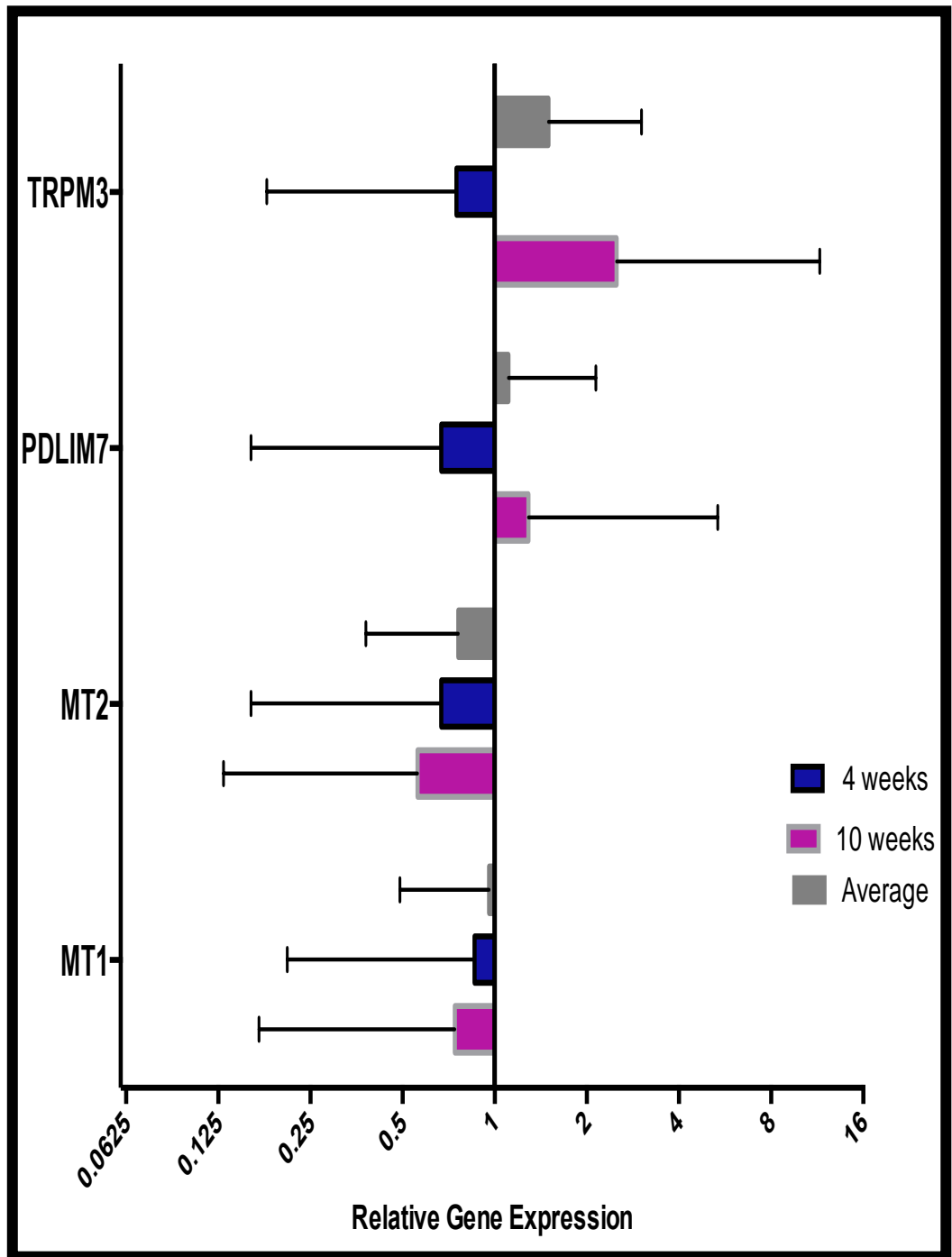
Figure 5.7 Zn binding proteins mRNA expression in db/db mice at 4 and 10 weeks of age and db/db mice.

RNA was isolated from control and db/db mice at 4 and 10 weeks of age. The cDNA was preamplified with Zn transporter genes MT1, MT2, PDLIM7 and TRPM3 (Taqman probes) and were loaded into a Taqman low density microfluidic cards containg these taqman genes, HPRT1 and 18S rRNA used as endogenous controls. n=6 mice were included in both the control and disease group. The blue in the figure represents db/db mice at 4 weeks, the pink bar graphs represents the db/db mice at 10 weeks and the grey bars represent the average over time in the genes in db/db mice. Data is presented as mean fold change ($\pm$95 Cl) compared to control (non-diabetic). *$p<0.05$, **$p<0.01$, ***$p<0.001$, NS, $p>0.05$.

5.4 Discussion

In order to investigate the gene regulation of Zn transporters, metal binding proteins and islet hormones, qPCR was used. The RNA from the whole pancreas of db/db mice at 4 and 10 weeks and age matched controls was obtained. The RNA was reverse transcribed to cDNA. The cDNA was then preamplified as described in chapter 2. There are limtations in obtaining optimal high quality and quantity RNA from pancreas tissues as they contain high proteases and nuclease which can degrade components including the RNA. The preamplification step is referred to as a nested PCR, as the cDNA is preamplified with the genes of interest (primers). The PCR product uses the same genes (primers) in the second round of RT-PCR. This is done in order to avoid further amplification of primer dimer artifacts or non specific products obtained from the primary PCR. Another advantage of using nested PCR is that the primers are internal in the PCR product and they have shorter amplicons and in the genes that are very lowely expressed the changes in the relative expression can be seen 2 cycles earlier and be amplified in the PCR. The second round of the PCR was done using low density microfluidic Taqman cards, containing endogenous control 18S and the control gene HPRT1 previously shown in the preliminary studies to be the best house keeping gene based on the most stable signal within both the control and disease samples.

Firstly, there was no significant change in the mRNA relative expression of islet hormones insulin and glucagon in the db/db mice pancreas in 4 week db/db mice compared with 4 week old control mice. The proinsulin mRNA levels in another study was reported to be significantly decreased in the db/db mice[388]. In support of this study, kaku et al[337] reported that there was a reduction of proinsulin mRNA in BLKS mice at 12 weeks of age. However, when they looked at the individual pancreatic insulin value, there was considerable variablity in the proinsulin mRNA in the db/db mice[389]. In our study insulin 1 gene was increased 1.47 fold in db/db mice at 10 weeks compared to age matched controls. However, this was not significant perhaps due to the high variability[388]. This indicates that the severity between mice and islets may influence the total insulin quantitation measured by PCR. The MT1 and MT2 mRNA levels did not change between controls and the early diabetic (4 week) group, consistant with the lack of change in total metallothionein protein in the pancreas. I investigated a Zn ion channel TRPM3 because a previous study using insulinoma cells (INS1), showed that

TRPM3 was a major Zn importer into beta cells. However, in the current study TRPM3 had very low expression levels in the pancreas in both the control and db/db mice, therefore I did not study this further.

In the ZnT family, ZnT3 and ZnT10 were detected only at low levels as confirmed in studies previously investigating Zn transporters in the pancreas of control mice[250]. The other Zn transporters were all expressed but not different between the db/db and the control mice group. Just prior to beginning experiments in this thesis, a paper appeared in the literature reporting that ZnT8 protein expression was strongly down-regulated in 5 week old db/db mice compared to controls[390].Tamaki et al[390] did not determine whether downregulation decreased further with the progression of type 2 diabetes nor did it look to see whether the down-regulation was at the transcriptional (mRNA) level or due to some post-transcriptional event. Here our study found that the db/db mice in the early diabetic mice.did not show a significant downregulation in ZnT8 mRNA. The reason for this is not clear, but it could be due to using scrapings of the whole pancreas and also not knowing how many islets are present in these scrapings.

Interestingly, Egefjord et al[391]reported that treatment of mouse islets and beta cells with IL-1β significantly downregulated ZnT8 gene expression. Cells overexpressing ZnT8 were more sensitive to the treatment of IL1β and increased the susceptibility to apoptotic death. IL-1β did not significantly alter other Zn transporters including ZIP5 and 6 and also ZNT, 4, 5 and 6[391]. No siginificant changes in the Zn tranporter genes was observed in the early or diabetic groups, especially in the diabetic group which is expected to have increase. Isolating the islet from these db/db mice might be an alternative method to observe these critical changes in these genes.

In the ZIP family, ZIP2 and ZIP12 were very lowely expressed in our pancreatic scrapings. ZIP3 was significantly downregulated in the db/db mice at 4 weeks compared to controls. No other genes changed including ZIP14, ZIP5 and ZIP7 were two of the highly expressed genes in the pancreas and also did not change. There was no significant changes in any of the Zn transporters, Zn binding protein and islet hormones at 10 weeks of age in db/db and control mice. The reason for this is not clear. A major limitation in this study is that the whole pancreas contains a number of tissues

including a variable number of inflammatory cells in the diabetic mice. These studies need to be confirmed by using isolated islets and laser capture microdissected islets.

CHAPTER 6 Protein expression of Islet ZnT Zn transporters ZnT7 and ZnT8 in db/db mice and age matched wild type (C57BL6J)

6.1 Introduction

The previous chapter showed very little change in gene expression of the Zn transporters in the db/db mice compared to age matched controls and no change in ZnT8 alone. The protein expression of two of the SLC30 family (ZnT) of Zn trasporters SLC30A7 and SLC30A8 will be investigated using immunofluorescence staining. ZnT7 and ZnT8 have been shown to be expressed in the pancreatic islets of wildtype mice[216,392] and have role in diabetes and diet induced obesity.

Zn is essential for many physiological processes in the body including function of metalloproteases, cell growth and division and secretion[393]. Deficiency in Zn is associated with immune suppression, growth retardation, skin and gastrointestinal disorders. The pancreatic islets cells are extremely rich in Zn, which is concentrated in the secretory granules and important for synthesis and storage of insulin and other pancreatic hormones. Insulin is synthesized firstly as a precursor polypeptide preproinsulin that is processed in the Golgi and the secretory vesicles to form proinsulin and insulin, respectively. Zn is important for both proinsulin and insulin. Firstly, with proinsulin Zn promotes the formation of Zn proinsulin hexamers in the Golgi and ER. More Zn is then needed in the secretory granules to form Zn insulin crystals which are stored until required for secretion.

The incorporation of Zn into proinsulin and insulin is dependent upon the action of specific Zn transporters. Three Zn transporters appear to be important for insulin synthesis and storage. ZnT5 and ZnT7 are required at the immature stage of insulin processing, while ZnT8 is critical for the later stage to form Zn insulin crystals in the secretory granules. ZnT5 was not studied in this thesis because of time and budgetary constraints. However, it may play a role similar to that of ZnT7.

ZnT7 is predominately expressed in the Golgi apparatus and mediates influx of Zn from the cytoplasm to the Golgi apparatus of beta cells[259], Chinese hamster ovary (CHO) cell[257]s and cerebellum[394] of mice. ZnT7 has also previously known to be expressed in the pancreatic islets of wildtype mice[258,259,395]. Huang et al recently reported that ZnT7 is expressed in pancreatic α-cells of mice and that overexpression of ZnT7 in beta cell

line increases insulin gene and protein expression and a high basal secretion of insulin in the cell, by increasing insulin promoter activity via Zn sensitive transcription factor in RIN5Mf cells[392]. Knock down of ZnT7 in mice made them more susceptible to insulin resistance and glucose tolerance[258,259]. It also resulted in low circulating leptin concentrations, but paradoxically low body weight was seen in these mice [395]. The role of ZnT7 in the early secretory pathway in the insulin synthesis and secretion and the pathogenesis of types 2 diabetes is still not well understood.

Previous studies have shown that ZnT8 is expressed very highly in the pancreatic islets especially in the alpha and beta cells. ZnT8 is expressed in the insulin containing secretory granules and knock down of ZnT8 specifically in beta cells resulted in loss of granular Zn, decreased dense granules (mature insulin) and increase in empty granules (proinsulin)[216,268]. In addition the mice were glucose intolerant. This suggests the importance Zn and ZnT8 for mature insulin processing. The importance of ZnT8 to type 1 diabetes arose out of finding of ZnT8 autoantibodies in this disease[396]. For example a recent Japanese study showed autoantibodies to ZnT8 in approximately 50% of patients with acute-onset type 1 diabetes, depending on the clinical phenotype [396]. Furthermore, a genome-wide association with disease susceptibility loci in type 2 diabetes, revealed a significant association of one allele of ZnT8 R325W with susceptibility in humans. Finally, knockdown of ZnT8 in mice results in defects in insulin crystallization in the beta cells [216]. Therefore these two Zn transporters ZnT7 and ZnT8 were studied in context of the db/db mouse model.

The aim of this study was to investigate two critical transporters ZnT7 and ZnT8 by using immunofluorescence staining to protein expression and subcellular distribution at different stages of diabetes.

It was hypothesized that:

- That ZnT8 will be significantly downregulated as early as 4 weeks of age and the protein will progressively decline as age increases, based on previous studies.

- There will be increased ZnT7 expression in the pancreatic islets of db/db mice to compensate for the loss of pancreatic islet Zn and ZnT8 and therefore impaired insulin processing.

6.2 Methods

Groups of db/db or WT mice (4 mice per group) were purchased from ARC at age groups 4,10 and 18 wk. Immunofluorescence stainings for ZnT8 and ZnT7 proteins were performed and staining intensities (mean grey values) quantified by ImageJ software. Data were log-normalized. Medians, fold-changes (relative to age-matched controls), confidence intervals and p values were determined using the R software. Some findings were confirmed by immunoperoxidase staining on formalin-fixed tissues. Data are tabulated in Table 6.1.

Tissues from WT (C57BL6J) and db/db mice at 4, 10 and 18 weeks of age were embedded in OCT medium and frozen. Sections, 5µm, were cut using a cryotome then fixed in cold acetone for 10 min. The sections were blocked in a humidified chamber for 60 min with serum from the secondary antibody host animal. Sections were incubated with rabbit polyclonal Anti-Slc30a7 (1:150; Cat no. HPA018034; Sigma Aldrich, USA), Rabbit polyclonal Anti Rat ZnT8 (1:100; Cat no. RZ8; Mellitech, France) and mouse monoclonal Anti-glucagon (K79Bb10) (1:50; Cat no. ab10988;Abcam, Sapphire Bioscience, Waterloo, NSW, Australia) overnight at 4°C. Excess primary antibody was removed by washing the slides with 1x PBS and incubated for 60 min with goat anti-rabbit Alexa488IgG(1:400; Cat no. 54533A Invitrogen) conjugate and rabbit anti-mouse Alexa594 conjugate IgG1γ (1:400;Cat no. 940829; Invitrogen). Sections were washed with PBS, nuclei were counter stained with DAPI(4', 6-diamidino-2-phenylindole; 1:1000) and mounted with fluorescent mounting medium (DAKO; Carpinteria, CA). Images were captured on a Zeiss Apoptome microscope (Carl Zeiss GmbH, Goettingen, Germany). The images were converted to JPEGS. Quantification of immunofluorescence was done by using FIGI image J software (NIH, Bethesda, MD, USA).

6.3 Results:

6.3.1 ZnT7

Figure 6.1 shows the co-staining of ZnT7 and glucagon in a typical control mouse islet. ZnT7 is expressed in the pancreatic islets of the mice with a bead-like distribution consistent with localization in the golgi apparatus, as also decribed by Huang et al[395] in mouse pancreatic islets. The ZnT7 gene was also expressed strongly in the pancreatic acinar tissue as shown by the circular like structures around the two islets in Figure 6.1 Frozen serial sections were obtained from the pancreata of the db/db mice at 4,10 and 18 weeks and age matched controls and stained for ZnT7 and glucagon. Figure 6.2 shows typical images and Figure 6.3 and Table 6.1 show the quantification of ZnT7 staining by Image J software. Overall, the db/db mice group had significantly higher ZnT7 compared to age matched controls ($p < 0.0005$). Individually however, there was only significant increase in ZnT7 staining at 4 wk (1.6 fold of control, $p < 0.05$). However, although the values for ZnT7 protein in the db/db mice at 10 and 18 wk of age, were 1.3 fold those of age-matched controls, these were not significant. Age alone did not have a significant effect on ZnT7 protein expression in the control mice.

6.3.2 ZnT8

Figure 6.4 shows the co-staining of ZnT8 and glucagon in a typical control mouse islet. ZnT8 was expressed homogenously throughout the islet especially in both the insulin producing beta cells and the glucagon producing alpha cells. It was not expressed in the acinar tissue. It was also noted that glucagon was stained in the periphery of the pancreatic islet consistent with the immunoperoxidase staining shown in (Figure 3.7 in chapter 3). Frozen serial sections were obtained from the pancreata of the db/db mice at 4,10 and 18 wk and age matched controls and stained for ZnT8 and glucagon. Negative controls (lacking primary antibody) were always included and were uniformly. Figure 6.5 shows typical images and figure 6.6 and Table 6.1 show the quantification of ZnT8 staining by Image J. There was a significant decrease in ZnT8 staining at each of the ages. Pancreatic Islet ZnT8 protein staining in the db/db mice was significantly decreased at 4 wk (0.52 fold of control, $p < 0.05$), 10 wk (0.2 fold, $p < 0.005$) and 18 wk (0.29 fold, $p < 0.005$). Thus, there was a large decrease in ZnT8 protein at 4 wk and

further decrease at 10 wk. Age alone did not have a significant effect in the control mice, but in the db/db mice there was a progressive loss of ZnT8 with progression of the disease. Figure 6.7 shows the stainings for ZnT8 (panel A) and glucagon (panel B) in the same islet of an 18 week chronic diabetic mice. Note that most of the ZnT8 is now colocalised with the glucagon indicating that ZnT8 is preferentially lost in the beta cells but is protected in the alpha cells.
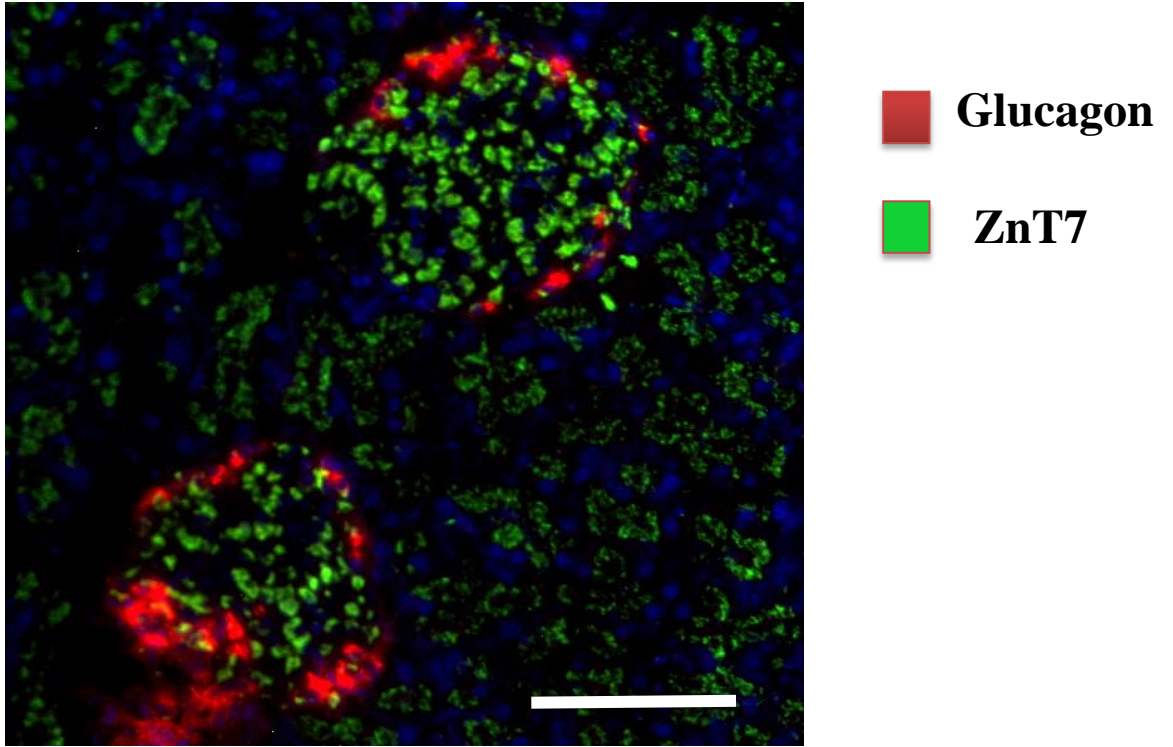
Figure 6.1 ZnT7 and glucagon staining of islet from 4 weeks wildtype C57BL6J mouse

Image of typical islet found in 4 week wild type mice that has been stained for expression of ZnT7 (indicated in green) and glucagon (in red). ZnT7 is expressed in Golgi like structures within the islet beta cells and there is little co-localization with glucagon. Scale Bar, 100 μm.
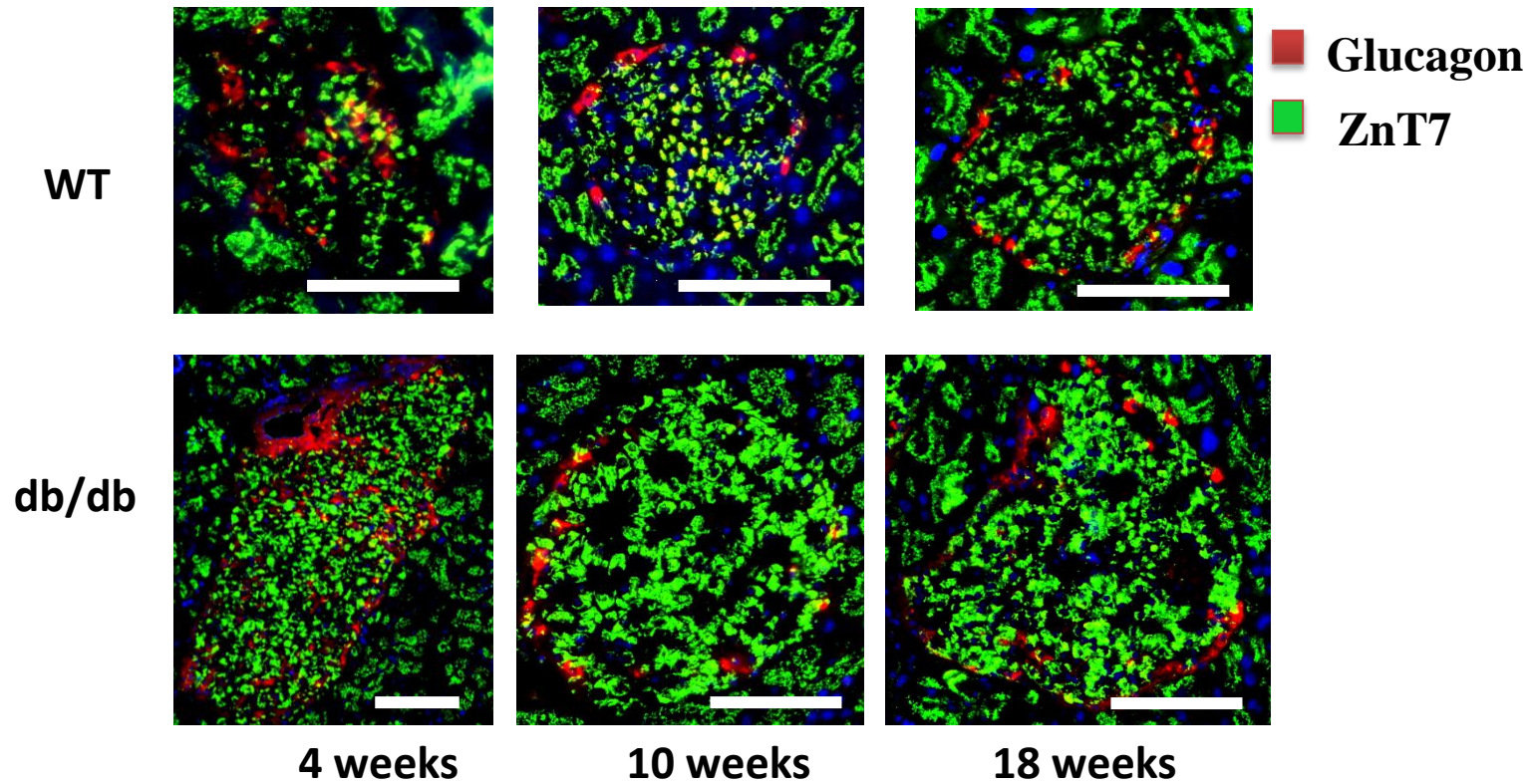
Figure 6.2 ZnT7 expression in wildtype and db/db mice

Figure shows representative images of co-staining of ZnT7 and glucagon. Upper panels show wild type mice, lower panels db/db mice. The columns represent 4, 10 and 18 weeks. Figure shows the staining of ZnT7 in the golgi like structures in islet cells in both wild type and db/db mice. Scale Bar, 100 μm.
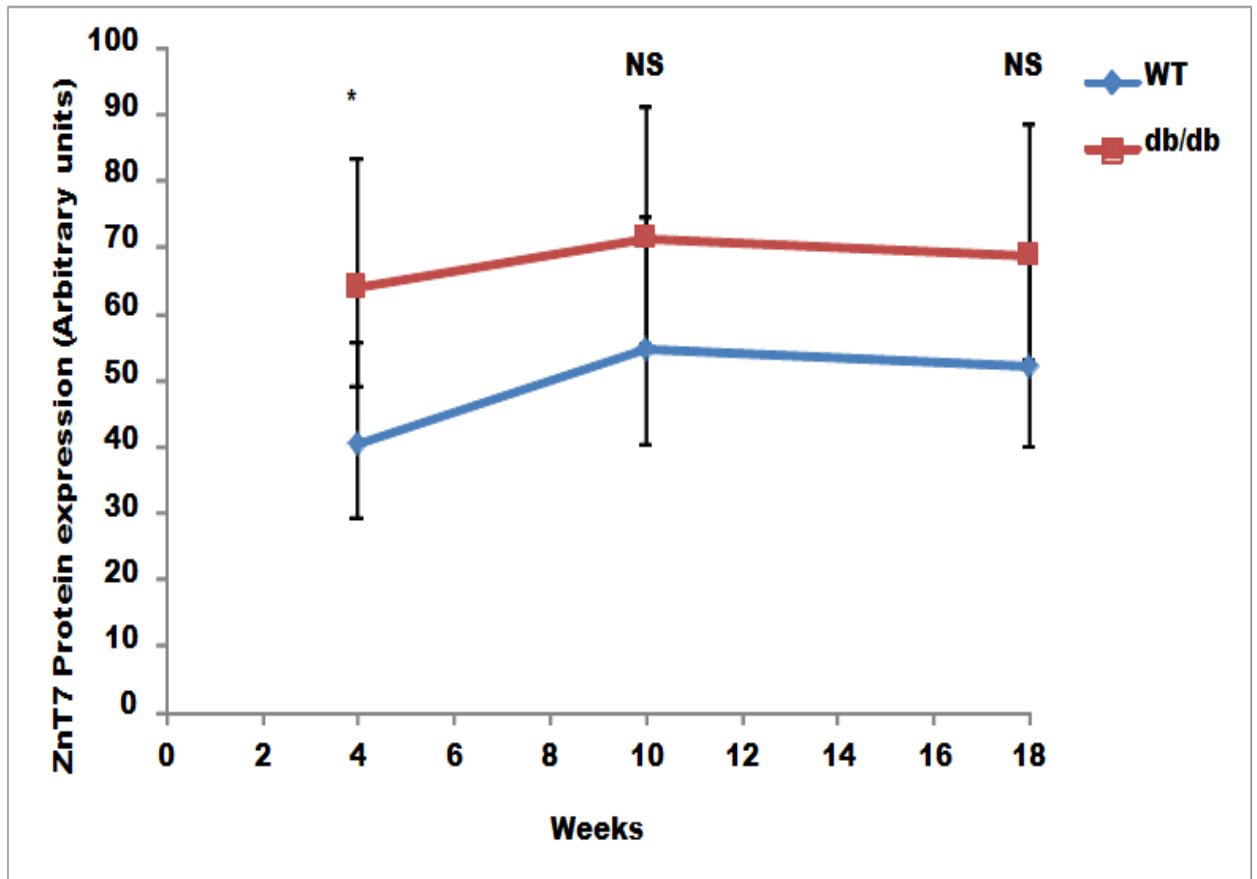
Figure 6.3 Effect of age and disease on ZnT7 protein in wildtype and db/db mice pancreatic islets

Figure shows that the db/db mice had significant upregulation of ZnT7 protein as early as 4 weeks compared to age matched wildtype mice. Further reduction of ZnT7 protein was observed at 10 and 18 weeks of age. The X axis represents the age of mice (weeks) and the Y axis represents the ZnT7 protein (arbitrary fluorescence units). Wild type mice are shown as the blue lines and the db/db mice are shown as the red lines. At each time point, 9 to 39 islets from 4 mice were measured for mean intensity by Just image J (FIGI). The data is shown as medians and the range as confidence intervals. * ($p<0.05$), NS $p.>0.05$. Statistical analysis was performed by type 2 ANOVA. 3-4 mice were used at each time point, and each point was a single ZnT7 protein measurement.
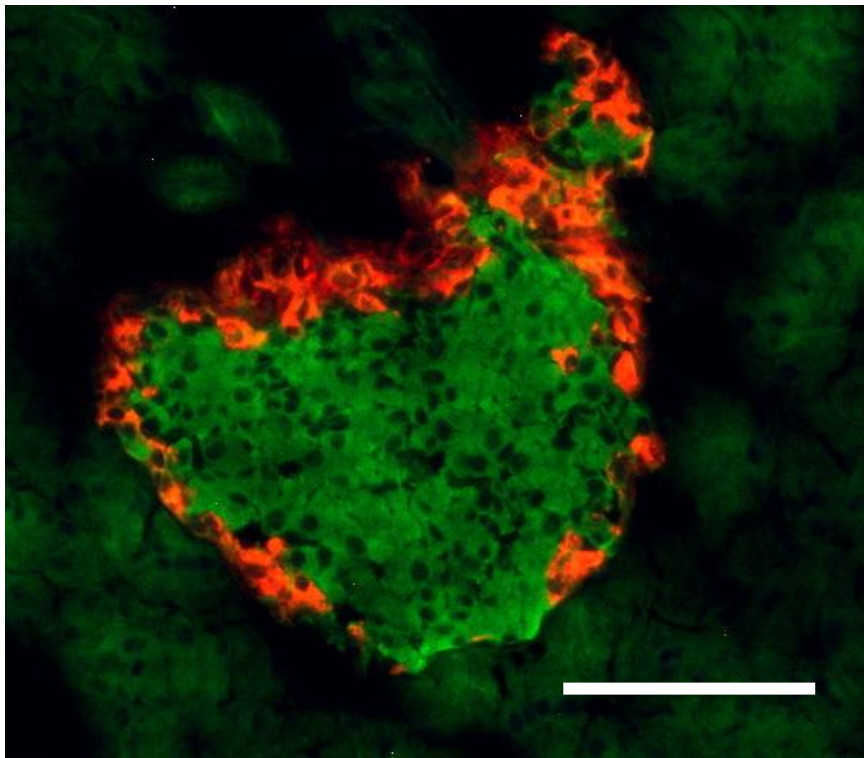
Glucagon

ZnT8

Figure 6.4 ZnT8 and glucagon staining of wild type C57BL6J mouse at 4 weeks

Image of typical islet found in 4 week wild type mice which shows co-staining of ZnT8 (indicated in green) and glucagon (in red). ZnT8 is expressed in both the beta cell-rich islet core and in glucagon producing alpha cells. It may also be expessed in the somatostatin producing delta cells but this needs testing.
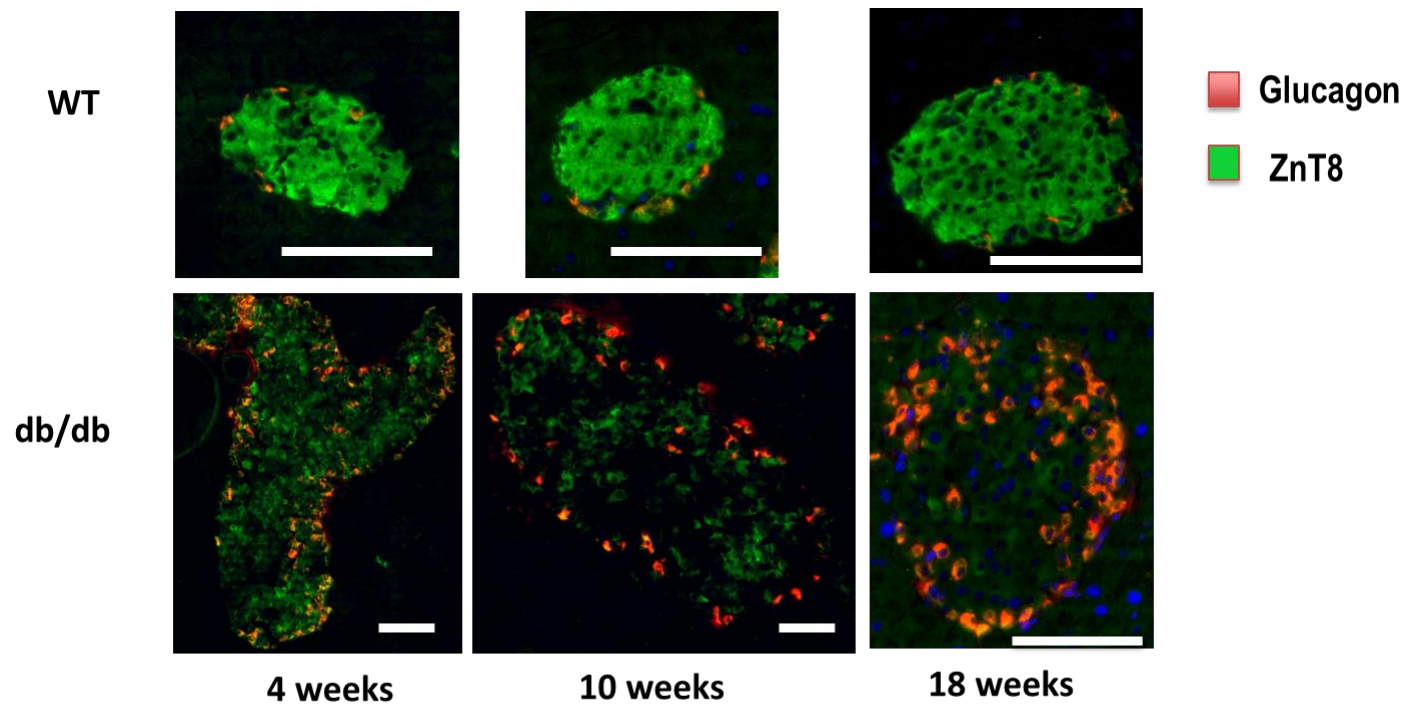
Figure 6.5 Effect of age and diabetes on ZnT8 protein expression in wild type and db/db mice pancreatic islets

Figure shows representative images of co-staining of ZnT8 and glucagon. Upper panels show wild type mice, lower panels db/db mice. The columns represent 4, 10 and 18 weeks. Figure shows the endogenous staining of ZnT8 in the beta cell-rich zone and in glucagon producing alpha cells in wildtype mice. In the db/db mice (bottom panels) ZnT8 is reduced at 4 weeks of age and further decreased at 10 and 18 weeks. ZnT8 is preserved in the glucagon producing alpha cells. Scale Bar, 100 μm.
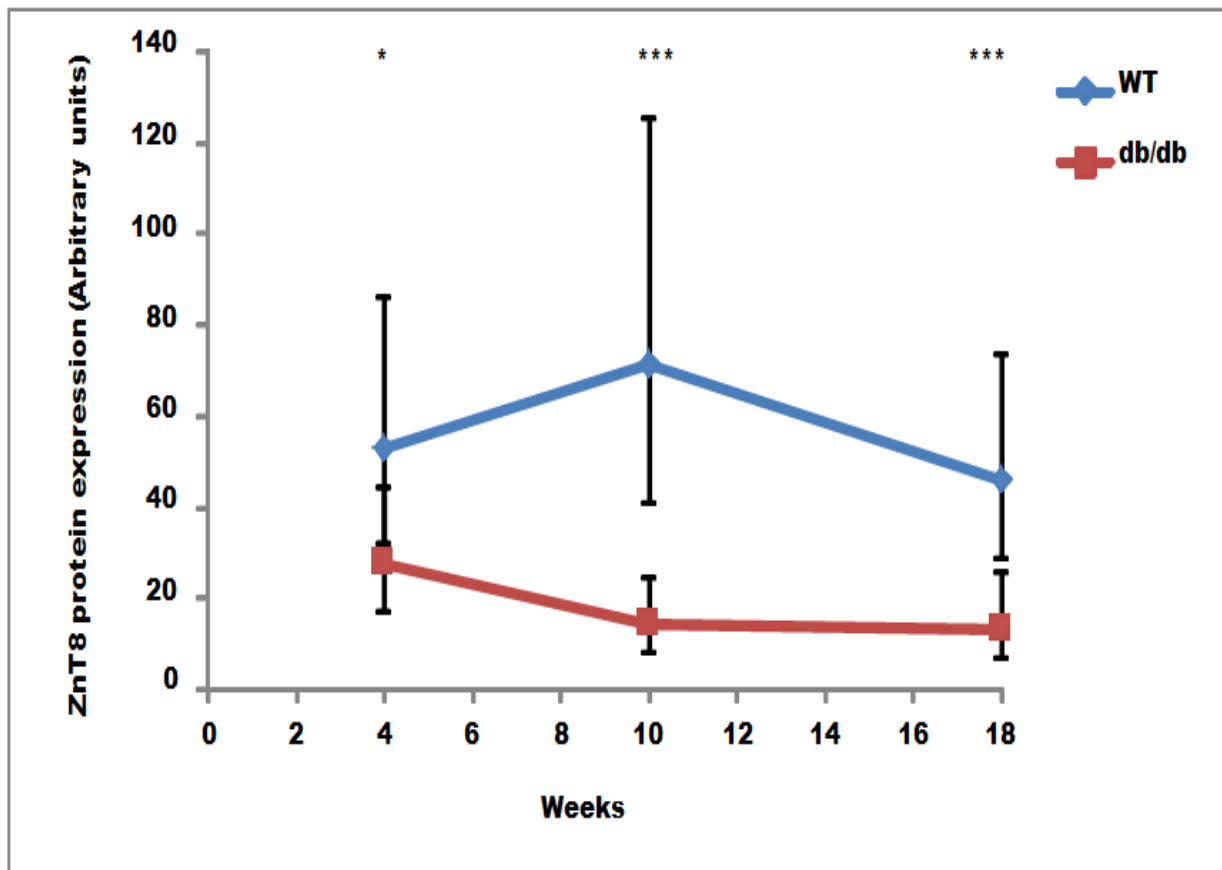
Figure 6.6 Effect of age and disease on ZnT8 expression in wild type and db/db mice pancreatic islets

Figure shows that the db/db mice had reduced ZnT8 as early as 4 weeks of age compared to age matched wild type mice. Further reduction of ZnT8 protein was observed at 10 and 18 weeks of age. The X axis represents the age of mice (weeks) and the Y axis represents the ZnT8 protein (arbitrary fluorescence units). Wild type mice are shown as the blue lines and the db/db mice are shown as the red lines. At each time point, between 25-54 islets from 4 mice were measured for mean intensity by Just image J (FIGI).The data is shown as medians and the range as confidence intervals. * ($p<0.05$), ** ($p<0.005$) and *** ($p<0.0005$). Statistical analysis was performed by type 2 ANOVA. 3-4 mice were used at each time point, and each point was a single ZnT8 measurement.
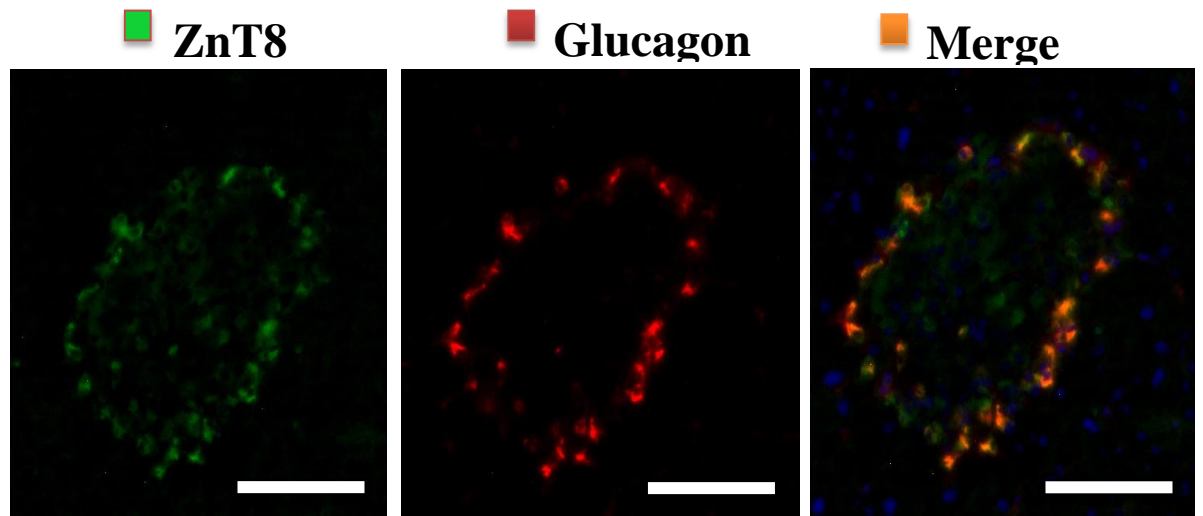
Figure 6.7 Preservation of ZnT8 in alpha cells

Figure shows representative co-staining images of a single islet from a chronic diabetic mouse (A)ZnT8, green,(B) Glucagon, red, C) merged image. There is co-localisation of ZnT8 and glucagon (orange).The images show that ZnT8 protein is preserved in the mantle of the islet. Scale Bar, 100 µM

6.4 Discussion:

Previous to these studies, ZnT8 had been shown to be important for maintaining Zn levels in beta cell granules and for correct insulin storage and release. Tamaki et al found that ZnT8 was first expressed at day 15 of embryogenesis in mice[390]. It had also been shown to be an autoantigen in type 1 diabetes while a single nucleotide polymorphism to ZnT8 increased the risk of both type 1 and 2 diabetes. In addition, Tamaki et al reported that ZnT8 is down-regulated in two animal models of type 2 diabetes including db/db mice. However they did not present any quantitative data and they compared female db/db mice with male C57BL6J controls. Previously, no one had shown whether ZnT8 is also altered in alpha cells in diabetes.

Here, the protein levels of ZnT7 protein in the dbdb model was also investigated because ZnT7 was found to be highly expressed in wildtype mice islets[259] and overexpression of ZnT7 in insulinoma cells increased insulin synthesis and secretion by promoting gene transcription of insulin[259]. Huang et al showed that ZnT7 knockout mice were more susceptible to diet induced glucose intolerance and insulin resistance[395].

In the current study, there was a modest but significant increase ($p < 0.05$, 1.6 fold increase) in islet ZnT7 protein expression levels as early as 4 weeks. ZnT7 in the pancreatic islets had a golgi- and ER-like distribution in the majority of the cells in both control and diabetic islets, consistent with a role for ZnT7 in the early stages of insulin synthesis. The finding that ZnT7 was not down-regulated in the mouse islets suggest that, in contrast to ZnT8, ZnT7 is not a target for impaired insulin production in the diabetic db/db mice. However, ZnT7 may play an important role in obesity. Huang et al investigated that ZnT7 deficient mice showed reduced body Zn and body fat accumulation[258]. They showed that ZnT7 is expressed highly in the adipocyte cells. Knocking out ZnT7 may block Zn influx into the adipocytes and alter adipogenesis.
In this study, ZnT7 showed a tubular like pattern in the acinar tissue, which has also not been previously known. But similar distribution was seen in huang et al study, that ZnT7 is expressed in a tubular distribution in the myoblast skeletal muscle. The function of ZnT7 in the acinar cells is unknown and will be addressed in future studies.

The present studies showed that the predominant loss of ZnT8 protein occurred at the early diabetes stage and there were further losses at 10 and 18 weeks as the diabetes progressed. Therefore the loss of ZnT8 was maintained through all stages of diabetes. There was no significant effect of age alone on the ZnT8 protein expression as seen in the control mice at all age groups. Simultaneously, another study appeared in the literature confirming the loss of ZnT8 at the early diabetes stage in db/db mice[390]. One implications of these findings is that down-regulation of ZnT8 is one of the early triggering factors in development of type 2 diabetes. A very recent study done by Tamaki et al 2013, reported the link between ZnT8 knockout (beta cell specific) and hepatic insulin clearance. The implications of this is not clear, especially concerning which type of insulin, pro-insulin or mature insulin, is being cleared and warrants further study.

Glucagon secretion is not lost in diabetes and alpha cells often replace beta cells during the progression of the disease [332]. Both of these were evident in the islets of the db/db mice. ZnT8 is known to be expressed in the alpha cells and the pancreatic polypeptide producing PP cells[390]. In this study, ZnT8 protein levels did not appear to change in the mantle cells (mostly alpha cells) in the db/db mice at 4,10 and 18 weeks of age, although it was not possible to specifically quantify this for the alpha cells as dual labeling of glucagon and ZnT8 were not possible with the antibodies available for this study. While preliminary, this is the first indication that alpha cell ZnT8 might not be altered in type 2 diabetes. If confirmed, it will suggest that whatever leads to loss of ZnT8 and Zn in the beta cells does not affect the alpha cells. In Chapter 4, Figure 4.6 the cells in the periphery of the islet did still contain Zn in them. This indicates that the alpha cell Zn may be preserved and protected in diabetes.

In diabetes, there is evidence of disorganization of alpha, delta and PP cells. It is not shown how the disorganization of islet hormones produced by these other cell types affects regulation of ZnT8 or other Zn transporters during this disease. Nor is it clear whether Zn released from islet cells has paracrine effects on neighboring islet cells.

Zn is important for correct protein folding of insulin in the ER and immature granules [397]. In Zn deficiency, there is misfolding of protein in the ER of yeast[398]. Since i)

protein misfolding is associated with ER stress and ii) ER stress occurs early in diabetes and leads to eventual loss of beta cells, there may be a link between Zn, insulin misfolding, ER stress and beta cell apoptosis. Whether ZnT8 is altered due to ER stress or whether the loss of ZnT8 (and Zn) contributes to ER stress is not clear.

One of the reasons why investigations into ZnT7 and ZnT8 are important in diabetes is that their cellular localization and function are unique in the beta cell. ZnT7 overexpression did not increase total Zn into cells but significantly increased insulin levels by gene transcription and translation[259]. However, overexpression of ZnT7 did not have profound effects on glucose induced insulin secretion. ZnT8 overexpression increased total Zn and did not alter total insulin content. However, ZnT8 overexpression did enhance glucose induced insulin secretion[395].

In summary the experiments in this chapter have shown strong islet staining for ZnT7 and ZnT8, two Zn transporters important for pro-insulin and insulin maturation and storage. One of the Zn transporters, ZnT8, was down regulated in db/db mice diabetes, while the other was modestly but significantly increased. Interestingly, ZIP transporters have been increasingly being implicated in a variety of different disease states such as asthma[399] and cancer[400]. However, no studies have investigated ZIP transporters in diabetes. The next chapter will investigate the location and regulation of ZIP4, ZIP5 and ZIP14 during the progression of diabetes.

Table 6.1 ZnT-related measurements in db/db model

Parameter	Wk	WT	db/db	Units	Fold-Change	Lower CI	Upper CI	n	P value
ZnT7	4	40	64	afu[a]	1.6	1.1	2.3	4	< 0.05
	10	55	71	afu[a]	1.3	0.9	1.9	4	ns[b]
	14	52	69	afu[a]	1.3	0.9	1.8	4	ns
ZnT8	4	53	28	afu[a]	0.52	0.28	0.97	4	< 0.05
	10	72	14	afu[a]	0.20	0.10	0.41	4	< 0.005
	14	46	14	afu[a]	0.29	0.14	0.61	4	< 0.005

a Arbitrary fluorescence units (Mean Gray Value)

b Not significant

CHAPTER 7 Protein expression of ZIP Zn transporters ZIP4, ZIP5 and ZIP14 in db/db mice and age matched wild type (C57BL6J)

7.1 Introduction:

In the previous chapter the protein expression of two of the ZnT transporters, ZnT7 and ZnT8 was described. The ZnT transporters are usually intracellular and involved in putting Zn into compartments of cells such as the Golgi and the secretory granules containing insulin. The Zn transporters that bring Zn into islet cells have not yet been identified. ZIP Zn transporters are generally thought to be the influx Zn transporters. Therefore in these studies the protein expression of three ZIP Zn transporters ZIP4, ZIP5 and ZIP14 was examined. ZIP4 was chosen because it is known to be one of the major Zn transporters involved in Zn absorption in the small intestine[233,311]. ZIP4 has a special link to the gastrointestinal system since ZIP4 is a major intestinal Zn transporter expressed on the apical surface of enterocytes[401] and increased in Zn deficiency[402].

Knockout of ZIP4 lead to loss of intestinal Zn especially in paneth cells, dysplasia of the intestinal crypts associated with increased catabolic metabolism and reduced protein synthesis and this leads to disorganisation of the absorptive epithelium[229]. It has been shown that ZIP4 is overexpressed in many pancreatic cancers, suggesting that it is important for malignant growth of pancreatic tumours[231], but whether the normal pancreatic islets express low levels of ZIP4 expression and whether ZIP4 is required for normal islet function has not been well investigated.Mutation in ZIP4 is responsible for a severe Zn deficiency in children called Acrodermatitis Enteropathica[229,310]. ZIP4 protein is upregulated in pancreatic cancer[402]. Another study done by Duffner Beattie et al[312] showed that ZIP4 was expressed in the pancreatic islet of a pregnant CD1 mice. This suggested that ZIP4 was one of the important proteins to investigate in the db/db mice model.

Another Zn transporter that is thought to be involved in Zn homeostasis by excreting Zn from the pancreas is ZIP5. Both ZIP4 and ZIP5 are closely related members of the LIV-1 subfamily of Zn transporters[311,312]. Recent studies have reported that ZIP5 is expressed in the basolateral membranes of intestinal enterocytes, visceral endoderm cells and pancreatic acinar cells. It was proposed that ZIP4 and ZIP5 have antagonistic functions in Zn homeostasis, ZIP4 mainly being involved in Zn uptake into the body

177

while ZIP5 was mainly involved in removing Zn from the body[312]. ZIP5 was chosen as it is known to be expressed abundantly in the acinar tissue of the pancreas, however it is not known whether this protein is expressed in islet cells nor whether it is altered in diabetes.

ZIP14 is an inflammation associated Zn transporter. Chronic inflammation is part of the pathogenesis of both type 1 and 2 diabetes. In type 2 diabetes, inflammation is caused by glucotoxicity, reactive oxygen species and proinflammatory cytokines which contribute to the decline of beta cell function. In addition, preliminary studies from our laboratory[403] reported that ZIP14 was expressed in the pancreas of human, marmoset and pig pancreatic islets. However, it was not clear from the images what cell type in the islet the ZIP14 was expressed in. ZIP14 is known to be also involved in hypozincemia, and iron homeostasis[243,245]. ZIP14 in the liver was shown to be upregulated in acute phase response, which leads to movement of Zn from plasma to the liver[234]. In addition, ZIP14 regulation was altered when hepatocytes were treated with LPS and IL-6[234]. In the db/db mice, there was significant iron loading in kidneys when fed with normal chow diet, but when they were fed iron deficient diet the iron decreased in their kidneys[404]. Macrophages play an important role in iron homeostasis and are increased in type 2 diabetic islets of humans and mice[45]. ZIP14 not only transports Zn but also iron and may also play a role in iron homeostasis although not much is known about this.

Therefore in this chapter immunostaining experiments for ZIP4, ZIP5 and ZIP14 in db/db mice pancreas are described.
The hypothesis of this study is that in both wildtype and db/db mice:

- There is a relationship between ZIP4 and the gut-islet interaction
- There is an inverse relationship between ZIP4 and ZIP5 staining because of their antagonistic actions.
- There is a relationship between islet inflammation and ZIP14 expression

7.2 Method

7.2.1 Immunofluorescence staining for ZIP4, ZIP5 and ZIP14

Tissues from WT (C57BL6J) and db/db mice at 4, 10 and 18 wk of age were embedded in OCT medium and frozen. Sections, 5μm, were cut using a cryotome then fixed in cold acetone for 10 min. The sections were blocked in a humidified chamber for 60 min with serum from the secondary antibody host animal. Sections were incubated with rabbit polyclonal Anti-ZIP4 (1:100; Cat no. PA5-210669; Thermoscientific, Rockford, USA) or rabbit polycolonal Anti-ZIP5 (1:150; Cat no. PA5-21070; Thermoscientific, Rockford, USA) and rabbit polycolonal Anti-ZIP14 (1:150; Cat no. PA5-21077; Thermoscientific, Rockford USA) and mouse monoclonal Anti-glucagon (K79Bb10) (1:50; Cat no. ab10988;Abcam, Sapphire Bioscience, Waterloo, NSW, Australia) overnight at 4°C. Excess primary antibody was removed by washing the slides with 1x PBS and incubated for 60 min with goat anti-rabbit Alexa488IgG (1:400; Cat no. 54533A Invitrogen,) conjugate and rabbit anti-mouse Alexa594 conjugate IgG1γ (1:400;Cat no. 940829; Invitrogen). Sections were washed with PBS, nuclei were counter stained with DAPI(4', 6-diamidino-2-phenylindole; 1:1000) and mounted with fluorescent mounting medium (DAKO; Carpinteria, CA). Images were captured on a Zeiss Apoptome microscope (Carl Zeiss GmbH, Goettingen, Germany). The images were converted to JPEGS. Quantification of immunofluorescence was done by using FIGI image J software (NIH, Bethesda, MD, USA).

7.2.2 Immunoperoxidase assay:

Tissue sections (4 μm) were cut, mounted on Superfrost Plus coated slides, labelled and then placed on a fully automated immunohistochemistry (IHC) staining Ventana Benchmark XT (Roche Diagnostics , Castle Hill, NSW, Australia) instrument. The section was then washed in reaction buffer followed by addition of Cell Conditioning 1 (CC1) solution (Roche Diagnostics, Castle Hill, NSW, Australia) for 30 min. CC1 was removed, washed, and the primary polyclonal Rabbit Anti-Glucagon at dilution 1/800 (Dako, Carpinteria, CA) added for 30 min whilst the slide was heated to 37°C. Staining was performed using *ultra*View DAB detection kit (Roche Diagnostics, Castle Hill, NSW, Australia) in accordance with the manufacturer's standard procedures followed

by counterstaining with haematoxylin 11(Roche Diagnostics, Castle Hill, NSW, Australia). The same procedure was used for Polyclonal Guinea Pig Anti-Swine Insulin (Dako, Carpinteria, CA) at 1/100 and ZIP4 (Thermo Scientific, Rockford, USA) at 1/400, ZIP 14 (Thermo Scientific Rockford, USA) at 1/1600, CD68 1/1500 (Dako, M0814 Clone KP1, Carpinteria, CA) and Polyclonal Rabbit Anti-human Somatostatin (Dako Carpinteria, CA) at 1/1600.Immunohistochemistry images were captured using a Nikon Eclipse 90i microscope (Nikon, Tokyo, Japan).

7.2.3   *Iron staining:*

Frozen section of normal human liver and chronic diabetic 18 wk (db/db) mice and control (human liver) were washed with distilled water. Equal parts of ferrocyanide and hydrochloric acid were added to the slides and slides incubated for 10 min. The slides were then washed with distilled water for 5 min. A counterstain with filtered neutral red stain (nuclei stain) was added for 5 min. The slides were air dried, and dehydrated with absolute ethanol and then mounted with coverslip. Positive staining for iron gives a purple colour.

7.2.4   *Western Blot:*

1.5×10^6 MIN6 cells were seeded into a 6 well tissue culture plate and grown to confluence. The cells were washed and lysed for 15mins at 4°C with M-PER buffer supplemented with phenylmethylsulfonyl fluoride (PMSF), Protease inhibitor cocktail and phosphatase inhibitors (Thermo scientific, Rockford, Illinois USA). Protein amount was quantified using a Pierce BCA kit (Thermo Scientific, , Rockford, Illinois USA). Protein amount was quantified using the DC™ Protein Assay Kit (Bio-Rad Laboratories Pty. Ltd., Gladesville, NSW, Australia). Protein lysates (30 μg/sample) were loaded on a sodium dodecyl sulfate/10% polyacrylamide gel and electrophoresed, prior to transfer onto PVDF membrane (GE Healthcare UK Ltd., Buckinghamshire, UK) or nitrocellulose and blocked with odyssey blocking buffer (OBB; LI-COR Biosciences, Millenium Science, Surrey Hills, VIC, Australia). Membranes were incubated overnight at 4°C with primary antibodies diluted in OBB (rabbit anti-ZIP 4, 5 and 14; 1/1000) or goat anti-actin (I-19, 1/5000; Santa Cruz Biotechnology, Inc., Santa Cruz, California, USA). After washing with 0.1% PBS/Tween-20, appropriate

secondary antibodies diluted in OBB (1/10,000 dilution IRDye® 800CW Donkey Anti-Goat Secondary or IRDye® 680LT Goat Anti-Rabbit Secondary; LI-COR Biosciences) were applied, followed by scanning with the Odyssey® Infrared Scanner and associated software (LI-COR Biosciences).

7.3 Results:

7.3.1   ZIP4

Frozen serial sections were obtained from the pancreata of the db/db mice at 4,10 and 18 wk and age matched controls and co-stained for ZIP4 and glucagon. Figure 7.1 shows the co-staining of ZIP4 and glucagon in control mouse pancreas at 4 wk of age. ZIP4 was weakly expressed in the acinar tissue but strongly expressed in clusters in the periphery of the islet. There was no co-localization of ZIP4 with the glucagon staining. Figure 7.2 shows typical images of stainings at 4, 10 and 18 wk while Figure 7.3 and Table 7.1 show the quantification of ZIP4 staining by ImageJ software. Negative control was omission of primary antibody. ZIP4 expression in the early diabetic, diabetic and chronic diabetic db/db mice was in both the peripheral mantle cells as well as the interior part of the pancreatic islet (Figure 7.2).There was no significant change in ZIP4 staining at any time point. Integrated density was used instead of mean gray value for ZIP4 because the staining was not homogenous across the islet but, instead, appeared to label only certain cells. At 4, 10 and 18wk, in db/db mice islets, ZIP4 protein staining was 1.4, 1.5 and 0.8-fold of age-matched controls, respectively (p value not significant, 14 to 36 islets from 4 mice per group were tested). There was no apparent effect of age alone on ZIP4 staining in WT mice.

ZIP4 staining was quite distinct from insulin staining (beta cells) and glucagon staining (alpha cells) in both control mouse and db/db mouse pancreatic sections. However, the staining patterns for ZIP4 and somatostatin (delta cells) in various tissue sections were very similar, prompting further search for evidence of their colocalization. Ideally, colocalization studies are done using multiple stainings on the same tissue section. It was not possible to do this for somatostatin and ZIP4 as the primary antibodies were both rabbit. Serial sections were therefore used. The use of serial sections for studies of co-localization is problematic for most small cells since the thickness of the tissue section (4 μm) is in the order of the diameter of the cell (5-10 μm). Another issue

concerns the binding of the primary antibodies to different parts of the cell, such as anti-ZIP14 to the plasma membrane and anti-somatostatin to the cytoplasmic granules of the delta cell. Despite these problems, it was possible to find sufficient co-localization between ZIP4 and somatostatin indicated by the arrows in figure 7.4 for control mice and Figure 7.5 for db/db mice at 4 weeks of age.

7.3.2 *ZIP5*

Figure 7.6 shows the co-staining of ZIP5 and glucagon in 4, 10 and 18 wk db/db mice and age-matched controls. The acinar shows a strong "starry sky" staining throughout the pancreas, however, there was little staining within the islets either chronic or diabetic. Therefore quantification of islets was not attempted.

7.3.3 *ZIP14*

Frozen serial sections were obtained from the pancreata of the db/db mice at 4,10 and 18 wk and age matched controls and stained for ZIP14 and glucagon. Figure 7.6 shows ZIP14 and glucagon co-staining in a pancreas section of a control mouse. Note the staining of blood vessels and the relative lack of staining of acinar and islets. However, islets of diabetic mice do stain in a particulate manner for ZIP14 as shown below.

Figure 7.7 shows typical images of stainings at the three age groups while Figure 7.8 and Table 7.1 show the quantification of ZIP14 staining by ImageJ software. There was significant increase in ZIP14 staining at all-time points in the diabetic mice. At 4, 10 and 18wk, in db/db mice islets, ZIP14 protein staining was 6.1, 3.9 and 3.1-fold of age-matched controls, respectively ($p < 0.005$, 19-55 islets from 4 mice per group were tested). There was a small but significant increase in control mice due to age alone from 4 to 10 wk.

To further test whether ZIP14 protein expression increases with islet size, the area of each islet was measured and plotted against ZIP14 expression. Figure 7.9 shows that the ZIP14 protein expression increased with islet size (r^2=0.56).

Since ZIP14 was clearly expressed in large blood vessels, the possibility existed that the staining of the islets was due to ZIP14 in intra-islet capillaries. To investigate whether ZIP14 is expressed in the capillaries of the islet an endothelium marker CD31 antibody was used. Figure 7.10 shows the immunofluorescence staining of the endothelium

marker CD31 in chronic diabetic mice pancreatic islets. CD31 did not colocalize with ZIP14, indicating that ZIP14 is not expressed in capillaries of the pancreatic islets.

To further investigate the identity of ZIP14 positive cells I used immunoperoxidase staining for ZIP14 in formalin fixed pancreatic sections at 4 wk db/db and age matched controls. In the db/db mice there was strong expression of ZIP14 in the pancreatic islets (confirming the immunofluorescence staining). The cells resembled macrophages. Therefore serial sections were stained for CD68, a macrophage marker. Figure 7.13 shows the colocalisation of ZIP14 and CD68 positive cells in 4-wk db/db mice, indicating that there is an increased infiltration of macrophages compared to age matched controls and these macrophages expressed ZIP14. While immunofluorescence labeling of ZIP14 appear to stain only macrophages, the immunoperoxidase staining in formalin fixed tissue stains macrophages strongly and there is also lesser staining in the beta cell zone. This is interesting for two reasons. Firstly, this suggests that beta cells do contain at least a low level of expression of ZIP14. This was further confirmed by western blot analysis for ZIP14 in MIN6 beta cell line (figure 7.14 right panel). Secondly, it has previously been proposed that alpha cells express ZIP14 based on studies with a human alpha cell line[405]. Finally, Figure 7.15 shows iron (hemosiderin) staining in A) positive controlhuman liver and B) 18 wk db/db mice pancreatic tissue. This figure shows that in the db/db mice pancreas there was no detectable amount of iron compared with the positive control liver .

Table 7.1 ZIP-related measurements in db/db model

Parameter	Wk	WT	db/db	Units	Fold-Change	Lower CI	Upper CI	n	P value
ZIP4	4	105272	148568	afu[a]	1.4	0.5	3.8	4	ns[b]
	10	90962	133452	afu[a]	1.5	0.4	5.7	4	ns
	18	152421	128888	afu[a]	0.8	0.3	2.1	4	ns
ZIP14	4	53322	325657	afu[a]	6.1	3.0	12.4	4	< 0.005
	10	191626	749229	afu[a]	3.9	1.7	9.2	4	< 0.005
	18	160637	500719	afu[a]	3.1	1.4	6.8	4	< 0.005

a Arbitrary fluorescence units (Integrated Density)

b Not significant
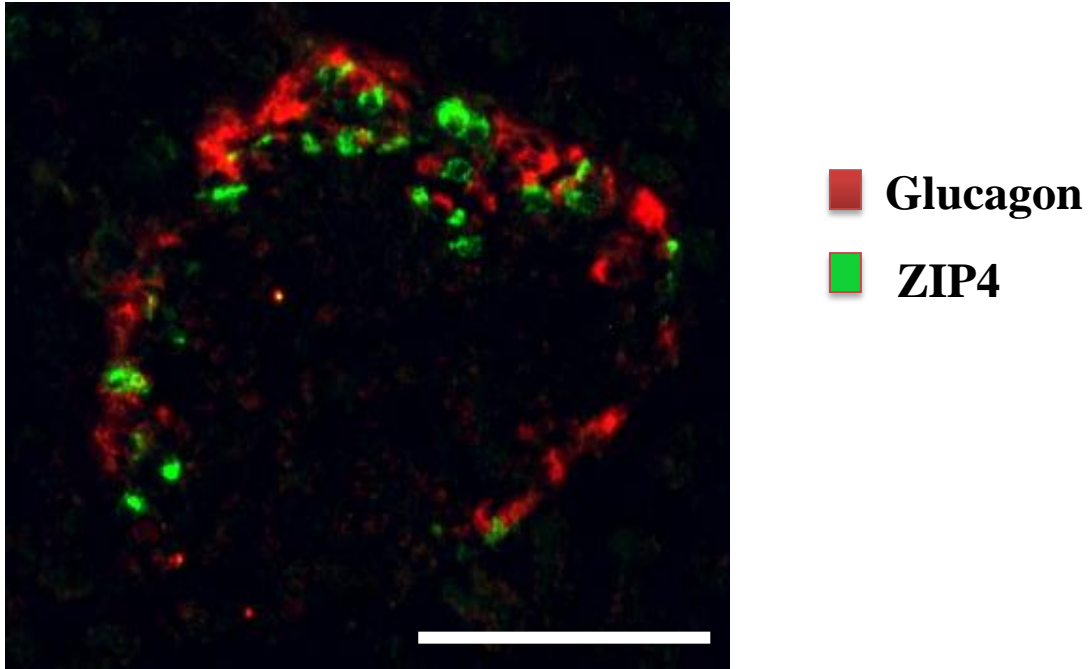
Figure 7.1 ZIP4 protein in the pancreatic islet of a control 4 week mouse

Image of typical islet found in 4 week wild type mice showing the expression (by immunofluorescence) of ZIP4 in the islet mantle. The figure shows a co-staining of ZIP4 (indicated in green) and glucagon (in red). It can be seen that ZIP4 is not expressed in the beta cell rich islet core as well as not in the majority (at least) of glucagon producing alpha cells. Scale Bar, 100 μm.
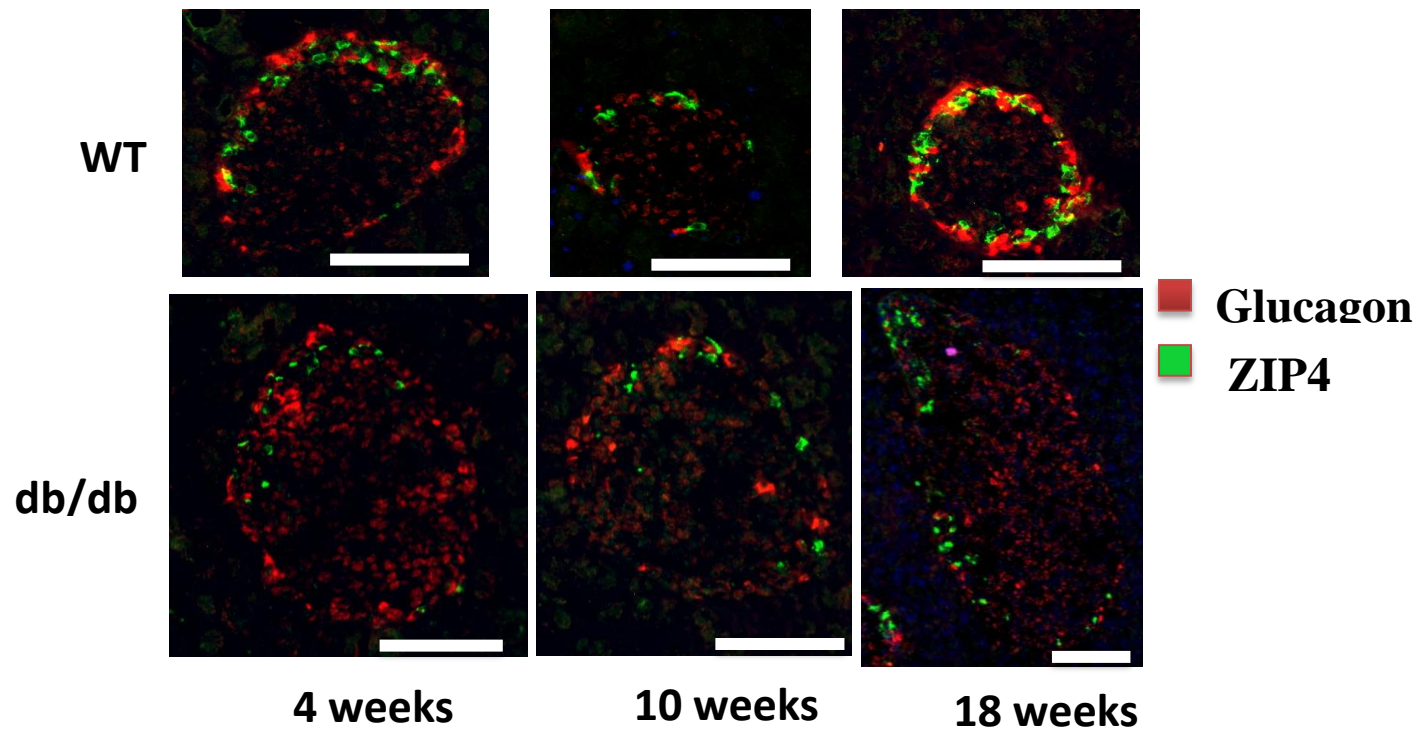
Figure 7.2 ZIP4 protein in islets of wildtype and db/db mice

Figure shows representative images of co-staining of ZIP4 and glucagon. Upper panels show wild type mice, lower panels db/db mice. The columns represent 4, 10 and 18 weeks. Figure shows the staining of ZIP4 in cells is largely restricted to the non-alpha cells in the mantle of the pancreatic islets of wild type mice. In the db/db mice (bottom panel), ZIP4 is scattered throughout the pancreatic islets. Scale Bar, 100 µm
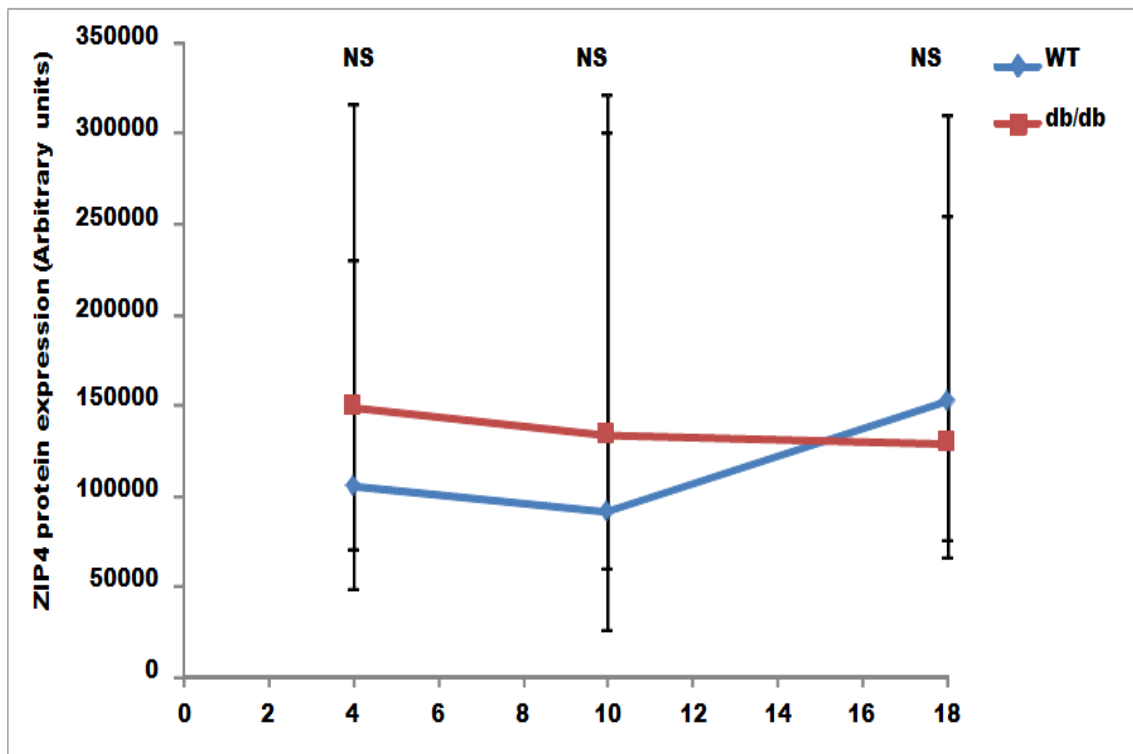
Figure 7.3 Effect of age and diabetes on ZIP4 protein

Figure shows that the db/db mice did not have significant differences in the protein expression of ZIP4 (by immunofluorescence) compared to aged matched wild type mice. The X axis represents the age of mice (weeks) and the Y axis represents the ZIP4 protein (arbitrary units). Wild type mice are shown as the blue lines and the db/db mice are shown as the red lines. At each time point, between 14 to 36 islets from 4 mice were measured by integrated density using Just image J (FIGI). The data is shown as medians and the range as confidence intervals. * ($p<0.05$), ** ($p<0.005$) and *** ($p<0.0005$). Statistical analysis was performed by type 2 ANOVA. 3-4 mice were used at each time point, and each point was a single ZIP4 protein measurement.

ZIP4   **Somatostatin**
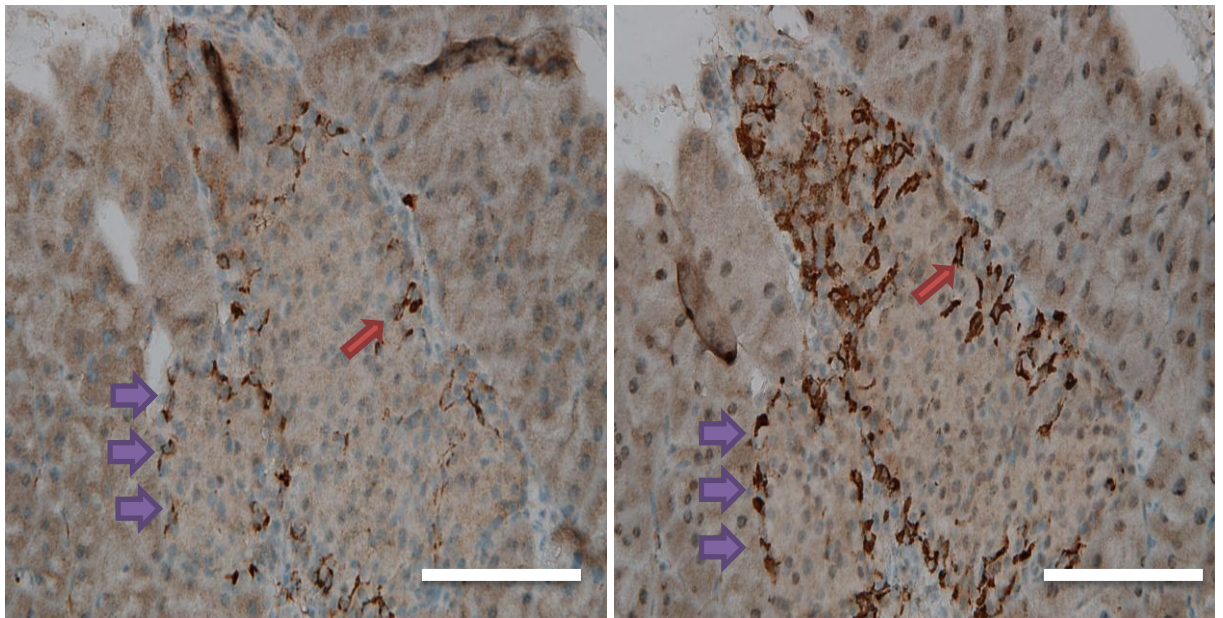
Figure 7.4 Co-localisation of ZIP4 and somatostatin in a pancreatic islet of a wild type mouse

Figure displays representative serial paraffin-embedded sections of immunoperoxidase staining of (A) ZIP4 and (B) somatostatin in the islet of a 4 week wild type mouse. The figure shows the co-localisation of ZIP4 and somatostatin in the pancreatic islet. It also shows that ZIP4 and somatostatin are expressed in the mantle of the pancreatic islet. Scale Bar, 100μm.
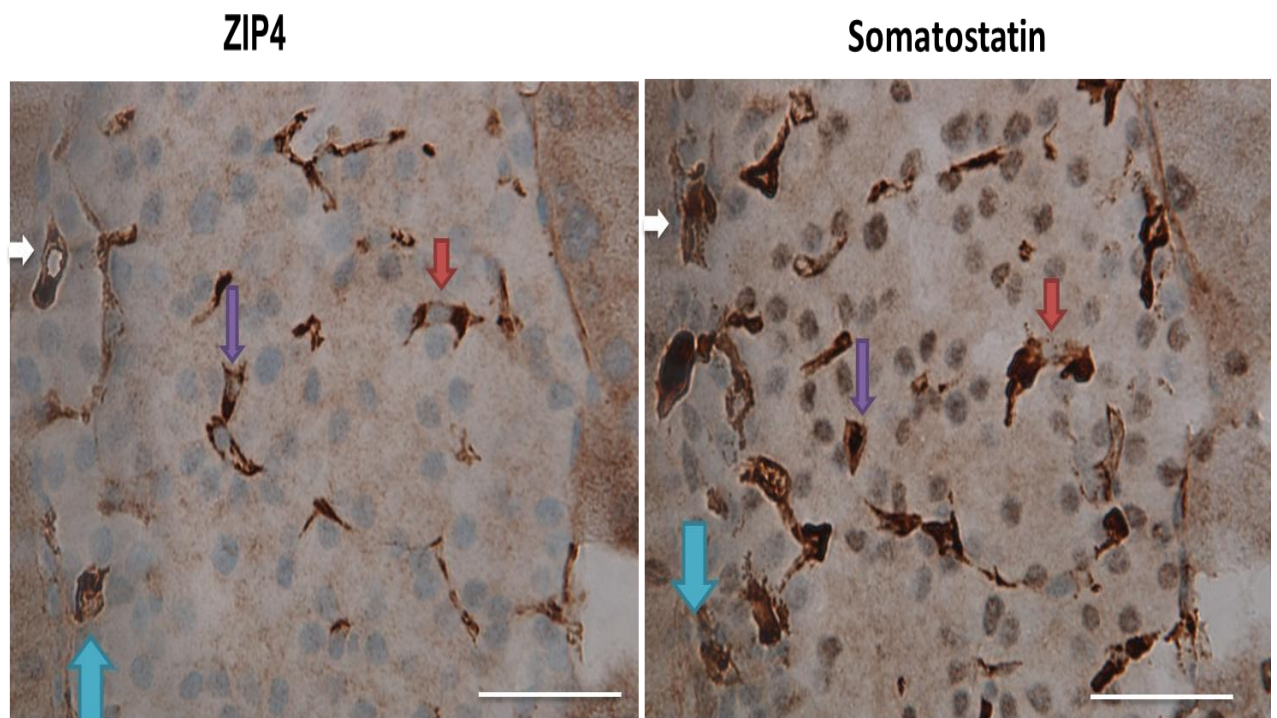
Figure 7.5 Co-localisation of ZIP4 and somatostatin in a pancreatic islet of a db/db mouse

Figure displays representative serial paraffin-embedded sections of immunoperoxidase staining of (A) ZIP4 and (B) somatostatin in the islet of a 4 week db/db mouse. The figure shows the co-localisation of ZIP4 and somatostatin in the pancreatic islet (see sets of arrows) and also shows that ZIP4 and somatostatin are expressed in the inner core of the islet. Scale Bar, 100 μm.
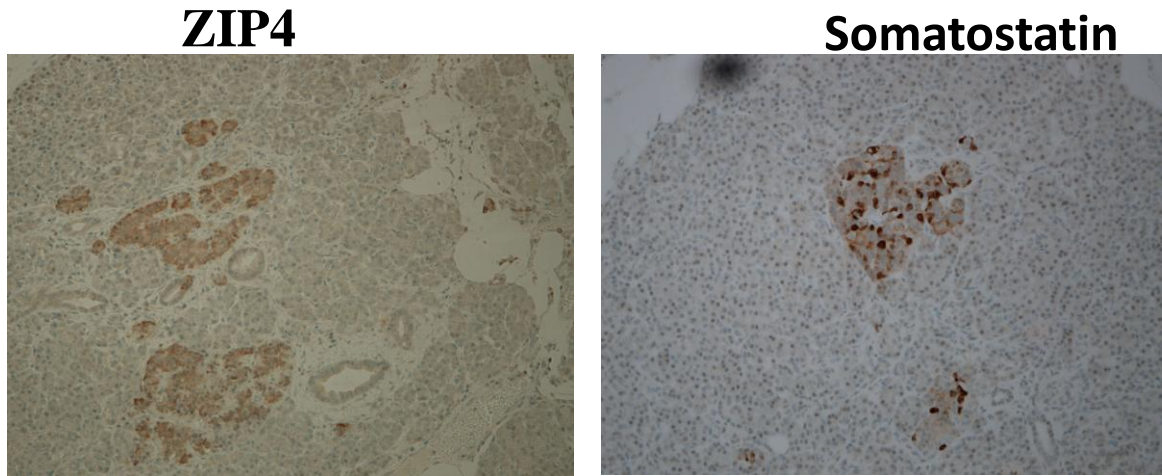
ZIP4   **Somatostatin**

Figure 7.6 Human ZIP4 and somatostatin protein expression in pancreatic islets

For species comparison, the figure shows ZIP4 (A) and somatostatin protein expression in pancreatic islets of a normal human. Note the different morphology of the human islet compared to that of the mouse. The somatostatin staining is strong in the inner core of the islet, but there is also a background staining across the islet. ZIP4 is expressed in a different pattern than in the mouse. However, the significance of this is unclear and needs a proper characterisation in normal and diabetic human islets. Scale Bar, 100 μm
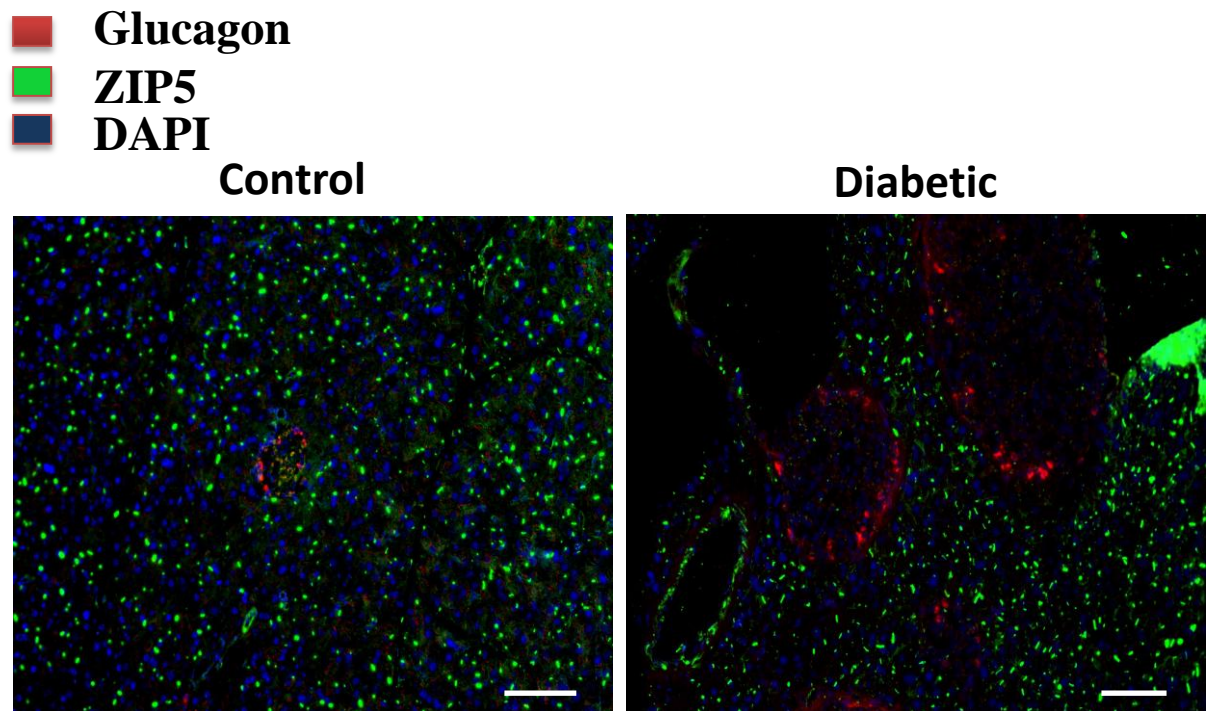
Figure 7.7 ZIP5 protein expression in control and db/db mice acinar and islet tissue at 4 weeks of age

Figure shows co-staining of ZIP5 (green),glucagon (red) and DAPI (blue) in pancreatic islets of wild type (left panel) and db/db (right panel) mice at 4 weeks of age. The figure shows that ZIP5 protein is highly expressed in the acinar tissue and almost no expression in the pancreatic islets in both wild type and db/db mice.
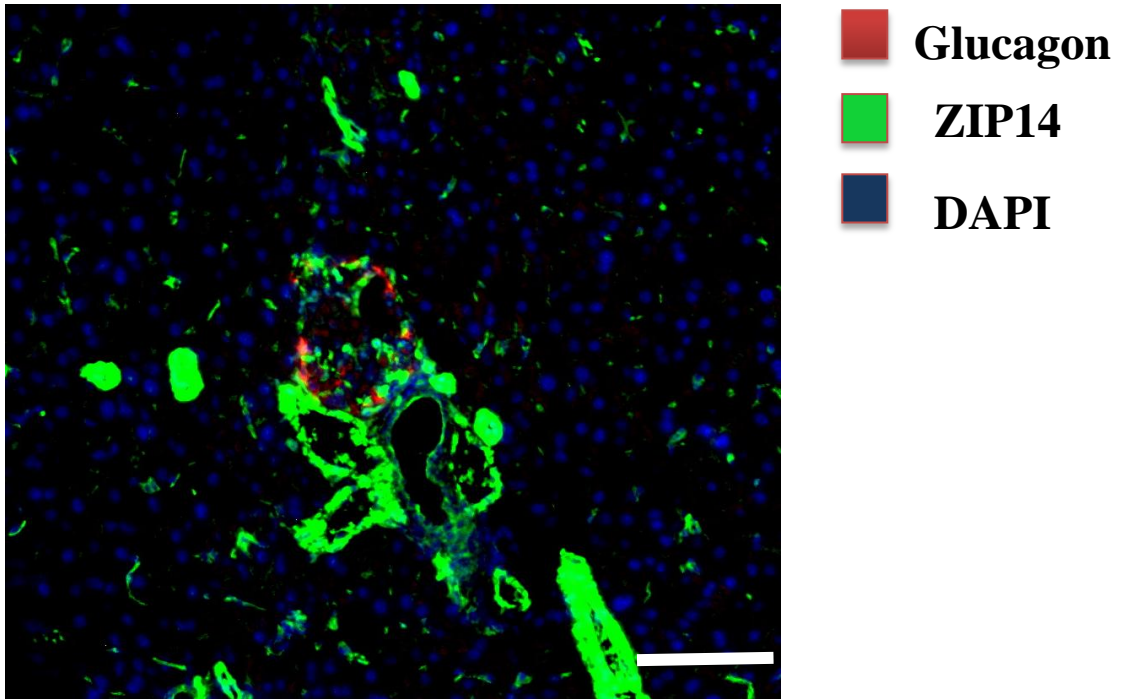
Figure 7.8 ZIP14 protein in the pancreatic islet and vasculature of a control 4 week mouse

Image of pancreatic section of a 4 week wild type miouse co-stained by immunofluorescence for ZIP14 (indicated in green) and glucagon (in red). ZIP14 is expressed in the blood vessels, acini and periphery of the pancreatic islet of wild type mice. Scale Bar, 100 μm
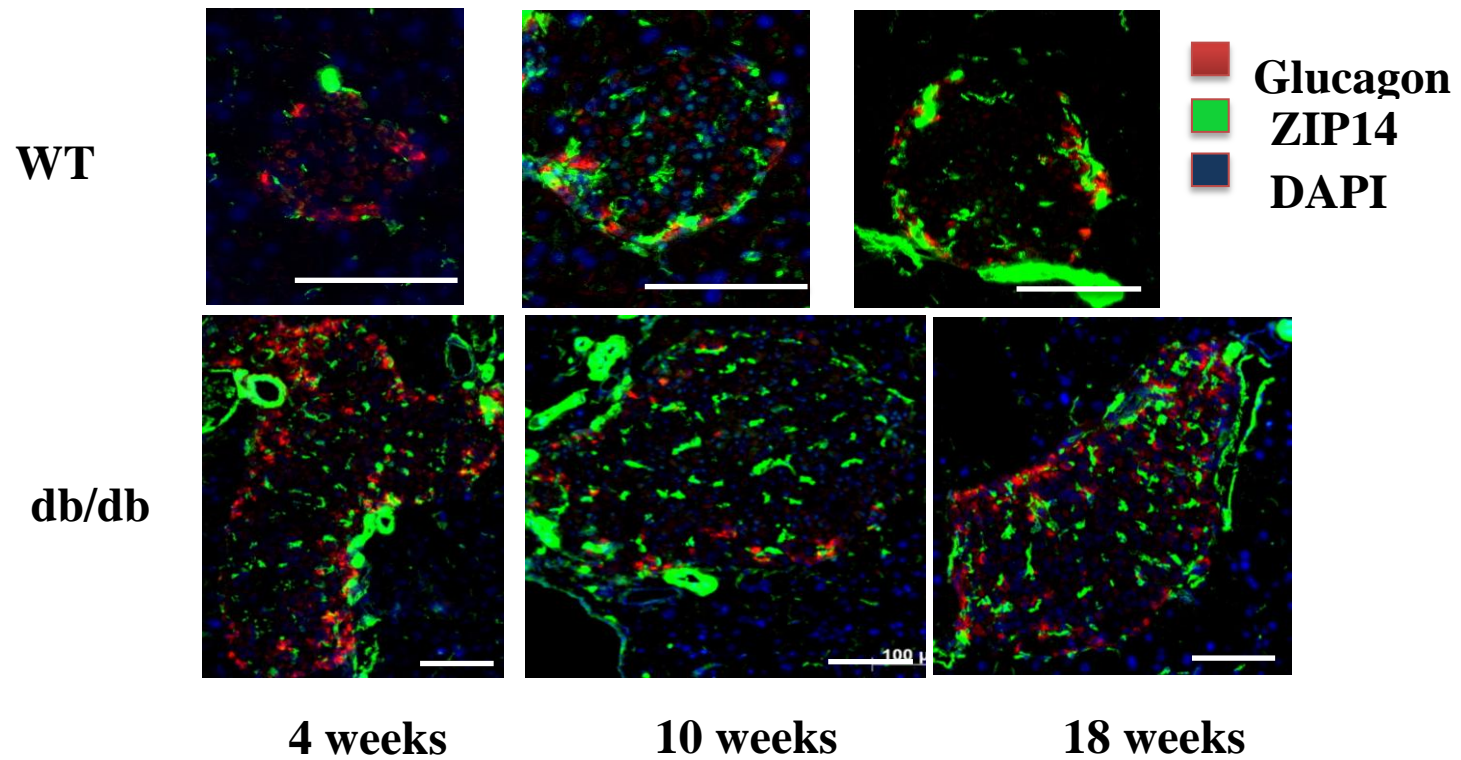
Figure 7.9 ZIP14 protein in wild type and db/db mice pancreatic islets

Figure shows representative images of co-staining of ZIP14 and glucagon. Upper panels show wild type mice, lower panels db/db mice. The columns represent 4, 10 and 18 weeks. ZIP14 is expressed in the periphery of the islets and in blood vessels (arrow) of wild type and db/db mice. In the db/db mice, the ZIP14 is increased within the pancreatic islets. Scale Bar, 100 μm.
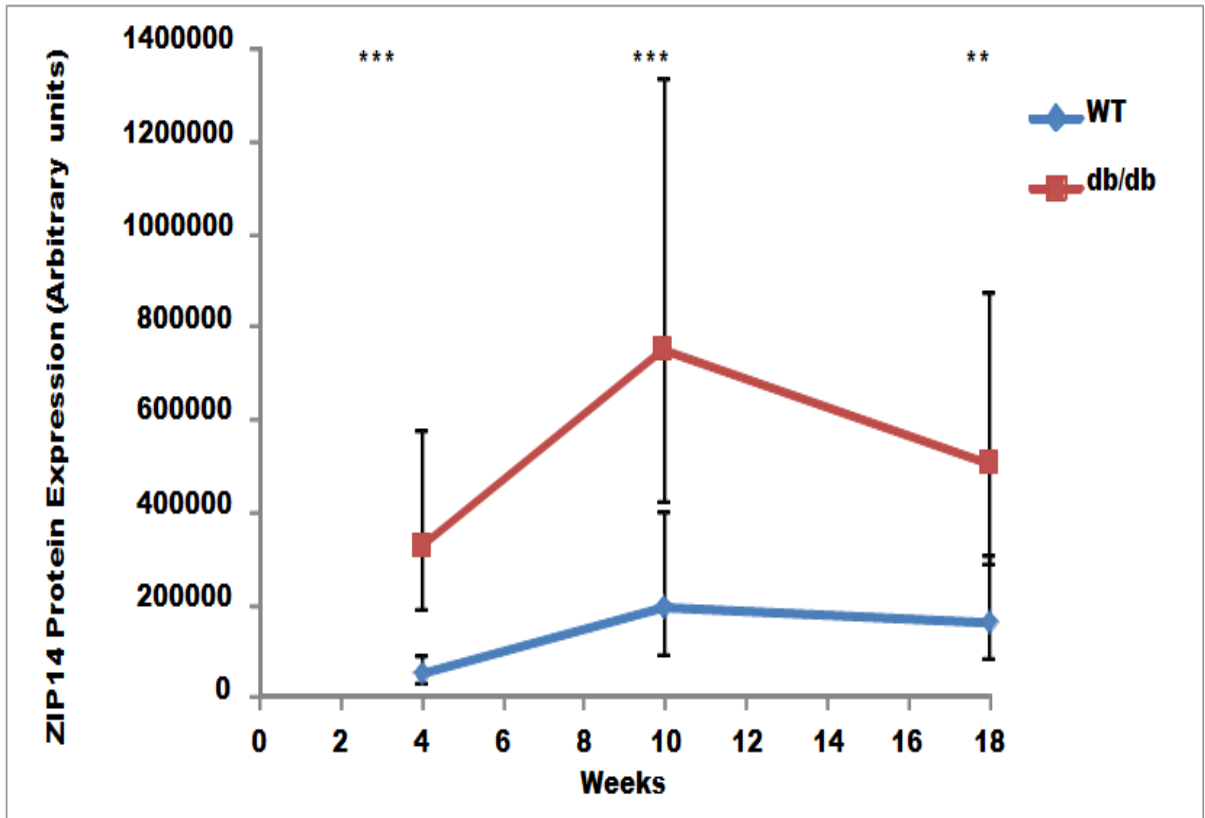
Figure 7.10 Effect of age and diabetes on ZIP14 protein in db/db mice pancreatic islets

Figure shows that ZIP14 protein was significantly up-regulated as early as 4 weeks in the db/db mice pancreatic islet and the peak up-regulation was seen at 10 and 18 weeks of age. The X axis represents the age of mice (weeks) and the Y axis represents the ZIP14 protein (arbitrary fluorescence units). Wild type mice are shown as the blue lines and the db/db mice are shown as the red lines. At each time point, between 19 and 55 islets from 4 mice were measured by integrated density using Just image J (FIGI). ZIP14 staining on blood vessels was excluded from the analysis. The data is shown as medians and the range as confidence intervals. * ($p < 0.05$), ** ($p < 0.005$) and *** ($p < 0.0005$). Statistical analysis was performed by type 2 ANOVA.
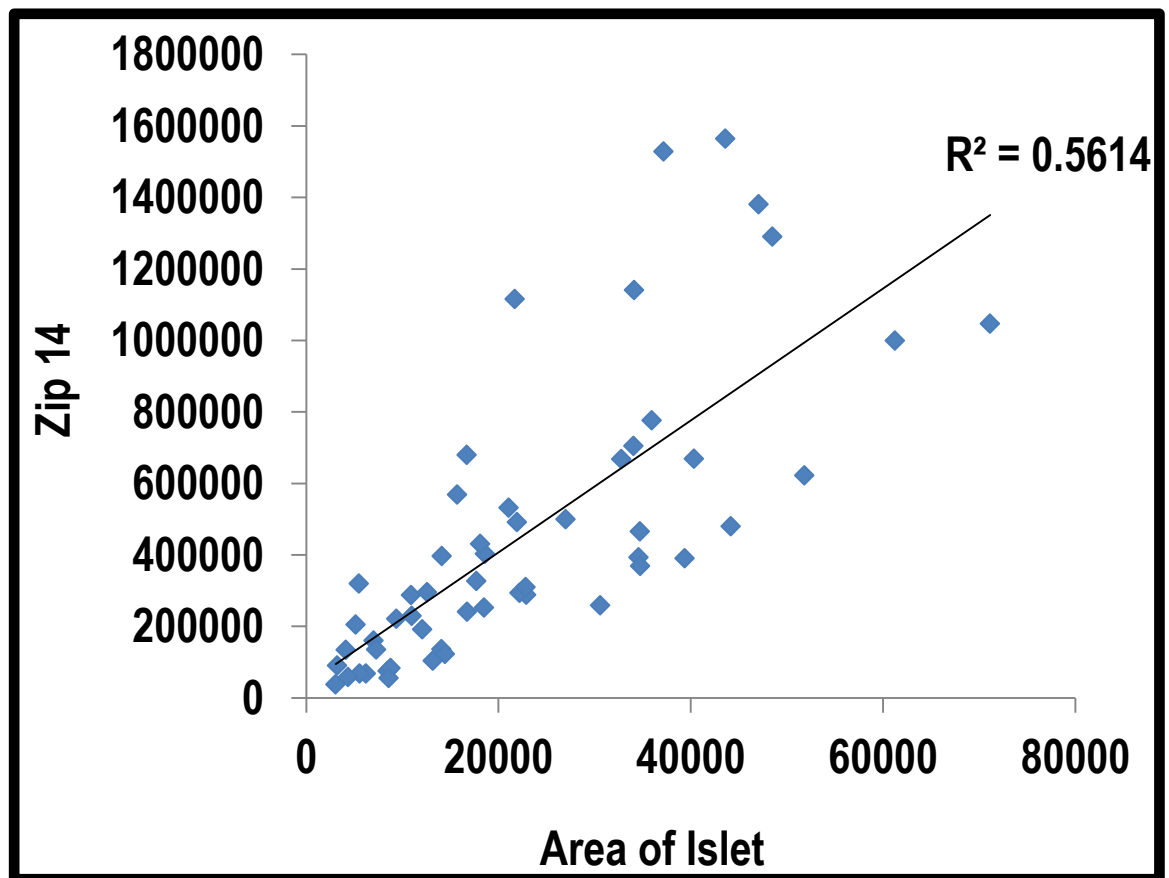
Figure 7.11 Correlation between ZIP14 protein expression and islet size

Islets from both wild type and db/db mice at 4 weeks of age were measured for ZIP14 staining and area in pixel. Data were pooled and the figure shows a strong correlation between ZIP14 protein staining intensity of the islets and area of islet (R^2=0.56).
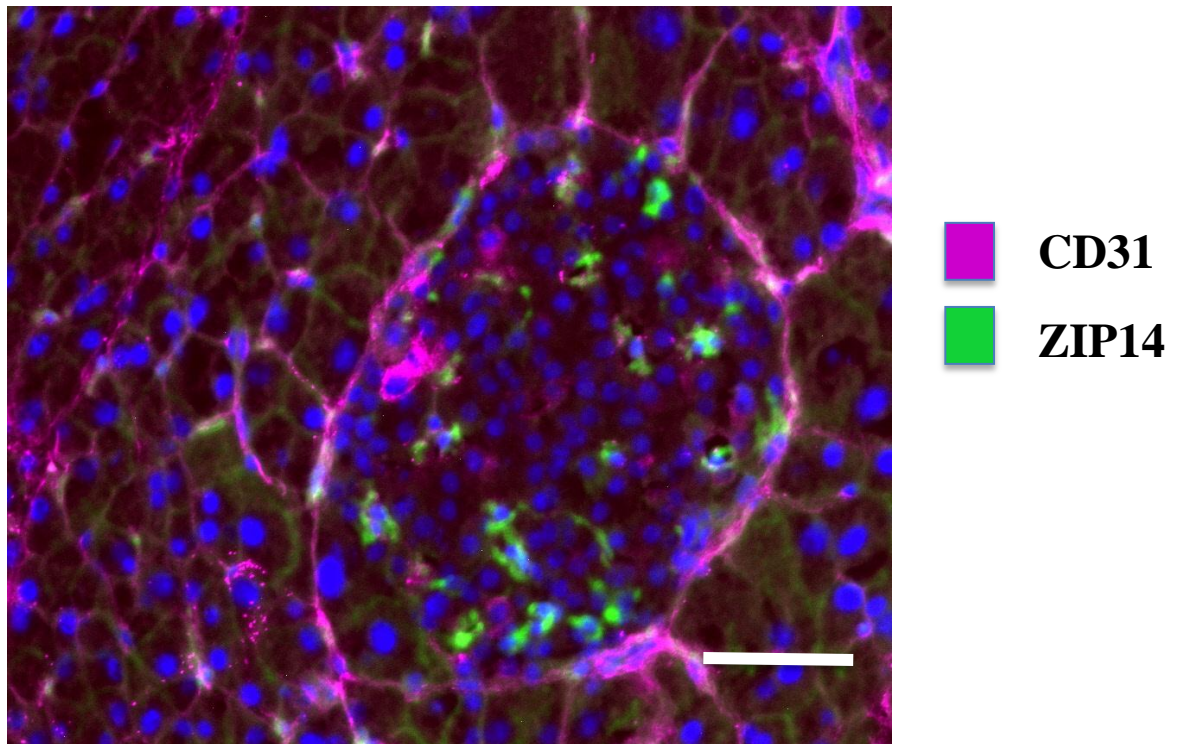
Figure 7.12 Co-localisation of CD31 and ZIP14 in db/db mice pancreatic islets

Figure shows a representative image of the co-staining of ZIP14 (green) and endothelial marker CD31 (magenta). It shows that ZIP14 does not co-localise with the endothelium marker CD31. Scale Bar, 100 μm.

CD6
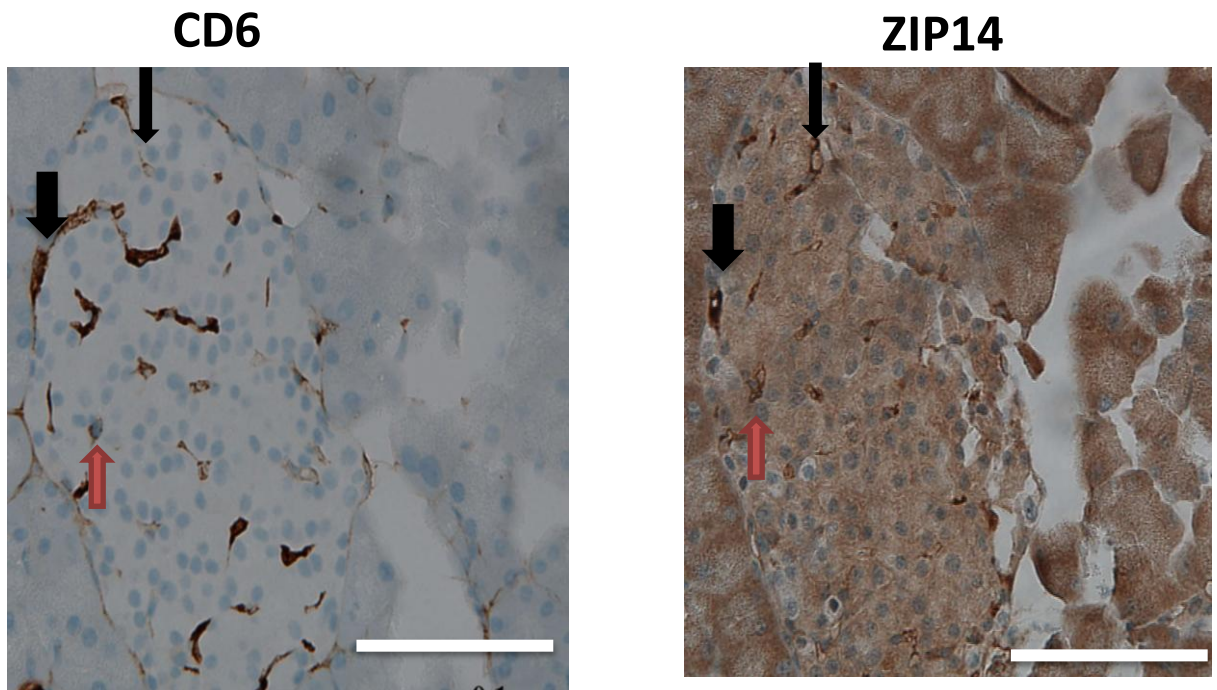
ZIP14

Figure 7.13 Co-localisation of CD68 (macrophage marker) and ZIP14 by immunoperoxidase in db/db mice pancreatic islet

Figure shows representative serial sections of staining of CD68 (left panel) and ZIP14 (right panel) that are expressed in 4 week db/db mice. The figure shows the co-localisation (arrow) of ZIP14 and macrophage marker CD68 in the pancreatic islet and also shows expression of ZIP14 in the inner core of the islet and the acinar tissue . Although these are serial sections, they are 4 μm apart and therefore there is not perfect alignment. Scale Bar, 100 μm
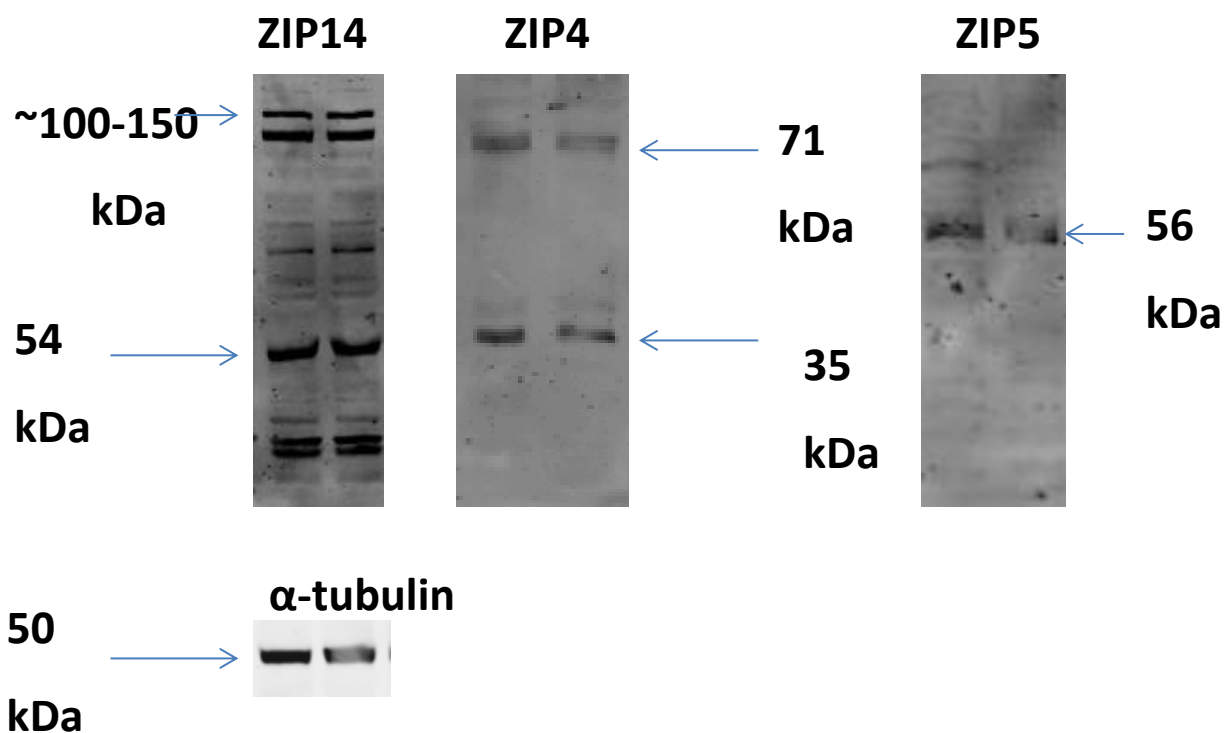
Figure 7.14 Expression of ZIP transporters in MIN6 beta cells

The figure shows protein expression (duplicate lanes) in MIN6 beta cell line by western blotting for Zip14 (left), ZIP4 (middle) and ZIP5 (right). α-tubulin was used as control for protein loading. For ZIP4, the two major bands which are 71kDa and the 35 kDa proteolytic fragment are indicated by arrows. For ZIP14, the doublet at 100-150 kDA and the monomeric form at 54kDa are indicated. For ZIP5, the single band at 56kDa is show
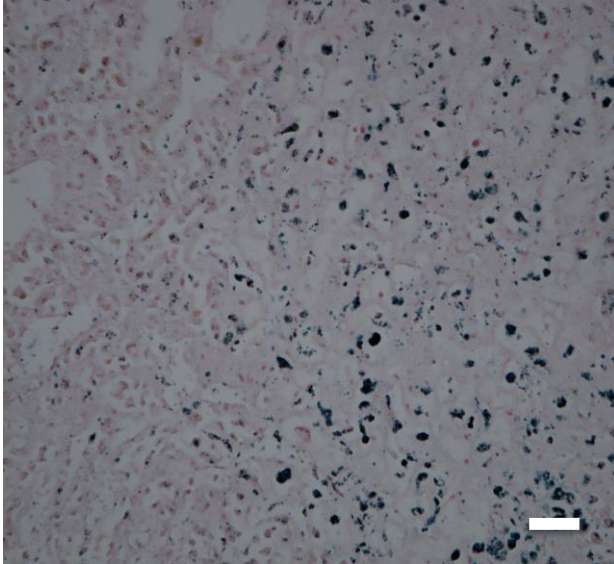
Human Liver   **db/db mice pancreas**
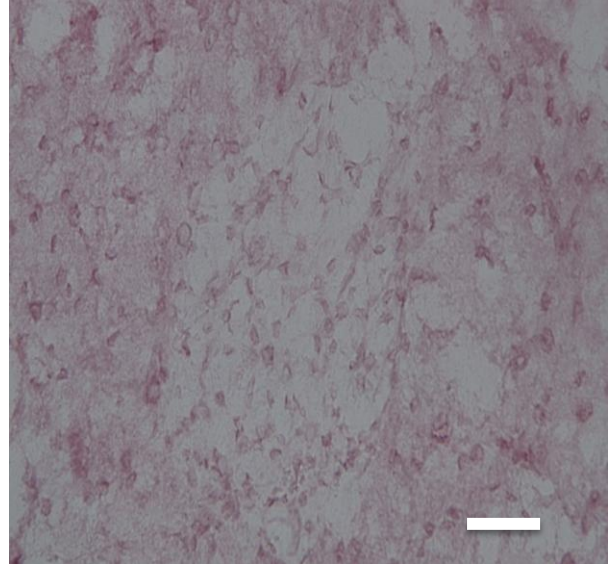
Figure 7.15 Iron staining of pancreas of db/db mice

Figure shows absence of staining for hemosiderin (tissue stain for iron) in pancreatic islets of chronic diabetic db/db mice. The positive violet blue staining for human liver is shown on the left. Counterstain was neutral red.Scale Bar, 100 μm.

7.4 Discussion

Although the finding that ZnT8 is critical to the Zn insulin story and the loss of Zn in diabetes (Chapter 6), it is not the whole picture. ZnT8 is restricted to the secretory granules of the beta cells and plays a role in granular levels of Zn. However, it cannot by itself move Zn into the beta cell as it is not a plasma membrane Zn transporter. It also cannot influence Zn levels in the golgi and ER which might be important for proinsulin folding and ER stress, respectively. Therefore, there is a need to identify other Zn transporters that influence beta cell Zn homeostasis in islets and which may be disturbed in diabetes.

ZIP4 has previously been shown to be a major Zn transporter responsible for Zn absorption at the luminal side of the small intestine; mutations in ZIP4 are responsible for a severe form of zinc deficiency affecting children (acrodermatitis enteropathica)[310]. ZIP4 is also expressed in other tissues[312] and may also be responsible for Zn uptake by these tissues. Whether ZIP4 is involved in pancreas and islet Zn uptake has not been well studied. Interestingly, the immunofluorescence studies were consistent with a localization of ZIP4 in delta cells of the pancreatic islets. ZIP4 did not co-localise with glucagon, nor did it have a comparable distribution to ZnT8 in beta cells. ZIP4 expression is disorganized in the pancreatic islet of db/db mice in correlation with the disorganized somatostain producing delta cells[110,112,332]. A previous study by Duffner Beattie et al[312] reported both the immunoperoxidase and immunofluorescence staining of ZIP4 throughout the islet with a pattern similar to beta cells. However, in their study ZIP4 was only lowly expressed and found in the beta cell zone. The reason for this discrepancy is unclear. In their study, pregnant db/db mice were used. ZIP4 may be an important influx transporter that brings Zn into the delta cells. Leiter et al investigated delta cells in 8-10 wk db/db mice pancreatic islets and showed by electron microscopy that number of delta cells increased in these mice[112]. The findings presented here support these results and show for the first time that these cells express an important Zn transporter, ZIP4.

Disorganization of alpha and delta cells in type 2 diabetes results in abnormal regulation and secretion of both insulin and glucagon[112,350,406]. The organization of the

islet cells is very important for the correct functioning of the islet cells. Hauge Evans 2009[407] investigated the role of somatostatin, by using somatostatin knockout mice and they reported that somatostatin has an inhibitory effect on insulin and glucagon synthesis and secretion[407]. In type 2 diabetes, because of the disorganization the delta cells are not able to function as efficiently[21]. In support Strowski et al 2008[350], observed that patients with type 2 diabetes have somatostatin levels that are normal, however, the rise of somatostatin in response to food ingestion or challenge with exogenous glucose was markedly reduced while insulin treatment restored the somatostatin response[350]. This indicates that delta cells are important for the function of islet cells and digestion.

ZIP4 may be involved in bringing Zn into the delta cells and possibly involved in paracrine regulation of both alpha and the beta cells. Disorganization of delta cells may contribute to altered Zn homeostasis and thereby lead to pathophysiological consequences described above. This raises the question why Zn transporters in one cell type within the islet such as the delta cell might be different from those in other islet cells such as the beta cell. It is possible that different Zn transporters are regulated differently in different islet cell types. Since the delta cells are also found in the intestine and ZIP4 is known to be a major Zn transporter in the intestine, islet delta cells may have Zn homeostasis pathway that are more in common with intestinal cells rather than with other islet cells. Of interest, I looked at ZIP4 expression in human pancreatic islets and found ZIP4 appeared to be lowly expressed in the insulin producing beta cells; however this need to be further confirmed. This species difference between human and mouse expression of ZIP4 could indicate that they may have functional differences.

Pancreatic ZIP5 is known to be important for Zn homeostasis and plays a role in the removal of Zn when systemic Zn is high and it is decreased in Zn deficiency[408]. It is located in the basolateral part of the acinar cells involved in uptake of Zn[311,409,410]. My study also confirmed that ZIP5 is expressed highly in the acinar tissue and very little in the islets cells. ZIP5 expression did not change in the early, mid and chronic diabetic db/db mice model compared to age matched WT group.

One of the most interesting and original findings in this thesis was the strong up-regulation of ZIP14 in early diabetic, diabetic and chronic diabetic islets. Previously, ZIP14 has been shown to be up-regulated in inflammation. Therefore, a study of ZIP14 in type 2 diabetes, where inflammation is thought to be important in the pathogenesis, was warranted. The ZIP14 protein expression did increase with age alone, but at all ages, the diabetic group had an up-regulation of ZIP14 compared to age-matched controls. ZIP14 was strikingly up-regulated when the db/db mice were overtly obese and hyperglycemic at 10 and 18 wk. Another study[411] showed that ZIP14 gene expression rapidly increased during early stages of adipocyte differentiation and the authors suggested that it plays an important role in bringing Zn into the adipocyte in early stages of adipogenesis.

In experiments described in this thesis, the db/db mice at 4 wk had significantly higher weight compared to the controls so ZIP14 might be upregulated in the db/db mice due to obesity. In obese and diabetic rodent models, it has been proposed that lipid mediators modulate immune cell function to cause low grade tissue inflammation, which in turn leads to adipocyte and metabolic dysfunction[412]. These lipid mediators acts through G protein coupled receptors. ZIP14 is known to work through a G protein coupled receptor; the lipid mediators could bind to these receptors thereby inducing ZIP14 expression and function[238] in obese db/db mice.

ZIP14 was also observed to be expressed in blood vessels adjacent to the islets, and this agrees with reports from the Pitt laboratory[413] showing ZIP14 in the endothelium of pulmonary blood vessels. Therefore, the possibility exists that ZIP14 is upregulated due to the altered vascularization of the islets in diabetes, particularly in islet capillaries. In a recent report, there was irregularity of the vasculature and decrease in VEGF mRNA expression in db/db mice pancreatic islets[27,414]. That the up-regulation of ZIP14 was due directly to changes in the vasculature is unlikely. Firstly, the increased immunostaining in the diabetic islets was consistent with cells or occasionally clusters of cells that resembled macrophages in appearance (Fig 7.13 showing immunoperoxidase staining of both CD68 and ZIP14). This was independently confirmed by a trained pathologist at The Queen Elizabeth Hospital. Secondly, the ZIP14 immunopositive cells were in the proximity of CD31-staining endothelial cells within the islets but did not directly

colocalise (Fig 7.12 showing pink and green cells) suggesting that the cells are clustered around the blood vessels, a feature consistent with infiltrating macrophages. The immunopositive cells had macrophage-like appearance consistent with the infiltration of macrophages seen during histological analysis of the islets. This is also consistent with recent reports in the literature that ZIP14 is expressed in macrophages in other tissues and upregulated by inflammatory stimuli LPS, IL6, TNF-alpha and IL-1beta[245]. ZIP14 may be a novel macrophage marker in diabetes. There was insufficient time to formally confirm that the ZIP14 positive cells are macrophages, but this will now be confirmed in our laboratory by co-staining for macrophage markers such as CD68.

If it can be confirmed that ZIP14 is labeling macrophages infiltrating the diabetic islets, the next step will be to determine the significance of this. In another study, db/db mice, when fed with normal diet, accumulated iron in their kidneys and developed kidney disease, whereas the db/db mice fed with an iron deficient diet were protected from disease. ZIP14 is not only a Zn transporter but also transports iron[236,415]. Such metal shifts may assist with islet amyloid plaque (IAPP) formation that is typical of type 2 diabetes. Consistent with this, Masters et al[416] showed, in another model of type 2 diabetes that macrophages colocalised with IAPP and were activated by it to produce inflammatory cytokines. In this context, it is possible that ZIP14 is being up-regulated on macrophages undergoing activation within the diabetic islets.

As ZIP14 is known also to be an iron transporter as well as a Zn transporter it will be interesting to study the relationship between ZIP14 and iron in islets. There was no detectable iron in the pancreatic islets in the chronic db/db mice pancreatic islets, but this may be due to the stain for hemosiderin not being sensitive enough to detect the small amount of iron released from macrophages. In future studies it will be interesting to investigate the iron regulatory peptide hepcidin which is known to be present in the secretory vesicles of insulin located in pancreatic beta cells where it has been suggested to be involved in the cross talk between iron and glucose metabolism[55,56].

The circulating cytokine profiles of the db/db and control mice were not significantly different for proinflammatory cytokines IL1β, TNFα and IL-6. Therefore, as suggested

earlier in this discussion, any inflammation in the db/db mice may be local rather than systemic (refer to Chapter 3). This was the conclusion also from the histological analyses, and confirmed by the hospital pathologist, that there was no overt inflammation in the pancreas of the db/db mice at any stage of diabetes but there was evidence of increased macrophage infiltration. It will be important now to look at staining of the cytokines in the islets themselves. In support of this, a recent study reported that IL-6, TNF-alpha and IL-1beta were upregulated in the pancreatic islets of these mice[417].

A recent study reported that ZIP14 knockout mice had upregulation of ZnT8 protein in the islets, increase in body weight, hypoglycemia, high insulin level, phosphorylation of insulin receptor and increased GLUT2 expression[240]. They also exhibited decreased release of circulating cytokines such as IL-6 and there was no change in the macrophage expression using CD68 staining. These knockout mice also showed impaired growth and glycogenesis and impairment of G coupled protein receptor signaling. GPCR signaling has an important role in the pathogenesis of type 2 diabetes and other diseases. in the islet as described earlier. Since knockout of ZIP14 in mice led to up-regulation of ZnT8[240] it is feasible that up-regulation of ZIP14 leads to down-regulation of ZnT8. How this might occur is not clear but may involve effects at the level of ZIP14 macrophages interacting with ZnT8 containing beta cells.

Here in this study, immunoperoxidase staining for ZIP14 in formalin fixed tissue shows some differences compared to immunofluorescence in frozen sections. Firstly, strong macrophage staining for ZIP14 was found in both methods. However, the immunoperoxidase staining showed a weaker staining for ZIP14 in the beta cell rich region and lack of staining in the mantle cells. The difference between the staining patterns may be due to increased sensitivity of the immunoperoxidase staining although usually immunofluorescence staining is more sensitive than immunohistochemical staining. It may be that formalin-preserved tissue gives a better morphology of the pancreatic islet and therefore improved localization of the Zn transporter.

These studies have now identified potentially important roles for ZIP4 and ZIP14 in two cell types relevant to diabetes, delta cells and infiltrating macrophages, respectively.

CHAPTER 8: Protein expression of Zn transporters in type 2 diabetic human compared to normal human pancreatic islets

8.1 Introduction

Previous chapters in this thesis showed significant changes in the Zn transporters proteins in the pancreatic islets of db/db mice compared to age matched controls. In summary, ZnT7 was primarily expressed in the beta cell-rich region of the islet and the protein was significantly upregulated in the islets of the db/db mice as early as 4 weeks of age. ZnT8 was expressed in both the alpha and the beta cells and, in diabetes, ZnT8 was reduced in the beta cells and was preserved in the alpha cells. ZIP14 was primarily expressed in islet macrophage while ZIP4 protein was expressed in the delta cells of the pancreatic islets in both db/db and age matched controls. It is now important to translate these murine findings to humans.

Zinc deficiency, including a reduction in pancreatic Zn, has long been documented in human patients with T2D[418]. A recent systematic review and meta analysis of 22 published studies in T2D concluded that Zn supplements improved glycaemic control and lipid parameters[355]. However whether Zn is lost in the islet is yet to be confirmed.

Much of what we know about Zn transporters in human islets concerns ZnT8. The importance of ZnT8 to type 2 human diabetes arose when genome wide studies in humans showed an association of the ZnT8 R325W polymorphic allele with increased susceptibility to type 2 diabetes[277]. Single nucleotide polymorphism of the ZnT8 gene in humans is linked to increased fasting glucose levels and type 2 diabetes[270,419]. The risk variant of ZnT8 had impaired Zn transport activity. A further recent study published in *Nature Genetics*[420], reported, paradoxically, that loss of function mutations in ZnT8 protected against type 2 diabetes in humans. In a large study, approximately 150,000 individuals were genotyped and 12 truncating variants in the protein ZnT8 were identified. The individuals who were carriers of the ZnT8 protein truncations had 65% reduced type 2 diabetic risk and showed reduced glucose levels. If correct this would contradict the previous findings suggesting that ZnT8 is protective against T2D. However, the interpretation of this recent study has now been challenged, suggesting age, hypoxic stress and other variables may have influence on whether ZnT8 is protective or not[421].

Variants in the ZnT8 protein may be potential drug targets in the therapy of type 2 diabetes. Insulinoma cells (INS-1E) over-expressing the low risk W325 variant, were

not susceptible to cyclosporine A suppression of glucose stimulated insulin secretion. However, the R325 variant over-expressing cells did show suppression of glucose stimulated insulin secretion by cyclosporine and other immunosuppressive drugs (tacrolimus and rapamycin)[261]. Therefore drugs may be developed that selectively target the high risk form of ZnT8.

The aim of the experiments described in this chapter was to investigate by immunofluorescence staining those Zn transporters that had shown significant changes in an animal model of type 2 diabetes (db/db) mice in normal and type 2 diabetic cadaver human frozen pancreatic tissue using.

It was hypothesised that (in line with the mouse studies) that:

- ZnT7 protein expression will be increased in in human T2D pancreatic islets compared to normals.
- ZnT8 protein will be dowregulatedin human T2D pancreatic islets compared to normals .
- There will be increased infiltration of macrophages containing ZIP14 in human T2D pancreatic islets compared to normal.
- There will be no change in expression of ZIP4 in human T2D pancreatic islets compared to normals

8.2 Methods

Pancreata from type 2 diabetic and normal humans were obtained from the Australian Islet Consortium with ethical clearance. The pancreas blocks were embedded in OCT medium and frozen in liquid nitrogen. Sections, 5µm, were cut using a cryotome then fixed in cold acetone for 10 min. The sections were blocked in a humidified chamber for 60 min with serum from the secondary antibody host animal. Sections were incubated with rabbit polyclonal Anti-Slc30a7 (1:150; Cat no. HPA018034; Sigma Aldrich, USA), Rabbit polyclonal Anti human ZnT8 (1:100; Cat no. PZ8; Mellitech, Grenoble Cedex, France),rabbit polyclonal rabbit polyclonal Anti-ZIP4 (1:100; Cat no. PA5-210669;Thermoscientific, Rockford, Illinois USA) or rabbit polycolonal Anti-ZIP5 (1:150; Cat no. PA5-21070; Thermoscientific, Rockford, Illinois USA) or rabbit polycolonaL Anti-ZIP14 (1:150; Cat no. PA5-21077;Thermoscientific, Rockford, Illinois USA) and mouse monoclonal Anti-glucagon (K79Bb10) (1:50; Cat no. ab10988;Abcam, , Melbourne, Victoria, Australia) overnight at 4°C. Excess primary antibody was removed by washing the slides with 1x PBS and incubated for 60 min with goat anti-rabbit Alexa488 IgG(1:400; Cat no. 54533A Invitrogen, Mulgrave, Victoria, Australia) conjugate and rabbit anti-mouse Alexa594 conjugate IgG1γ (1:400;Cat no. 940829; Invitrogen, Mulgrave, Victoria, Australia). Sections were washed with PBS and nuclei were counter-stained with DAPI(4', 6-diamidino-2-phenylindole; 1:1000).

8.3 Results

Immunofluorescence was performed for ZnT7, ZnT8, ZIP4 and ZIP14 proteins in pancreatic sections from normal human and T2D donors. Typical fluorescence images are shown in Figs 8.1-8.7

8.3.1   ZnT7

Figure 8.1 and 8.2 shows the staining of ZnT7 in typical normal human and type 2 diabetic pancreatic islets, respectively. ZnT7 was expressed in the pancreatic islets of the mice with a bead-like distribution consistent with localization in the golgi apparatus, as also described by Huang et al[258] in mouse pancreatic islets. There was a lack of co-localisation of ZnT7 with glucagon. Occasionally, ZnT7 was also expressed strongly in the pancreatic acinar tissue as shown in Figure 8.1 similar to the mouse pancreas in Figure 6. There was no obvious differences in the ZnT7 protein distribution in the human type 2 diabetics (figure 8.2).

8.3.2   ZnT8

Figure 8.3 and 8.4 shows the staining of ZnT8 in typical normal human and type 2 diabetic pancreatic islets, respectively. ZnT8 was expressed homogenously throughout the normal human islet especially in both the insulin producing beta cells and the glucagon producing alpha cells. Some ZnT8 protein expression was seen in the acinar tissue. Note the intense ZnT8 staining in the inner beta cell core of the normal islet compared with the diabetic islet. Also note the co-localization of ZnT8 and glucagon (orange colour) largely in the periphery of the normal islet but dispersed throughout the diabetic islet, suggesting the presence of ZnT8 in alpha cells and preservation of alpha cell ZnT8 in T2D. In the type 2 diabetic pancreatic as seen in figure 8.1 (B), ZnT8 protein expression was decreased in the pancreatic islet and was preserved in the alpha cells of the pancreatic islets as seen in the db/db mice at all ages figure 6.5. Negative controls (lacking primary antibody) were always included and were negative of staining.

210

8.3.3   ZIP4

Figure 8.5 shows the staining of ZIP4 in normal human islets and figure 8.6 shows ZIP4 staining in type 2 diabetic pancreatic islets. In normal pancreas, ZIP4 was not expressed in the acinar tissue but there was scattered expression in the islets. There was some co-localization of ZIP4 with the glucagon staining. ZIP4 staining was also quite distinct from insulin staining (beta cells) and glucagon staining (alpha cells) in both control and type 2 diabetic human pancreatic sections. Mostly the ZIP4 and glucagon cells were not co-localised similar to as seen in mouse islets (Figure 7.2). There was insufficient time to investigate the co-localisation of ZIP4 and Somatostatin in human islets by immunoperoxidase as was done in mouse islets.

8.3.4   ZIP14

Figure 8.7 shows the staining of ZIP14 in normal human islets and Figure 8.8 shows ZIP14 staining in type 2 diabetic pancreatic islets. ZIP14 staining in normal human islets was particulate but only infrequent and not in every islet. There appear to be differences between subjects. ZIP14 was also expressed in the blood vessels around the islets as seen in the mouse. ZIP14 in the type 2 diabetic human pancreatic islet was also expressed in a particulate manner and appear to be upregulated.

8.3.5   Quantification of Zn transporter immunofluorescences for individual human subjects

Image J software allowed semi-quantitative expression of protein levels (Fig 8.9). ZnT7 protein data was not quantified because of lack of time. Fig 8.9A shows data for ZnT8 staining in individual normal versus T2D subjects. The levels of ZnT8 fluorescence varied for different normal pancreata (mean fluorescence intensity $\pm$ SD was 90.5 $\pm$ 20.9, n =7 subjects). By contrast, all T2D subjects had low expression of ZnT8 in their islets (60.0 $\pm$ 7.4, n =5 subjects) and the overall mean for the group was significantly lower ($p<0.05$) than that for the normals. Fig 8.9B shows that the levels of ZIP4 fluorescence varied for different normal pancreata and there was no significant difference between the overall means for normals (18.2 $\pm$ 4.1, n = 7) and T2D subjects

(26.8 $\pm$ 7.0, n = 5). Fig 8.9C shows variable levels of ZIP14 fluorescence between subjects (normal and T2D). In particular, one of the seven normal subjects and three of the eight diabetic subjects tested had strong islet ZIP14 staining. There was no significant difference between the overall means for normals (44.3 $\pm$ 35.5, n = 7) and T2D subjects (62.4 $\pm$ 42.7, n = 8).

Thus, significant changes occur in ZnT8 in human diabetes and there is variable expression of two influx Zn transporters ZIP4 and ZIP14 on different islet cell types.
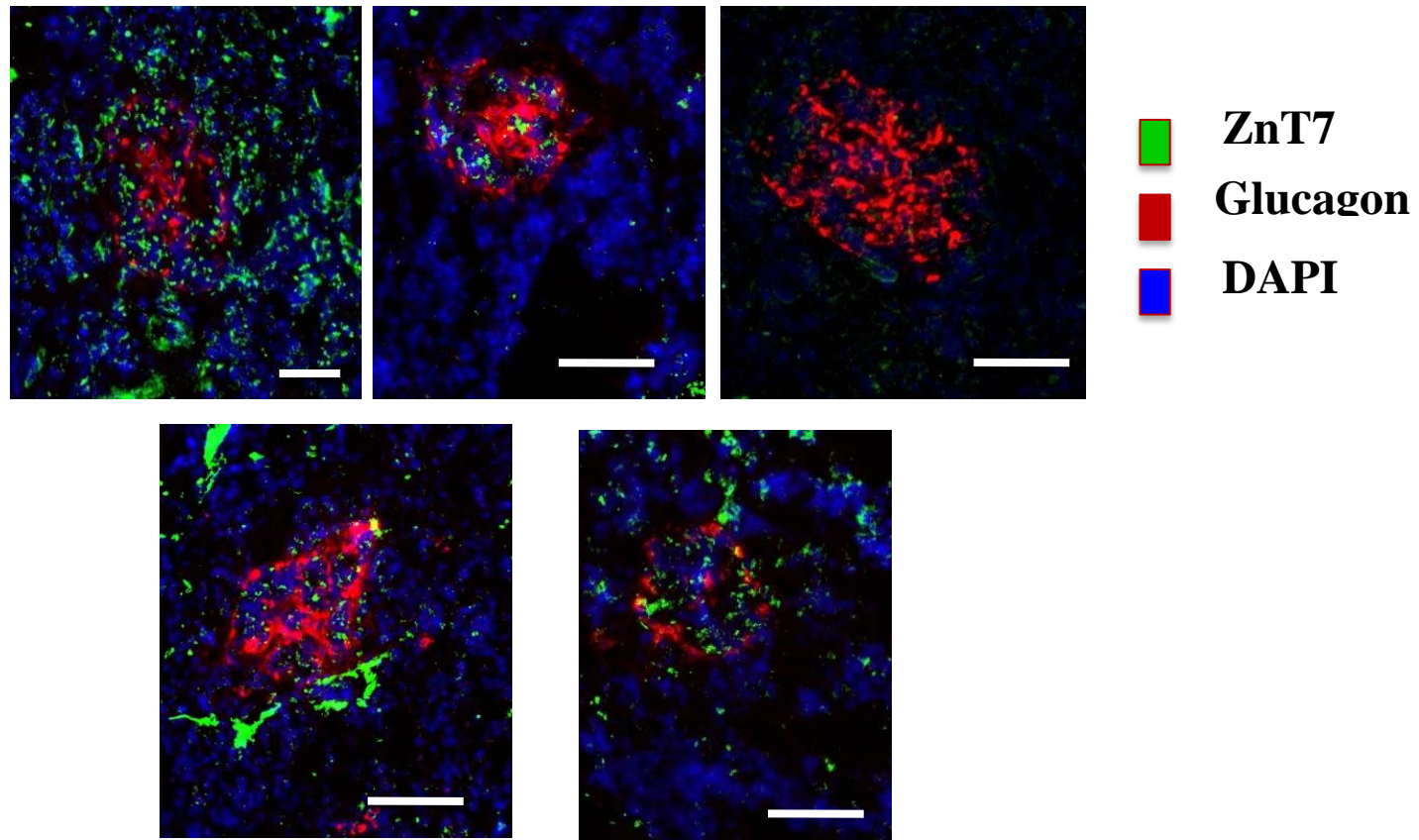
Figure 8.1 ZnT7 protein in islets of normal human patients

Figure shows representative images of co-staining of ZnT7 (green), glucagon (red) and DAPI (blue). Upper and lower panels show ZnT7 protein expression from 5 normal human pancreatic islets. ZnT7 is expressed in Golgi like structures within the islet beta cells and there is little co-localization with glucagon. Scale Bar, 100 μm
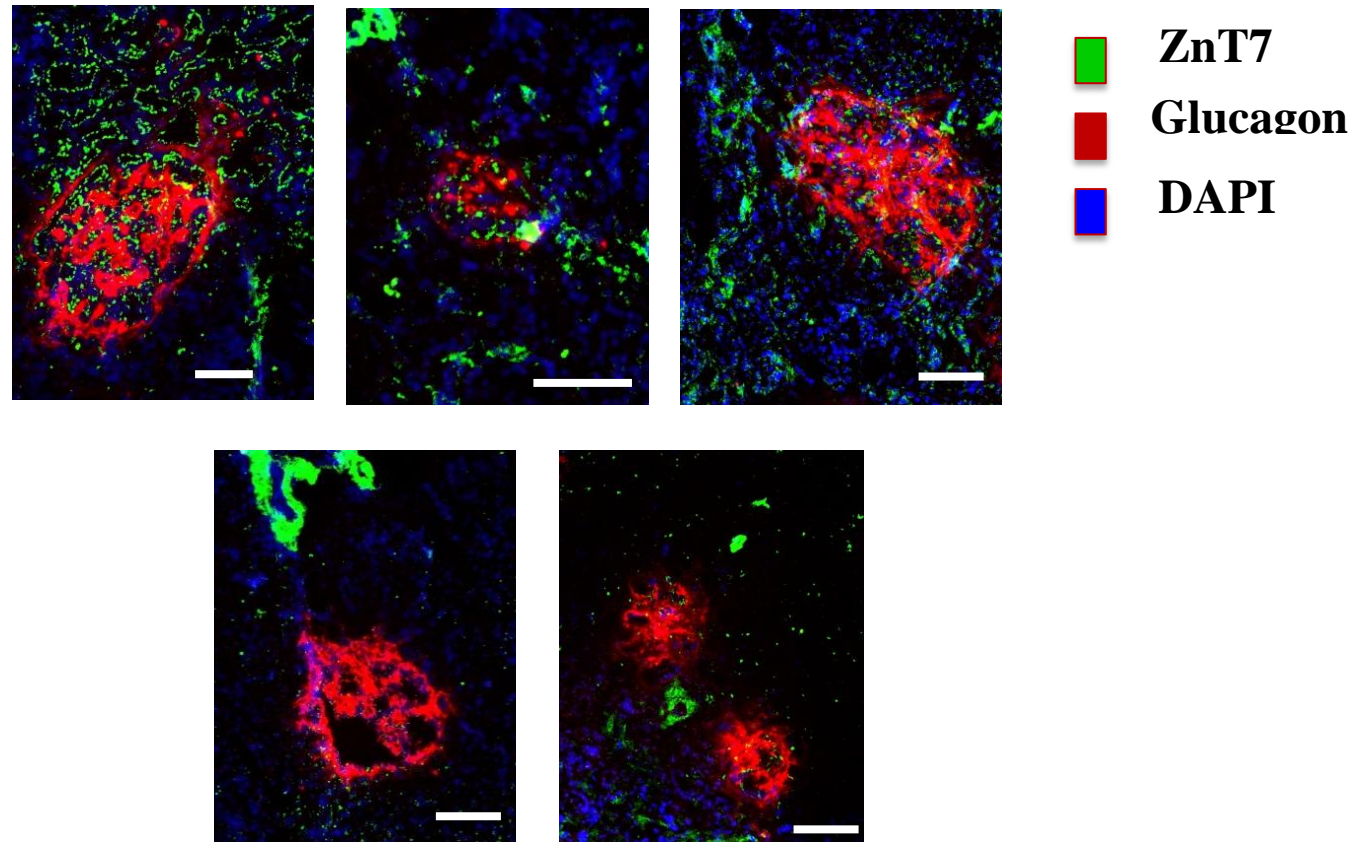
Figure 8.2 ZnT7 protein in islets of type 2 diabetic human patients

Figure shows representative images of co-staining of ZnT7 (green), glucagon (red) and DAPI (blue). Upper and lower panels show ZnT7 protein expression from 5 normal human pancreatic islets. ZnT7 is expressed in Golgi like structures within the islet beta cells and there is little co-localization with glucagon. ZnT7 were not expressed in many islets due to alpha cell invasion in the islets of type 2 diabetic patients. Scale Bar, 100 μm
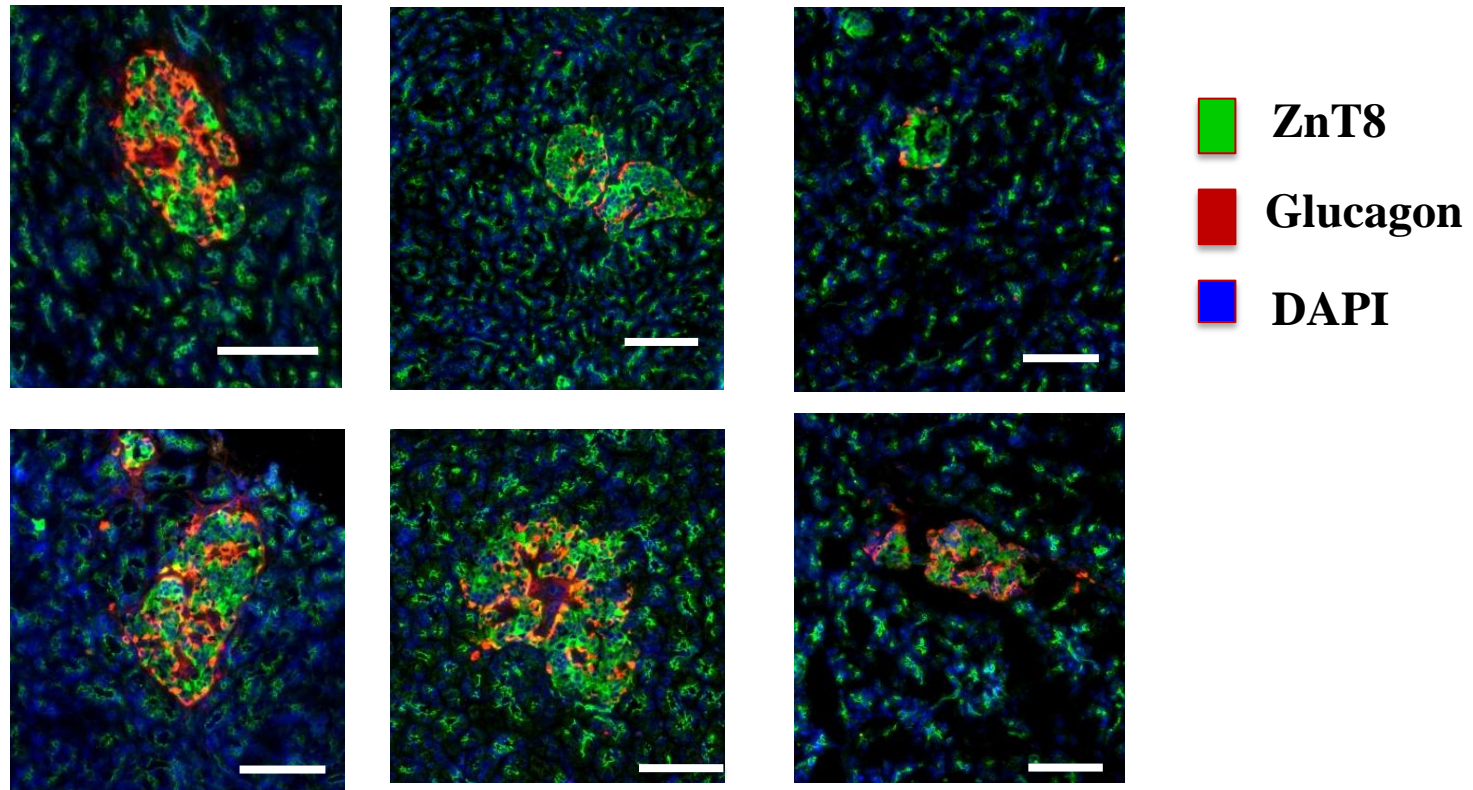
Figure 8.3 ZnT8 protein in pancreatic islets of normal human patients

Figure shows representative images of co-staining of ZnT8 and glucagon. Upper panel and lower panel show pancreatic islets from 6 normal human patients. Figure shows endogenous staining of ZnT8 , all cells in the pancreatic islets including alpha and beta cells express the protein ZnT8. The expression of ZnT8 in delta cells was not confirmed. Scale Bar, 100 μm
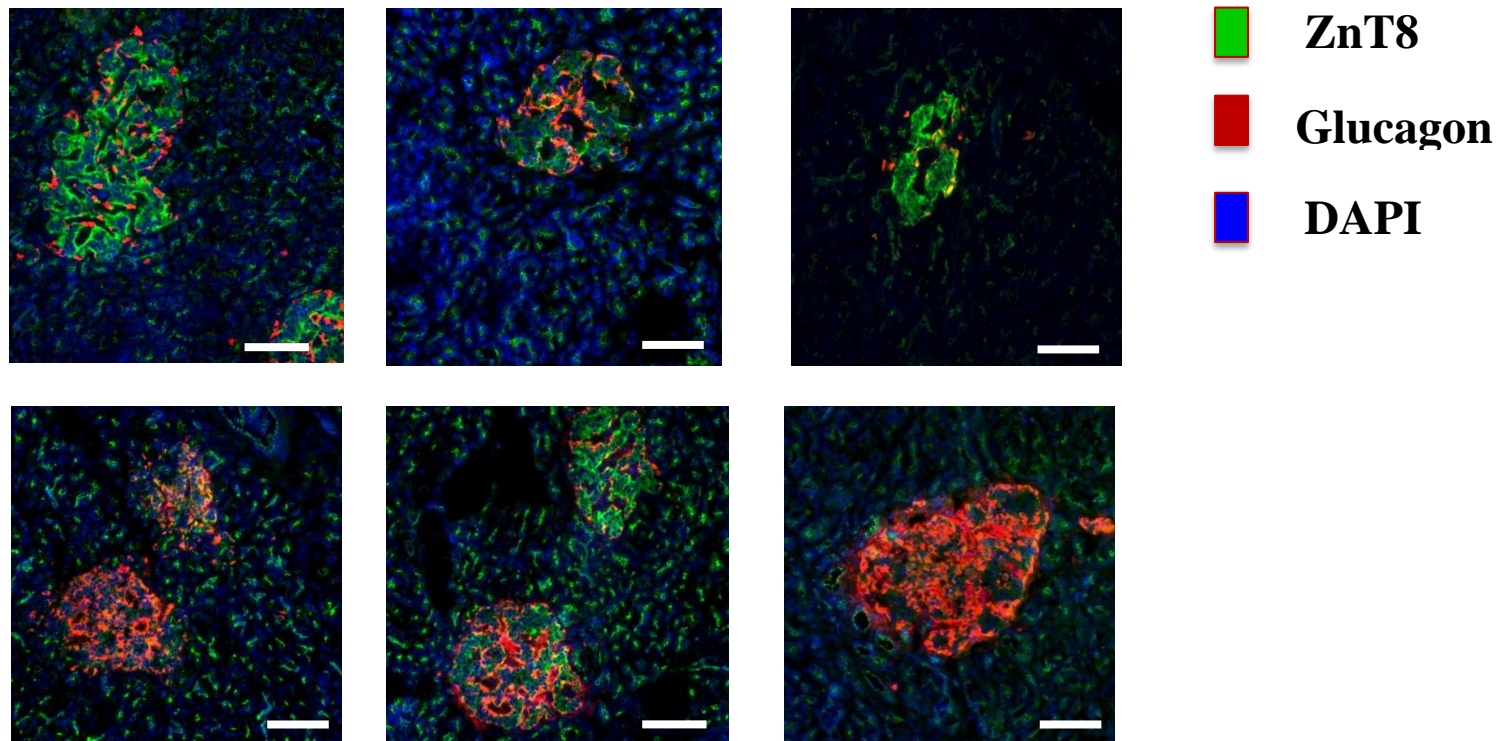
Figure 8.4 ZnT8 protein in pancreatic islets of diabetic human patients

Figure shows representative images of co-staining of ZnT8 and glucagon. Upper panel and lower panel show pancreatic islets from 6 type 2 diabetic human patients. Figure shows endogenous staining of ZnT8, all cells in the pancreatic islets including alpha and beta cells express the protein ZnT8.ZnT8 was preserved in alpha cells and there was variable expression of ZnT8 in beta cells in the patients with type 2 diabetes. Scale Bar, 100 μm
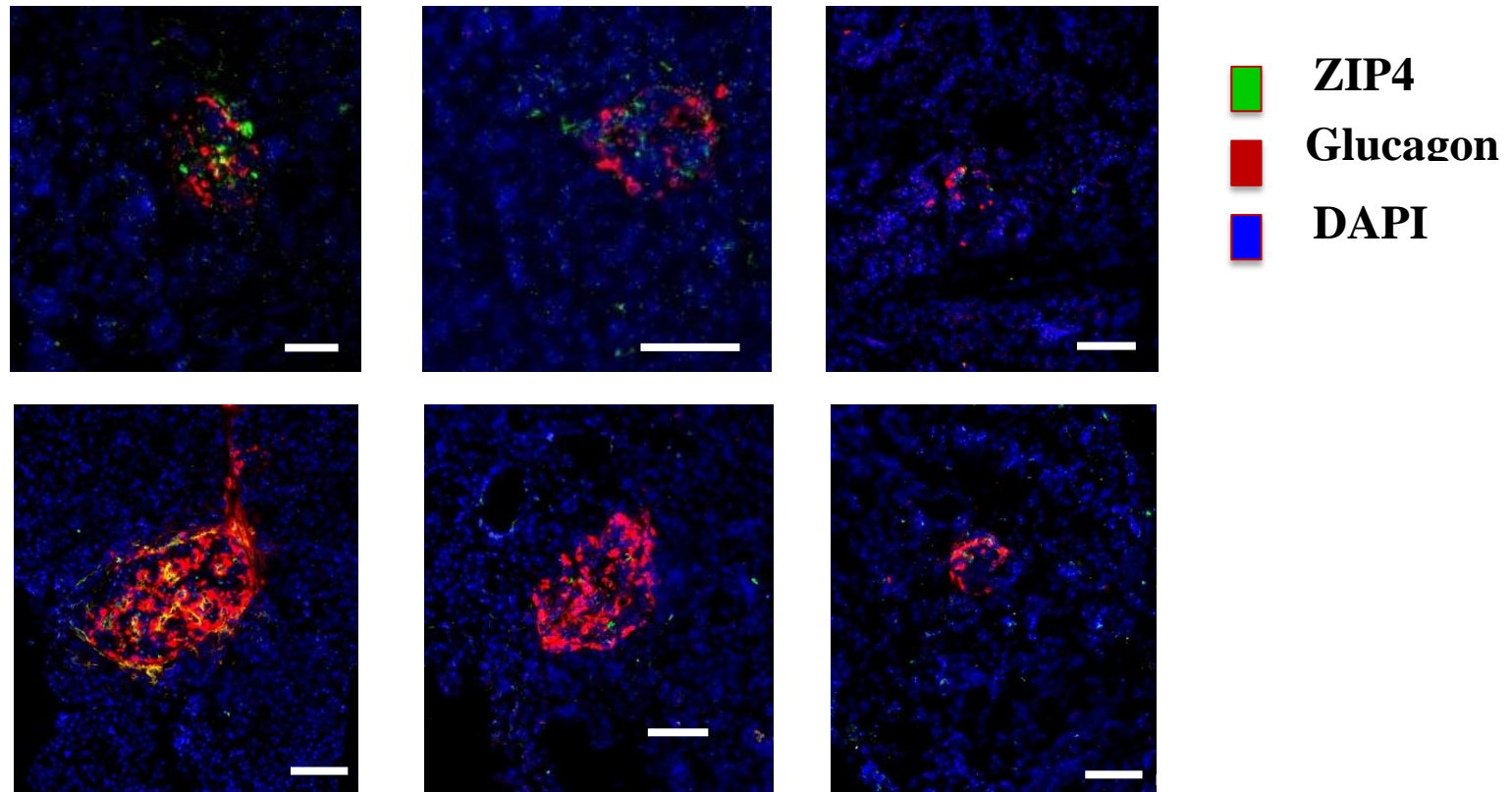
Figure 8.5 ZIP4 protein in islets of normal human pancreatic islets.

Figure shows representative images of co-staining of ZIP4 (green), glucagon (red) and DAPI (blue). Upper and lower panels show pancreatic islets from 6 normal human patients. Figure shows the staining of ZIP4 in cells is largely restricted to the non-alpha cells in the mantle of the pancreatic islets normal humans. ZIP4 is scattered throughout the pancreatic islets. However in occasional islets there are some co-localisation of ZIP4 and glucagon. Scale Bar, 100 μm
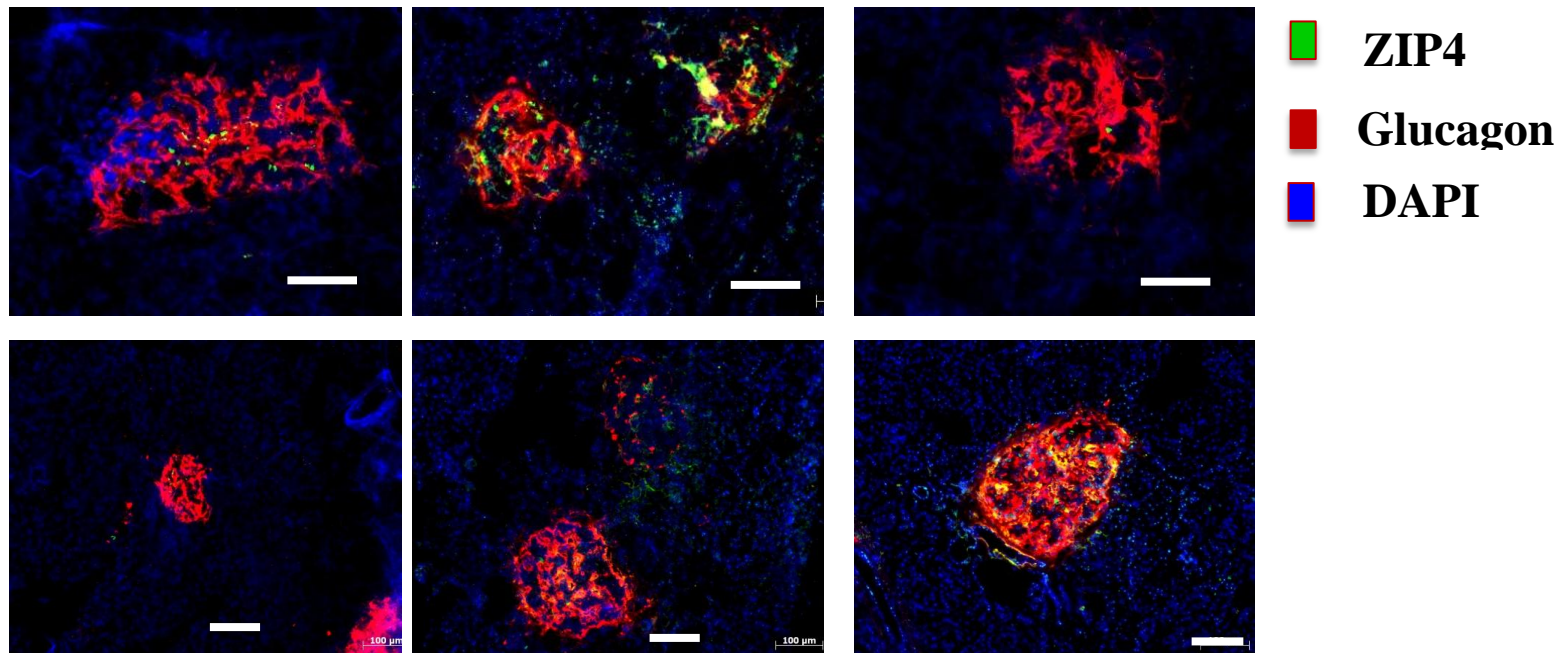
Figure 8.6 ZIP4 protein in islets of type 2 diabetic human pancreatic islets.

Figure shows representative images of co-staining of ZIP4 (green), glucagon (red) and DAPI (blue). Upper and lower panels shows pancreatic islets from 6 type 2 diabetic human patients. Figure shows the staining of ZIP4 in cells is largely restricted to the non-alpha cells in the mantle of the pancreatic islets of type 2 diabetic patients. ZIP4 is scattered throughout the pancreatic islets. However in occasional islets there are some co-localisation of ZIP4 and glucagon. There were variability in expression in the ZIP4 protein in the pancreatic islets of the type 2 diabetic patients. Scale Bar, 100 μm
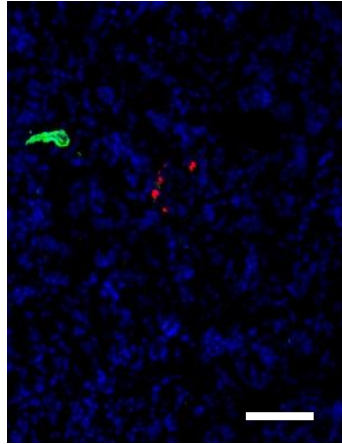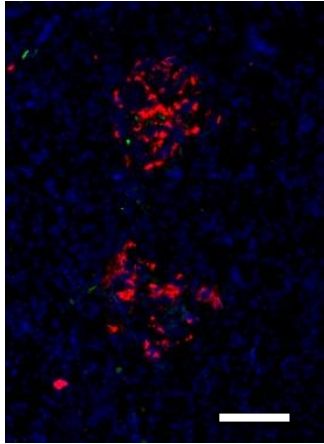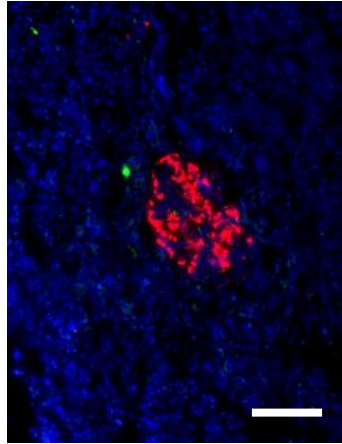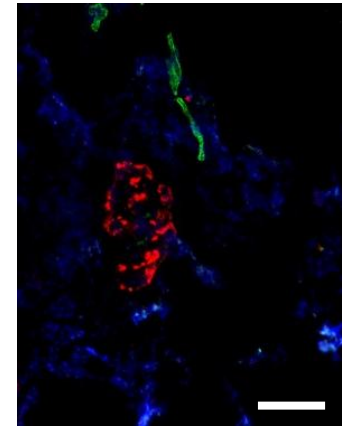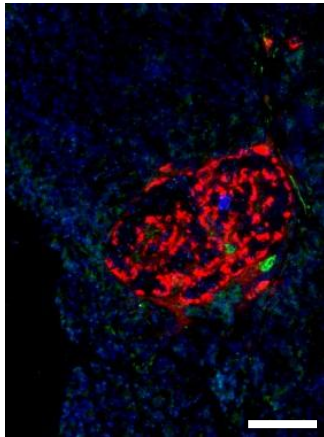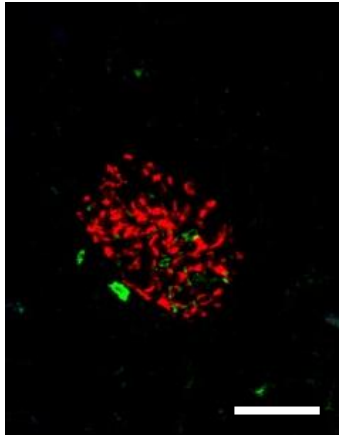
Figure 8.7 ZIP14 protein in islets of normal human patients.

Figure shows representative images of co-staining of ZIP14 (green), glucagon (red) and DAPI (blue). Upper and lower panels shows pancreatic islets from 6 normal human patients. Figure shows the staining of ZIP14 in cells is largely restricted to non-alpha, beta and delta cells, but macrophage like cells.it also shows that there is low expression of ZIP4 in normal human islets. Scale Bar, 100 μm
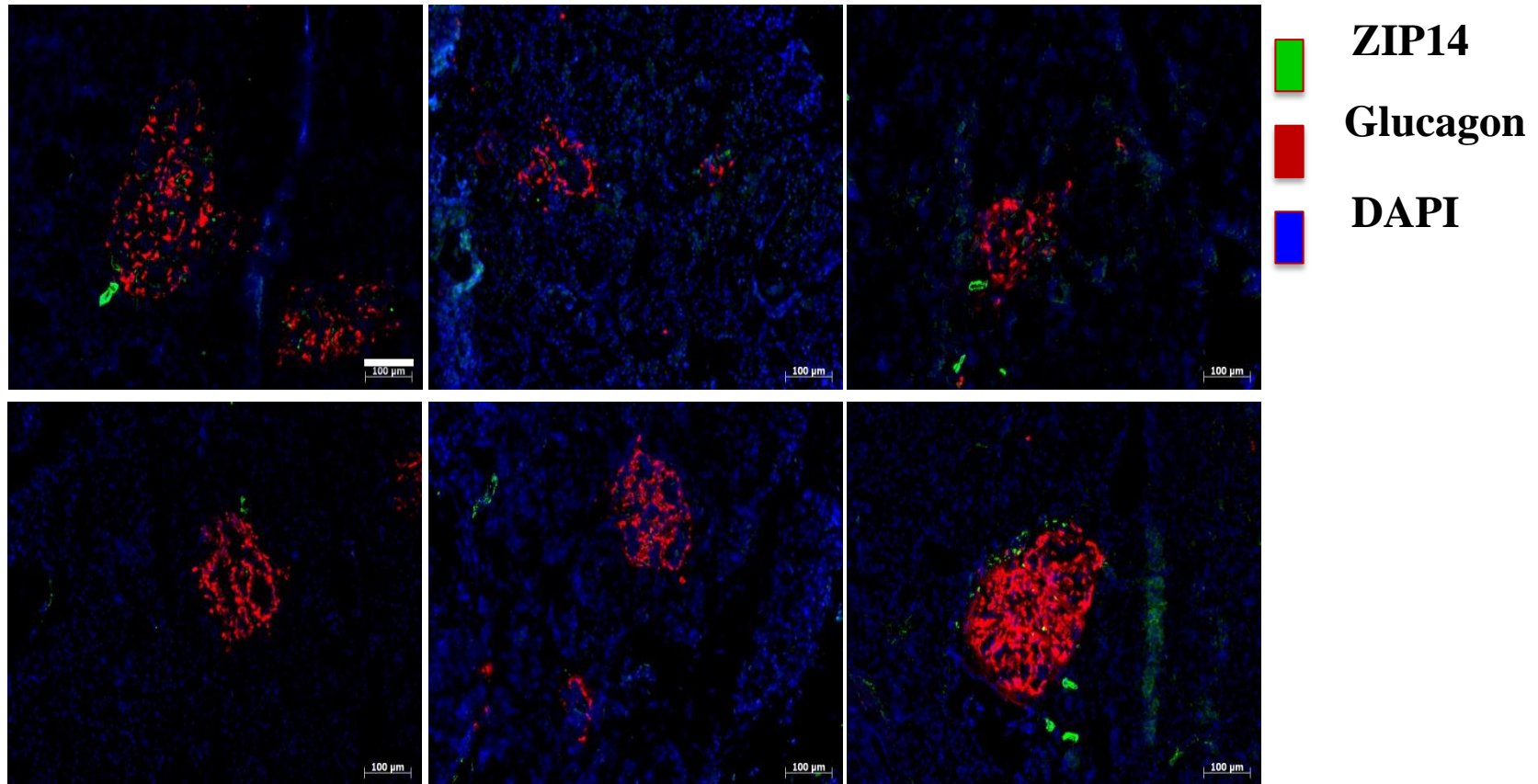
Figure 8.8 ZIP14 protein in islets of type 2 diabetic patients.

Figure shows representative images of co-staining of ZIP14 (green), glucagon (red) and DAPI (blue). Upper and lower panels shows pancreatic islets from 6 normal human patients. Figure shows the staining of ZIP14 in cells is largely restricted to non-alpha, beta and delta cells, but macrophage like cells. It also shows the variability in the ZIP14 containing macrophages in the patients with type 2 diabetes. Scale Bar, 100 µm
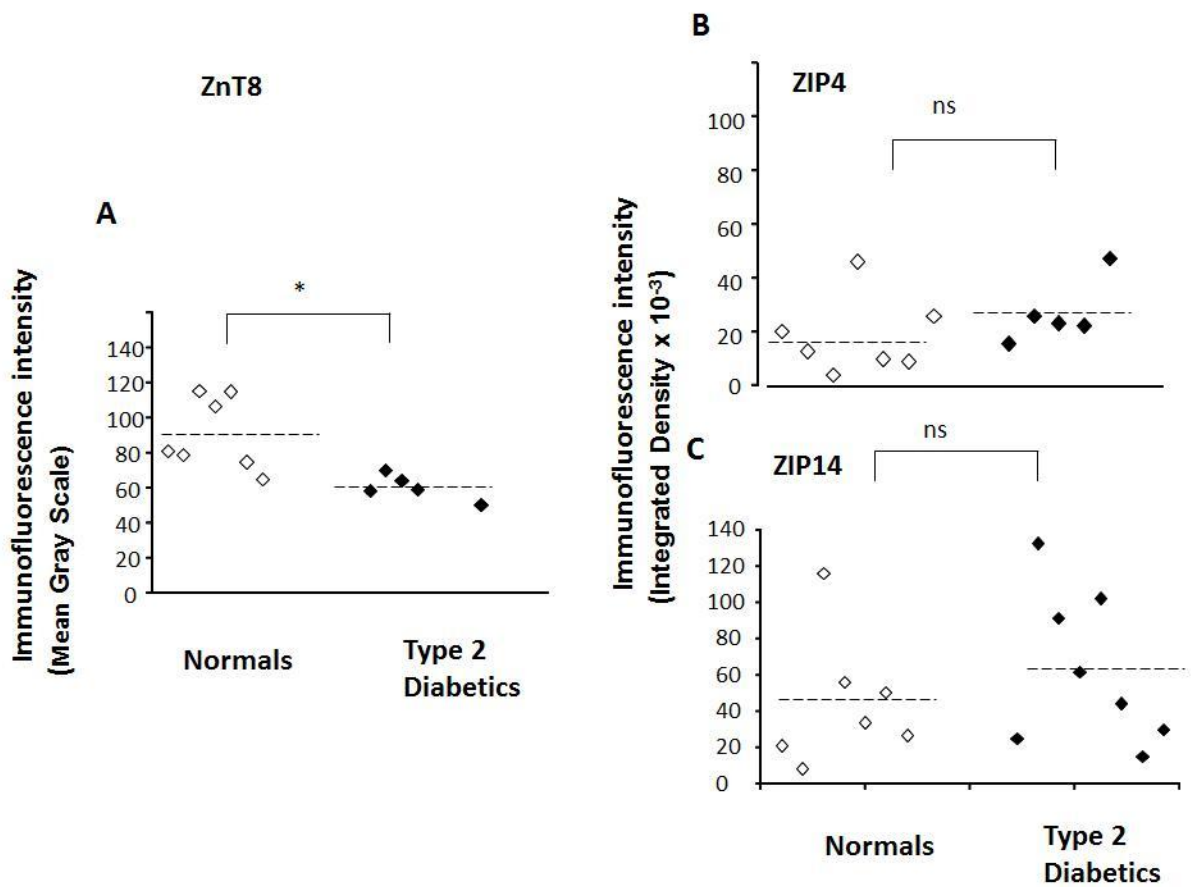
Figure 8.9 Differences in Zn transporter expression between islets of normal and T2D human subjects

Data show immunofluorescence intensities (arbitrary units) of ZnT8 (A), ZIP4 (B) and ZIP14 (C) in islets of individual normal (n = 7) and T2D (n = 5-8) subjects. Note the variable intensities of ZnT8 in different normal subjects. Dashed line shows means for each group. The only significant changes in expression between the normal and diabetics was in ZnT8 (A) although three of the 8 cases of T2D had substantially increased staining for ZIP14 (C). Fluorescence was quantified using ImageJ with mean gray scale for the more homogeneous staining pattern of ZnT8 and integrated density for the more particulate staining patterns of ZIP4 and ZIP14. 214 islets from normal and 301 islets from T2D were quantified. * P <0.05   ns = not significant.

8.4 Discussion

A bonus of our study was access to human T2D pancreata which are otherwise difficult to obtain. We show, for the first time, the expression and islet cell distribution of ZnT8, ZIP4, and Zip 14 in the human pancreatic islets, and changes in human T2D. The major findings in human T2D were ZnT8 was downregulated on islet beta cells but preserved on alpha cells and ZIP4 and ZIP14 were selectively expressed in the islets on somatostatin producing delta cells and macrophages, respectively.

One of the unexpected findings in the normal human pancreas was the widely differing levels of protein expression of ZnT8 between different subjects. Other studies from our group have also confirmed this for gene expression as shown for mRNA by RT-PCR and micro-array. Whether this is a consequence of ZnT8 polymorphisms or some other factor related to prediabetes, obesity or glycaemic control requires further investigation. It is estimated that about one in three normal subjects have prediabetes (US statistics) and this might account for the lower ZnT8 protein expressions seen in Fig 8.2.

This study is the first report of alpha cells containing ZnT8 in both diabetic humans and mice. Loss of ZnT8 in the beta cell rich zone but retention of ZnT8 on alpha cells in diabetes might provide an explanation for the impairment of insulin production and retention of glucagon production in T2D. It also suggests that whatever leads to loss of ZnT8 (and Zn) in the beta cells does not affect the alpha cells. Rather these cells progressively replace beta cells during the development of type 2 diabetes.

There is very little known about ZIP transporters in pancreatic islets and diabetes. These are likely to be relevant because they regulate the influx of Zn into the cytosol of the cell and control cytoplasmic enzymes. Our studies show, for the first time, a strong up-regulation of ZIP14 in early and chronic diabetic islets. This is also consistent with recent reports in the literature that ZIP14 is expressed in macrophages in other tissues and is upregulated by inflammatory stimuli[236,237,240,245]. ZIP14 may therefore be a novel macrophage marker in type 2 diabetes. The relationship of ZIP14 to islet macrophage activation state needs to be clarified. Lipopolysaccharide has been shown to upregulate ZIP14 in macrophages and ZIP14 knockout attenuated downstream cytokine signaling. This has implications for inflammation in type 2 diabetes[245]. In the db/db mice

pancreatic islet it is known that the pro-inflammatory M1 subtype increases and there is no change in the trophic M2 subtype expression[28]. In view of this it is likely that ZIP14 is expressed on the proinflammatory macrophages and may be involved in processes such as beta cell apoptosis and beta cell de-differentiation. The strong positive correlation between islet area and ZIP14 protein expression raises the possibility that ZIP14 up-regulation is a factor in the early islet hyperplasia in T2D. Since ZIP14 knockout in C57BL/6 mice leads to upregulation of ZnT8 protein in the islets as well as increase in body weight, phosphorylation of insulin receptor and increased GLUT2 expression[240], it is feasible that up-regulation of ZIP14 leads to down-regulation of ZnT8. How this might occur is not clear but our findings are consistent with effects at the level of ZIP14 macrophages interacting with ZnT8 containing beta cells.

Our finding that normal pancreatic islet delta cells almost exclusively express ZIP4, a major Zn transporter responsible for Zn absorption in the intestine[312], is consistent with the existence of a gut islet somatotrophin axis. ZIP4 expressed in delta cells of the islets could be important for gut islet interaction and homeostasis. While we found no significant change in the ZIP4 expression in the diabetic islets, disorganisation of delta cells containing ZIP4 could have functional implications in type 2 diabetes involved in gut related roles. Since ZIP4 is overexpressed in many pancreatic cancers[402], the role of ZIP4 in islet cell function and islet hyperplasia needs to be investigated.

These findings now point to an important role for changes in islet Zn metabolism in the onset of Type 2 diabetes. We hypothesize that down-regulation of beta cell ZnT8 at the gene level results in an early loss of Zn from the pancreatic islet and contributes to the development of type 2 diabetes by causing a block in insulin maturation and decline in beta cell function. We also propose that the retention of ZnT8 in alpha cells of diabetics preserves glucagon production. Up-regulation of ZIP14 on islet macrophages in diabetes may contribute to islet inflammation. In addition, ZIP4 may be a major influx transporter for Zn in delta cells.

CHAPTER 9 Final discussion

9.1 Gap in literature and hypothesis and aims

It has long been known that Zn is required for the correct storage of insulin in beta cell granules of the islets of Langerhans and that total Zn is reduced in human type 2 diabetic pancreata compared to normal human pancreata[418]. This suggests that a critical Zn-dependent pathway in the production and/or secretion of insulin, may be compromised in type 2 diabetes. Recently, several studies have identified the secretory granule zinc transporter ZnT8 as an important mediator of zinc homeostasis in the islets and have shown anomalies in ZnT8 in both type 2 diabetes models[262,390]. When I commenced the experiments for this thesis, two major gaps in the Zn islet literature existed. Firstly, although ZnT8 was known to be critical for insulin storage in the beta cells, it was not clear whether diabetes-associated changes in ZnT8 were an early event or secondary to the disease process. Secondly, since ZnT8 is only involved in uptake of Zn into beta cell granules, other, yet to be identified, Zn transporters may control uptake and efflux of Zn across the plasma membrane as well as across other organelle membranes in the beta cell such as the ER and golgi.

The major aim of this thesis was to investigate the role of labile Zn, total Zn and Zn transporters in the pathogenesis of normal and type two diabetic pancreatic islets, using the well-characterized type 2 diabetic db/db mice model. To date there is limited information available on the physiological role of Zn and Zn transporters in normal and diabetic db/db mice. What has been shown previously in this model is that zinc is reduced in the pancreas of 8 week old type 2 diabetic db/db mice [370], ZnT8 expression was down-regulated in the early stage of diabetes [390] and dietary zinc supplementation reduces hyperglycemia in db/db mice [362]. During the course of this thesis, a further study showed that ZnT8 was also reduced in the adipose tissue of these mice and that Exendin-4 up-regulated ZnT-8 gene expression in the pancreas but not adipose tissue of the db/db mice [382]. To date it is not clear whether other Zn transporters and Zn binding proteins may also be involved and, if so, whether alteration in Zn transporters in diabetes occurs at the transcriptional or the posttranscriptional level and how this may influence insulin maturation, synthesis and release. It is also unclear whether any of the known risk factors of diabetes (obesity, inflammation, and hyperglycemia) lead to altered Zn homeostasis in islets. Knowledge of the interrelationship between Zn and Zn

transporters in the pathogenesis of type 2 diabetes will give us greater understanding of the mechanisms linking type 2 diabetes with altered Zn homeostasis and impaired insulin synthesis and release in beta cells.

9.2 Summary of the major findings:

The murine db/db model of type 2 diabetes and obesity was selected for the studies in this thesis. Diabetic status was confirmed by hyperinsulinemia, hyperglycemia, reduced glucose tolerance, islet cell hyperplasia and disorganisation of alpha, beta and delta cells as described in Chapter 3. In experiments described in Chapter 4, loss of pancreatic Zn with diabetes was confirmed and extended to show that loss occurred in the labile Zn pools in the islet beta cells early in onset of diabetes (4 weeks, early diabetes). The most important and original findings of this study (Chapter 5-7) are that loss of Zn in the diabetic mice was associated with early changes in three members of the membrane Zn transporter families:- ZnT8, which was downregulated at the protein (but not mRNA) level in islet beta cells but not alpha cells. ZIP14, staining was signficantly increased and coincided with macrophage like cells but mRNA levels did not change. There was a significant increase in ZnT7 protein in the db/db mice compared to age matched controls. It was also shown for the first time that ZIP4 is expressed predominatly in the somatostatin-producing delta cells. These changes in islet Zn homeostasis occurred in the absence of depletion of systemic Zn levels (liver Zn), athough there was a small but significant increase in plasma Zn. There was also no change in the Zn-buffering cytosolic protein metallothionein. However, it should be noted that there was considerable heterogeniety between individual islets in the early diabetic mice. None of the other zinc transporters tested were significantly affected in diabetes in this model. Finally, there was opportunity to look at changes in these Zn transporters in a limited number of pancreatic tissues in human T2D compared to normals. Changes in Zn transporter protein expression may be an early event leading to the loss of islet beta granule Zn. In addition, ZIP4 may be the major influx transporter for Zn in delta cells, ZnT8 is the transporter regulating Zn in insulin secretory granules and ZIP14 may be a novel marker of macrophage infiltration in diabetic islets.

9.3 Discussion of findings

The db/db mice developed a diabetes with many features of human type 2 diabetes mellitus

In my animal model, I found that the hyperinsulinemia and hyperplasia of islets were already maximal at 4 weeks while obesity and hyperglycaemia were significant at 4 wk but progressively increased over the following 3-4 months. The db/db mice had less immunoreactive staining towards insulin and there was evidence of degranulation in the large proportion of beta cells. There was more immunoreactivity for glucagon in the db/db mice indicative of the increased number of alpha cells. My animal model futher confirmed previous results from the db/db and other animal models of diabetes, showing disorganised islet architecture. For example, the distribution of the alpha cells was in the inner core of the islets of the db/db mice whereas in the control mice the alpha cells were in the periphery of the islet. This disorganization may be due to various mechanisms including alpha-cell hyperplasia and beta cell loss due to apoptosis or dedifferentiation of beta cells into alpha cells[101].Increase in delta cell numbers in the db/db mice pancreatic islets could further influence the maturation and secretory capacity of pancretic islets[328]. Differences between this model and human type 2 diabetes are discussed at the end of this chapter.

Loss of Zn in the pancreas of db/db mice occurred early in diabetes and was maintained into late diabetes, compared to age matched controls

Previous studies have not established whether the Zn loss in the pancreas during diabetes is a late event and therefore a consequence of diabetes or an early event that may be influencing the development of type 2 diabetes. Therefore, as described in chapter 4 of this thesis, both total Zn (measured by AAS) and labile Zn (visualized and measured by Zn fluorophore Zinpyr-1) were studied in db/db mice versus controls at three ages: 4 weeks (early diabetes), 10 weeks (diabetes) and 18 weeks (chronic diabetes). The major decrease in Zn was during early diabetes (4 weeks) and at 10 and

18 weeks the difference was less pronounced as there was a decrease in islet Zn in normal mice with age. There is substantial evidence that tissue Zn is reduced during aging in multiple organ systems.

There was loss of labile zinc in the islet beta cells but not in the alpha cells

In 1984, Figlewicz et al [367] determined that there were three distinct pools of exchangeable Zn in pancreatic islets:- namely, Zn in secretory granules, extra granular pools and a poorly-defined metabolic labile islet compartment. A more recent study [216] showed there were at least two pools of beta cell Zn as Zn flurophore Zinquin labelled the secretory granules while another Zn fluorophore FluoZin-3 labelled cytosolic Zn. Zinquin has some disadvantages including its requirement for UV excitation and rapid quenching of fluorescence. Other fluorophores for Zn have since been developed. One of the best of these is ZINPYR-1 and this was chosen for the experiments in this thesis. To my knowledge no one has previously tried ZINPYR-1 on db/db mice islets.

Labile Zn detected using ZINPYR-1 in the islets of the control mice had a granular-like pattern, which likely corresponds to the beta cell insulin-containing secretory vesicles. The staining was heterogeneous. Some islets were stained more brightly than others; this may indicate different levels of Zn in the granules due to the islets being in different phases of secretion. For example, an islet which has recently secreted insulin would be expected to have less Zn than one in resting phase.

Limited studies report the role and function of Zn in alpha cells and how this could influence the role and function of insulin. Alpha cells might be involved in secreting Zn which could act to inhibit insulin release, thereby elevating the glucose level in the blood. In 2001, Kristiansen et al[375] reported zinc in the periphery of granules in alpha cells using electron microscopy following staining of Zn by autometallography [422] a process which allows ultrastructural monitoring of Zn in cells). Consistent with this, the peripheral alpha cells (identified by glucagon staining) also fluoresced strongly with ZINPYR-1, indicating they are also rich in labile Zn.

The islets in the early diabetic and diabetic mice had substantial loss of ZINPYR-1 detectable Zn in the beta cells (p<0.05); however, the non beta cells retained their normal levels of Zn. This observation could be correlated with the retention of somatostatin and glucagon staining in the early diabetic and diabetic islets. Not all beta cells of the islet showed a decrease in Zn. There were areas in which beta cells appeared to lose Zn first. This is consistent with the alpha cells progressively replacing the beta cells during the development of the type 2 diabetes. In the chronic diabetic mice, it could be seen that the Zn was still retained in the non beta cells and there was almost complete loss of Zn in the beta cells.

An interesting question is whether ZINPYR-1 detects Zn complexed within the stored insulin-Zn crystals or whether it only fluoresces with granule Zn that has not yet incorporated into the crystals. These studies suggest that ZINPYR-1 will be a useful Zn fluorophore for islet cell Zn measurements.

Zn is involved in making the proinsulin more soluble in solution and is involved in hexamerisation of proinsulin[377]. In low zinc concentrations it was reported that the mature insulin precipitates; however, proinsulin remains stable in the rough endoplasmic reticulum and transport to the Golgi apparatus where the process of conversion of the pro-insulin to the mature insulin occurs. In the 4 week db/db mice (early diabetes), insulin was reduced compared to wildtype mice. Therefore the loss of Zn could be a factor in the precipitation and exhaustion of mature insulin in beta cells in early diabetes. In my study due to limited time and resources, it was not possible to investigate the pro-insulin to mature insulin ratio in the plasma and the pancreatic islets of these mice.

There was no change in early diabetes in liver Zn levels in db/db mice

An important question is whether the loss of Zn in the diabetics islets is a consequence of a systemic zinc deficiency. Therefore, it was important to determine whether changes in systemic levels of Zn occur in db/db mice, especially during early diabetes when Zn loss in the pancreas and islets is already apparent. Three measures of systemic Zn used in this thesis were liver Zn, plasma Zn and liver metallothionein. Both pancreas and

liver have been considered to be reservoirs of Zn in the body. There was no loss of systemic Zn in db/db mice. A small early increase in plasma Zn in the db/db mice compared to age matched controlsmay be due to pancreatic Zn being released into the circulation during the easrly hyperinsulinemia in these mice

There was no difference in pancreatic metallothionein levels between db/db and control mice. Therefore, changes in Zn levels during the diabetes are unlikely to be a consequence of changes in metallothionein levels in the beta cell cytososol; metallothionein may therefore not be a major player in the altered zinc homeostasis in db/db mice.

There was no down-regulation of gene expression for ZnT8 in db/db islets

In order to investigate the gene regulation of zinc transporters, metal binding proteins and islet hormones, qPCR was used on whole pancreas of db/db mice and age matched controls. There are limtations in obtaining optimal high quality and quantity RNA from pancreas tissues as they contain high proteases and nuclease which can degrade components including the RNA.There was no significant change in the relative expression of islet hormones insulin and glucagon in the db/db mice pancreas at 4 weeks. The proinsulin mRNA levels in another study was reported to be significantly decreased in the db/db mice. In support of this study, kaku et al [337]reported that there was a reduction of proinsulin mRNA in BLKS mice at 12 weeks of age. However, when they looked at the individual pancreatic insulin values, there was considerable variablity in the proinsulin mRNA in the db/db mice[389]. In my study insulin gene expression was increased 1.5 fold in db/db mice at 10 weeks compared to age matched controls. However, this was not significant perhaps due to the high variability due to both disease severity between mice and islet heterogenity.The MT1 and MT2 mRNA levels did not change between controls and the early diabatic group, consistant with the lack of change in total metallothionein protein in the pancreas. I investigated a Zn ion channel TRPM3 because in a previous study using insulinoma cells (INS1), it was reported to be a major Zn importer for beta cells under depolarizing conditions.

However, in my study TRPM3 had very low expression levels in the pancreas in both the control and db/db mice; therefore I did not study this further.

In the ZnT family, ZnT3 and ZnT10 were detected only at low levels as confirmed in previous studies investigating Zn transporters in pancreas in control mice[250]. The other Zn transporters were all expressed but not different between the db/db and the control mice group. Just prior to beginning experiments in this thesis, a paper appeared in the literature reporting that ZnT8 protein expression was strongly down-regulated in 5 week old db/db mice compared to controls. This study did not determine whether downregulation decreased further with the progression of type 2 diabetes. It also did not look to see whether the down-regulation was at the transcriptional (mRNA) level or due to some post-transcriptional event. I found that the db/db mice at 4 weeks did not show a significant downregulation in ZnT8 mRNA. Limitations in this study include use of whole pancreas rather than isolated pancreatic islets. Interestingly, Egefjord et al reported that treatment of mouse islets and beta cells with IL-1β significantly downregulated ZnT8 gene expression without altering other Zn transporters including ZIP5,6 and ZnT, 4, 5 and 6[391].

In my study, ZIP2 and ZIP12 were very lowly expressed. ZIP5 and ZIP7 were two of the highly expressed genes in the pancreas and also did not change. There was no significant changes in any of the zinc transporters, Zn binding protein and islet hormones at 10 weeks of age in db/db and control mice.

Islet ZnT7 protein was up-regulated early in db/db mice

The protein levels of ZnT7 protein was investigated because ZnT7 was found to be highly expressed in wildtype mice islets and overexpression of ZnT7 in insulinoma cells increased insulin synthesis and secretion by promoting gene transcription of insulin[259]. Huang et al showed that ZnT7 knockout mice were more susceptible to diet induced glucose intolerance and insulin resistance [395].

In my studies, there was a modest but significant increase (p<0.05) in islet ZnT7 protein expression levels as early as 4 weeks. ZnT7 in the pancreatic islets had a Golgi- and ER-like distribution in the majority of the cells in both control and diabetic islets, consistent with a role for ZnT7 in the early stages of insulin synthesis. Lack of down-regulation of ZnT7 in the mouse islets suggests that, in contrast to ZnT8, ZnT7 is not a target for impaired insulin production in the diabetic db/db mice. The pattern of ZnT7 staining in the acinar cells was tubular like and resembled a pattern of staining seen previously in skeletal muscle and representing Golgi like staining.

ZnT8 protein was down-regulated early in beta cells of db/db mice

Previous to these studies, ZnT8 had been shown to be important for maintaining Zn levels in beta cell granules and for correct insulin storage and release. It had also been shown to be an autoantigen in Type 1 diabetes. It was not clear, however, whether ZnT8 is also expressed in alpha cells and whether it is affected in diabetes.

These studies showed that the predominant loss of ZnT8 protein occurred at the early diabetic stage and there were further losses at 10 and 18 weeks as the diabetes progressed. There was no significant effect of age alone on the ZnT8 protein expression as seen in the control mice at all age groups. The loss of ZnT8 in early diabetes in db/db mice has also been shown by another group [390].

Collectively, the results in this thesis suggest that, in db/db mice at least, ZnT8 is not altered at the mRNA level, but it is altered at the protein level. Post-translational effects may include phosporylation or enhanced degradation. Further study by Western blotting in a beta cell line exposed to high glucose concentrations may provide further clues.

ZnT8 protein was maintained in alpha cells of db/db mice :

Two observations on type 2 diabetes are relevant. Glucagon secretion is not lost in diabetes and alpha cells often replace beta cells during the progression of the disease. Both of these were evident in my thesis studies. It is interesting that, in the db/db diabetic mice, ZnT8 was not down-regulated on the alpha cells as shown by double

labeling for glucagon. This is, to my knowledge, the first report of alpha cell containing ZnT8 in diabetic mice. It suggests that whatever leads to loss of ZnT8 (and Zn) in the beta cells does not affect the alpha cells.

In db/db mice ER stress is evident in early diabetes leading to loss of beta cells later in the disease pathogenesis. However, whether ZnT8 is altered due to ER stress or the loss of ZnT8 (and Zn) leads to ER stress is not evident in the studies. In addition, Zn is important for correct protein folding of insulin in the ER and immature granules [397].

ZIP4 is a marker of delta cells in mice

ZIP4 has previously been shown to be a major Zn transporter responsible for Zn absorption at the luminal side of the small intestine; mutation in ZIP4 is responsible for a severe form of zinc deficiency affecting children (acrodermatitis enteropathica)[180,410,423]. ZIP4 is expressed in other tissues and may also be responsible for Zn uptake by these tissues. Whether ZIP4 is involved in pancreas and islet Zn uptake has not been well studied. Duffner Bettie et al suggested that ZIP4 is expressed on beta cells of CD1 mouse islets based on immunofluorescence staining. However they looked at ZIP4 expression in pregnant mice and not in normal settings or diabetes[311,312]. There might be increase in demand in ZIP4 expression levels in pregnancy compared to normal settings, which may not give a true picture of the normal setting. Their immunoperoxidase staining is a bit contradictory as some of the insulin producing cells were not stained for ZIP4, whereas there were some unidentified more darkly staining cells. My studies have now identified the major staining cells in normal and db/db mice pancreas as being the somatostatin producing delta cells. Firstly, there were areas of ZIP4 stained cells in the mantle next to the glucagon staining cells and not identical to them. This suggested that the ZIP4 positive cells were not alpha cells. Therefore, the stained cells could be one of the non-alpha and non-beta cells in the mantle and the core. Co-staining of somatostatin and ZIP4 was performed by immunoperoxidase labelling and colocalisation of somatostatin and ZIP4 was found. Whether other cells such as the PP cells also express ZIP4 needs to be determined. In these studies there was no significant change in the ZIP4 expression in the db/db mice pancreatic islets. However, disorganisation of delta cells containing ZIP4 could have

functional implications in type 2 diabetes involved in gut related roles. The immunoperoxidase staining described in chapter 7 shows apparently a lower level of expression of ZIP4 in the beta cell rich area; however the significance of this is not clear, it might be due to overstaining. Interestingly this staining was not seen in the alpha rich cell zone in the mantle and the immunofluorescence studies appear to only show the delta cells to be positive. Therefore, the presence of ZIP4 on isolated beta cells needs to be confirmed. In preliminary studies towards the end of my studies for this thesis I showed that the beta cell line MIN6 expresses ZIP4 by western blot analysis. Since delta cells control insulin and glucagon secretion, disorganisation of delta cells containing ZIP4 might lead to a disruption in endocrine function of the islets.

ZIP14 is is a maker of islet macrophages and is up-regulated in db/db mice

One of the most interesting and original findings in this thesis was the strong up-regulation of ZIP14 in early diabetic, diabetic and chronic diabetic islets. Previously, ZIP14 has been shown to be up-regulated in inflammation. Therefore, a study of ZIP14 in type 2 diabetes, where inflammation is thought to be important in the pathogenesis, was warranted.

The ZIP14 protein expression did increase with age alone, but this was due to the increase in islet size. There was a strong positive correlation between islet area and ZIP14 protein expression and in the control mice there was an increase in islet size with age. The diabetic group had an up-regulation of ZIP14 compared to age-matched controls. ZIP14 was also observed to be expressed in blood vessels adjacent to the islets. Therefore, the possibility existed that ZIP14 is upregulated due to the altered vascularization of the islets in diabetes, particularly in islet capillaries. In a recent report, there was irregularity of the vasculature and decrease in VEGF mRNA expression in db/db mice pancreatic islets [414].

However, other evidence argues against the up-regulation of ZIP14 being due directly to changes in the vasculature. Firstly, endothelial cells that stained positive for CD31 within the islets did not colocalise with ZIP14 positive cells. Secondly, the increased immunostaining for ZIP14 in the diabetic islets was consistent with cells or

occasionally clusters of cells that resembled macrophages in appearance. This was confirmed by showing co-staining for ZIP14 and the macrophage marker CD68. This is also consistent with recent reports in the literature that ZIP14 is expressed in macrophages in other tissues and is upregulated by inflammatory stimuli LPS, IL6, TNF-alpha and IL-1beta[234,237,247]. ZIP14 may therefore be a novel macrophage marker in type 2 diabetes. There are two types of macrophages M1 which are the pro-inflammatory macrophages and M2 which is the trophic macrophage that is involved in general macrophage functions (see chapter 1.3.5 to 1.3.8). In the db/db mice pancreatic islet it is known that M1 subtype increases and there is no change in the M2 subtype expression[44]. In view of this it is likely that ZIP14 is expressed on the proinflammatory macrophages and may be involved in processes such as beta cell apoptosis and beta cell dedifferentiation.

ZIP14 is also known to be an iron transporter and has implications such as the iron overload in type 2 diabetes in haematochrosis. Interestingly, In another study, db/db mice, when fed with normal chow diet, accumulated iron in their kidneys and developed kidney disease, whereas the db/db mice fed with an iron deficient diet were protected from disease[404]. ZIP14 might play a role in iron accumulation in islets and assisting with the islet amyloid plaque (IAPP) formation that is typical of type 2 diabetes. Consistent with this, Masters et al showed, in another model of type 2 diabetes that macrophages colocalised with IAPP and were activated by it to produce inflammatory cytokines[416]. Hepcidin is expressed higly in the insulin granules of the pancreatic islets[55]. Therefore, a study of the role of ZIP14 in iron movements within the islets is warranted. As a preliminary study I stained for iron in the db/db mouse islets, using hemosiderin as a marker for iron in tissue pathology. There was no staining, although this might simply be due to the low sensitivity of the assay. Future studies should look at hepcidin and ferroportins and other cellular markers of iron accumulation.

Lipopolysaccharide has been shown to upregulate ZIP14 in macrophages and ZIP14 knockout attenuated downstream cytokine signaling. This has implications for inflammation in type 2 diabetes[245]. The circulating cytokine profiles of the db/db and control mice were not significantly different for proinflammatory cytokines IL1b, TNFa

and IL6. Therefore, as suggested earlier in this discussion, any inflammation in the db/db mice may be local rather than systemic. This was the conclusion also from the histological analyses showing that there was no overt inflammation in the pancreas of the db/db mice at any stage of diabetes but there was evidence of increased macrophage infiltration. It will be important now to look at staining of the cytokines in the islets themselves.

A recent study reported that ZIP14 knockout in C57BL/6 mice had upregulation of ZnT8 protein in the islets, increase in body weight, hypoglycemia, high insulin level, phosphorylation of insulin receptor and increased GLUT2 expression[240]. They also exhibited decreased release of circulating cytokines such as IL-6 and there was no change in the macrophage expression using CD68 staining. These knock out mice also showed impaired growth and glycogenesis and impairment of GPCR signaling. GPCR signaling has an important role in the pathogenesis of type 2 diabetes and other diseases. It is also known that GPCR and insulin signaling act in an autocrine and paracrine fashion[238]. It is feasible that up-regulation of ZIP14 leads to down-regulation of ZnT8 in db/db mice and thereby, leading to loss of beta cell Zn and impaired beta cell function. How this might occur is not clear but may involve effects at the level of ZIP14 macrophages interacting with ZnT8 containing beta cells. This could be tested in an in vitro co-culture model with activated ZIP14 positive macrophages and MIN6 or isolated mouse islet cells.

Some findings in mouse model were also seen in human type 2 diabetes

ZnT8 showed variable expression in normal human islets. As for the db/db mice, there was significant down-regulation of ZnT8 protein in beta cells in diabetes, but no down-regulation in alpha cells. ZIP14 was up-regulated in islets of 3 of the diabetic pancreata similar to the up-regulation in db/db mice. Also, the pattern of labelling for ZIP14 was similar to that seen in mouse islets and may therefore also be due to infiltrating macrophages. As in db/db mice, there was no change in excpression of ZIP4 in human diabetes. The pattern of labelling for ZIP4 was similar to that seen in mouse islets and may therefore also be due to delta cells. In summary, the changes seen in db/db mice were largely mimicked in human diabetes with the reservation that there was much

more variability of expression in the human islets which may reflect variability in such things as age, obesity, prediabetes, duration and severity of diabetes and medications.

A model to explain some findings in this thesis is described in figure 9.1 for the normal mouse and 9.2 for the diabetic mouse.

9.4 Medical significance

There are three major medical significances of this project.

I have confirmed that Zn and ZnT8 protein are lost in type 2 diabetes and have now extended this to show that the changes in Zn occur as an early event in the disease pathogenesis and therefore may be part of the mechanism driving the diabetes. The importance of this is that if it is an early event it may be able to restore Zn levels by giving Zn supplements early in diabetes. This has been achieved in the db/db mice where pancreatic Zn was normalised and hyperglycemia was attenuated by dietary Zn supplements [362]. Following this study Wany et al investigated Zn supplementation in streptozotocin (STZ) treated wistar rats. It was found that Zn supplementation improved the symptoms of diabetes such as polydipsia and led to a reduction of cholesterol levels[370].

In humans, however, the results have been controversial. For example, Rossel et al 2003 investigated Zn supplementation for six months in type 2 diabetic patients and showed that the circulating Zn levels in these patients increased significantly, they had reduced oxidative stress, but did not have any changes in hyperglycemia. Also Foster et al 2013 reported that Zn supplementation in women with type 2 diabetes did not have significant outcomes on glucose homeostasis and lipidemia [424]. However, recently Jayawandara et al, did a meta analysis on 12 studies of Zn supplementation in type 2 diabetic patients and concluded that Zn supplementation improved glycaemia control and increased HDL levels in the blood [355].

My studies are the first to identify ZIP4 in the delta cells; this suggests that ZIP4 is involved in controlling Zn levels in these cells and appears to be less important for the

other islet cells. Since ZIP4 is important for gastrointestinal function, the effects of ZIP4 dysregulation on somatostatin production by delta cells needs to be examined, as well as the effect of diabetes on ZIP4 expression in human islets and whether this has influence on gastrointestinal function.

These studies are the first to identify ZIP14 on macrophage in islet cells in type 2 diabetes. If ZIP14 was knocked down in the macrophages, this could reduce the islet related changes that occur in diabetes such as the loss of ZnT8. However, it is still not clear whether ZIP14 has a positive or negative role in islet cell biology. Development of antagonists of ZIP14 may be useful to upregulate ZnT8 levels and restore insulin sysnthesis.

9.5 Limitations in these studies:

The main studies described in this thesis involved researching novel aspects of zinc homeostasis in a mouse model of type 2 diabetes. There were a number of limitations in these studies.

Limitations of characterising the db/db mice model:

The db/db mouse model is a very well-characterised model of type 2 diabetes. The findings with the db/db mice such as the ZIP4 present on delta cells and ZIP14 on islet macrophages now need to be confirmed in the other type 2 diabetes and obese rodent models such as Zucker diabetic rats and ob/ob mice. The mouse model of type 2 diabetes and obesity is a good model to investigate the mechanisms and pathways of the disease. However, there are limitations with these mouse models as good models of human disease. For example, the db/db mice model is due to a leptin receptor mutation unlike the majority of the human type 2 diabetes. The severity of the disease in these mice is greater than what exists in the human. Human type 2 diabetes is a heterogeneous disease comprising of various factors such as the environment, diet, polymorphisms, family history and lifestyle. Therefore the interpretation of the results obtained from db/db mice may not necessarily apply to humans. All of the findings need to be confirmed in normal and diabetic human islets.

Limitations in gene expression study:

In this study I used whole pancreas to investigate the relative expression of zinc transporters (ZnT1-10, ZIP1-14, Zn binding proteins and islet hormones). It would have been preferable to use isolated islets or laser capture microdissected islets rather than native pancreatic tissue. I did explore this using laser capture microdissection but the quality and quantity of the RNA from the islets were suboptimal. Genes such as ZnT8, insulin, and glucagon are islet specific genes and they can be detected accurately in whole pancreas. However other Zn transporters for example ZIP14 are expressed in the blood vessels, macrophages and also islets and give a mixed signal. Another limitation of this study was getting good quality RNA from whole pancreas tissue as it contains many proteases and RNAases especially in the acinar tissue where digestive enzymes are being secreted. In order to obtain more cDNA from the RNA being used I included a preamplification step. An advantage of these studies was the use of multiple genes in triplicates embedded on microfluidic card and the normalisation to two house keeping genes.
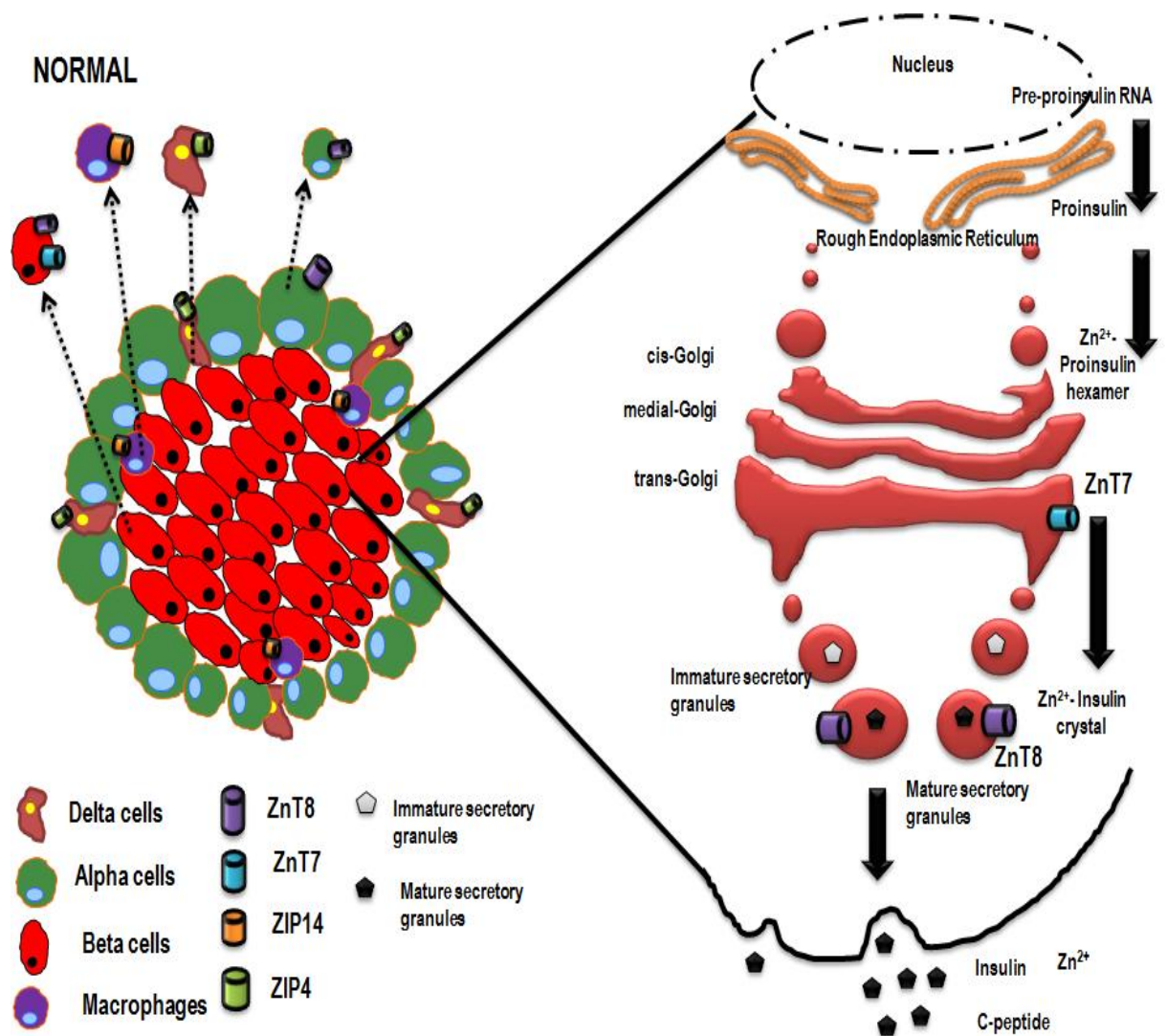
Figure 9.1 Schematic diagram of the localization and role of Zn transporters in wildtype islets

The left panel shows a typical mouse islet with a mantle rich in alpha and delta cells and a central core rich in beta cells. Only occasional macrophages are present. The Zn transporter ZnT7 is expressed in the beta cells and some alpha cells. ZnT8 is expressed on both alpha and beta cells. Delta cells strongly expresses the gut related protein ZIP4; this has implications for Zn uptake by these cells and also gut-islet interactions. Nothing is known about other Zn transporters in the delta cells. ZIP14 is expressed on the macrophages but the relationship to the state of macrophage activation needs to be determined. The right panel shows insulin is derived by two proteolysis steps 1) conversion of pre-proinsulin to proinsulin in the rough endoplasmic reticulum (RER) and 2) cleavage of proinsulin to the alpha and beta insulin chains in the early secretory

vesicles. Zn is important for both Zn-proinsulin hexamerisation in the RER/golgi and Zn insulin crystallisation in mature insulin vesicles. Findings in chapter 6 shows that ZnT7 staining had golgi like distribution (consistent with findings in other tissues) and ZnT7 is therefore likely involved in bringing Zn into the RER/golgi of the beta cell.

the role of ZnT7 and ZnT8 in the mature insulin formation. ZnT7 is involved in bringing Zn into the Golgi where pro-insulin hexamers predominate and processed into immature secretory granules. ZnT8 is involved in bringing Zn into the secretory granules where maturation can be completed and mature insulin crystals are predominant

ZnT8

ZIP4

ZIP14

TYPE 2 DIABETES (db/db mice)

Nucleus

Pre-proinsulin RNA

Proinsulin

Rough Endoplasmic Reticulum

Zn^{2+}-Proinsulin hexamer

cis-Golgi

medial-Golgi

trans-Golgi

ZnT7

Immature secretory granules

ZnT8

Zn^{2+}- Insulin crystal

Zn^{2+}

Mature secretory granules

Proinsulin

Insulin Zn^{2+}

C-peptide

243
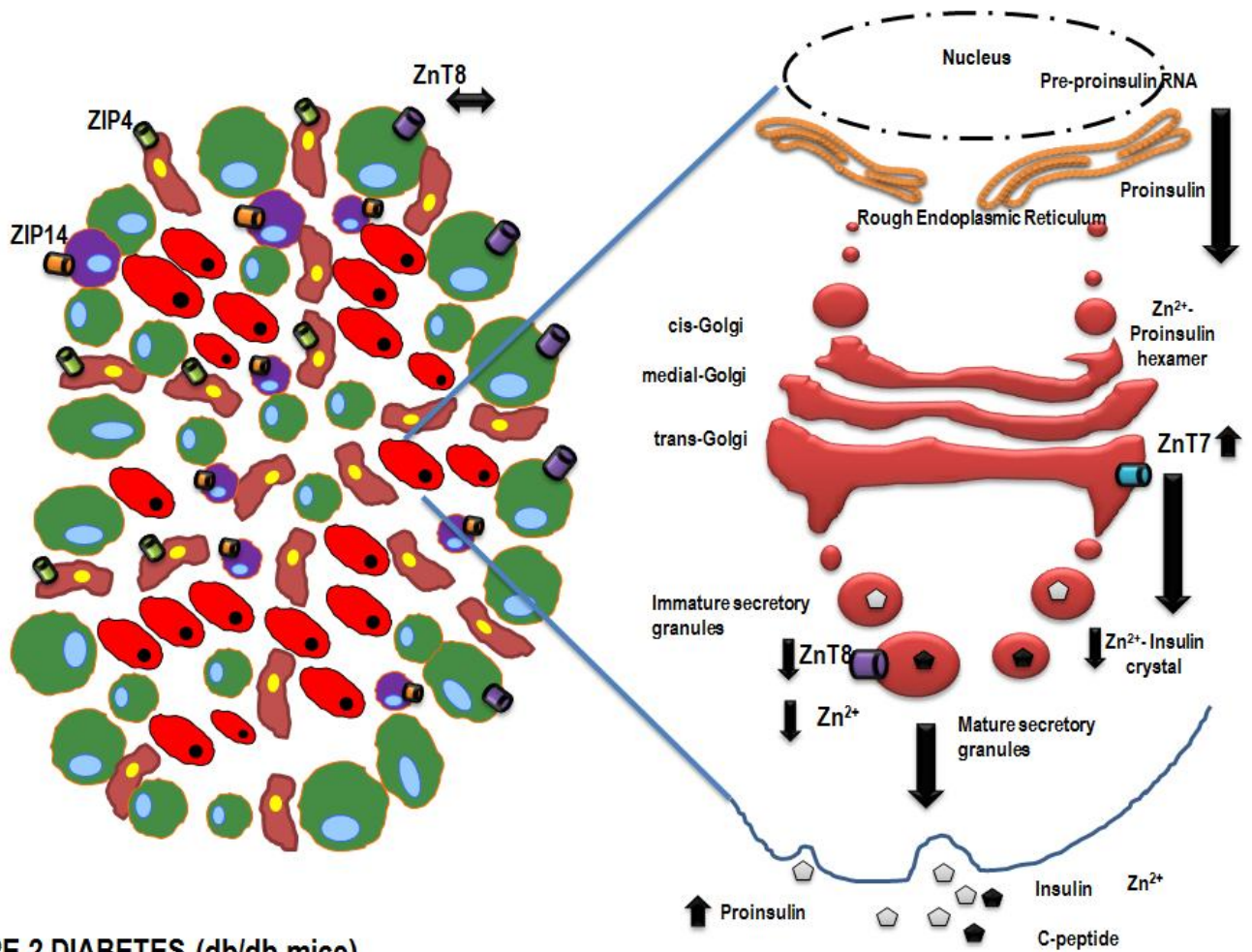
Figure 9.2 Schematic diagram of the localization and role of Zn transporters in db/db mice islets

The figure hows a typical diabetic mouse islet with a hypertrophic and disorganised islet structure. The alpha and delta cells move to the central core of the islet or are beta cells that have been reprogrammed to non beta cells. The consequence of this is that the tight regulation of islet hormone secretion is lost. It is not clear what implications it has on Zn homeostasis in these islet cell types for two reasons firstly; it is not clear whether Zn released from beta cells has a paracrine effect on the neighbouring alpha and delta cells and vice versa; Secondly; it is not known whether disorganisation of alpha and delta cells interferes with the uptake of Zn and other nutrients from islet capillaries. ZnT7 expression is up-regulated in the Golgi of the islet cells to increase insulin production to compensate for the hyperglycaemia in type 2 diabetes. ZnT8 expression is down-regulated in the beta cells but not in the alpha cells. The increase in ZnT7 and decrease in ZnT8 expression leads to a block in the insulin maturation with an increase in proinsulin hexamers (immature secretory granules being secreted). This would be consistent with accumulation of immature granules containing Zn proinsulin hexamers replacing the mature insulin secretory granules in the db/db mice. The immature granules preferentially exocytose releasing proinsulin into the circulation[83]. Therefore in the db/db mice it is proposed that there is a block in maturation of proinsulin to insulin formation, secondary to changes in ZnT7 and ZnT8. The ZnT8 was decreased in the beta cells in the early phase of diabetes and further reductions occurred as diabetes progressed. This confirms other findings including those of liu et al 2011 and Tamaki 2009 et al. and in the experiments described in this thesis this is extended to show that both Zn and ZnT8 are preserved in the alpha cells in the diabetic mice. Preservation of Zn and ZnT8 in the alpha cells may facilitate glucagon secretion and thereby play an important role in worsening the hyperglycaemia.

ZIP14 is up-regulated in the islets. This up-regulation is at least partly due to increase in macrophage number within the islet. There was no increase in the amount of ZIP14 in each macrophage in early diabetes but the immunofluorescence images suggest that they may be increase in the amount of ZIP14 in the later stages of diabetes and this could be due to increased macrophage activation correlating with more severe

hyperglycemia and obesity. In a study done by Cucak et al showed an increase in macrophages of the M1 proinflammatory subtype (Cucak 2013), in db/db mice pancreatic islets. It is not known whether ZIP14 is associated with macrophage subset, but it is known that inflammatory stimuli such as LPS, turpentine, IL-6 increase its expression greatly suggesting that the ZIP14 may be a marker of activated inflammatory macrophage but this needs to be confirmed. It would be interesting to cross ZIP14 knockout mice with db/db to see whether this affects macrophage infiltration into the islets as well as the effects on the progression of diabetes. ZIP14 is also expressed in blood vessels but the relationship to diabetes is not known.

ZIP4 did not appear to change in diabetes but because delta cells do increase in the inner core of the islet, this need to be further investigated. Disorganisation of delta cells containing ZIP4 may have a functional consequence in diabetes, as the regulation of the insulin and glucagon may be altered. Knockout of ZIP4 could give us functional clues on the role of Zn in delta cell function.

9.6 Final conclusions and Future directions

Studies in this thesis have raised some interesting questions that need to be addressed in future studies. It would be interesting to look for ZIP4 and ZIP14 polymorphisms in diabetes type 1 and 2, as well as autoantibodies in type 1 diabetes, which might further give us clues on the mechanisms of the disease .Repeating these studies in human islets of control and diabetic patients is important to confirm findings with the mouse model of diabetes. Crosses of ZIP14 or ZnT8 knockout mice with db/db mice may shed light on whether ZIP14 knockout improves diabetes and whether ZnT8 knockout increases the severity of the disease. In future studies the two models db/db vs ob/ob mice (which do not have a leptin receptor mutation) could be compared. This would have enabled to see what role obesity plays in the altered Zn homeostasis. This would give further clues as to whether the leptin gene mutation or leptin receptor gene mutation have similar effects on Zn transporter regulation.

This thesis provides new data on the role of Zn and Zn transporters in the pancreatic islets which should lead to a better understanding of how Zn is involved in islet hormone synthesis and storage and abnormalities in type 2 diabetes. There are two potential clinical implications of these studies. The first is in understanding better the critical early events in development of type 2 diabetes, how these are influenced by Zn status and whether Zn supplements have a role to play in slowing down the transition from pre-diabetes to established diabetes. Low dietary intake of Zn might be a factor in diabetes and zinc supplements could therefore prove useful as aids to therapy. Secondly, whether Zn is an important factor in islet viability may have implications for transplantation of islets in type 1 diabetics. A study of the Zn and Zn transporter status in islets that are to be transplanted into patients may lead to improvements in islet viability and successful outcomes.

References

1. Kahn SE, Hull RL, Utzschneider KM. Mechanisms linking obesity to insulin resistance and type 2 diabetes. Nature 2006;444:840-6.
2. Cnop M, Welsh N, Jonas J-C, Jörns A, Lenzen S, Eizirik DL. Mechanisms of Pancreatic β-Cell Death in Type 1 and Type 2 Diabetes: Many Differences, Few Similarities. Diabetes 2005;54:S97-S107.
3. Meigs JB. Epidemiology of Type 2 Diabetes and Cardiovascular Disease: Translation From Population to Prevention: The Kelly West Award Lecture 2009. Diabetes Care 2010;33:1865-71.
4. Hu FB. Globalization of Diabetes: The role of diet, lifestyle, and genes. Diabetes Care 2011;34:1249-57.
5. Twigg SM, Kamp MC, Davis TM, Neylon EK, Flack JR. Prediabetes: a position statement from the Australian Diabetes Society and Australian Diabetes Educators Association. Med J Aust 2007;186:461-5.
6. Weir GC, Bonner-Weir S. Five Stages of Evolving Beta-Cell Dysfunction During Progression to Diabetes. Diabetes 2004;53:S16-S21.
7. Laybutt DR, Kaneto H, Hasenkamp W, Grey S, Jonas J-C, Sgroi DC, Groff A, Ferran C, Bonner-Weir S, Sharma A, Weir GC. Increased Expression of Antioxidant and Antiapoptotic Genes in Islets That May Contribute to β-Cell Survival During Chronic Hyperglycemia. Diabetes 2002;51:413-23.
8. Del Prato S. Role of glucotoxicity and lipotoxicity in the pathophysiology of Type 2 diabetes mellitus and emerging treatment strategies. Diabetic Medicine 2009;26:1185-92.
9. Olefsky JM, Glass CK. Macrophages, Inflammation, and Insulin Resistance. Annual Review of Physiology 2010;72:219-46.
10. Hummasti S, Hotamisligil GS. Endoplasmic Reticulum Stress and Inflammation in Obesity and Diabetes. Circulation Research 2010;107:579-91.
11. Sano R, Reed JC. ER stress-induced cell death mechanisms. Biochimica et Biophysica Acta (BBA) - Molecular Cell Research 2013;1833:3460-70.
12. DeFronzo RA. Insulin resistance, lipotoxicity, type 2 diabetes and atherosclerosis: the missing links. The Claude Bernard Lecture 2009. Diabetologia 2010;53:1270-87.
13. Goldstein BJ. Insulin resistance as the core defect in type 2 diabetes mellitus. The American Journal of Cardiology 2002;90:3-10.
14. Donath MY, Ehses JA, Maedler K, Schumann DM, Ellingsgaard H, Eppler E, Reinecke M. Mechanisms of β-Cell Death in Type 2 Diabetes. Diabetes 2005;54:S108-S13.
15. Bi Y, Wang T, Xu M, Xu Y, Li M, Lu J, Zhu X, Ning G. Advanced research on risk factors of type 2 diabetes. Diabetes/Metabolism Research and Reviews 2012;28:32-9.
16. Lebovitz HE. Type 2 Diabetes: An Overview. Clinical Chemistry 1999;45:1339-45.
17. Baetens D, Malaisse-Lagae F, Perrelet A, Orci L. Endocrine pancreas: three-dimensional reconstruction shows two types of islets of langerhans. Science 1979;206:1323-5.

18. Aguayo-Mazzucato C, Sanchez-Soto C, Godinez-Puig V, Gutiérrez-Ospina G, Hiriart M. Restructuring of Pancreatic Islets and Insulin Secretion in a Postnatal Critical Window. PLoS ONE 2006;1:e35.

19. Pandol SJ. The exocrine pancreas: San Rafael (CA): Morgan & Claypool Life Sciences; 2010.

20. Cabrera O, Berman DM, Kenyon NS, Ricordi C, Berggren P-O, Caicedo A. The unique cytoarchitecture of human pancreatic islets has implications for islet cell function. Proceedings of the National Academy of Sciences of the United States of America 2006;103:2334-9.

21. Hauge-Evans AC, King A, Fairhall K, Jones PM. A role for islet somatostatin in mediating sympathetic regulation of glucagon secretion. Islets 2010;2:341-4.

22. Hauge-Evans AC, King AJ, Carmignac D, Richardson CC, Robinson ICAF, Low MJ, Christie MR, Persaud SJ, Jones PM. Somatostatin secreted by islet δ-cells fulfils multiple roles as a paracrine regulator of islet function. Diabetes 2008.

23. Yaginuma N, Takahashi T, Saito K, Kyoguku M. The Microvasculature of the Human Pancreas and Its Relation to Langerhans Islets and Lobules. Pathology - Research and Practice 1986;181:77-84.

24. Ballian N, Brunicardi FC. Islet Vasculature as a Regulator of Endocrine Pancreas Function. World Journal of Surgery 2007;31:705-14.

25. Richards OC, Raines SM, Attie AD. The Role of Blood Vessels, Endothelial Cells, and Vascular Pericytes in Insulin Secretion and Peripheral Insulin Action. Endocrine Reviews 2010;31:343-63.

26. Bonner-Weir S, Orci L. New Perspectives on the Microvasculature of the Islets of Langerhans in the Rat. Diabetes 1982;31:883-9.

27. Agudo J, Ayuso E, Jimenez V, Casellas A, Mallol C, Salavert A, Tafuro S, Obach M, Ruzo A, Moya M, Pujol A, Bosch F. Vascular Endothelial Growth Factor–Mediated Islet Hypervascularization and Inflammation Contribute to Progressive Reduction of β-Cell Mass. Diabetes 2012;61:2851-61.

28. Pollard JW. Trophic macrophages in development and disease. Nat Rev Immunol 2009;9:259-70.

29. Pradere J-P, Kluwe J, De Minicis S, Jiao J-J, Gwak G-Y, Dapito DH, Jang M-K, Guenther ND, Mederacke I, Friedman R, Dragomir A-C, Aloman C, Schwabe RF. Hepatic macrophages but not dendritic cells contribute to liver fibrosis by promoting the survival of activated hepatic stellate cells in mice. Hepatology 2013;58:1461-73.

30. Raivich G, Banati R. Brain microglia and blood-derived macrophages: molecular profiles and functional roles in multiple sclerosis and animal models of autoimmune demyelinating disease. Brain Research Reviews 2004;46:261-81.

31. Hume DA. Macrophages as APC and the Dendritic Cell Myth. The Journal of Immunology 2008;181:5829-35.

32. Kurushima H, Ramprasad M, Kondratenko N, Foster DM, Quehenberger O, Steinberg D. Surface expression and rapid internalization of macrosialin (mouse CD68) on elicited mouse peritoneal macrophages. Journal of Leukocyte Biology 2000;67:104-8.

33. Kelly J, Ali Khan A, Yin J, Ferguson TA, Apte RS. Senescence regulates macrophage activation and angiogenic fate at sites of tissue injury in mice. J Clin Invest 2007;117:3421-6.

34. Koh TJ, DiPietro LA. Inflammation and wound healing: the role of the macrophage. Expert Rev Mol Med 2011;13:e23.

35.   Newman A, Hughes C. Macrophages and angiogenesis: a role for Wnt signaling. Vascular Cell 2012;4:1-7.

36.   Dickhout JG, Basseri S, Austin RC. Macrophage Function and Its Impact on Atherosclerotic Lesion Composition, Progression, and Stability: The Good, the Bad, and the Ugly. Arteriosclerosis, Thrombosis, and Vascular Biology 2008;28:1413-5.

37.   Kzhyshkowska J, Neyen C, Gordon S. Role of macrophage scavenger receptors in atherosclerosis. Immunobiology 2012;217:492-502.

38.   Lamharzi N, Renard CB, Kramer F, Pennathur S, Heinecke JW, Chait A, Bornfeldt KE. Hyperlipidemia in Concert With Hyperglycemia Stimulates the Proliferation of Macrophages in Atherosclerotic Lesions: Potential Role of Glucose-Oxidized LDL. Diabetes 2004;53:3217-25.

39.   Van Wesenbeeck L, Odgren PR, MacKay CA, D'Angelo M, Safadi FF, Popoff SN, Van Hul W, Marks SC. The osteopetrotic mutation toothless (tl) is a loss-of-function frameshift mutation in the rat Csf1 gene: Evidence of a crucial role for CSF-1 in osteoclastogenesis and endochondral ossification. Proceedings of the National Academy of Sciences 2002;99:14303-8.

40.   Dai X-M, Zong X-H, Sylvestre V, Stanley ER. Incomplete restoration of colony-stimulating factor 1 (CSF-1) function in CSF-1–deficient Csf1op/Csf1op mice by transgenic expression of cell surface CSF-1. Blood 2004;103:1114-23.

41.   Maedler K, Schumann DM, Sauter N, Ellingsgaard H, Bosco D, Baertschiger R, Iwakura Y, Oberholzer J, Wollheim CB, Gauthier BR, Donath MY. Low Concentration of Interleukin-1β Induces FLICE-Inhibitory Protein–Mediated β-Cell Proliferation in Human Pancreatic Islets. Diabetes 2006;55:2713-22.

42.   Ehses JA, Perren A, Eppler E, Ribaux P, Pospisilik JA, Maor-Cahn R, Gueripel X, Ellingsgaard H, Schneider MK, Biollaz G, Fontana A, Reinecke M, Homo-Delarche F, Donath MY. Increased number of islet-associated macrophages in type 2 diabetes. Diabetes 2007;56:2356-70.

43.   Eguchi K, Manabe I. Macrophages and islet inflammation in type 2 diabetes. Diabetes, Obesity and Metabolism 2013;15:152-8.

44.   Cucak H, Grunnet LG, Rosendahl A. Accumulation of M1-like macrophages in type 2 diabetic islets is followed by a systemic shift in macrophage polarization. Journal of Leukocyte Biology 2013.

45.   Ganz T. Macrophages and Systemic Iron Homeostasis. Journal of Innate Immunity 2012;4:446-53.

46.   Recalcati S, Locati M, Cairo G. Systemic and cellular consequences of macrophage control of iron metabolism. Seminars in Immunology 2012;24:393-8.

47.   Steinbicker A, Muckenthaler M. Out of Balance—Systemic Iron Homeostasis in Iron-Related Disorders. Nutrients 2013;5:3034-61.

48.   Beutler E. Hemochromatosis: Genetics and Pathophysiology. Annual Review of Medicine 2006;57:331-47.

49.   Pietrangelo A. Hereditary Hemochromatosis — A New Look at an Old Disease. New England Journal of Medicine 2004;350:2383-97.

50.   Krause A, Neitz S, Mägert H-J, Schulz A, Forssmann W-G, Schulz-Knappe P, Adermann K. LEAP-1, a novel highly disulfide-bonded human peptide, exhibits antimicrobial activity. FEBS Letters 2000;480:147-50.

51.   Pigeon C, Ilyin G, Courselaud B, Leroyer P, Turlin B, Brissot P, Loréal O. A New Mouse Liver-specific Gene, Encoding a Protein Homologous to Human Antimicrobial Peptide Hepcidin, Is Overexpressed during Iron Overload. Journal of Biological Chemistry 2001;276:7811-9.

52. Kulaksiz H, Schmid A, Hönscheid M, Ramaswamy A, Cetin Y. Clara Cell Impact in Air-Side Activation of CFTR in Small Pulmonary Airways. Proceedings of the National Academy of Sciences of the United States of America 2002;99:6796-801.

53. Ganz T, Nemeth E. The Hepcidin-Ferroportin System as a Therapeutic Target in Anemias and Iron Overload Disorders. ASH Education Program Book 2011;2011:538-42.

54. Camaschella C. Iron and hepcidin: a story of recycling and balance. ASH Education Program Book 2013;2013:1-8.

55. Kulaksiz H, Fein E, Redecker P, Stremmel W, Adler G, Cetin Y. Pancreatic β-cells express hepcidin, an iron-uptake regulatory peptide. Journal of Endocrinology 2008;197:241-9.

56. Fernández-Real JM, López-Bermejo A, Ricart W. Cross-Talk Between Iron Metabolism and Diabetes. Diabetes 2002;51:2348-54.

57. Hentze MW, Muckenthaler MU, Andrews NC. Balancing acts: molecular control of mammalian iron metabolism. Cell 2004;117:285-97.

58. Banting FG, Best CH. The Journal of Laboratory and Clinical Medicine: Vol. VII St. Louis, February, 1922 No. 5. Nutrition Reviews 1987;45:55-7.

59. Chan SJ, Noyes BE, Agarwal KL, Steiner DF. Construction and selection of recombinant plasmids containing full-length complementary DNAs corresponding to rat insulins I and II. Proc Natl Acad Sci U S A 1979;76:5036-40.

60. Støy J, Steiner D, Park S-Y, Ye H, Philipson L, Bell G. Clinical and molecular genetics of neonatal diabetes due to mutations in the insulin gene. Reviews in Endocrine and Metabolic Disorders 2010;11:205-15.

61. Paronen J, Moriyama H, Abiru N, Sikora K, Melanitou E, Babu S, Bao FEI, Liu E, Miao D, Eisenbarth GS. Establishing Insulin 1 and Insulin 2 Knockout Congenic Strains on NOD Genetic Background. Annals of the New York Academy of Sciences 2003;1005:205-10.

62. Liu M, Hodish I, Haataja L, Lara-Lemus R, Rajpal G, Wright J, Arvan P. Proinsulin misfolding and diabetes: mutant INS gene-induced diabetes of youth. Trends in Endocrinology & Metabolism 2010;21:652-9.

63. Haataja L, Snapp E, Wright J, Liu M, Hardy AB, Wheeler MB, Markwardt ML, Rizzo M, Arvan P. Proinsulin Intermolecular Interactions during Secretory Trafficking in Pancreatic β Cells. Journal of Biological Chemistry 2013;288:1896-906.

64. Bogan JS. Regulation of Glucose Transporter Translocation in Health and Diabetes. Annual Review of Biochemistry 2012;81:507-32.

65. Fridlyand L, Philipson L. Glucose sensing in the pancreatic beta cell: a computational systems analysis. Theoretical Biology and Medical Modelling 2010;7:15.

66. Itoh N, Okamoto H. Translational control of proinsulin synthesis by glucose. Nature 1980;283:100-2.

67. Guest PC, Bailyes EM, Rutherford NG, Hutton JC. Insulin secretory granule biogenesis. Co-ordinate regulation of the biosynthesis of the majority of constituent proteins. Biochem J 1991;274:73-8.

68. Prentki M, Tornheim K, Corkey BE. Signal transduction mechanisms in nutrient-induced insulin secretion. Diabetologia 1997;40 Suppl 2:S32-41.

69. Prentki M. New insights into pancreatic β-cell metabolic signaling in insulin secretion. European Journal of Endocrinology 1996;134:272-86.

70.   Schuit F, De Vos A, Farfari S, Moens K, Pipeleers D, Brun T, Prentki M. Metabolic Fate of Glucose in Purified Islet Cells: Glucose-regulated anaplerosis in β cells Journal of Biological Chemistry 1997;272:18572-9.

71.   Peter-Riesch B, Fathi M, Schlegel W, Wollheim CB. Glucose and carbachol generate 1,2-diacylglycerols by different mechanisms in pancreatic islets. The Journal of Clinical Investigation 1988;81:1154-61.

72.   Farese RV, Dimarco PE, Barnes DE, Sabir MA, Larson RE, Davis JS, Morrison AD. Rapid Glucose-Dependent Increases in Phosphatidic Acid and Phosphoinositides in Rat Pancreatic Islets. Endocrinology 1986;118:1498-503.

73.   Aronoff SL, Berkowitz K, Shreiner B, Want L. Glucose Metabolism and Regulation: Beyond Insulin and Glucagon. Diabetes Spectrum 2004;17:183-90.

74.   Cushman SW, Wardzala LJ. Potential mechanism of insulin action on glucose transport in the isolated rat adipose cell. Apparent translocation of intracellular transport systems to the plasma membrane. Journal of Biological Chemistry 1980;255:4758-62.

75.   Suzuki K, Kono T. Evidence that insulin causes translocation of glucose transport activity to the plasma membrane from an intracellular storage site. Proceedings of the National Academy of Sciences 1980;77:2542-5.

76.   Dieni CA, Bouffard MC, Storey KB. Glycogen synthase kinase-3: cryoprotection and glycogen metabolism in the freeze-tolerant wood frog. The Journal of Experimental Biology 2012;215:543-51.

77.   Koch L, Wunderlich FT, Seibler J, xF, nner AC, Hampel B, Irlenbusch S, Brabant G, Kahn CR, Schwenk F, Br, xFc, ning JC. Central insulin action regulates peripheral glucose and fat metabolism in mice. The Journal of Clinical Investigation 2008;118:2132-47.

78.   Barthel A, Schmoll D. Novel concepts in insulin regulation of hepatic gluconeogenesis. American Journal of Physiology - Endocrinology and Metabolism 2003;285:E685-E92.

79.   Karpe F, Dickmann JR, Frayn KN. Fatty Acids, Obesity, and Insulin Resistance: Time for a Reevaluation. Diabetes 2011;60:2441-9.

80.   Butler AE, Janson J, Bonner-Weir S, Ritzel R, Rizza RA, Butler PC. β-Cell Deficit and Increased β-Cell Apoptosis in Humans With Type 2 Diabetes. Diabetes 2003;52:102-10.

81.   Del Guerra S, Marselli L, Lupi R, Boggi U, Mosca F, Benzi L, Del Prato S, Marchetti P. Effects of prolonged in vitro exposure to sulphonylureas on the function and survival of human islets. Journal of Diabetes and its Complications 2005;19:60-4.

82.   Marchetti P, Bugliani M, Lupi R, Marselli L, Masini M, Boggi U, Filipponi F, Weir GC, Eizirik DL, Cnop M. The endoplasmic reticulum in pancreatic beta cells of type 2 diabetes patients. Diabetologia 2007;50:2486-94.

83.   Masini M, Marselli L, Bugliani M, Martino L, Masiello P, Marchetti P, Tata V. Ultrastructural morphometric analysis of insulin secretory granules in human type 2 diabetes. Acta Diabetologica 2012;49:247-52.

84.   Kimball CP, Murlin JR. Aqueous extracts of pancreas: III. Some precipitation reactions of Insulin. Journal of Biological Chemistry 1923;58:337-46.

85.   Staub A, Behrens OK. The Glucagon Content of Crystalline Insulin Preparations. The Journal of Clinical Investigation 1954;33:1629-33.

86.   Dunning BE, Gerich JE. The Role of α-Cell Dysregulation in Fasting and Postprandial Hyperglycemia in Type 2 Diabetes and Therapeutic Implications. Endocrine Reviews 2007;28:253-83.

87.   Raju B, Cryer PE. Loss of the Decrement in Intraislet Insulin Plausibly Explains Loss of the Glucagon Response to Hypoglycemia in Insulin-Deficient Diabetes: Documentation of the Intraislet Insulin Hypothesis in Humans. Diabetes 2005;54:757-64.

88.   Drucker DJ. Minireview: The Glucagon-Like Peptides. Endocrinology 2001;142:521-7.

89.   Heinrich G, Gros P, Lund PK, Bentley RC, Habener JF. Pre-Proglucagon Messenger Ribonucleic Acid: Nucleotide and Encoded Amino Acid Sequences of the Rat Pancreatic Complementary Deoxyribonucleic Acid. Endocrinology 1984;115:2176-81.

90.   Rouillé Y, Westermark G, Martin SK, Steiner DF. Proglucagon is processed to glucagon by prohormone convertase PC2 in alpha TC1-6 cells. Proceedings of the National Academy of Sciences 1994;91:3242-6.

91.   Dhanvantari S, Seidah NG, Brubaker PL. Role of prohormone convertases in the tissue-specific processing of proglucagon. Molecular Endocrinology 1996;10:342-55.

92.   Furuta M, Zhou A, Webb G, Carroll R, Ravazzola M, Orci L, Steiner DF. Severe Defect in Proglucagon Processing in Islet A-cells of Prohormone Convertase 2 Null Mice. Journal of Biological Chemistry 2001;276:27197-202.

93.   Furuta M, Yano H, Zhou A, Rouillé Y, Holst JJ, Carroll R, Ravazzola M, Orci L, Furuta H, Steiner DF. Defective prohormone processing and altered pancreatic islet morphology in mice lacking active SPC2. Proceedings of the National Academy of Sciences 1997;94:6646-51.

94.   Quesada I, Villalobos C, Nunez L, Chamero P, Alonso M, Nadal A, Garcia-Sancho J. Glucose induces synchronous mitochondrial calcium oscillations in intact pancreatic islets. Cell Calcium 2008;43:39 - 47.

95.   Jiang Y, Cypess AM, Muse ED, Wu C-R, Unson CG, Merrifield RB, Sakmar TP. Glucagon receptor activates extracellular signal-regulated protein kinase 1/2 via cAMP-dependent protein kinase. Proceedings of the National Academy of Sciences 2001;98:10102-7.

96.   Exton JH. Glucagon Signal-Transduction Mechanisms. In: Comprehensive Physiology: John Wiley & Sons, Inc.; 2010.

97.   Ouyang D, Dhall D, Yu R. Pathologic pancreatic endocrine cell hyperplasia. World J Gastroenterol 2011;17:137-43.

98.   Ehses JA, Ellingsgaard H, Boni-Schnetzler M, Donath MY. Pancreatic islet inflammation in type 2 diabetes: from alpha and beta cell compensation to dysfunction. Arch Physiol Biochem 2009;115:240-7.

99.   Willcox A, Richardson SJ, Bone AJ, Foulis AK, Morgan NG. Evidence of increased islet cell proliferation in patients with recent-onset type 1 diabetes. Diabetologia 2010;53:2020-8.

100.   Cho J-H, Kim J-W, Shin J-A, Shin J, Yoon K-H. β-cell mass in people with type 2 diabetes. Journal of Diabetes Investigation 2011;2:6-17.

101.   Talchai C, Xuan S, Lin Hua V, Sussel L, Accili D. Pancreatic β Cell Dedifferentiation as a Mechanism of Diabetic β Cell Failure. Cell 2012;150:1223-34.

102.   Veronica Hurtado IR, Enrique Blazquez, Elvira Alvarez and Carmen Sanz Glucagon-Like Peptide-1 and Its Implications in Obesity, Hot Topics in Endocrine and Endocrine-Related Diseases; 2013.

103.   Delfs J, Robbins R, Connolly JL, Dichter M, Reichlin S. Somatostatin production by rat cerebral neurones in dissociated cell culture. Nature 1980;283:676-7.

104. Hasegawa Y, Miyamoto K, Nomura M, Igarashi M, Kangawa K, Matsuo H. Isolation and amino acid compositions of four Somatostatin–Like substances in chicken Hypothalamic extract. Endocrinology 1984;115:433-5.

105. Gunawardene AR, Corfe BM, Staton CA. Classification and functions of enteroendocrine cells of the lower gastrointestinal tract. International Journal of Experimental Pathology 2011;92:219-31.

106. de Herder WW, Lamberts SWJ. Somatostatin and somatostatin analogues: diagnostic and therapeutic uses. Current Opinion in Oncology 2002;14:53-7.

107. Li M, Fisher WE, Kim HJ, Wang X, Brunicardi CF, Chen C, Yao Q. Somatostatin, somatostatin receptors, and pancreatic cancer. World J Surg 2005;29:293-6.

108. Kailey B, van de Bunt M, Cheley S, Johnson PR, MacDonald PE, Gloyn AL, Rorsman P, Braun M. SSTR2 is the functionally dominant somatostatin receptor in human pancreatic beta- and alpha-cells. Am J Physiol Endocrinol Metab 2012;303:E1107-16.

109. Celinski SA, Fisher WE, Amaya F, Wu YQ, Yao Q, Youker KA, Li M. Somatostatin receptor gene transfer inhibits established pancreatic cancer xenografts. Journal of Surgical Research 2003;115:41-7.

110. Gapp DA, Leiter EH, Coleman DL, Schwizer RW. Temporal changes in pancreatic islet composition in c57bl/6j-db/db (diabetes) mice. Diabetologia 1983;25:439-43.

111. Benninger RKP, Head WS, Zhang M, Satin LS, Piston DW. Gap junctions and other mechanisms of cell–cell communication regulate basal insulin secretion in the pancreatic islet. The Journal of Physiology 2011;589:5453-66.

112. Leiter EH, Gapp DA, Eppig JJ, Coleman DL. Utrastructural and morphometric studies of delta cells in pancreatic islets from C57BL/Ks diabetes mice. Diabetologia 1979;17:297-309.

113. Lonovics J, Devitt P, Watson LC, Rayford PL, Thompson JC. Pancreatic polypeptide: A review. Archives of Surgery 1981;116:1256-64.

114. Farooqi IS, O'Rahilly S. Leptin: a pivotal regulator of human energy homeostasis. The American Journal of Clinical Nutrition 2009;89:980S-4S.

115. Pelleymounter M, Cullen M, Baker M, Hecht R, Winters D, Boone T, Collins F. Effects of the obese gene product on body weight regulation in ob/ob mice. Science 1995;269:540-3.

116. Campfield L, Smith F, Guisez Y, Devos R, Burn P. Recombinant mouse OB protein: evidence for a peripheral signal linking adiposity and central neural networks. Science 1995;269:546-9.

117. Halaas J, Gajiwala K, Maffei M, Cohen S, Chait B, Rabinowitz D, Lallone R, Burley S, Friedman J. Weight-reducing effects of the plasma protein encoded by the obese gene. Science 1995;269:543-6.

118. Tartaglia LA, Dembski M, Weng X, Deng N, Culpepper J, Devos R, Richards GJ, Campfield LA, Clark FT, Deeds J, Muir C, Sanker S, Moriarty A, Moore KJ, Smutko JS, Mays GG, Wool EA, Monroe CA, Tepper RI. Identification and expression cloning of a leptin receptor, OB-R. Cell 1995;83:1263-71.

119. Lee G-H, Proenca R, Montez JM, Carroll KM, Darvishzadeh JG, Lee JI, Friedman JM. Abnormal splicing of the leptin receptor in diabetic mice. Nature 1996;379:632-5.

120. Marroquí L, Gonzalez A, Ñeco P, Caballero-Garrido E, Vieira E, Ripoll C, Nadal A, Quesada I. Role of leptin in the pancreatic β-cell: effects and signaling pathways. Journal of Molecular Endocrinology 2012;49:R9-R17.

121. Tudurí E, Marroquí L, Soriano S, Ropero AB, Batista TM, Piquer S, López-Boado MA, Carneiro EM, Gomis R, Nadal A, Quesada I. Inhibitory Effects of Leptin on Pancreatic α-Cell Function. Diabetes 2009;58:1616-24.

122. Ingalls AM, Dickie MM, Snell GD. Obese, A new mutation in the mouse Journal of Heredity 1950;41:317-8.

123. Hellman B. The occurrence of Argyrophil cells in the islets of langerhans of American obese-hyperglycamic mice Acta Endocrinologica 1961;36:596-602.

124. Hellman B. Studies in obese-Hyperglycemic mice*. Annals of the New York Academy of Sciences 1965;131:541-58.

125. Coleman DL. Obese and diabetes: Two mutant genes causing diabetes-obesity syndromes in mice. Diabetologia 1978;14:141-8.

126. Herberg L, Coleman DL. Laboratory animals exhibiting obesity and diabetes syndromes. Metabolism 1977;26:59-99.

127. Lord JM, Atkins TW. Effect of age on hepatocyte and soleus muscle insulin receptor binding in lean and genetically obese diabetic (ob/ob) mice. Diabetes Res 1985;2:259-65.

128. Westman S. Degradation of insulin in vitro by liver and epididymal adipose tissue from obese-hyperglycaemic mice. Biochem J 1968;106:543-7.

129. Chan JY, Luzuriaga J, Bensellam M, Biden TJ, Laybutt DR. Failure of the Adaptive Unfolded Protein Response in Islets of Obese Mice Is Linked With Abnormalities in β-Cell Gene Expression and Progression to Diabetes. Diabetes 2013;62:1557-68.

130. Corsetti JP, Sparks JD, Peterson RG, Smith RL, Sparks CE. Effect of dietary fat on the development of non-insulin dependent diabetes mellitus in obese Zucker diabetic fatty male and female rats. Atherosclerosis 2000;148:231-41.

131. Terrettaz J, Jeanrenaud B. In Vivo Hepatic and Peripheral Insulin Resistance in Genetically Obese (fa/fa) Rats. Endocrinology 1983;112:1346-51.

132. Hummel KP, Dickie MM, Coleman DL. Diabetes, a new mutation in the mouse. Science 1966;153:1127-8.

133. Coleman DL. Diabetes-obesity syndromes in mice. Diabetes 1982;31:1-6.

134. Chen H, Charlat O, Tartaglia LA, Woolf EA, Weng X, Ellis SJ, Lakey ND, Culpepper J, More KJ, Breitbart RE, Duyk GM, Tepper RI, Morgenstern JP. Evidence That the Diabetes Gene Encodes the Leptin Receptor: Identification of a Mutation in the Leptin Receptor Gene in db/db Mice. Cell 1996;84:491-5.

135. Belke DD, Severson DL. Diabetes in Mice with Monogenic Obesity: The db/db Mouse and Its Use in the Study of Cardiac Consequences. In: Animal Models in Diabetes Research; 2012:47-57.

136. Wyse BM, Dulin WE. The influence of age and dietary conditions on diabetes in the db mouse. Diabetologia 1970;6:268-73.

137. Coleman DL, Hummel K. Hyperinsulinemia in pre-weaning diabetes (db) mice. Diabetologia 1974;10:607-10.

138. Hummel K, Coleman D, Lane P. The influence of genetic background on expression of mutations at the diabetes locus in the mouse. I. C57BL/KsJ and C57BL/6J strains. Biochemical Genetics 1972;7:1-13.

139. Wang Y-w, Sun G-d, Sun J, Liu S-j, Wang J, Xu X-h, Miao L-n. Spontaneous Type 2 Diabetic Rodent Models. Journal of Diabetes Research 2013;2013:8.

140. Friedman JM, Halaas JL. Leptin and the regulation of body weight in mammals. Nature 1998;395:763-70.

141. Cava AL, Matarese G. The weight of leptin in immunity. Nat Rev Immunol 2004;4:371-9.

142. Weir GC, Bonner-Weir S. Finally! A human pancreatic beta cell line. J Clin Invest 2011;121:3395-7.

143. Dionne KE, Colton CK, Lyarmush M. Effect of Hypoxia on Insulin Secretion by Isolated Rat and Canine Islets of Langerhans. Diabetes 1993;42:12-21.

144. Halban PA, Praz GA, Wollheim CB. Abnormal glucose metabolism accompanies failure of glucose to stimulate insulin release from a rat pancreatic cell line (RINm5F). Biochem J 1983;212:439-43.

145. Cheng K, Delghingaro-Augusto V, Nolan CJ, Turner N, Hallahan N, Andrikopoulos S, Gunton JE. High Passage MIN6 Cells Have Impaired Insulin Secretion with Impaired Glucose and Lipid Oxidation. PLoS ONE 2012;7:e40868.

146. Skelin M, Rupnik M, Cencic A. Pancreatic beta cell lines and their applications in diabetes mellitus research. ALTEX 2010;27:105-13.

147. Ishihara H, Asano T, Tsukuda K, Katagiri H, Inukai K, Anai M, Kikuchi M, Yazaki Y, Miyazaki JI, Oka Y. Pancreatic beta cell line MIN6 exhibits characteristics of glucose metabolism and glucose-stimulated insulin secretion similar to those of normal islets. Diabetologia 1993;36:1139-45.

148. Maret W, Sandstead HH. Zinc requirements and the risks and benefits of zinc supplementation. Journal of Trace Elements in Medicine and Biology 2006;20:3-18.

149. Prasad AS. Zinc: an overview. Nutrition 1995;11:93-9.

150. Vallee BL, Falchuk KH. The biochemical basis of zinc physiology. Physiological reviews 1993;73:79-118.

151. Cousins RJ, McMahon RJ. Integrative Aspects of Zinc Transporters. Journal of Nutrition 2000;130:1384S-7.

152. Prasad AS, Miale A, Jr, Farid ZZ, Sandstead HH, Schulert AR, Darby WJ. BIochemical studies on dwarfism,hypogonadism, and anemia. Archives of Internal Medicine 1963;111:407-28.

153. Sandstead HH. Human Zinc Deficiency: Discovery to Initial Translation. Advances in Nutrition: An International Review Journal 2013;4:76-81.

154. Menard MP, Cousins RJ. Zinc Transport by Brush Border Membrane Vesicles from Rat Intestine. Journal of Nutrition 1983;113:1434-42.

155. Semrad C. Zinc and intestinal function. Current gastroenterology reports 1999;1:398-403.

156. Pattison SE, Cousins RJ. Zinc uptake and metabolism by hepatocytes. Federation proceedings 1986;45:2805-9.

157. Dreosti IE. Recommended dietary intakes of iron, zinc, and other inorganic nutrients and their chemical form and bioavailability. Nutrition 1993;9:542-5.

158. Trumbo P, Yates AA, Schlicker S, Poos M. Dietary Reference Intakes: Vitamin A, Vitamin K, Arsenic, Boron, Chromium, Copper, Iodine, Iron, Manganese, Molybdenum, Nickel, Silicon, Vanadium, and Zinc. Journal of the American Dietetic Association 2001;101:294-301.

159. Lambein F, Haque R, Khan JK, Kebede N, Kuo YH. From soil to brain: zinc deficiency increases the neurotoxicity of Lathyrus sativus and may affect the susceptibility for the motorneurone disease neurolathyrism. Toxicon 1994;32:461-6.

160. Jayawardena R, Ranasinghe P, Galappatthy P, Malkanthi R, Constantine G, Katulanda P. Effects of zinc supplementation on diabetes mellitus: a systematic review and meta-analysis. Diabetol Metab Syndr 2012;4:13.

161. Kambe T, Narita H, Yamaguchi-Iwai Y, Hirose J, Amano T, Sugiura N, Sasaki R, Mori K, Iwanaga T, Nagao M. Cloning and Characterization of a Novel Mammalian Zinc Transporter, Zinc Transporter 5, Abundantly Expressed in Pancreatic β Cells. Journal of Biological Chemistry 2002;277:19049-55.

162. Ranaldi G, Perozzi G, Truong-Tran A, Zalewski P, Murgia C. Intracellular distribution of labile Zn(II) and zinc transporter expression in kidney and MDCK cells. American journal of physiology Renal physiology 2002;283:1365-75.

163. Hambidge KM, Miller LV, Westcott JE, Sheng X, Krebs NF. Zinc bioavailability and homeostasis. The American journal of clinical nutrition 2010;91:1478S-83.

164. Krishna SS, Majumdar I, Grishin NV. Structural classification of zinc fingers: survey and summary. Nucleic acids research 2003;31:532-50.

165. Schmid G, Chittolini R, Raiteri L, Bonanno G. Differential effects of zinc on native GABAA receptor function in rat hippocampus and cerebellum. Neurochemistry International 1999;34:399-405.

166. Hafiez AA, el-Kirdassy ZH, Mansour MM, Sharada HM, el-Zayat EM. Role of zinc in regulating the testicular function. Part 1. Effect of dietary zinc deficiency on serum levels of gonadotropins, prolactin and testosterone in male albino rats. Nahrung 1989;33:935-40.

167. Costello LC, Feng P, Milon B, Tan M, Franklin RB. Role of zinc in the pathogenesis and treatment of prostate cancer: critical issues to resolve. Prostate Cancer Prostatic Dis 2004;7:111-7.

168. Mutch PB, Hurley LS. Mammary gland function and development: effect of zinc deficiency in rat. The American journal of physiology 1980;238:E26-31.

169. El Muayed M, Billings L, Raja M, Zhang X, Park P, Newman M, Kaufmen D, O'Halloran T, Lowe W. Acute Cytokine Mediated Downregulation of the Zinc Transporter ZnT8 Alters Pancreatic Beta Cell Function. Journal of Endocrinology 2010:1-26.

170. Ho LH, Ruffin RE, Murgia C, Li L, Krilis SA, Zalewski PD. Labile Zinc and Zinc Transporter ZnT4 in Mast Cell Granules: Role in Regulation of Caspase Activation and NF-{kappa}B Translocation. Journal of immunology 2004;172:7750-60.

171. Frederickson CJ. Neurobiology of zinc and zinc-containing neurons. International review of neurobiology 1989;31:145-238.

172. Zalewski P, Truong-Tran A, Lincoln S, Ward D, Shankar A, Coyle P, Jayaram L, Copley A, Grosser D, Murgia C, Lang C, Ruffin R. Use of a zinc fluorophore to measure labile pools of zinc in body fluids and cell-conditioned media. Biotechniques 2006;40:509-20.

173. Keil DE, Berger-Ritchie J, McMillin GA. Testing for Toxic Elements: A Focus on Arsenic, Cadmium, Lead, and Mercury. Lab Medicine 2011;42:735-42.

174. Nolan EM, Lippard SJ. Small-Molecule Fluorescent Sensors for Investigating Zinc Metalloneurochemistry. Accounts of Chemical Research 2008;42:193-203.

175. Zalewski P, Millard S, Forbes I, Kapaniris O, Slavotinek A, Betts W, Ward A, Lincoln S, Mahadevan I. Video image analysis of labile zinc in viable pancreatic islet cells using a specific fluorescent probe for zinc. The Journal of Histochemistry and Cytochemistry 1994;42:877-84.

176.   Truong-Tran AQ, Ruffin RE, Zalewski PD. Visualization of labile zinc and its role in apoptosis of primary airway epithelial cells and cell lines. American journal of physiology Lung cellular and molecular physiology 2000;279:1172-83.

177.   Huang Z, Lippard SJ. Chapter twenty-three - Illuminating Mobile Zinc with Fluorescence: From Cuvettes to Live Cells and Tissues. In: Conn PM, ed. Methods in Enzymology: Academic Press; 2012:445-68.

178.   You Y, Tomat E, Hwang K, Atanasijevic T, Nam W, Jasanoff AP, Lippard SJ. Manganese displacement from Zinpyr-1 allows zinc detection by fluorescence microscopy and magnetic resonance imaging. Chemical Communications 2010;46:4139-41.

179.   Kowalczyk T, Lin Z, Van Voorhis T. Fluorescence quenching by photoinduced electron transfer in the Zn2+ sensor zinpyr-1: a computational investigation. The journal of physical chemistry A 2010;114:10427-34.

180.   Maverakis E, Fung MA, Lynch PJ, Draznin M, Michael DJ, Ruben B, Fazel N. Acrodermatitis enteropathica and an overview of zinc metabolism. Journal of the American Academy of Dermatology 2007;56:116-24.

181.   Sturniolo GC, Leo VD, Ferronato A, D'Odorico A, D'Incà R. Zinc supplementation tightens ldquoLeaky Gutrdquo in Crohn's disease. Inflammatory Bowel Diseases 2001;7:94-8.

182.   Sturniolo GC, Fries W, Mazzon E, Di Leo V, Barollo M, D'Inca R. Effect of zinc supplementation on intestinal permeability in experimental colitis. Journal of Laboratory and Clinical Medicine 2002;139:311-5.

183.   Colvin RA. Characterization of a plasma membrane zinc transporter in rat brain. Neuroscience letters 1998;247:147-50.

184.   Assaf SY, Chung SH. Release of endogenous Zn2+ from brain tissue during activity. Nature 1984;308:734-6.

185.   Adamo A, Zago M, Mackenzie G, Aimo L, Keen C, Keenan A, Oteiza P. The Role of Zinc in the Modulation of Neuronal Proliferation and Apoptosis. Neurotoxicity Research 2010;17:1-14.

186.   Truong-Tran AQ, Ruffin RE, Zalewski PD. Visualization of labile zinc and its role in apoptosis of primary airway epithelial cells and cell lines. American Journal of Physiology - Lung Cellular and Molecular Physiology 2000;279:L1172-L83.

187.   Hennig B, Meerarani P, Ramadass P, Toborek M, Malecki A, Slim R, McClain CJ. Zinc nutrition and apoptosis of vascular endothelial cells: implications in atherosclerosis. Nutrition 1999;15:744-8.

188.   Hennig B, Wang Y, Ramasamy S, McClain CJ. Zinc Deficiency Alters Barrier Function of Cultured Porcine Endothelial Cells. The Journal of nutrition 1992;122:1242-7.

189.   Sazawal S, Black RE, Jalla S, Mazumdar S, Sinha A, Bhan MK. Zinc Supplementation Reduces the Incidence of Acute Lower Respiratory Infections in Infants and Preschool Children: A Double-blind, Controlled Trial. Pediatrics 1998;102:1-5.

190.   Soutar A, Seaton A, Brown K. Bronchial reactivity and dietary antioxidants. Thorax 1997;52:166-70.

191.   Truong-Tran AQ, Grosser D, Ruffin RE, Murgia C, Zalewski PD. Apoptosis in the normal and inflamed airway epithelium: role of zinc in epithelial protection and procaspase-3 regulation. Biochemical pharmacology 2003;66:1459-68.

192.   Lang C, Murgia C, Leong M, Tan L-W, Perozzi G, Knight D, Ruffin R, Zalewski P. Anti-inflammatory effects of zinc and alterations in zinc transporter mRNA

in mouse models of allergic inflammation. American Journal of Physiology - Lung Cellular and Molecular Physiology 2007;292:L577-L84.

193.   Lansdown ABG, Mirastschijski U, Stubbs N, Scanlon E, Ågren MS. Zinc in wound healing: Theoretical, experimental, and clinical aspects. Wound Repair and Regeneration 2007;15:2-16.

194.   Moynahan EJ. Letter: Acrodermatitis enteropathica: a lethal inherited human zinc-deficiency disorder. Lancet 1974;2:399-400.

195.   Lonnerdal B. Trace element transport in the mammary gland. Annual Review of Nutrition 2007;27:165-77.

196.   Huang L, Gitschier J. A novel gene involved in zinc transport is deficient in the lethal milk mouse. Nature genetics 1997;17:292-7.

197.   Kelleher SL, Seo YA, Lopez V. Mammary gland zinc metabolism: regulation and dysregulation. Genes & nutrition 2009;4:83-94.

198.   Hsieh HS, Navia JM. Zinc Deficiency and Bone Formation in Guinea Pig Alveolar Implants. The Journal of nutrition 1980;110:1581-8.

199.   Yamaguchi M. Role of zinc in bone formation and bone resorption. The Journal of Trace Elements in Experimental Medicine 1998;11:119-35.

200.   Rossi L, Migliaccio S, Corsi A, Marzia M, Bianco P, Teti A, Gambelli L, Cianfarani S, Paoletti F, Branca F. Reduced Growth and Skeletal Changes in Zinc-Deficient Growing Rats Are Due to Impaired Growth Plate Activity and Inanition. The Journal of nutrition 2001;131:1142-6.

201.   Oner G, Bhaumick B, Bala RM. Effect of zinc deficiency on serum somatomedin levels and skeletal growth in young rats. Endocrinology 1984;114:1860-3.

202.   Fraker PJ, DePasquale-Jardieu P, Zwickl CM, Luecke RW. Regeneration of T-cell helper function in zinc-deficient adult mice. Proceedings of the National Academy of Sciences of the United States of America 1978;75:5660-4.

203.   Fraker PJ, Haas SM, Luecke RW. Effect of Zinc Deficiency on the Immune Response of the Young Adult A/J Mouse. The Journal of Nutrition 1977;107:1889-95.

204.   Dowd PS, Kelleher J, Guillou PJ. T-lymphocyte subsets and interleukin-2 production in zinc-deficient rats. The British journal of nutrition 1986;55:59-69.

205.   Zalewski PD. Zinc and Immunity. Journal of Nutritional Immunology 1996;4:39-101.

206.   Prasad AS. Zinc: Mechanisms of Host Defense. The Journal of Nutrition 2007;137:1345-9.

207.   Karl L, Chvapil M, Zukoski CF. Effect of Zinc on the Viability and Phagocytic Capacity of Peritoneal Macrophages. Experimental Biology and Medicine 1973;142:1123-7.

208.   Tone K, Suzuki T, Todoroki T. Influence of zinc deficiency on phagocytosis in mice. Kitasato Arch Exp Med 1991;64:263-9.

209.   Wirth JJ, Fraker PJ, Kierszenbaum F. Zinc requirement for macrophage function: effect of zinc deficiency on uptake and killing of a protozoan parasite. Immunology 1989;68:114-9.

210.   Kim YJ, Kang JH, Yang MP. Zinc increases the phagocytic capacity of canine peripheral blood phagocytes in vitro. Vet Res Commun 2009;33:251-61.

211.   Joshi PC, Mehta A, Jabber WS, Fan X, Guidot DM. Zinc Deficiency Mediates Alcohol-Induced Alveolar Epithelial and Macrophage Dysfunction in Rats. American Journal of Respiratory Cell and Molecular Biology 2009;41:207-16.

212. Wu FYH, Wu CW. Zinc in DNA Replication and Transcription. Annual Review of Nutrition 1987;7:251-72.

213. Nygaard S, Larsen A, Knuhtsen A, Rungby J, Smidt K. Effects of zinc supplementation and zinc chelation on in vitro beta-cell function in INS-1E cells. BMC Research Notes 2014;7:84.

214. Coffman FD, Dunn MF. Insulin-metal ion interactions: the binding of divalent cations to insulin hexamers and tetramers and the assembly of insulin hexamers. Biochemistry 1988;27:6179-87.

215. Kadima W, Roy M, Lee RW, Kaarsholm NC, Dunn MF. Studies of the association and conformational properties of metal-free insulin in alkaline sodium chloride solutions by one- and two-dimensional 1H NMR. Journal of Biological Chemistry 1992;267:8963-70.

216. Lemaire K, Ravier MA, Schraenen A, Creemers JWM, Van de Plas R, Granvik M, Van Lommel L, Waelkens E, Chimienti F, Rutter GA, Gilon P, Veld PAit, Schuit FC. Insulin crystallization depends on zinc transporter ZnT8 expression, but is not required for normal glucose homeostasis in mice. Proceedings of the National Academy of Sciences 2009;106:14872-7.

217. Zhou H, Zhang T, Harmon JS, Bryan J, Robertson RP. Zinc, Not Insulin, Regulates the Rat α-Cell Response to Hypoglycemia In Vivo. Diabetes 2007;56:1107-12.

218. Egefjord L, Petersen AB, Rungby J. Zinc, alpha cells and glucagon secretion. Current diabetes reviews 2010;6:52-7.

219. Maret W, Krezel A. Cellular zinc and redox buffering capacity of metallothionein/thionein in health and disease. Molecular medicine 2007;13:371-5.

220. Tanaka N, Kawachi M, Fujiwara T, Maeshima M. Zinc-binding and structural properties of the histidine-rich loop of Arabidopsis thaliana vacuolar membrane zinc transporter MTP1(). FEBS Open Bio 2013;3:218-24.

221. Jenkitkasemwong S, Wang C-Y, Mackenzie B, Knutson M. Physiologic implications of metal-ion transport by ZIP14 and ZIP8. BioMetals 2012;25:643-55.

222. Alam S, Kelleher SL. Cellular Mechanisms of Zinc Dysregulation: A Perspective on Zinc Homeostasis as an Etiological Factor in the Development and Progression of Breast Cancer. Nutrients 2012;4:875-903.

223. Krane SM. A new look at a rare old disease. IBMS BoneKEy 2008;5:253-7.

224. Schmitt-Ulms G, Ehsani S, Watts JC, Westaway D, Wille H. Evolutionary Descent of Prion Genes from the ZIP Family of Metal Ion Transporters. PLoS ONE 2009;4:e7208.

225. Jou M-Y, Hall AG, Philipps AF, Kelleher SL, Lönnerdal B. Tissue-Specific Alterations in Zinc Transporter Expression in Intestine and Liver Reflect a Threshold for Homeostatic Compensation during Dietary Zinc Deficiency in Weanling Rats. The Journal of Nutrition 2009;139:835-41.

226. Yang J, Zhang Y, Cui X, Yao W, Yu X, Cen P, Hodges SE, Fisher WE, Brunicardi FC, Chen C, Yao Q, Li M. Gene profile identifies zinc transporters differentially expressed in normal human organs and human pancreatic cancer. Curr Mol Med 2013;13:401-9.

227. Weaver BP, Dufner-Beattie J, Kambe T, Andrews GK. Novel zinc-responsive post-transcriptional mechanisms reciprocally regulate expression of the mouse Slc39a4 and Slc39a5 zinc transporters (Zip4 and Zip5). Biol Chem 2007;388:1301-12.

228. Dufner-Beattie J, Kuo YM, Gitschier J, Andrews GK. The adaptive response to dietary zinc in mice involves the differential cellular localization and zinc regulation of the zinc transporters ZIP4 and ZIP5. J Biol Chem 2004;279:49082-90.

229. Geiser J, Venken KJT, De Lisle RC, Andrews GK. A Mouse Model of Acrodermatitis Enteropathica: Loss of Intestine Zinc Transporter ZIP4 (Slc39a4) Disrupts the Stem Cell Niche and Intestine Integrity. PLoS Genet 2012;8:e1002766.

230. Wang F, Kim B-E, Dufner-Beattie J, Petris MJ, Andrews G, Eide DJ. Acrodermatitis enteropathica mutations affect transport activity, localization and zinc-responsive trafficking of the mouse ZIP4 zinc transporter. Human Molecular Genetics 2004;13:563-71.

231. Zhang Y, Yang J, Cui X, Chen Y, Zhu VF, Hagan JP, Wang H, Yu X, Hodges SE, Fang J, Chiao PJ, Logsdon CD, Fisher WE, Brunicardi FC, Chen C, Yao Q, Fernandez-Zapico ME, Li M. A novel epigenetic CREB-miR-373 axis mediates ZIP4-induced pancreatic cancer growth. EMBO Molecular Medicine 2013;5:1322-34.

232. Kambe T, Andrews GK. Novel Proteolytic Processing of the Ectodomain of the Zinc Transporter ZIP4 (SLC39A4) during Zinc Deficiency Is Inhibited by Acrodermatitis Enteropathica Mutations. Molecular and Cellular Biology 2009;29:129-39.

233. Antala S, Dempski RE. The Human ZIP4 Transporter Has Two Distinct Binding Affinities and Mediates Transport of Multiple Transition Metals. Biochemistry 2012;51:963-73.

234. Liuzzi JP, Lichten LA, Rivera S, Blanchard RK, Aydemir TB, Knutson MD, Ganz T, Cousins RJ. Interleukin-6 regulates the zinc transporter Zip14 in liver and contributes to the hypozincemia of the acute-phase response. Proceedings of the National Academy of Sciences of the United States of America 2005;102:6843-8.

235. Thorsen K, Mansilla F, Schepeler T, Øster B, Rasmussen MH, Dyrskjøt L, Karni R, Akerman M, Krainer AR, Laurberg S, Andersen CL, Ørntoft TF. Alternative Splicing of SLC39A14 in Colorectal Cancer is Regulated by the Wnt Pathway. Molecular & Cellular Proteomics 2011;10.

236. Liuzzi JP, Aydemir F, Nam H, Knutson MD, Cousins RJ. Zip14 (Slc39a14) mediates non-transferrin-bound iron uptake into cells. Proceedings of the National Academy of Sciences 2006;103:13612-7.

237. Lichten LA, Liuzzi JP, Cousins RJ. Interleukin-1β contributes via nitric oxide to the upregulation and functional activity of the zinc transporter Zip14 (Slc39a14) in murine hepatocytes. American Journal of Physiology - Gastrointestinal and Liver Physiology 2009;296:G860-G7.

238. Hojyo S, Fukada T, Shimoda S, Ohashi W, Bin B-H, Koseki H, Hirano T. The Zinc Transporter SLC39A14/ZIP14 Controls G-Protein Coupled Receptor-Mediated Signaling Required for Systemic Growth. PLoS ONE 2011;6:e18059.

239. Tominaga K, Kagata T, Johmura Y, Hishida T, Nishizuka M, Imagawa M. SLC39A14, a LZT protein, is induced in adipogenesis and transports zinc. FEBS Journal 2005;272:1590-9.

240. Beker Aydemir T, Chang SM, Guthrie GJ, Maki AB, Ryu MS, Karabiyik A, Cousins RJ. Zinc transporter ZIP14 functions in hepatic zinc, iron and glucose homeostasis during the innate immune response (endotoxemia). PloS one 2012;7:e48679.

241. Bataller R, xF, Brenner DA. Liver fibrosis. The Journal of Clinical Investigation 2005;115:209-18.

242.   Liuzzi JP, Aydemir F, Nam H, Knutson MD, Cousins RJ. Zip14 (Slc39a14) mediates non-transferrin-bound iron uptake into cells. Proceedings of the National Academy of Sciences of the United States of America 2006;103:13612-7.

243.   Nam H, Wang C-Y, Zhang L, Zhang W, Hojyo S, Fukada T, Knutson MD. ZIP14 and DMT1 in the liver, pancreas, and heart are differentially regulated by iron deficiency and overload: implications for tissue iron uptake in iron-related disorders. Haematologica 2013;98:1049-57.

244.   Anderson ER, Shah YM. Iron Homeostasis in the Liver. In: Comprehensive Physiology: John Wiley & Sons, Inc.; 2013.

245.   Sayadi A, Nguyen A-T, Bard F, Bard-Chapeau E. Zip14 expression induced by lipopolysaccharides in macrophages attenuates inflammatory response. Inflammation Research 2013;62:133-43.

246.   Moshage H. Cytokines and the hepatic acute phase response. The Journal of Pathology 1997;181:257-66.

247.   Min K-S, Takano M, Amako K, Ueda H, Tanaka K. Involvement of the essential metal transporter Zip14 in hepatic Cd accumulation during inflammation. Toxicology Letters 2013;218:91-6.

248.   Dadke S, Kusari A, Kusari J. Phosphorylation and activation of protein tyrosine phosphatase (PTP) 1B by insulin receptor. Molecular and Cellular Biochemistry 2001;221:147-54.

249.   Cousins RJ, Liuzzi JP, Lichten LA. Mammalian Zinc Transport, Trafficking, and Signals. Journal of Biological Chemistry 2006;281:24085-9.

250.   Kelleher SL, McCormick NH, Velasquez V, Lopez V. Zinc in Specialized Secretory Tissues: Roles in the Pancreas, Prostate, and Mammary Gland. Advances in Nutrition: An International Review Journal 2011;2:101-11.

251.   Hoch E, Lin W, Chai J, Hershfinkel M, Fu D, Sekler I. Histidine pairing at the metal transport site of mammalian ZnT transporters controls Zn2+ over Cd2+ selectivity. Proceedings of the National Academy of Sciences of the United States of America 2012;109:7202-7.

252.   Coudray N, Valvo S, Hu M, Lasala R, Kim C, Vink M, Zhou M, Provasi D, Filizola M, Tao J, Fang J, Penczek PA, Ubarretxena-Belandia I, Stokes DL. Inward-facing conformation of the zinc transporter YiiP revealed by cryoelectron microscopy. Proceedings of the National Academy of Sciences 2013;110:2140-5.

253.   Lu M, Fu D. Structure of the Zinc Transporter YiiP. Science 2007;317:1746-8.

254.   Harrison C, Katayama S, Dhut S, Chen D, Jones N, Bähler J, Toda T. SCFPof1-ubiquitin and its target Zip1 transcription factor mediate cadmium response in fission yeast. The EMBO Journal 2005;24:599-610.

255.   Huang L, Tepaamorndech S. The SLC30 family of zinc transporters - a review of current understanding of their biological and pathophysiological roles. Molecular aspects of medicine 2013;34:548-60.

256.   Lu M, Chai J, Fu D. Structural basis for autoregulation of the zinc transporter YiiP. Nature Structural Molecular Biology 2009;16:1063-7.

257.   Kirschke CP, Huang L. ZnT7, a Novel Mammalian Zinc Transporter, Accumulates Zinc in the Golgi Apparatus. Journal of Biological Chemistry 2003;278:4096-102.

258.   Huang L, Yu YY, Kirschke CP, Gertz ER, Lloyd KKC. Znt7 (Slc30a7)-deficient Mice Display Reduced Body Zinc Status and Body Fat Accumulation. Journal of Biological Chemistry 2007;282:37053-63.

259. Huang L, Yan M, Kirschke CP. Over-expression of ZnT7 increases insulin synthesis and secretion in pancreatic [beta]-cells by promoting insulin gene transcription. Experimental Cell Research 2010;316:2630-43.

260. Pound LD, Sarkar SA, Benninger RKP, Wang Y, Suwanichkul A, Shadoan MK, Printz RL, Oeser JK, Lee CE, Piston DW, McGuinness OP, Hutton JC, Powell DR, O'Brien RM. Deletion of the mouse Slc30a8 gene encoding zinc transporter-8 results in impaired insulin secretion. Biochemical Journal 2009;421:371-6.

261. Kim I, Kang ES, Yim YS, Ko SJ, Jeong SH, Rim JH, Kim YS, Ahn CW, Cha BS, Lee HC, Kim CH. A low-risk ZnT-8 allele (W325) for post-transplantation diabetes mellitus is protective against cyclosporin A-induced impairment of insulin secretion. The pharmacogenomics journal 2010.

262. Fu Y, Tian W, Pratt EB, Dirling LB, Shyng SL, Meshul CK, Cohen DM. Down-regulation of ZnT8 expression in INS-1 rat pancreatic beta cells reduces insulin content and glucose-inducible insulin secretion. PLoS One 2009;4:e5679.

263. Achenbach P, Lampasona V, Landherr U, Koczwara K, Krause S, Grallert H, Winkler C, Pfluger M, Illig T, Bonifacio E, Ziegler AG. Autoantibodies to zinc transporter 8 and SLC30A8 genotype stratify type 1 diabetes risk. Diabetologia 2009;52:1881-8.

264. Wenzlau JM, Moua O, Liu Y, Eisenbarth GS, Hutton JC, Davidson HW. Identification of a major humoral epitope in Slc30a8 (ZnT8). Annals of the New York Academy of Sciences 2008;1150:252-5.

265. Nicolson TJ, Bellomo EA, Wijesekara N, Loder MK, Baldwin JM, Gyulkhandanyan AV, Koshkin V, Tarasov AI, Carzaniga R, Kronenberger K, Taneja TK, da Silva Xavier G, Libert S, Froguel P, Scharfmann R, Stetsyuk V, Ravassard P, Parker H, Gribble FM, Reimann F, Sladek R, Hughes SJ, Johnson PR, Masseboeuf M, Burcelin R, Baldwin SA, Liu M, Lara-Lemus R, Arvan P, Schuit FC, Wheeler MB, Chimienti F, Rutter GA. Insulin storage and glucose homeostasis in mice null for the granule zinc transporter ZnT8 and studies of the type 2 diabetes-associated variants. Diabetes 2009;58:2070-83.

266. Wijesekara N, Chimienti F, Wheeler M. Zinc, a regulator of islet function and glucose homeostasis. Diabetes Obes Metab 2009;11:202 - 14.

267. Chimienti F, Devergnas S, Pattou F, Schuit F, Garcia-Cuenca R, Vandewalle B, Kerr-Conte J, Van Lommel L, Grunwald D, Favier A, Seve M. In vivo expression and functional characterization of the zinc transporter ZnT8 in glucose-induced insulin secretion. Journal of cell science 2006;119:4199-206.

268. Wijesekara N, Dai F, Hardy A, Giglou P, Bhattacharjee A, Koshkin V, Chimienti F, Gaisano H, Rutter G, Wheeler M. Beta cell-specific Znt8 deletion in mice causes marked defects in insulin processing, crystallisation and secretion. Diabetologia 2010:1656-68.

269. Wenzlau JM, Juhl K, Yu L, Moua O, Sarkar SA, Gottlieb P, Rewers M, Eisenbarth GS, Jensen J, Davidson HW, Hutton JC. The cation efflux transporter ZnT8 (Slc30A8) is a major autoantigen in human type 1 diabetes. Proceedings of the National Academy of Sciences 2007;104:17040-5.

270. Wenzlau JM, Liu Y, Yu L, Moua O, Fowler KT, Rangasamy S, Walters J, Eisenbarth GS, Davidson HW, Hutton JC. A Common Nonsynonymous Single Nucleotide Polymorphism in the SLC30A8 Gene Determines ZnT8 Autoantibody Specificity in Type 1 Diabetes. Diabetes 2008;57:2693-7.

271.   Gohlke H, Ferrari U, Koczwara K, Bonifacio E, Illig T, Ziegler A-G. SLC30A8 (ZnT8) Polymorphism is Associated with Young Age at Type 1 Diabetes Onset. The Review of Diabetic Studies 2008;5:25-7.

272.   Vaziri-Sani F, Oak S, Radtke J, Lernmark K, Lynch K, Agardh CD, Cilio CM, Lethagen AL, Ortqvist E, Landin-Olsson M, Torn C, Hampe CS. ZnT8 autoantibody titers in type 1 diabetes patients decline rapidly after clinical onset. Autoimmunity 2010;43:598-606.

273.   Yan H, Yuan W, Velculescu VE, Vogelstein B, Kinzler KW. Allelic Variation in Human Gene Expression. Science 2002;297:1143.

274.   Lo HS, Wang Z, Hu Y, Yang HH, Gere S, Buetow KH, Lee MP. Allelic Variation in Gene Expression Is Common in the Human Genome. Genome Research 2003;13:1855-62.

275.   Sladek R, Rocheleau G, Rung J, Dina C, Shen L, Serre D, Boutin P, Vincent D, Belisle A, Hadjadj S, Balkau B, Heude B, Charpentier G, Hudson TJ, Montpetit A, Pshezhetsky AV, Prentki M, Posner BI, Balding DJ, Meyre D, Polychronakos C, Froguel P. A genome-wide association study identifies novel risk loci for type 2 diabetes. Nature 2007;445:881-5.

276.   Harvard DGIoBIo, MIT LU, Novartis Institutes of BioMedical Research, Saxena R, Voight BF, Lyssenko V, Burtt NP, de Bakker PIW, Chen H, Roix JJ, Kathiresan S, Hirschhorn JN, Daly MJ, Hughes TE, Groop L, Altshuler D, Almgren P, Florez JC, Meyer J, Ardlie K, Bengtsson Bostrom K, Isomaa B, Lettre G, Lindblad U, Lyon HN, Melander O, Newton-Cheh C, Nilsson P, Orho-Melander M, Rastam L, Speliotes EK, Taskinen M-R, Tuomi T, Guiducci C, Berglund A, Carlson J, Gianniny L, Hackett R, Hall L, Holmkvist J, Laurila E, Sjogren M, Sterner M, Surti A, Svensson M, Svensson M, Tewhey R, Blumenstiel B, Parkin M, DeFelice M, Barry R, Brodeur W, Camarata J, Chia N, Fava M, Gibbons J, Handsaker B, Healy C, Nguyen K, Gates C, Sougnez C, Gage D, Nizzari M, Gabriel SB, Chirn G-W, Ma Q, Parikh H, Richardson D, Ricke D, Purcell S. Genome-Wide Association Analysis Identifies Loci for Type 2 Diabetes and Triglyceride Levels. Science 2007;316:1331-6.

277.   Scott LJ, Mohlke KL, Bonnycastle LL, Willer CJ, Li Y, Duren WL, Erdos MR, Stringham HM, Chines PS, Jackson AU, Prokunina-Olsson L, Ding C-J, Swift AJ, Narisu N, Hu T, Pruim R, Xiao R, Li X-Y, Conneely KN, Riebow NL, Sprau AG, Tong M, White PP, Hetrick KN, Barnhart MW, Bark CW, Goldstein JL, Watkins L, Xiang F, Saramies J, Buchanan TA, Watanabe RM, Valle TT, Kinnunen L, Abecasis GR, Pugh EW, Doheny KF, Bergman RN, Tuomilehto J, Collins FS, Boehnke M. A Genome-Wide Association Study of Type 2 Diabetes in Finns Detects Multiple Susceptibility Variants. Science 2007;316:1341-5.

278.   Steinthorsdottir V, Thorleifsson G, Reynisdottir I, Benediktsson R, Jonsdottir T, Walters GB, Styrkarsdottir U, Gretarsdottir S, Emilsson V, Ghosh S, Baker A, Snorradottir S, Bjarnason H, Ng MC, Hansen T, Bagger Y, Wilensky RL, Reilly MP, Adeyemo A, Chen Y, Zhou J, Gudnason V, Chen G, Huang H, Lashley K, Doumatey A, So WY, Ma RC, Andersen G, Borch-Johnsen K, Jorgensen T, van Vliet-Ostaptchouk JV, Hofker MH, Wijmenga C, Christiansen C, Rader DJ, Rotimi C, Gurney M, Chan JC, Pedersen O, Sigurdsson G, Gulcher JR, Thorsteinsdottir U, Kong A, Stefansson K. A variant in CDKAL1 influences insulin response and risk of type 2 diabetes. Nature genetics 2007;39:770-5.

279.   Staiger H, Machicao F, Stefan N, Tschritter O, Thamer C, Kantartzis K, Schäfer SA, Kirchhoff K, Fritsche A, Häring H-U. Polymorphisms within Novel Risk Loci for Type 2 Diabetes Determine β-Cell Function. PLoS One 2007;2:e832.

280. Palmer ND, Goodarzi MO, Langefeld CD, Ziegler J, Norris JM, Haffner SM, Bryer-Ash M, Bergman RN, Wagenknecht LE, Taylor KD, Rotter JI, Bowden DW. Quantitative Trait Analysis of Type 2 Diabetes Susceptibility Loci Identified From Whole Genome Association Studies in the Insulin Resistance Atherosclerosis Family Study. Diabetes 2008;57:1093-100.

281. Xiang J, Li X-Y, Xu M, Hong J, Huang Y, Tan J-R, Lu X, Dai M, Yu B, Ning G. Zinc Transporter-8 Gene (SLC30A8) Is Associated with Type 2 Diabetes in Chinese. The Journal of clinical endocrinology and metabolism 2008;93:4107-12.

282. Pascoe L, Tura A, Patel SK, Ibrahim IM, Ferrannini E, Zeggini E, Weedon MN, Mari A, Hattersley AT, McCarthy MI, Frayling TM, Walker M. Common Variants of the Novel Type 2 Diabetes Genes CDKAL1 and HHEX/IDE Are Associated With Decreased Pancreatic β-Cell Function. Diabetes 2007;56:3101-4.

283. Hertel J, Johansson S, Ræder H, Midthjell K, Lyssenko V, Groop L, Molven A, Njølstad P. Genetic analysis of recently identified type 2 diabetes loci in 1,638 unselected patients with type 2 diabetes and 1,858 control participants from a Norwegian population-based cohort (the HUNT study). Diabetologia 2008;51:971-7.

284. Weijers R. Three-dimensional structure of beta-cell-specific zinc transporter, ZnT-8, predicted from the type 2 diabetes-associated gene variant SLC30A8 R325W. Diabetology & Metabolic Syndrome 2010;2:33.

285. Kang ES, Kim MS, Kim YS, Kim CH, Han SJ, Chun SW, Hur KY, Nam CM, Ahn CW, Cha BS, Kim SI, Lee HC. A Polymorphism in the Zinc Transporter Gene SLC30A8 Confers Resistance Against Posttransplantation Diabetes Mellitus in Renal Allograft Recipients. Diabetes 2008;57:1043-7.

286. Hijova E. Metallothioneins and zinc: their functions and interactions. Bratislavske lekarske listy 2004;105:230-4.

287. Wu JP, Ma BY, Ren HW, Zhang LP, Xiang Y, Brown MA. Characterization of metallothioneins (MT-I and MT-II) in the yak. Journal of Animal Science 2007;85:1357-62.

288. Coyle P, Philcox JC, Carey LC, Rofe AM. Metallothionein: the multipurpose protein. Cell Mol Life Sci 2002;59:627-47.

289. Miles AT, Hawksworth GM, Beattie JH, Rodilla V. Induction, Regulation, Degradation, and Biological Significance of Mammalian Metallothioneins. Critical Reviews in Biochemistry and Molecular Biology 2000;35:35-70.

290. Tomita T, Matsubara O. Immunocytochemical Localization of Metallothionein in Human Pancreatic Islets. Pancreas 2000;20:21-4.

291. Peschke E, Bähr I, Mühlbauer E. Melatonin and Pancreatic Islets: Interrelationships between Melatonin, Insulin and Glucagon. International Journal of Molecular Sciences 2013;14:6981-7015.

292. El Muayed M, Raja MR, Zhang X, MacRenaris KW, Bhatt S, Chen X, Urbanek M, O'Halloran TV, Lowe WL, Jr. Accumulation of cadmium in insulin-producing beta cells. Islets 2012;4:405-16.

293. Chen H, Carlson EC, Pellet L, Moritz JT, Epstein PN. Overexpression of Metallothionein in Pancreatic β-Cells Reduces Streptozotocin-Induced DNA Damage and Diabetes. Diabetes 2001;50:2040-6.

294. Vriens J, Owsianik G, Hofmann T, Philipp Stephan E, Stab J, Chen X, Benoit M, Xue F, Janssens A, Kerselaers S, Oberwinkler J, Vennekens R, Gudermann T, Nilius B, Voets T. TRPM3 Is a Nociceptor Channel Involved in the Detection of Noxious Heat. Neuron 2011;70:482-94.

295. Frühwald J, Camacho Londoño J, Dembla S, Mannebach S, Lis A, Drews A, Wissenbach U, Oberwinkler J, Philipp SE. Alternative Splicing of a Protein Domain Indispensable for Function of Transient Receptor Potential Melastatin 3 (TRPM3) Ion Channels. Journal of Biological Chemistry 2012;287:36663-72.

296. Vriens J, Owsianik G, Hofmann T, Philipp SE, Stab J, Chen X, Benoit M, Xue F, Janssens A, Kerselaers S, Oberwinkler J, Vennekens R, Gudermann T, Nilius B, Voets T. TRPM3 is a nociceptor channel involved in the detection of noxious heat. Neuron 2011;70:482-94.

297. Hogstrand C, Kille P, Nicholson RI, Taylor KM. Zinc transporters and cancer: a potential role for ZIP7 as a hub for tyrosine kinase activation. Trends in Molecular Medicine 2009;15:101-11.

298. Stuart GW, Searle PF, Palmiter RD. Identification of multiple metal regulatory elements in mouse metallothionein-I promoter by assaying synthetic sequences. Nature 1985;317:828-31.

299. Westin G, Schaffner W. A zinc-responsive factor interacts with a metal-regulated enhancer element (MRE) of the mouse metallothionein-I gene. The EMBO journal 1988;7:3763-70.

300. Heuchel R, Radtke F, Georgiev O, Stark G, Aguet M, Schaffner W. The transcription factor MTF-1 is essential for basal and heavy metal-induced metallothionein gene expression. The EMBO journal 1994;13:2870-5.

301. Lazarczyk M, Pons C, Mendoza J-A, Cassonnet P, Jacob Y, Favre M. Regulation of cellular zinc balance as a potential mechanism of EVER-mediated protection against pathogenesis by cutaneous oncogenic human papillomaviruses. The Journal of Experimental Medicine 2008;205:35-42.

302. Seo YA, Lopez V, Kelleher SL. A histidine-rich motif mediates mitochondrial localization of ZnT2 to modulate mitochondrial function. American Journal of Physiology - Cell Physiology 2011;300:C1479-C89.

303. Ranaldi G, Perozzi G, Truong-Tran A, Zalewski P, Murgia C. Intracellular distribution of labile Zn(II) and zinc transporter expression in kidney and MDCK cells. American Journal of Physiology - Renal Physiology 2002;283:F1365-F75.

304. Huang L, Kirschke CP, Gitschier J. Functional Characterization of a Novel Mammalian Zinc Transporter, ZnT6. Journal of Biological Chemistry 2002;277:26389-95.

305. Fukada T, Yamasaki S, Nishida K, Murakami M, Hirano T. Zinc homeostasis and signaling in health and diseases. JBIC Journal of Biological Inorganic Chemistry 2011;16:1123-34.

306. Devergnas S, Chimienti F, Naud N, Pennequin A, Coquerel Y, Chantegrel J, Favier A, Seve M. Differential regulation of zinc efflux transporters ZnT-1, ZnT-5 and ZnT-7 gene expression by zinc levels: a real-time RT-PCR study. Biochemical pharmacology 2004;68:699-709.

307. Milon B, Dhermy D, Pountney D, Bourgeois M, Beaumont C. Differential subcellular localization of hZip1 in adherent and non-adherent cells. FEBS Letters 2001;507:241-6.

308. Costello LC, Liu Y, Zou J, Franklin RB. Evidence for a Zinc Uptake Transporter in Human Prostate Cancer Cells Which Is Regulated by Prolactin and Testosterone. Journal of Biological Chemistry 1999;274:17499-504.

309. Wang F, Dufner-Beattie J, Kim B-E, Petris MJ, Andrews G, Eide DJ. Zinc-stimulated Endocytosis Controls Activity of the Mouse ZIP1 and ZIP3 Zinc Uptake Transporters. Journal of Biological Chemistry 2004;279:24631-9.

310. Dufner-Beattie J, Wang F, Kuo Y-M, Gitschier J, Eide D, Andrews GK. The Acrodermatitis Enteropathica Gene ZIP4 Encodes a Tissue-specific, Zinc-regulated Zinc Transporter in Mice. Journal of Biological Chemistry 2003;278:33474-81.

311. Weaver BP, Dufner-Beattie J, Kambe T, Andrews GK. Novel zinc-responsive post-transcriptional mechanisms reciprocally regulate expression of the mouse Slc39a4 and Slc39a5 zinc transporters (Zip4 and Zip5). Biological Chemistry 2007;388:1301-12.

312. Dufner-Beattie J, Kuo Y-M, Gitschier J, Andrews GK. The Adaptive Response to Dietary Zinc in Mice Involves the Differential Cellular Localization and Zinc Regulation of the Zinc Transporters ZIP4 and ZIP5. Journal of Biological Chemistry 2004;279:49082-90.

313. Mao X, Kim B-E, Wang F, Eide DJ, Petris MJ. A Histidine-rich Cluster Mediates the Ubiquitination and Degradation of the Human Zinc Transporter, hZIP4, and Protects against Zinc Cytotoxicity. Journal of Biological Chemistry 2007;282:6992-7000.

314. Kim B-E, Wang F, Dufner-Beattie J, Andrews GK, Eide DJ, Petris MJ. Zn2+-stimulated Endocytosis of the mZIP4 Zinc Transporter Regulates Its Location at the Plasma Membrane. Journal of Biological Chemistry 2004;279:4523-30.

315. Yamashita S, Miyagi C, Fukada T, Kagara N, Che Y-S, Hirano T. Zinc transporter LIVI controls epithelial-mesenchymal transition in zebrafish gastrula organizer. Nature 2004;429:298-302.

316. Taylor KM. A distinct role in breast cancer for two LIV-1 family zinc transporters. Biochemical Society Transactions 2008;36:1247-51.

317. Besecker B, Bao S, Bohacova B, Papp A, Sadee W, Knoell DL. The human zinc transporter SLC39A8 (Zip8) is critical in zinc-mediated cytoprotection in lung epithelia. American Journal of Physiology - Lung Cellular and Molecular Physiology 2008;294:L1127-L36.

318. Napolitano JR, Liu M-J, Bao S, Crawford M, Nana-Sinkam P, Cormet-Boyaka E, Knoell DL. Cadmium-mediated toxicity of lung epithelia is enhanced through NF-κB-mediated transcriptional activation of the human zinc transporter ZIP8. American Journal of Physiology - Lung Cellular and Molecular Physiology 2012;302:L909-L18.

319. Hogstrand C, Kille P, Ackland ML, Hiscox S, Taylor KM. A mechanism for epithelial-mesenchymal transition and anoikis resistance in breast cancer triggered by zinc channel ZIP6 and STAT3 (signal transducer and activator of transcription 3). The Biochemical journal 2013;455:229-37.

320. Bin B-H, Fukada T, Hosaka T, Yamasaki S, Ohashi W, Hojyo S, Miyai T, Nishida K, Yokoyama S, Hirano T. Biochemical Characterization of Human ZIP13 Protein: A homo-dimerized zinc transporter involved in the spondylocheiro dysplastic ehlers-Danlos syndrome. Journal of Biological Chemistry 2011;286:40255-65.

321. Nishida K, Hasegawa A, Nakae S, Oboki K, Saito H, Yamasaki S, Hirano T. Zinc transporter Znt5/Slc30a5 is required for the mast cell–mediated delayed-type allergic reaction but not the immediate-type reaction. The Journal of Experimental Medicine 2009;206:1351-64.

322. Haase H, Ober-Blöbaum JL, Engelhardt G, Hebel S, Heit A, Heine H, Rink L. Zinc Signals Are Essential for Lipopolysaccharide-Induced Signal Transduction in Monocytes. The Journal of Immunology 2008;181:6491-502.

323. Team RC. R: A language and environment for statistical computing. Vienna, Austria: R Foundation for Statistical Computing; 2013.

324. Douglas Bates MM, Ben Bolker and Steven Walker lme4: Linear mixed-effects models using Eigen and S4. In; 2013.

325. Weisberg JFaS. Companion to Applied Regression. Thousand Oaks CA; 2011.

326. Hothorn T, Bretz F, Westfall P. Simultaneous Inference in General Parametric Models. Biometrical Journal 2008;50:346-63.

327. Kim A, Miller K, Jo J, Kilimnik G, Wojcik P, Hara M. Islet architecture: A comparative study. Islets 2009;1:129-36.

328. Kharouta M, Miller K, Kim A, Wojcik P, Kilimnik G, Dey A, Steiner DF, Hara M. No mantle formation in rodent islets—The prototype of islet revisited. Diabetes Research and Clinical Practice 2009;85:252-7.

329. Steiner DJ, Kim A, Miller K, Hara M. Pancreatic islet plasticity: Interspecies comparison of islet architecture and composition. Islets 2010;2:135-45.

330. Simeone DM, Zhang L, Treutelaar MK, Zhang L, Graziano K, Logsdon CD, Burant CF. Islet hypertrophy following pancreatic disruption of Smad4 signaling. American Journal of Physiology - Endocrinology and Metabolism 2006;291:E1305-E16.

331. Homo-Delarche F, Calderari S, Irminger J-C, Gangnerau M-N, Coulaud J, Rickenbach K, Dolz M, Halban P, Portha B, Serradas P. Islet Inflammation and Fibrosis in a Spontaneous Model of Type 2 Diabetes, the GK Rat. Diabetes 2006;55:1625-33.

332. Baetens D, Stefan Y, Ravazzola M, Malaisse-Lagae F, Coleman DL, Orci L. Alteration of Islet Cell Populations in Spontaneously Diabetic Mice. Diabetes 1978;27:1-7.

333. Ehses JA, Perren A, Eppler E, Ribaux P, Pospisilik JA, Maor-Cahn R, Gueripel X, Ellingsgaard H, Schneider MKJ, Biollaz G, Fontana A, Reinecke M, Homo-Delarche F, Donath MY. Increased Number of Islet-Associated Macrophages in Type 2 Diabetes. Diabetes 2007;56:2356-70.

334. Kanda H, Tateya S, Tamori Y, Kotani K, Hiasa K-i, Kitazawa R, Kitazawa S, Miyachi H, Maeda S, Egashira K, Kasuga M. MCP-1 contributes to macrophage infiltration into adipose tissue, insulin resistance, and hepatic steatosis in obesity. The Journal of Clinical Investigation 2006;116:1494-505.

335. King AJF. The use of animal models in diabetes research. British Journal of Pharmacology 2012;166:877-94.

336. Surwit RS, Kuhn CM, Cochrane C, McCubbin JA, Feinglos MN. Diet-induced type II diabetes in C57BL/6J mice. Diabetes 1988;37:1163-7.

337. Kaku K, Fiedorek FT, Jr., Province M, Permutt MA. Genetic analysis of glucose tolerance in inbred mouse strains. Evidence for polygenic control. Diabetes 1988;37:707-13.

338. Tesch GH, Lim AKH. Recent insights into diabetic renal injury from the db/db mouse model of type 2 diabetic nephropathy. American Journal of Physiology - Renal Physiology 2011;300:F301-F10.

339. Meissner M, Herrema H, van Dijk TH, Gerding A, Havinga R, Boer T, Müller M, Reijngoud D-J, Groen AK, Kuipers F. Bile Acid Sequestration Reduces Plasma Glucose Levels in *db/db* Mice by Increasing Its Metabolic Clearance Rate. PLoS ONE 2011;6:e24564.

340. Orci L, Baetens D, Rufener C, Amherdt M, Ravazzola M, Studer P, Malaisse-Lagae F, Unger RH. Hypertrophy and hyperplasia of somatostatin-containing D-cells in diabetes. Proceedings of the National Academy of Sciences 1976;73:1338-42.

341.	Pick A, Clark J, Kubstrup C, Levisetti M, Pugh W, Bonner-Weir S, Polonsky KS. Role of apoptosis in failure of beta-cell mass compensation for insulin resistance and beta-cell defects in the male Zucker diabetic fatty rat. Diabetes 1998;47:358-64.
342.	Kloppel G, Lohr M, Habich K, Oberholzer M, Heitz PU. Islet pathology and the pathogenesis of type 1 and type 2 diabetes mellitus revisited. Surv Synth Pathol Res 1985;4:110-25.
343.	Parsons JA, Brelje TC, Sorenson RL. Adaptation of islets of Langerhans to pregnancy: increased islet cell proliferation and insulin secretion correlates with the onset of placental lactogen secretion. Endocrinology 1992;130:1459-66.
344.	Bonner-Weir S, Baxter LA, Schuppin GT, Smith FE. A second pathway for regeneration of adult exocrine and endocrine pancreas. A possible recapitulation of embryonic development. Diabetes 1993;42:1715-20.
345.	Bonner-Weir S, Smith FE. Islet cell growth and the growth factors involved. Trends in Endocrinology & Metabolism 1994;5:60-4.
346.	Garris DR, Garris BL. Cytochemical analysis of pancreatic islet hypercytolipidemia following diabetes (db/db) and obese (ob/ob) mutation expression: influence of genomic background. Pathobiology 2004;71:231-40.
347.	Kaung H-lC. Growth dynamics of pancreatic islet cell populations during fetal and neonatal development of the rat. Developmental Dynamics 1994;200:163-75.
348.	Dalbøge LS, Almholt DLC, Neerup TSR, Vassiliadis E, Vrang N, Pedersen L, Fosgerau K, Jelsing J. Characterisation of Age-Dependent Beta Cell Dynamics in the Male db/db Mice. PLoS ONE 2013;8:e82813.
349.	Emanueli C, Caporali A, Krankel N, Cristofaro B, Van Linthout S, Madeddu P. Type-2 diabetic Lepr(db/db) mice show a defective microvascular phenotype under basal conditions and an impaired response to angiogenesis gene therapy in the setting of limb ischemia. Front Biosci 2007;12:2003-12.
350.	Strowski MZ, Parmar RM, Blake AD, Schaeffer JM. Somatostatin Inhibits Insulin and Glucagon Secretion via Two Receptor Subtypes: An in Vitro Study of Pancreatic Islets from Somatostatin Receptor 2 Knockout Mice. Endocrinology 2000;141:111-7.
351.	Lönnerdal B. Dietary Factors Influencing Zinc Absorption. The Journal of Nutrition 2000;130:1378S-83S.
352.	Cousins RJ. Gastrointestinal Factors Influencing Zinc Absorption and Homeostasis. International Journal for Vitamin and Nutrition Research 2010;80:243-8.
353.	Ananda SP. Zinc deficiency. BMJ 2003;326.
354.	Prasad AS. Effects of zinc deficiency on immune functions. The Journal of Trace Elements in Experimental Medicine 2000;13:1-20.
355.	Jayawardena R, Ranasinghe P, Galappatthy P, Malkanthi R, Constantine G, Katulanda P. Effects of zinc supplementation on diabetes mellitus: a systematic review and meta-analysis. Diabetology & Metabolic Syndrome 2012;4:13.
356.	Pidduck H, Wren P, Evans D. Hyperzincuria of diabetes mellitus and possible genetical implications of this observation. Diabetes 1970;19:240 - 7.
357.	Garg V, Gupta R, Goyal R. Hypozincemia in diabetes mellitus. J Assoc Physicians India 1994;42:720 - 1.
358.	Al-Maroof R, Al-Sharbatti S. Serum zinc levels in diabetic patients and effect of zinc supplementation on glycemic control of type 2 diabetics. Saudi Medical Journal 2006;27:344 - 50.
359.	Chausmer A. Zinc, insulin and diabetes. J Am Coll Nutr 1998;17:109 - 15.

360. Priel T, Aricha-Tamir B, Sekler I. Clioquinol attenuates zinc-dependent β-cell death and the onset of insulitis and hyperglycemia associated with experimental type I diabetes in mice. European Journal of Pharmacology 2007;565:232-9.

361. Bolkent S, Yanardag R, Mutlu O. The Influence of Zinc Supplementation on the Pancreas of Streptozotocin-Diabetic Rats. Digestive diseases and sciences 2009.

362. Simon SF, Taylor CG. Dietary Zinc Supplementation Attenuates Hyperglycemia in db/db Mice. Experimental biology and medicine 2001;226:43-51.

363. Li Y. Zinc and insulin in pancreatic beta-cells. Endocrine 2013:1-12.

364. Vallee BL, Auld DS. Zinc coordination, function, and structure of zinc enzymes and other proteins. Biochemistry 1990;29:5647-59.

365. Devirgiliis C, Murgia C, Danscher G, Perozzi G. Exchangeable zinc ions transiently accumulate in a vesicular compartment in the yeast Saccharomyces cerevisiae. Biochemical and Biophysical Research Communications 2004;323:58-64.

366. Murgia C, Devirgiliis C, Mancini E, Donadel G, Zalewski P, Perozzi G. Diabetes-linked zinc transporter ZnT8 is a homodimeric protein expressed by distinct rodent endocrine cell types in the pancreas and other glands. Nutrition, Metabolism and Cardiovascular Diseases 2009;19:431-9.

367. Figlewicz DP, Forhan SE, Hodgson AT, Grodsky GM. 65Zinc and Endogenous Zinc Content and Distribution in Islets in Relationship to Insulin Content. Endocrinology 1984;115:877-81.

368. Jindal RM, Gray DW, McShane P, Morris PJ. Zinc-specific N-(6-methoxy-8-quinolyl)-para-toluenesulfonamide as a selective nontoxic fluorescence stain for pancreatic islets; 1993.

369. Grant K. Walkup SCB, ‡, Stephen J. Lippard, ‡ and Roger Y. Tsien*,†,§. A New Cell-Permeable Fluorescent Probe for Zn2+. Journal of American Chemical Society 2000;122:5644-5.

370. Levine AS, McClain CJ, Handwerger BS, Brown DM, Morley JE. Tissue zinc status of genetically diabetic and streptozotocin-induced diabetic mice. The American Journal of Clinical Nutrition 1983;37:382-6.

371. Sahai A, Malladi P, Pan X, Paul R, Melin-Aldana H, Green RM, Whitington PF. Obese and diabetic db/db mice develop marked liver fibrosis in a model of nonalcoholic steatohepatitis: role of short-form leptin receptors and osteopontin. American Journal of Physiology - Gastrointestinal and Liver Physiology 2004;287:G1035-G43.

372. Yamaguchi K, Itoh Y, Yokomizo C, Nishimura T, Niimi T, Umemura A, Fujii H, Okanoue T, Yoshikawa T. Blockade of IL-6 signaling exacerbates liver injury and suppresses antiapoptotic gene expression in methionine choline-deficient diet-Fed db/db mice. Lab Invest 2011;91:609-18.

373. Foster M, Samman S. Zinc and Regulation of Inflammatory Cytokines: Implications for Cardiometabolic Disease. Nutrients 2012;4:676-94.

374. Hobel C, Culhane J. Role of Psychosocial and Nutritional Stress on Poor Pregnancy Outcome. The Journal of Nutrition 2003;133:1709S-17S.

375. Kristiansen LH, Rungby J, Sondergaard LG, Stoltenberg M, Danscher G. Autometallography allows ultrastructural monitoring of zinc in the endocrine pancreas. Histochemistry and cell biology 2001;115:125-9.

376. Liu Z, Kim W, Chen Z, Shin Y-K, Carlson OD, Fiori JL, Xin L, Napora JK, Short R, Odetunde JO, Lao Q, Egan JM. Insulin and Glucagon Regulate Pancreatic α-Cell Proliferation. PLoS ONE 2011;6:e16096.

377. Emdin SO, Dodson GG, Cutfield JM, Cutfield SM. Role of zinc in insulin biosynthesis. Diabetologia 1980;19:174-82.

378. Liuzzi JP, Cousins RJ. Mammalian zinc transporters. Annual Review of Nutrition 2004;24:151-72.

379. Zheng D, Feeney GP, Kille P, Hogstrand C. Regulation of ZIP and ZnT zinc transporters in zebrafish gill: zinc repression of ZIP10 transcription by an intronic MRE cluster. Physiological genomics 2008;34:205-14.

380. Gaither LA, Eide DJ. Eukaryotic zinc transporters and their regulation. Biometals : an international journal on the role of metal ions in biology, biochemistry, and medicine 2001;14:251-70.

381. Myers SA, Nield A, Myers M. Zinc transporters, mechanisms of action and therapeutic utility: implications for type 2 diabetes mellitus. Journal of nutrition and metabolism 2012;2012:173712.

382. Liu BY, Jiang Y, Lu Z, Li S, Lu D, Chen B. Down-regulation of zinc transporter 8 in the pancreas of db/db mice is rescued by Exendin-4 administration. Molecular medicine reports 2011;4:47-52.

383. Wagner TJ, Drews A, Loch S, Mohr F, Philipp S, Lambert S, Oberwinkler J. TRPM3 channels provide a regulated influx pathway for zinc in pancreatic beta cells. Pflügers Archiv - European Journal of Physiology 2010;460:755-65.

384. Bach I. The LIM domain: regulation by association. Mechanisms of Development 2000;91:5-17.

385. Kodani M, Yang G, Conklin LM, Travis TC, Whitney CG, Anderson LJ, Schrag SJ, Taylor TH, Beall BW, Breiman RF, Feikin DR, Njenga MK, Mayer LW, Oberste MS, Tondella MLC, Winchell JM, Lindstrom SL, Erdman DD, Fields BS. Application of TaqMan Low-Density Arrays for Simultaneous Detection of Multiple Respiratory Pathogens. Journal of Clinical Microbiology 2011;49:2175-82.

386. Abruzzo LV, Lee KY, Fuller A, Silverman A, Keating MJ, Medeiros LJ, Coombes KR. Validation of oligonucleotide microarray data using microfluidic low-density arrays: a new statistical method to normalize real-time RT-PCR data. Biotechniques 2005;38:785-92.

387. Langmann T, Mauerer R, Schmitz G. Human ATP-Binding Cassette Transporter TaqMan Low-Density Array: Analysis of Macrophage Differentiation and Foam Cell Formation. Clinical Chemistry 2006;52:310-3.

388. Orland MJ, Permutt MA. Quantitative analysis of pancreatic proinsulin mRNA in genetically diabetic (db/db) mice. Diabetes 1987;36:341-7.

389. Kaku K, Province M, Permutt MA. Genetic analysis of obesity-induced diabetes associated with a limited capacity to synthesize insulin in C57BL/KS mice: evidence for polygenic control. Diabetologia 1989;32:636-43.

390. Tamaki M, Fujitani Y, Uchida T, Hirose T, Kawamori R, Watada H. Downregulation of ZnT8 expression in pancreatic beta-cells of diabetic mice. Islets 2009;1:124-8.

391. Egefjord L, Jensen J, Bang-Berthelsen C, Petersen A, Smidt K, Schmitz O, Karlsen A, Pociot F, Chimienti F, Rungby J, Magnusson N. Zinc transporter gene expression is regulated by pro-inflammatory cytokines: a potential role for zinc transporters in beta-cell apoptosis? BMC Endocrine Disorders 2009;9:7.

392. Huang L, Yan M, Kirschke CP. Over-expression of ZnT7 increases insulin synthesis and secretion in pancreatic β-cells by promoting insulin gene transcription. Experimental Cell Research 2010;316:2630-43.

393. Truong-Tran AQ, Carter J, Ruffin R, Zalewski PD. New insights into the role of zinc in the respiratory epithelium. Immunol Cell Biol 2001;79:170-7.

394. Gao HL, Feng WY, Li XL, Xu H, Huang L, Wang ZY. Golgi apparatus localization of ZNT7 in the mouse cerebellum. Histology and histopathology 2009;24:567-72.

395. Huang L, Kirschke CP, Lay YA, Levy LB, Lamirande DE, Zhang PH. Znt7-null mice are more susceptible to diet-induced glucose intolerance and insulin resistance. The Journal of biological chemistry 2012;287:33883-96.

396. Kawasaki E. ZnT8 and type 1 diabetes. Endocr J 2012;59:531-7.

397. Huang XF, Arvan P. Intracellular Transport of Proinsulin in Pancreatic -Cells: Structural maturation probed by disulfide accessibility Journal of Biological Chemistry 1995;270:20417-23.

398. Ellis CD, Wang F, MacDiarmid CW, Clark S, Lyons T, Eide DJ. Zinc and the Msc2 zinc transporter protein are required for endoplasmic reticulum function. The Journal of Cell Biology 2004;166:325-35.

399. Xu TF, Wang XL, Yang JZ, Hu XY, Wu WF, Guo L, Kang LD, Zhang LY. Overexpression of Zip-2 mRNA in the leukocytes of asthmatic infants. Pediatric pulmonology 2009;44:763-7.

400. Taylor KM, Vichova P, Jordan N, Hiscox S, Hendley R, Nicholson RI. ZIP7-Mediated Intracellular Zinc Transport Contributes to Aberrant Growth Factor Signaling in Antihormone-Resistant Breast Cancer Cells. Endocrinology 2008;149:4912-20.

401. Wang K, Zhou B, Kuo Y-M, Zemansky J, Gitschier J. A Novel Member of a Zinc Transporter Family Is Defective in Acrodermatitis Enteropathica. The American Journal of Human Genetics 2002;71:66-73.

402. Li M, Zhang Y, Liu Z, Bharadwaj U, Wang H, Wang X, Zhang S, Liuzzi JP, Chang S-M, Cousins RJ, Fisher WE, Brunicardi FC, Logsdon CD, Chen C, Yao Q. Aberrant expression of zinc transporter ZIP4 (SLC39A4) significantly contributes to human pancreatic cancer pathogenesis and progression. Proceedings of the National Academy of Sciences 2007;104:18636-41.

403. Mohanasundaram D, Drogemuller C, Brealey J, Jessup CF, Milner C, Murgia C, Lang CJ, Milton A, Zalewski PD, Russ GR, Coates PT. Ultrastructural analysis, zinc transporters, glucose transporters and hormones expression in New world primate (Callithrix jacchus) and human pancreatic islets. General and comparative endocrinology 2011;174:71-9.

404. Ikeda Y, Enomoto H, Tajima S, Izawa-Ishizawa Y, Kihira Y, Ishizawa K, Tomita S, Tsuchiya K, Tamaki T. Dietary iron restriction inhibits progression of diabetic nephropathy in db/db mice. American Journal of Physiology - Renal Physiology 2013;304:F1028-F36.

405. Gyulkhandanyan AV, Lu H, Lee SC, Bhattacharjee A, Wijesekara N, Fox JEM, MacDonald PE, Chimienti F, Dai FF, Wheeler MB. Investigation of Transport Mechanisms and Regulation of Intracellular Zn2+ in Pancreatic α-Cells. Journal of Biological Chemistry 2008;283:10184-97.

406. Rutter GA. Regulating Glucagon Secretion: Somatostatin in the Spotlight. Diabetes 2009;58:299-301.

407. Hauge-Evans AC, King AJ, Carmignac D, Richardson CC, Robinson ICAF, Low MJ, Christie MR, Persaud SJ, Jones PM. Somatostatin Secreted by Islet δ-Cells Fulfills Multiple Roles as a Paracrine Regulator of Islet Function. Diabetes 2009;58:403-11.

408. Dufner-Beattie J, Kuo YM, Gitschier J, Andrews GK. The adaptive response to dietary zinc in mice involves the differential cellular localization and zinc regulation of

the zinc transporters ZIP4 and ZIP5. The Journal of biological chemistry 2004;279:49082-90.

409. Wang F, Kim BE, Petris MJ, Eide DJ. The mammalian Zip5 protein is a zinc transporter that localizes to the basolateral surface of polarized cells. The Journal of biological chemistry 2004;279:51433-41.

410. Wang X, Zhou B. Dietary zinc absorption: A play of Zips and ZnTs in the gut. IUBMB Life 2010;62:176-82.

411. Tominaga K, Kagata T, Johmura Y, Hishida T, Nishizuka M, Imagawa M. SLC39A14, a LZT protein, is induced in adipogenesis and transports zinc. The FEBS journal 2005;272:1590-9.

412. Smidt K, Pedersen SB, Brock B, Schmitz O, Fisker S, Bendix J, Wogensen L, Rungby J. Zinc-transporter genes in human visceral and subcutaneous adipocytes: Lean versus obese. Molecular and Cellular Endocrinology 2007;264:68-73.

413. Lee SM, McLaughlin JN, Frederick DR, Zhu L, Thambiayya K, Wasserloos KJ, Kaminski I, Pearce L, Peterson J, Li J, Latoche JD, Peck-Palmer O, Beer-Stolz D, Fattman CL, Alcorn JF, Oury TD, Angus DC, Pitt BR, Kaynar AM. Metallothionein-induced zinc partitioning exacerbates hyperoxic acute lung injury. American journal of physiology Lung cellular and molecular physiology 2012.

414. Li X, Zhang L, Meshinchi S, Dias-Leme C, Raffin D, Johnson JD, Treutelaar MK, Burant CF. Islet Microvasculature in Islet Hyperplasia and Failure in a Model of Type 2 Diabetes. Diabetes 2006;55:2965-73.

415. Girijashanker K, He L, Soleimani M, Reed JM, Li H, Liu Z, Wang B, Dalton TP, Nebert DW. Slc39a14 Gene Encodes ZIP14, A Metal/Bicarbonate Symporter: Similarities to the ZIP8 Transporter. Molecular Pharmacology 2008;73:1413-23.

416. Masters SL, Dunne A, Subramanian SL, Hull RL, Tannahill GM, Sharp FA, Becker C, Franchi L, Yoshihara E, Chen Z, Mullooly N, Mielke LA, Harris J, Coll RC, Mills KHG, Mok KH, Newsholme P, Nunez G, Yodoi J, Kahn SE, Lavelle EC, O'Neill LAJ. Activation of the NLRP3 inflammasome by islet amyloid polypeptide provides a mechanism for enhanced IL-1[beta] in type 2 diabetes. Nat Immunol 2010;11:897-904.

417. Leung JC, Chan LY, Lam MF, Tang SC, Chow CW, Lim AI, Lai KN. The role of leptin and its short-form receptor in inflammation in db/db mice infused with peritoneal dialysis fluid. Nephrology, dialysis, transplantation : official publication of the European Dialysis and Transplant Association - European Renal Association 2012;27:3119-29.

418. Scott DA, Fisher AM. The Insulin and the Zinc Content of Normal and Diabetic Pancreas. The Journal of clinical investigation 1938;17:725-8.

419. Kagawa Y, Dever GJ, Otto CT, Charupoonphol P, Supannatas S, Yanagisawa Y, Sakuma M, Hasegawa K. Single nucleotide polymorphism and lifestyle-related diseases in the Asia-Pacific region: comparative study in Okinawa, Palau and Thailand. Asia Pac J Public Health 2003;15 Suppl:S10-4.

420. Pearson E. Zinc transport and diabetes risk. Nat Genet 2014;46:323-4.

421. Flannick J, Thorleifsson G, Beer NL, Jacobs SBR, Grarup N, Burtt NP, Mahajan A, Fuchsberger C, Atzmon G, Benediktsson R, Blangero J, Bowden DW, Brandslund I, Brosnan J, Burslem F, Chambers J, Cho YS, Christensen C, Douglas DA, Duggirala R, Dymek Z, Farjoun Y, Fennell T, Fontanillas P, Forsén T, Gabriel S, Glaser B, Gudbjartsson DF, Hanis C, Hansen T, Hreidarsson AB, Hveem K, Ingelsson E, Isomaa B, Johansson S, Jørgensen T, Jørgensen ME, Kathiresan S, Kong A, Kooner J, Kravic J, Laakso M, Lee J-Y, Lind L, Lindgren CM, Linneberg A, Masson G, Meitinger T, Mohlke KL, Molven A, Morris AP, Potluri S, Rauramaa R, Ribel-Madsen

R, Richard A-M, Rolph T, Salomaa V, Segrè AV, Skärstrand H, Steinthorsdottir V, Stringham HM, Sulem P, Tai ES, Teo YY, Teslovich T, Thorsteinsdottir U, Trimmer JK, Tuomi T, Tuomilehto J, Vaziri-Sani F, Voight BF, Wilson JG, Boehnke M, McCarthy MI, Njølstad PR, Pedersen O, the Go TDc, the TDGc, Groop L, Cox DR, Stefansson K, Altshuler D. Loss-of-function mutations in SLC30A8 protect against type 2 diabetes. Nature genetics 2014;46:357-63.

422.   Danscher G, Juhl Sr, Stoltenberg M, Krunderup B, Schr⊘der HD, Andreasen A. Autometallographic Silver Enhancement of Zinc Sulfide Crystals Created in Cryostat Sections from Human Brain Biopsies: A New Technique that Makes it Feasible to Demonstrate Zinc Ions in Tissue Sections from Biopsies and Early Autopsy Material. Journal of Histochemistry & Cytochemistry 1997;45:1503-10.

423.   Wang F, Kim BE, Dufner-Beattie J, Petris MJ, Andrews G, Eide DJ. Acrodermatitis enteropathica mutations affect transport activity, localization and zinc-responsive trafficking of the mouse ZIP4 zinc transporter. Human molecular genetics 2004;13:563-71.

424.   Foster M, Petocz P, Caterson ID, Samman S. Effects of zinc and α-linolenic acid supplementation on glycemia and lipidemia in women with type 2 diabetes mellitus: a randomized, double-blind, placebo-controlled trial. Journal of Diabetes Research and Clinical Metabolism 2013;2.

Appendix 1: Reagents

Ultrasensitive Insulin Elisa Kit (Crystal chem, Downers Grove, IL USA)

Mouse Cytokine 3 plex (Cat no Y6000000X1) Biorad

Mouse Insulin Elisa Kit (10-1247-01) Mercodia

BCA Protein Assay Kit (Product no 233227) Thermoscientific

0.8ml LH Lithium Heparin sep (ref 450479) Mini spin

Tissue Tek 2 OCT compound for frozen tissue specimens Siemens

Mould Cryogenic plastic Disposable
15x15x5mm (Intermediate cryomold) Siemens

Borex tubes

Nitric acid Suprapur 1L (Z233441) Merck

Primary antibodies:

Monoclonal Anti-Mouse Glucagon IgG1 (K79Bb10) Abcam
Cat no. ab10988

PolyclonalRabbit Anti-ZnT7IgG Sigma-Aldrich

Polyclonal Rabbit Anti-Rat ZnT8 1gG (Cat no. RZ8) Mellitech
(France)

Polyclonal Rabbit Anti-ZIP4 IgG
	Thermoscientific

Rabbit Anti-ZIP5 IgG   Thermoscientific

Rabbit Anti-ZIP14 IgG   ThermoScientific

Polyclonal Rabbit Anti-human Somatostatin (Cat A0566)   Dako   Carpinteria,
CA

Polyclonal Guinea Pig Anti-Swine Insulin 1/100 (Cat A0564)   Dako   Carpinteria,
CA

Polyclonal Rabbit Anti-Glucagon (Cat A0565)   Dako   Carpinteria,
CA

CD68 1/1500 (Cat M0814 Clone KP1)   Dako   Carpinteria,
CA

Secondary Antibodies:

Anti-rabbit Alexa flour 488 IgG (FITC)   Invitrogen

Anti-MouseAlexa flour 584 IgG1 gamma 1   Invitrogen

Dako Fluroscent Mounting Medium (Cat no. E7023-500ML)   Dako

RNA and Polymerase chain reaction reagents:

Omniscript RT Kit 50 Reactions   Qiagen

Oligo DT primers (Cat no 79105)   Qiagen

RNase Zap wipes   Ambion

Experion STDS Reagents and supplies for 25 chips (Cat no 7007104)Biorad

Ethanol, absolute 200 proof for molecular biology   Sigma-Aldrich

Chloroform (Prod 10077)   AnalaR

Trizol (Cat: 15596018)   Invirogen

RNeasy mini kit (Cat no 74106)   Qiagen

RNA aqueous micro kit (Cat no 1931)   Ambion

RNase free DNase kit (Cat: 79254)   Qiagen

Taqman Universal master mix   (Cat; 4304437)   Applied
Biosystems

Applied Biosystems inventoried Taqman gene expression assays

Zn transporters	Accession codes:
ZIP1	Mm01605921_g1
ZIP2	Mm01314597_g1
ZIP3	Mm00460290_m1
ZIP4	Mm00511151m1
ZIP5	Mm00511105_m1
ZIP6	Mm00507295_m1
ZIP7	Mm00433930_m1
ZIP8	Mm00470855_m1
ZIP9	Mm00470907_m1
ZIP10	Mm00554174_m1
ZIP11	Mm04206888_m1
ZIP12	Mm01325273_m1
ZIP13	Mm01329757_m1
ZIP14	Mm01317439_m1
ZnT1	Mm00437377_m1
ZnT2	Mm01185317_m1
ZnT3	Mm00442148_m1
Znt4	Mm00442155_m1
ZnT5	Mm00458158_m1
ZnT6	Mm00460610_m1
ZnT7	Mm00458239_m1
ZnT8	Mm00496660_m1
ZnT9	Mm01315481_m1
ZnT10	Mm01315481_m1
MT1	Mm00496660_g1
MT2	Mm04207591_g1
TPRM3	Mm01210379_m1
PDLIM7	Mm00482816_m1
INS1	Mm01259683_g1
GLUCAGON	Mm01269055_m1

Working diluent for atomic flame absorption:

600ml of high purity water

50ml of Butan-1-ol (Univar)

1.5ml of Brij-35 (30%)

8.9ml of concentrated hydrochloric acid

Preparation of 10mM TRIS buffer pH 8.2 for homogenisation of organs:

1. The molecular weight of TRIS buffer (sigma Chemicals, St. Louis, MO) IS 121 MV and we want to prepare a 10mM solution of TRIS buffer, 1.21g TRIS is diluted in 1L deionised water (~17oC).

2. The TRIS and water were mixed thoroughly

3. A pH meter was placed to get the solution to pH7 reading(+/- 0.2)

4. If required, a small volume of acid was added to decrease the pH or alkaline to increase the pH until the meter reds 8.2

5. When the correct pH is reached, the pH meter is rinsed using deionised water and is left in the standard solution.

Preparation of 30mM TRIS buffer pH 7.4:

1. The molecular weight of TRIS BUFFER (Sigma Chemicals, St Louis, MO) is 121 MV, and we want to prepare a 30Mm solution of TRIS BUFFER, 3.63G TRIS is diluted in 1L deionised water (~17oC).

2. The TRIS and water was mixed thoroughly

3. A pH meter was placed in the solution, acid or alkaline was added to increase or decrease the pH until the meter reached the pH of 7.4.

4. When the correct pH is reached, the pH meter is rinsed using deionised water and is left in the standard solution.

Preparation of 2x Acrylamide SDS gels

10ml separation gel:

H_2O	4ml
30% Acrylamide mix	3.3ml
1.5 M Tris (pH 8.8)	2.5ml
10% SDS	100µl
10% APS	100µl
TEMED	4µl

A layer of water was added on top of the gels to prevent them from drying out as the gels set.

Stack gel-6ml

The water layer was discarded

H_2O	3.6mL
30% Acrylamide mix	1.0mL
0.5M Tris (pH 6.8)	1.5mL
10% SDS	60µl
10% APS	60µl
TEMED	6µl

10x Transfer Buffer

288g of Glycine
60g of Tris base
2L Milli Q water

These reagents were placed in a beaker with an magnetic stirrer until all was dissolved

1x Transfer Buffer

100ml o 10x buffer

700ml of COLD Mille Q water

200ml of Methanol

5x Running Buffer

287.5g Glucose

60g Tris base

10g SDS

2L Mille Q H20

These reagents were placed in a beaker with a magnetic stirrer until everything was dissolved

The 5x running buffer was diluted 1:5 in Mille Q water before use

PBS-T

1ml of tween in 1 litre of 1x PBS

Western Blot

The western blot was run with 1x running buffer. The gel was run at 150V for 1hour for 25 mins at room temperature.

Transfer: 800ml transfer buffer and 200ml of methanol was mixed and poured into a tube for transfer of the membranes.

The transfer of the membranes were done manually:

Black = Gel =Negative (sponge-filter paper-membrane-filter paper-sponge)

The membrane was transferred at 100V for 1 hour and 15 mins with an ice block in the tank.

The membranes were then rinsed with 5ml PBS-T.

ZIP4, ZIP5 and ZIP14 weer diluted 1:1000 in Odyssey buffer and was incubated overnight at 4°C. The membranes were washed 3 times for 15 mins with PBS Tween.

The secondary antibody was incubated at room temperature in the dark with α-rabbit (Cat: IRI Dye 800CW-green) diluted 1:10000 in odyssey buffer and mouse α-human tubulin was diluted in PBS-t 1:10000 (sapphire Bioscience-Abcam Cat 120-72910) for

1 hour . The membranes were then washed 3 times with PBS-T for 15 mins and viewed using Odyssey (Lincor) machine to captured the bands of interest.

Appendix 2: Equipment used

My cycler thermal heating block	Biorad
Bioplex 200 system	Biorad
Biorad Bioplex Pro 11 wash system	Biorad
Epifluoresence microscope with AxioVision software version Axiovs40v4.82.0.	
Nikon Eclipse 90i microscope	(Nikon, Tokyo, Japan).
Flame atomic absorption spectrometer	Perkin–Elmer
3030 Atomic Absorption spectrometer,	Überlingen, Germany
Automatic gamma counter	Perkin Elmer Germany
9700ht Qpcr	Applied Biosystems USA
Diluter for flame atomic absorption spectrometry	
Experion Automated Electrophoresis Station	Biorad
Microscope	
Cryotome	Leica
Microplate reader	Biorad

Appendix 3: Papers

Paper 1

Role of Zn and Zn Transporters in the Pathogenesis of Type 2 Diabetes

Mariea D. Bosco,[1,2] Daisy Mohanasundaram[3], Claire F. Jessup[1,6], Darling Rojas-Canales[1], Chris Drogemuller[1], Tom Loudovaris[7], Tom W.H. Kay[7,8], Susan E. Lester[4], Shane T. Grey[5], Peter D. Zalewski[1+] and Patrick. T. Coates[1+]**

[1]Renal Transplantation and Immunobiology Laboratory, The Royal Adelaide Hospital, Adelaide, South Australia, Australia.

[2]Discipline of Medicine 5B, University of Adelaide, The Queen Elizabeth Hospital, Woodville South, South Australia, Australia 5011

[3]Department of Immunology, Flinders Medical Centre and Flinders University, Bedford Park, South Australia, Australia

[4]Rheumatology Unit, The Queen Elizabeth Hospital, Woodville South, South Australia, Australia 5011

[5]Garvan Institute of Medical Research, 384 Victoria Street, Darlinghurst, NSW 2010, Australia

[6]Department of Anatomy & Histology and Centre for Neuroscience, Flinders University of SA, Bedford Park

[7] Immunology and Diabetes Unit, St. Vincent's Institute of Medical Research, 9 Princes St, Fitzroy, Victoria 3065, Australia

[8] University of Melbourne, Department of Medicine, St Vincent's Hospital, Fitzroy, Victoria 3065, Australia

[+]PDZ and PTC are equal co-senior authors on this paper

** Author for correspondence

Professor P. Toby H. Coates Renal Transplantation and Immunobiology Laboratory, Central Northern Adelaide Renal & Transplantation Service, Royal Adelaide Hospital, North Terrace, ADELAIDE 5000. Tel: +61 8 8222 0900 Fax: +61 8 8222 0970 Email: toby.coates@health.sa.gov.au

Running Title: Zn and Zn Transporters in type 2 diabetes

Word count current (192 currently)

Abstract

Zn is essential for insulin production and abnormalities in Zn homeostasis contribute to the development of diabetes. Zn homeostasis is regulated by the concerted action of two families of importer (ZIP) and exporter (ZnT) membrane Zn transporter proteins. Animal and human studies have shown a critical role for secretory granule ZnT8 in insulin production and genome-wide association studies suggest that ZnT8 is a disease susceptibility gene for Type-2 diabetes (T2D). However, little is known about the expression of ZnT8 and other Zn transporter proteins in normal islets and T2D. Here we show that, in T2D human and db/db mouse pancreatic islets, 1) ZnT8 protein is significantly decreased in the beta cells but retained on the alpha cells, 2) ZIP4 is expressed on somatostatin-producing delta cells in normal islets but also on alpha cells in T2D and 3) ZIP14 is up-regulated on islet macrophages in some diabetics. Retention of ZnT8 on alpha cells may contribute to alpha cell hyperplasia and sustained glucagon production in diabetes. Changes in islet Zn and Zn transporters were amongst the earliest events in the db/db mice and may constitute a new risk factor for disease progression in pre-diabetes.

Introduction

Zinc (Zn) is an essential trace element which plays critical roles in hormone metabolism and immune function. Pancreatic islet cells have amongst the highest content of Zn in the human body. Zn promotes the formation of Zn pro-insulin hexamers in the Golgi and, subsequently, Zn insulin crystals in the secretory granules which are stored until release. Abnormalities in Zn biology have been shown to play roles in diabetes (reviewed in [1, 2]). Zinc deficiency, including a reduction in pancreatic Zn, has long been documented in patients with T2D [3]. A recent systematic review and meta analysis of 22 published studies in T2D concluded that Zn supplements improved glycaemic control and lipid parameters [4]. Zn supplements also lowered blood glucose levels in the db/db mouse model of T2D [5].

Intracellular Zn levels are maintained by two large families of membrane Zn transporter proteins: the ZnT protein family, encoded by the genes solute carrier family (SLC)30A1-10, that are involved in the efflux of Zn from the cytosol to the extracellular space or sequestration into intracellular organelles and the ZIP protein family, encoded by genes SLC39A1-14, that are involved in the influx of Zn or release from organelles thereby increasing cytosolic Zn concentrations. The Zn transporter SLC30A8 (ZnT8) is expressed specifically in endocrine cells including insulin-secreting beta cells and glucagon-secreting alpha cells [6]. Down-regulation of ZnT8 in vitro in cultured beta cell lines or primary beta cells resulted in reduced intracellular zinc, insulin production and insulin secretion in response to high glucose challenge [7, 8]. ZnT8 is also down regulated in pancreatic islets of a type 2 diabetic rodent db/db mice model [9]. Single nucleotide polymorphism of the ZnT8 gene in humans is linked

to increased fasting glucose levels and type 2 diabetes [10, 11]. The risk variant of ZnT8 had impaired Zn transport activity [12]. A recent report in Nature Genetics, showing that loss-of-function mutations in *SLC30A8* in humans protects against T2D, has muddied the water, although the interpretation of this finding has recently been challenged [13]. There are also extra-pancreatic effects of ZnT8. Mice with β cell–specific knock-down of ZnT8 had enhanced hepatic degradation and clearance of the insulin in liver, thereby providing an alternative explanation for low peripheral blood insulin levels despite insulin hypersecretion from pancreatic β cells [14]. Interestingly, Zn secreted with insulin suppressed hepatic insulin clearance by inhibiting clathrin-dependent insulin endocytosis [14]. Despite these studies there is relatively little detailed immunobiology of Zn transporters in pancreatic islets and little known about changes in expression of ZnT8 and other Zn transporter proteins at different stages in the development of T2D.

To investigate the relevance of Zn transporter proteins in normal pancreatic islets and in diabetes we initially studied their expression by real time PCR in healthy organ pancreatic donors and by micro array analysis. We then extended this analysis to pancreata from donors with or without T2D. Finally we used the well characterized db/db murine model of T2D to address the issue of changes in Zn transporters in both early and late T2D. The db/db mouse lacks a functional leptin receptor and develops both obesity and diabetes [15]. As discussed by Belke and Severson (2012) [16], the natural progression of the diabetes, with insulin resistance followed by an impairment of insulin secretion, is very similar to the pathogenesis of T2D in humans. Initial early hyperphagia and insulin resistance are quickly followed by compensatory responses of

hyperinsulinemia, beta-cell hyperplasia and islet hypertrophy, before hyperglycemia occurs at the age of 4 to 8 weeks.

For the immunofluorescence studies we focused on two ZnT Zn transporters ZnT7 and ZnT8 since both have been shown to be involved in the incorporation of Zn into proinsulin and insulin. It is likely that one or more members of the ZIP family are involved in bringing Zn into islet cells but these have yet to be identified. We therefore focused on two ZIP Zn transporters ZIP4 and ZIP14. ZIP4 was chosen because it is one of the major influx Zn transporters and is overexpressed in many pancreatic cancers while ZIP14 was chosen because it is an inflammation-associated Zn transporter and chronic inflammation is part of the pathogenesis of type 2 diabetes.

Our studies indicate that there is a wide variation in Zn transporters in human, that significant changes occur in diabetes, including Zn transporters on other islet cells and, using the small animal model and that changes in Zn transporters occur before the development of T2D highlighting the important role of these proteins in pancreatic function in health and disease susceptibility.

Research Design and Methods

Human pancreata

Access to pancreatic tissue was provided through the pancreatic islet transplant program Australian Islet Consortium (RAH 100205b and St Vincent's Hospital Melbourne (SVH HREC-D 103/05). Consent for donated human pancreata for research in all cases was obtained through Donate Life Australia. Human pancreatic islets were purified from donor pancreas using a modified Ricordi method as previously described [17].

Total RNA was purified from isolated human islets, purified acinar tissue and OCT-embedded frozen whole pancreas pieces using TRIzol reagent (Invitrogen, Carlsbad, CA, USA). mRNA was separated and purified by RNAeasy mini column (Qiagen, Hilden, Germany). The quality and quantity of RNA was determined using standard sensitivity RNA chips analysed by Experion (Bio-Rad, CA). High quality RNA samples were reverse transcribed to cDNA using Omni script RT kit (Qiagen, Hilden, Germany).

Animals

All experimental procedures were approved by the SA Pathology Animal Ethics (141a.10) and the University of Adelaide Animal Ethics Committees (M-2010-166A) and conformed with National Health and Medical Research Council Guidelines for Use and Care of Laboratory Animals. Male db/db mice aged 4, 10 and 14-18 weeks and aged-matched wildtype (WT) mice (C57BL/6J) were purchased from the Animal Resource Centre (Perth) and University of Adelaide. Mice were maintained in an animal house at 22°C and subjected to a 12h light/dark cycle. All animals had free access to water and rodent chow.

Human Real Time PCR

Real time quantitative PCR was carried out using an ABI7300 PCR machine and Taqman™ primer and probes (Applied Biosystems) designed to gene specific human sequences (Supplementary Methods 1). A pre-amplification step of the samples was performed using Taqman pre-AMP Master mix kit protocol (Supplementary Methods 1). Relative gene expression was calculated using the $2^{\Delta\Delta CT}$ method

Immunofluorescence staining for ZnT8, ZIP4 and ZIP14:

Cryosections, 5µm, were fixed in ice-cold acetone for 10 min. The sections were blocked in a humidified chamber for 60 min with serum from the secondary antibody host animal. Sections were incubated overnight at 4°C with rabbit polyclonal antibodies to ZnT8 (1:100; Mellitech, France), ZIP4 (1:100; Thermoscientific, Rockford, IL, USA), or ZIP14 (1:150; Thermo- scientific, Rockford, IL, USA) and mouse monoclonal anti-glucagon (Sigma Aldrich, North Ryde, New South Wales, Australia). Slides were washed (1x PBS) and incubated for 60 min with goat anti-rabbit Alexa488 conjugate and rabbit anti-mouse Alexa594 conjugate (1:400; Life technologies, Mulgrave, Victoria, Australia). Sections were washed, nuclei were counter stained with DAPI (4', 6-diamidino-2-phenylindole) and mounted with fluorescent mounting medium (Dako Australia Pty. Ltd, Nth Sydney, NSW, Australia).

The images were captured on a Zeiss Apoptome microscope (Carl Zeiss GmbH, Goettingen, Germany) and analysed by FIGI image J software. Mean gray value was used for ZnT7 and ZnT8 as they were homogeneous in expression. Integrated density was used instead of mean gray value for ZIP4 and ZIP14 because the staining was not homogenous across the islet.

Immunoperoxidase staining:

Tissue sections (4 µm) were cut, mounted on Superfrost Plus coated slides, labelled and then placed on a fully automated immunohistochemistry (IHC) staining Ventana Benchmark XT (Roche Diagnostics) instrument. Antibodies used were polyclonal rabbit anti-glucagon (1/800), polyclonal guinea pig anti-swine insulin (1/100),

monoclonal anti-CD68 (1/1500, M0814 Clone KP1) and polyclonal rabbit anti-human somatostatin (1/1600) all from Dako Carpinteria, CA, anti-ZIP4 (1/400) and anti-ZIP 14 (1/1600) from Thermo Scientific Rockford, USA) followed by counterstaining with haematoxylin 11(Roche Diagnostics). Images were captured using a Nikon Eclipse 90i microscope (Nikon, Tokyo, Japan).

ZINPYR-1 staining for Zn in pancreatic islets

Cryosections of mouse pancreas from both db/db and control mice at 4,10 and 18 weeks of age were incubated with 1μM of ZINPYR-1 (Cat no ZP1, Mellitech, France) for 15 min at 37°C. Sections were washed with phosphate buffered saline (pH 7.4, 1x PBS), mounted and images captured as for immunofluorescence (above).

Measurement of pancreatic and liver Zn and metallothionein (MT)

Whole pancreas and liver were removed from db/db and WT mice and total Zn and MT content were measured using atomic absorption spectrometry and the cadmium haemoglobin binding assay, respectively [18].

Statistical Analysis

Analysis was performed by an ANOVA approach, using likelihood ratio tests, as the datasets were not completely balanced. A two-factor interaction model (Group*Time) was estimated for each response. All data was log-transformed prior to analysis because of non-constant variance. The fitted "means" were estimated by back-transforming the fitted log-means, and therefore represent medians. Gaussian generalised linear models (GLMs) were used for datasets where there was a single observation for each mouse,

and gaussian generalised linear mixed models (GLMMs) were used for datasets where there were repeated observations on each individual (i.e. random effect = animal). Statistical analysis was performed using R software V 3.0.1[19].GLM models were estimated using base functions in R. GLMM (random effect models) were estimated using the lme4 library V1.0-5 [20].Type II Likelihood ratio ANOVA tables were generated by the Anova function in the car library V2.0-19 [21]. Planned comparisons, corrected for multiple comparisons, were performed between db/db and wildtype mice at each time point using the multcomp library V1.3-1[22].

Results

1. Human studies

Human Zn transporter gene expression studies

To investigate the tissue expression of Zn transporters in normal pancreas and disease, real time PCR was performed on 10 isolated human islet preparations, 3 acinar preparations and 4 whole pancreas preparations. Using the PCR approach a range of Zn transporters were found to be expressed in the normal human pancreas, in comparison to acinar tissue. The most highly expressed Zn transporters in the islet were ZnT8, ZIP7, ZIP14 and ZIP1, with ZnT8 and ZIP14 showing marked preferential expression in the islet compared to whole pancreatic tissue or isolated acinar tissues. A separate cohort of human pancreatic islets (n=8) were also assayed for Zn transporter expression using Affymetrix gene array. There was good concordance between the identified Zn transporters using both techniques in two separate cohorts indicating the robustness of the findings. Within the human islet preparations assayed, ZIP 14 displayed the highest

expression, followed by ZIP6 and ZnT8. Although their expression was not as high as insulin, glucagon and somatostatin, a range of Zn transporters were expressed at higher levels in isolated human islet preparations compared to the GLP-1 receptor and the GLUT1 and GLUT2 transporters. Using the array these transporters were expressed at consistent levels across the isolated islet preparations.

To assess whether Zn transporters changed in disease, 6 donor pancreata from patients with T2D were also studied with real time PCR for Zn transporter genes. The mean duration of diabetes for individuals with T2D was 6 years. Out of 24 zinc transporters genes three of the influx transporters Zip2, Zip4 and Zip 12 and two of the efflux transporters ZnT3 and ZnT10 were not detected at the transcriptional level in either control or diabetic pancreata. Out of all the influx transporters Zip 5 was the most abundantly expressed followed by Zip8, Zip7 and Zip6. For ZnTs the most abundantly expressed gene was ZnT9 followed by ZnT2, ZnT8, and ZnT7. There was reduced gene expression of ZnT8 in T2D diabetic pancreata.

Gene expression studies on whole pancreas do not indicate whether the changes seen also manifest at the protein level and which islet cell types are involved. We therefore performed immunofluorescence for ZnT8, ZIP4 and ZIP14 proteins in pancreatic sections from normal human and T2D donors. Details about the two groups are presented in Table 1. Of note is the age of control donor pancreas and BMI which are both younger and less obese than T2D. Image J software allowed semi-quantitative expression of protein levels.

Human Zn transporter immunofluorescence studies

294

Fig 1A shows typical immunofluorescence images (green) for ZnT8, ZIP4 and ZIP14 in islets from normal humans (Left) and type 2 diabetics (Right). Islets were co-labelled for glucagon (red) to identify the islets and to show alpha cells. Fig 1B shows quantitative data by ImageJ analysis for individual subjects, normal versus T2D.

ZnT8

There was intense and largely homogeneous staining for ZnT8 in normal human islets including both the beta and alpha cell compartments, the latter shown by co-localization with glucagon. In T2D patients, there was loss of ZnT8 in the beta cell compartment while the expanded alpha cell population retained strong ZnT8 expression. The levels of ZnT8 fluorescence varied for different normal pancreata (mean fluorescence intensity $\pm$ SD was 90.5 ± 20.9, n =7 subjects). By contrast, all T2D subjects had low expression of ZnT8 in their islets (60.0 ± 7.4, n =5 subjects) and the overall mean for the group was significantly lower ($p<0.05$) than that for the normal (Fig 1B).

ZIP4

There was occasional staining of cells for ZIP4 in normal human islets, the majority of which did not appear to be beta or alpha cells (Fig 1A). However, there was striking co-localization of ZIP4 and glucagon staining in some of the T2D subjects, with many alpha cells now expressing ZIP4. The levels of ZIP4 fluorescence varied for different normal pancreata and there was no significant difference between the overall means for normals (18.2 ± 4.1, n = 7) and T2D subjects (26.8 ± 7.0, n = 5), Fig 1B.

<u>ZIP14</u>

There was occasional staining of cells for ZIP14 in normal and T2D human islets (Fig 1A). As for ZIP4, these did not appear to be beta or alpha cells. They were larger than the ZIP4+ve cells and had a macrophage-like appearance. Fig 1B shows variable levels of ZIP14 fluorescence between subjects (normal and T2D). In particular, one of the seven normal subjects and three of the eight diabetic subjects tested had strong islet ZIP14 staining. There was no significant difference between the overall means for normals (44.3 ± 35.5, n = 7) and T2D subjects (62.4 ± 42.7, n = 8).

Thus, we report for the first time in human T2D, significant down-regulation in ZnT8 and no change in two influx Zn transporters ZIP4 and ZIP14.

2. Murine db/db studies

To further investigate changes in Zn transporter proteins, the db/db mouse model of T2D was used, with an emphasis on changes in Zn parameters in diabetes both early (4 wk) and late (10 wk and beyond).

The time-dependent progression of various diabetic parameters in the db/db versus wild-type (WT) mice is shown in Supplementary Fig 1. In brief, peak hyper-insulinemia (9.5 fold increase, $p<0.005$) and islet hyperplasia (4.9 fold, $p<0.005$) occurred at 4 wk while peak obesity (1.8 fold, $p<0.005$) and hyperglycaemia (5.0 fold, $p<0.005$) occurred at 10wk and beyond. Immunoperoxidase staining in the WT mice showed dense and closely packed insulin staining throughout the interior of the islet where beta cells are present (Supplementary Figure S2). In the db/db mice the insulin

296

staining was patchy, more loosely packed and showed evidence of beta cell degranulation. Glucagon in the WT mice was largely present in the periphery (or mantle) of the islet where the alpha cells predominate. In the db/db mice, however, the glucagon staining was more disorganized existing in the periphery and the inner core of the islets, even in early diabetes. Somatostatin in the WT mice was present in the periphery (or mantle) of the islet where the delta cells predominate. In the db/db mice however, the somatostatin staining was more disorganized and increased in expression in the inner core of the islets, even in early diabetes.

Islet and systemic Zn levels in db/db mice:

There were no systemic changes in Zn levels at any age in the db/db mice, as assessed by no significant decrease in plasma Zn, liver Zn and liver and pancreas metallothionein (Table 2). However, there were significant decreases in pancreas Zn as early as 4wk (0.44 fold of control, p<0.005). To determine whether the early loss of pancreatic Zn was in the endocrine or exocrine compartments, the Zn fluorophore ZinPyr-1 was used to investigate the levels and distribution of labile Zn in cryosections of the pancreata.

In WT mice, ZinPyr-1 stained both acinar tissue and islets. However, islets stained much more intensely than acini. There was a heterogenous, granular-like labile Zn distribution in the WT islets at 4 wk (Fig 2A, panel a). Interestingly, islet Zn fluorescence in WT mice was much less at 18 wk than at 4 wk (Fig 2A panel c). This was confirmed by Image J analysis of between 14 and 55 islets from 4 mice at each time point (Fig 2B) and matched the significant decrease in whole pancreatic Zn content between 4 and 18 wk in the WT mice (Table 2). This suggests some decrease in pancreas and islet Zn content as C57Bl mice age.

As early as 4 wk, in db/db mice, there was a uniform loss of islet ZinPyr-1 fluorescence (Fig 2A, panel b) which was significant (0.66 fold of that in WT p<0.05). Therefore, the early loss of Zn in the db/db mice pancreas was in the islets rather than in the acinar tissue. (Fig 2B). This low level of islet Zn in db/db mice at 4 wk largely persisted at 18 wk (Fig 2B) although now occasional islet cells fluoresced intensely (arrow in Fig 2A, panel d). These may represent a subset of Zn-rich cells that are expanded during the course of the diabetes.

Immunofluorescence of Zn transporter proteins in wildtype and db/db mice

ZnT8

ZnT8 was expressed homogenously throughout the normal mouse islet especially in both the insulin producing beta cells and the glucagon producing alpha cells at 4 and 18 wk (Fig 3A panels a,c, respectively). ZnT8 staining was significantly decreased in the db/db mice (Fig 3A panels b,d). Decrease at 4 wk was 0.52 fold of control (p<0.05), 10 wk (0.2 fold, p<0.005) and 18 wk (0.29 fold, p<0.005, Fig 3B).

In typical db/db islets, most of the ZnT8 was colocalised with glucagon (see Fig 3A panel d) indicating that, during diabetes, ZnT8 is preferentially lost in the beta cells but is retained in the alpha cells.

ZIP4

ZIP4 was weakly expressed in the acinar tissue but strongly expressed in clusters of cells in the periphery of the WT islet at 4 and 18 wk (Fig 3A panels e,g, respectively). There was no co-localization of ZIP4 with glucagon staining. ZIP4 expression in the

early diabetic and chronic diabetic db/db mice was in both the peripheral mantle cells as well as the interior part of the pancreatic islet (Fig 3A panels f,h). At 4, 10 and 18wk, in db/db mice islets, ZIP4 protein staining was 1.4, 1.5 and 0.8-fold of age-matched controls, respectively (p value not significant, 14 to 36 islets from 4 mice per group were tested, Fig 3B).

ZIP14

ZIP14 was expressed on occasional cells throughout the WT islets at 4 and 18 wk (Fig 3A panels i,k, respectively). There was significant increase in ZIP14 staining at all-time points in the db/db mice (Fig 3A panels j,l). There was also a small but significant increase in WT mice due to age alone from 4 to 10 weeks (Figure 3B). At 4, 10 and 18wk, in db/db mice islets, ZIP14 protein staining was 6.1, 3.9 and 3.1-fold of age-matched controls, respectively (p < 0.005, 19-55 islets from 4 mice per group were tested, Fig 3B). Not only was there a significant increase in cells expressing ZIP14 in the db/db mice but the average staining intensity per cells was also increased (data not shown) suggesting an up-regulation of ZIP14 on the ZIP14+ve cells in diabetes.

Zip4 and somatostatin staining

ZIP4 staining was quite distinct from insulin staining (beta cells) and glucagon staining (alpha cells) in both control mouse and db/db mouse pancreatic sections. However, the staining patterns for ZIP4 and somatostatin (delta cells) in various tissue sections were very similar. Immunoperoxidase staining for ZIP4 and somatostatin in serial sections confirmed colocalization in db/db islets (arrows in Fig 4a,b for db/db mice at 4 weeks of age) as well as WT islets (not shown).

Zip14 and macrophage staining

ZIP14+ve islet cells had a macrophage-like morphology. This was confirmed by staining of ZIP14 and the macrophage marker CD68 in serial sections of the same diabetic islet (arrows in Fig4 c,d). There was less macrophage staining and ZIP14 in the islets of wildtype mice (data not shown) consistent with the immunofluorescence studies. A positive correlation was found between ZIP14 protein expression and islet size regardless of diabetic status (r^2=0.56).

Discussion

In this study we obtained access to normal human islets, normal human pancreas and T2D pancreata which are otherwise difficult to obtain and were able to study the expression of Zn transporters in these tissues. This study reports the islet cell distribution of ZnT8, ZIP4, and Zip 14 in the human and mouse pancreatic islets, and changes in human and mouse T2D. Using the db/db mouse model of T2D also showed that loss of Zn and changes in Zn transporters occur very early in onset of diabetes and was not accompanied by systemic changes in Zn. The other major findings were that, in both mouse and human T2D, ZnT8 was downregulated on islet beta cells but preserved on alpha cells and ZIP4 and ZIP14 were selectively expressed in the islets on somatostatin producing delta cells and macrophages, respectively.

An important issue is whether the loss of Zn in the diabetics islets is a consequence of a systemic Zn deficiency (e.g. due to inadequate dietary Zn intake, malabsorption of Zn or excessive Zn excretion in the urine) or, alternatively, a consequence of dysregulation of Zn homeostasis within the pancreas. Therefore, it was important to determine

whether changes in systemic levels of Zn occur in db/db mice, especially during early diabetes when Zn loss in the pancreas and islets is already apparent. There was no evidence of systemic Zn changes (liver Zn, plasma Zn and liver metallothionein) suggesting Zn abnormalities in diabetes are mainly restricted to the pancreas.

As Zn transporters control local tissue levels of Zn their expression in the pancreas was then studied. One of the unexpected findings in the normal human pancreas was the widely differing levels of expression of ZnT8 between different subjects as shown for mRNA by RT-PCR and micro-array and protein. Whether this is a consequence of ZnT8 polymorphisms or some other factor related to obesity or glycaemic control requires further investigation. The reduction in Znt8 mRNA and protein expression in human T2D subjects was both consistent and significant.

Whether the changes in Zn occur early or late in the pathogenesis of diabetes cannot be determined using human disease samples and thus a well-defined animal model was employed to address this issue. Using the db/db mouse model, which has numerous features of human T2D, we have now established that the major decrease in pancreatic islet Zn and ZnT8 occurs very early during diabetes (by 4 weeks). The main Zn-dependent step in insulin synthesis and storage occurs in the secretory granules and involves insulin crystallization. ZnT8 had been shown to be important for maintaining Zn levels in beta cell granules and for correct insulin storage and release. Down-regulation of ZnT8 might therefore be an early triggering factor in development of type 2 diabetes.

Two further observations on type 2 diabetes are relevant to our findings. Glucagon, which has opposing actions to insulin in glycaemic control, is not lost in type 2 diabetes and alpha cells often replace beta cells during the progression of the disease [23-27]. Like beta cells, alpha cells are rich in Zn within their granules [28] and may therefore be involved in glucagon storage and synthesis. This study is the first report of alpha cells containing ZnT8 in both diabetic humans and mice. The bright ZinPyr-1 fluorescent cells in Fig3A (panel d) appear to correspond in frequency and islet distribution to the preserved and expanding alpha cell population in the chronic diabetics (Fig4A, panel d) and presumably represent alpha cella which have retained both ZnT8 and Zn. Loss of ZnT8 in the beta cell rich zone but retention of ZnT8 on alpha cells in diabetes might provide an explanation for the impairment of insulin production and retention of glucagon production in T2D. It also suggests that whatever leads to loss of ZnT8 (and Zn) in the beta cells does not affect the alpha cells. Rather these cells progressively replace beta cells during the development of type 2 diabetes.

There is very little known about ZIP transporters in pancreatic islets and diabetes. These are likely to be relevant because they regulate the influx of Zn into the cytosol of the cell and control cytoplasmic enzymes. Our studies show, for the first time, a strong up-regulation of ZIP14 in early and chronic diabetic islets. This is also consistent with recent reports in the literature that ZIP14 is expressed in macrophages in other tissues and is upregulated by inflammatory stimuli [29-31]. ZIP14 may therefore be a novel macrophage marker in type 2 diabetes. The relationship of ZIP14 to islet macrophage activation state needs to be clarified. Lipopolysaccaride has been shown to upregulate ZIP14 in macrophages and ZIP14 knockout attenuated downstream cytokine signaling. This has implications for inflammation in type 2 diabetes[32]. In the db/db mice

302

pancreatic islet it is known that the pro-inflammatory M1 subtype increases and there is no change in the trophic M2 subtype expression [33]. In view of this it is likely that ZIP14 is expressed on the proinflammatory macrophages and may be involved in processes such as beta cell apoptosis and beta cell de-differentiation. The strong positive correlation between islet area and ZIP14 protein expression raises the possibility that ZIP14 up-regulation is a factor in the early islet hyperplasia in T2D. Since ZIP14 knockout in C57BL/6 mice leads to upregulation of ZnT8 protein in the islets as well as increase in body weight, phosphorylation of insulin receptor and increased GLUT2 expression [34], it is feasible that up-regulation of ZIP14 leads to down-regulation of ZnT8. How this might occur is not clear but our findings are consistent with effects at the level of ZIP14 macrophages interacting with ZnT8 containing beta cells.

The finding that normal pancreatic islet delta cells almost exclusively express ZIP4, a major Zn transporter responsible for Zn absorption in the intestine [35], is consistent with   the existence of a gut islet somatotrophin axis. ZIP4 expressed in delta cells of the islets could be important for gut islet interaction and homeostasis. While we found no significant change in the ZIP4 expression in the diabetic islets, disorganisation of delta cells containing ZIP4 could have functional implications in type 2 diabetes involved in gut related roles. Since ZIP4 is overexpressed in many pancreatic cancers [36], the role of ZIP4 in islet cell function and islet hyperplasia needs to be investigated.

Our findings now point to an important role for changes in islet Zn metabolism in the onset of Type 2 diabetes. We hypothesize that down-regulation of beta cell ZnT8 at the

gene level results in an early loss of Zn from the pancreatic islet and contributes to the development of type 2 diabetes by causing a block in insulin maturation and decline in beta cell function. We also propose that the retention of ZnT8 in alpha cells of diabetics preserves glucagon production. Up-regulation of ZIP14 on islet macrophages in diabetes may contribute to islet inflammation. In addition, ZIP4 may be a major influx transporter for Zn in delta cells.

Authors Contributions:

Mariea Dencey Bosco mouse data, protein staining of Zn transporters, Zn (ZINPYR-1), Design of experiments, interpretation of results, writing of manuscript.

Daisy Mohanasundram: human ZnT islet PCR analysis, manuscript review

Chris Drogemuller: human pancreatic islet ZnT PCR analysis, design of experiments, interpretation of results and manuscript review and discussion

Shane Grey: human islet micro-array, manuscript review and intellectual input

Susan lester: Statistical analysis and intellectual input

Peter Zalewski: Manuscript writing, zinc experiments, intellectual input.

Patrick Toby Coates: manuscript review, experimental design

Darling Rojas: manuscript review

Claire Jessup: manuscript review

Table 1 Clinical characteristics of T2D and control donors

Parameters	Control subjects (n=6)	T2D (N=6)
Age (mean ± SD)	50± 19	58 ± 8
Gender M/F	3/3	5/1
BMI (kg/m^2)	25± 6	33± 3
Duration (years)	-	6±6.3
*Medication diet/oral/insulin/unknown	-	2/2/1/1

*Out of six T2D, two received were under diet control and two were taking oral anti diabetic drugs, one with insulin and one unknown.

Table 2 Zn-related measurements in db/db mice and wild type control

Parameter	Wk	WT	db/db	Fold-Change	Lower CI	Upper CI	n	P value
Liver Zn	4	1904	1701	0.9	0.69	1.15	6-8	ns[b]
	10	1193	1193	1.0	0.78	1.29	6-8	ns
	14	1683	909	0.54	0.42	0.70	6-8	**
Liver MT	4	7	7.3	1.0	0.5	2.0		ns
	10	5.2	4.7	0.90	0.4	1.9		ns
	14	7.1	5.7	0.80	0.4	1.8		ns
Plasma Zn	4	9.8	12.7	1.3	0.9	1.9		ns
	10	8.7	11.3	1.3	0.8	2.9		ns
	14	9.7	12.2	1.3	0.8	2.1		ns
Pancreatic Zn	4	2295	1019	0.44	0.34	0.59	6-8	**
	10	1435	945	0.66	0.50	0.86	6-8	**
	14	1582	1227	0.78	0.59	1.02	6-8	ns
Pancreatic MT	4	33	35	1.1	0.5	2.3		ns
	10	28	24	0.8	0.4	1.7		ns
	14	34	23	0.7	0.3	1.4		ns
Islet Zn	4	110	73	0.66	0.43	1.01	6-8	*
	18	75	66	0.87	0.58	1.29	6-8	ns

a Liver Zn, Liver MT, pancreatic Zn and pancreatic MT are in nmol/g. Plasma Zn is in

μmol/L and islet Zn is in arbitrary fluorescence units

b * p<0.05, ** p<0.005, ns = Not significant

Figure legends:

Figure 1 Fluorescence labelling for ZnT8, ZIP4 and ZIP14 in normal and diabetic human islets

A: Panels show representative images of islet fluorescence in normal human pancreata (Left) or T2D diabetic pancreata (Right) for ZnT8 (Upper), ZIP4 (Middle) and ZIP14 (Lower). Islets were stained for glucagon (red) to identify the islets and nuclei were stained blue with DAPI; Zn transporter immunofluorescences are in green. Note the intense ZnT8 staining in the inner beta cell core of the normal islet (Upper Left) compared with the diabetic islet (Upper Right). Also note the co-localization of ZnT8 and glucagon (orange colour) largely in the periphery of the normal islet but dispersed throughout the diabetic islet, suggesting the presence of ZnT8 in alpha cells and preservation of alpha cell ZnT8 in T2D. ZIP4 was present on occasional (non-alpha, non-beta) cells in the normal islet (Middle Left) but expressed on alpha cells (orange) in the T2D sample (Middle Right). Not all T2D subjects showed this apparent alpha cell ZIP4. ZIP14 was expressed on occasional macrophage-like cells in islets of both normals (Lower Left) and T2D (Lower Right).

Scale Bar in all images was 100 μm.

B: Panels show immunofluorescence intensities (arbitrary units) of ZnT8, ZIP4 and ZIP14 in islets of individual normal (n = 7) and T2D (n = 5-8) subjects. Note the

variable intensities of ZnT8 in different normal subjects. Dashed line shows means for each group. The only significant changes in expression between the normal and diabetics was in ZnT8 although three of the 8 cases of T2D and one normal had substantially increased staining for ZIP14. Fluorescence was quantified using ImageJ with mean gray scale for the more homogeneous staining pattern of ZnT8 and integrated density for the more particulate staining patterns of ZIP4 and ZIP14. 214 islets from normal and 301 islets from T2D were quantified.

* $P < 0.05$ ns = not significant

Figure 2. Effect of early and chronic diabetes on islet Zn in db/db mice.

A: Panels show representative images of islet ZinPyr-1 fluorescence (green) for Zn during early diabetes (4 wk, panel b) or chronic diabetes (18 wk, panel d). Corresponding WT controls are shown at 4 wk (panel a) and 18 wk (panel c). Islets were stained for glucagon (red) to identify the islets and nuclei were stained blue with DAPI. Note the intense staining for Zn throughout the islets in the WT mice at 4 wk (a) and the loss of fluorescence in the db/db mouse islets at 4 wk (b). Islet Zn also decreased in WT mice during the period from 4 to 18 wk (compare a and c), although clusters of more brightly fluorescent cells were seen in chronic diabetes (arrows in d).

B: As early as 4 wk, islet Zn was significantly decreased in db/db mice compared to age matched wild type WT mice. Note also the decrease in islet Zn in normal mice with age.

The X axis represents the age of mice (weeks) and the Y axis represents the ZinPyr-1 fluorescence of islet Zn. Wild type (WT) mice are shown as the closed diamonds and

the db/db mice as the open squares. At each time point, between 14 and 55 islets from 4 mice were measured. Fluorescence was quantified using ImageJ (mean gray scale). The data is shown as medians and the range as confidence intervals. Statistical analysis was performed by Type 2 ANOVA. * ($p<0.05$), ** ($p<0.005$) and *** ($p<0.0005$).

Figure 3. Effect of early and chronic diabetes on islet Zn transporter proteins in db/db mice.

A: Panels a-l shows representative images of fluorescence in db/db mouse islets for ZnT8, ZIP4 and ZIP14 during early diabetes (4 wk, panels b, f, j respectively) or chronic diabetes (18 wk, panels d, h, l respectively). Corresponding WT controls are shown at 4 wk (panels a, e, i respectively) and 18 wk (panels c, g, k respectively). Islets were stained for glucagon (red) to identify the islets and nuclei were stained blue with DAPI; Zn transporter immunofluorescences are in green. Note the intense staining for ZnT8 throughout the islets in the WT mice at 4 wk (panel a) and the loss of fluorescence in the db/db mouse islets at 4 wk (panel b). ZnT8 is preserved in the glucagon producing alpha cells in diabetes as shown by the orange (merged green and red) fluorescence in b and d. In WT mice, ZIP4 was expressed on occasional cells in the non-beta cell islet periphery and distinct from the alpha cells (red, panels e and g). There was no change in the frequency of ZIP4+ve cells in diabetes (panels f and h). In WT mice, ZIP14 was also expressed on occasional cells distinct from alpha and beta cells (panels i and k) and there were markedly increased in the diabetic mice (panels j and l).

B: As early as 4 wk, islet ZnT8 was significantly down-regulated and ZIP14 was significantly up-regulated in db/db mice compared to age matched WT mice. The X

axis represents the age of mice (weeks) and the Y axis represents the immunofluorescence of ZnT8, ZIP4 or ZIP14. WT mice are shown as the closed diamonds and the db/db mice as the open squares. At each time point, between 14 and 55 islets from 4 mice were measured. Fluorescence was quantified using ImageJ with mean gray scale for the more homogeneous staining pattern of ZnT8 while integrated density was used for the more particulate staining patterns of ZIP4 and ZIP14. The data is shown as medians and the range as confidence intervals. Statistical analysis was performed by Type 2 ANOVA. * ($p<0.05$), ** ($p<0.005$) and *** ($p<0.0005$).

Figure 4 ZIP4-somatostatin and ZIP14-macrophage co-localization studies

Panels a-b: Immunoperoxidase staining of serial sections for ZIP4 (panel a) and delta cell marker somatostatin (SMST, panel b).

Panels c-d: Immunoperoxidase staining of serial sections for ZIP14 (panel c) and macrophage marker CD68 (panel d).

The different sets of arrows show co-localizations where evident. Because the section thickness 4 μm is close to the diameter of the cells, co-localization in serial sections can only occasionally be detected.

Scale Bar in all images was 100 μm.

Legends to Supplementary Figures

Suppl Fig S1. Effect of age (wk) on various diabetic parameters in db/db mice. Hyperinsulinemia and islet hyperplasia were maximal at 4 wk in db/db mice while maximal obesity and hyperglycaemia occurred several weeks later.

The X axis represents the age of mice (weeks) and the Y axis represents the diabetic parameter:- body weight in g (A), random blood glucose level in mmol/L (B), plasma insulin in μmol/L (C) and mean islet area in pixel squared (D). Wild type (WT) mice are shown as the closed diamonds and the db/db mice as the open squares. 6-8 mice were used at each time point, and each point was a single measurement. For islet hyperplasia studies in D, at each time point, between 18 and 67 islets were analyzed.

The data is shown as medians and the range as confidence intervals. Statistical analysis was performed by Type 2 ANOVA. * ($p<0.05$), ** ($p<0.005$) and *** ($p<0.0005$).

Suppl Figure S2. *Islet hormone architecture.* Figure shows typical islets stained for islet hormones in immunoperoxidase-labelled paraffin embedded sections of 4 week old wild type mice (upper panel) and db/db mice (bottom panel). The hormones assayed were insulin (left), glucagon (centre) and somatostatin (right) for beta cells, alpha cells and delta cells, respectively. Insulin staining in the wild type mice is in the inner core of the islets while glucagon and somatostatin are predominantly in the mantle. In the db/db

mice, the insulin is in a more degranulated form and the glucagon and somatostatin cells are disorganised in the inner core.

References: 50 references maximum

1.   Bosco, M.D., et al., *Zinc and zinc transporter regulation in pancreatic islets and the potential role of zinc in islet transplantation.* Rev Diabet Stud, 2010. **7**(4): p. 263-74.

2.   Rutter, G., *Think zinc: New roles for zinc in the control of insulin secretion.* Islets, 2010. **2**: p. 49 - 50.

3.   Scott, D.A. and A.M. Fisher, *The Insulin and the Zinc Content of Normal and Diabetic Pancreas.* The Journal of clinical investigation, 1938. **17**(6): p. 725-8.

4.   Jayawardena, R., et al., *Effects of zinc supplementation on diabetes mellitus: a systematic review and meta-analysis.* Diabetology & metabolic syndrome, 2012. **4**(1): p. 13.

5.   Simon, S.F. and C.G. Taylor, *Dietary Zinc Supplementation Attenuates Hyperglycemia in db/db Mice.* Experimental biology and medicine, 2001. **226**(1): p. 43-51.

6.   Murgia, C., et al., *Diabetes-linked zinc transporter ZnT8 is a homodimeric protein expressed by distinct rodent endocrine cell types in the pancreas and other glands.* Nutrition, Metabolism and Cardiovascular Diseases, 2009. **19**(6): p. 431-439.

7.   Fu, Y., et al., *Down-regulation of ZnT8 expression in INS-1 rat pancreatic beta cells reduces insulin content and glucose-inducible insulin secretion.* PLoS One, 2009. **4**(5): p. e5679.

8.   El Muayed, M., et al., *Acute Cytokine Mediated Downregulation of the Zinc Transporter ZnT8 Alters Pancreatic Beta Cell Function.* Journal of Endocrinology, 2010: p. 1-26.

9.   Tamaki, M., et al., *Downregulation of ZnT8 expression in pancreatic beta-cells of diabetic mice.* Islets, 2009. **1**(2): p. 124-8.

10.   Sladek, R., et al., *A genome-wide association study identifies novel risk loci for type 2 diabetes.* Nature, 2007. **445**(7130): p. 881-5.

11.   Dupuis, J., et al., *New genetic loci implicated in fasting glucose homeostasis and their impact on type 2 diabetes risk.* Nat Genet, 2010. **42**(2): p. 105-16.

12.   Nicolson, T.J., et al., *Insulin storage and glucose homeostasis in mice null for the granule zinc transporter ZnT8 and studies of the type 2 diabetes-associated variants.* Diabetes, 2009. **58**(9): p. 2070-83.

13.   Rutter, G.A. and F. Chimienti, *SLC30A8 mutations in type 2 diabetes.* Diabetologia, 2014.

14.   Tamaki, M., et al., *The diabetes-susceptible gene SLC30A8/ZnT8 regulates hepatic insulin clearance.* J Clin Invest, 2013. **123**(10): p. 4513-24.

15.   Chen, H., et al., *Evidence That the Diabetes Gene Encodes the Leptin Receptor: Identification of a Mutation in the Leptin Receptor Gene in db/db Mice.* Cell, 1996. **84**(3): p. 491-495.

16.   Belke, D.D. and D.L. Severson, *Diabetes in Mice with Monogenic Obesity: The db/db Mouse and Its Use in the Study of Cardiac Consequences*, in *Animal Models in Diabetes Research*. 2012. p. 47-57.

17.   O'Connell, P.J., et al., *Multicenter Australian trial of islet transplantation: improving accessibility and outcomes.* Am J Transplant, 2013. **13**(7): p. 1850-8.

18.   Philcox, J.C., et al., *Endotoxin-induced inflammation does not cause hepatic zinc accumulation in mice lacking metallothionein gene expression.* The Biochemical journal, 1995. **308 (Pt 2)**: p. 543-6.

19.   Team, R.C., *R: A language and environment for statistical computing*. 2013, Vienna, Austria: R Foundation for Statistical Computing.

20.   Douglas Bates, M.M., Ben Bolker and Steven Walker *lme4: Linear mixed-effects models using Eigen and S4*, 2013.

21.   Weisberg, J.F.a.S., *Companion to Applied Regression*. Second Edition. 2011, Thousand Oaks CA.

22.   Hothorn, T., F. Bretz, and P. Westfall, *Simultaneous Inference in General Parametric Models.* Biometrical Journal, 2008. **50**(3): p. 346-363.

23. Baetens, D., et al., *Alteration of Islet Cell Populations in Spontaneously Diabetic Mice.* Diabetes, 1978. **27**(1): p. 1-7.

24. Gapp, D.A., et al., *Temporal changes in pancreatic islet composition in c57bl/6j-db/db (diabetes) mice.* Diabetologia, 1983. **25**(5): p. 439-443.

25. Kitamura, T., *The role of FOXO1 in [beta]-cell failure and type 2 diabetes mellitus.* Nat Rev Endocrinol, 2013. **9**(10): p. 615-623.

26. Kharouta, M., et al., *No mantle formation in rodent islets—The prototype of islet revisited.* Diabetes Research and Clinical Practice, 2009. **85**(3): p. 252-257.

27. Kim, A., et al., *Islet architecture: A comparative study.* Islets, 2009. **1**(2): p. 129-136.

28. Kristiansen, L.H., et al., *Autometallography allows ultrastructural monitoring of zinc in the endocrine pancreas.* Histochemistry and cell biology, 2001. **115**(2): p. 125-9.

29. Liuzzi, J.P., et al., *Interleukin-6 regulates the zinc transporter Zip14 in liver and contributes to the hypozincemia of the acute-phase response.* Proceedings of the National Academy of Sciences of the United States of America, 2005. **102**(19): p. 6843-6848.

30. Lichten, L.A., J.P. Liuzzi, and R.J. Cousins, *Interleukin-1β contributes via nitric oxide to the upregulation and functional activity of the zinc transporter Zip14 (Slc39a14) in murine hepatocytes.* American Journal of Physiology - Gastrointestinal and Liver Physiology, 2009. **296**(4): p. G860-G867.

31. Min, K.-S., et al., *Involvement of the essential metal transporter Zip14 in hepatic Cd accumulation during inflammation.* Toxicology Letters, 2013. **218**(1): p. 91-96.

32. Sayadi, A., et al., *Zip14 expression induced by lipopolysaccharides in macrophages attenuates inflammatory response.* Inflammation Research, 2013. **62**(2): p. 133-143.

33. Cucak, H., L.G. Grunnet, and A. Rosendahl, *Accumulation of M1-like macrophages in type 2 diabetic islets is followed by a systemic shift in macrophage polarization.* Journal of Leukocyte Biology, 2013.

34. Beker Aydemir, T., et al., *Zinc transporter ZIP14 functions in hepatic zinc, iron and glucose homeostasis during the innate immune response (endotoxemia).* PloS one, 2012. **7**(10): p. e48679.

35.   Dufner-Beattie, J., et al., *The Acrodermatitis Enteropathica Gene ZIP4 Encodes a Tissue-specific, Zinc-regulated Zinc Transporter in Mice.* Journal of Biological Chemistry, 2003. **278**(35): p. 33474-33481.

36.   Donahue, T. and O.J. Hines, *The ZIP4 pathway in pancreatic cancer.* Cancer Biol Ther, 2010. **9**(3): p. 243-5.

Supplementary Methods 1

Gene name is followed by Taqman gene expression No. ZIP1 (SLC39A1)- Hs, ZIP2 (SLC39A2)- Hs, ZIP3 (SLC39A3)- Hs, ZIP4 (SLC39A4)- Hs, ZIP5 (SLC39A5)- Hs, ZIP6 (SL39A6)- Hs, ZIP7 (SLC39A7)- Hs, ZIP8 (SLC39A8)- Hs, ZIP9 (SLC39A9)- Hs, ZIP10 (SLC39A10)- Hs, ZIP11 (SLC39A11)- Hs, ZIP12 (SLC39A12)- Hs, ZIP13 (SLC39A13)- Hs, Zip14 (SLC39A14)- Hs00299262_ml, ZnT1 (SLC30A1)- Hs, ZnT2 (SLC30A2)- Hs, ZnT3 (SLC30A3)- Hs, ZnT4 (SLC30A4)- Hs 00203308_ml, ZnT5 (SLC30A5)- Hs, ZNT6 (SLC30A6)- Hs00215827_ml, ZnT7 (SLC30A7)- Hs, ZnT8 (SCL30A8)- Hs00545183_ml, ZnT9 (SLC30A9)- Hs, ZnT10 (SLC30A10)- Hs, Insulin- Hs 02741908_ml, Glucagon- Hs00174967_ml, Somatostatin- Hs00174949_ml, GLUT2 (SLC2A1)- Hs00165775_ml, GLUT1 (SLC2A1)- Hs00892681_ml, glucoskinase- Hs00175951_ml and HPRT- Hs99999909.

Preamplification of cDNA targets:

The pre-amplification step of the samples was performed using Taqman pre-AMP Master mix kit protocol (part number 4384557). 31 Taqman gene expression assays ZnT1-10, ZIP1-14, insulin, glucagon, MT1, MT2, TPRM3 and PDLIM7 were pooled together to make 0.2X final concentration. Subsequently 12.5µl of the pooled assay mix (0.2x) were combined with 12.5µl neat cDNA sample and 25µl of the Taqman Preamp Master Mix (2x) to make the final volume of 50µl. The reactions were incubated in an Applied Biosystems (Mulgrave, Victoria, Australia) 7300 thermocycler for 10 mins at 95°C followed by 10 cycles of 95°C for 15 seconds and 60°C for 4 mins and then held at 4°C. 50µl of the preamp sample product, 30µl of 1x TE buffer and 80µl of Taqman

Gene Expression Master Mix were added to each individual port of the Taqman array

plates and were run on the 7900HT fast real time PCR system.
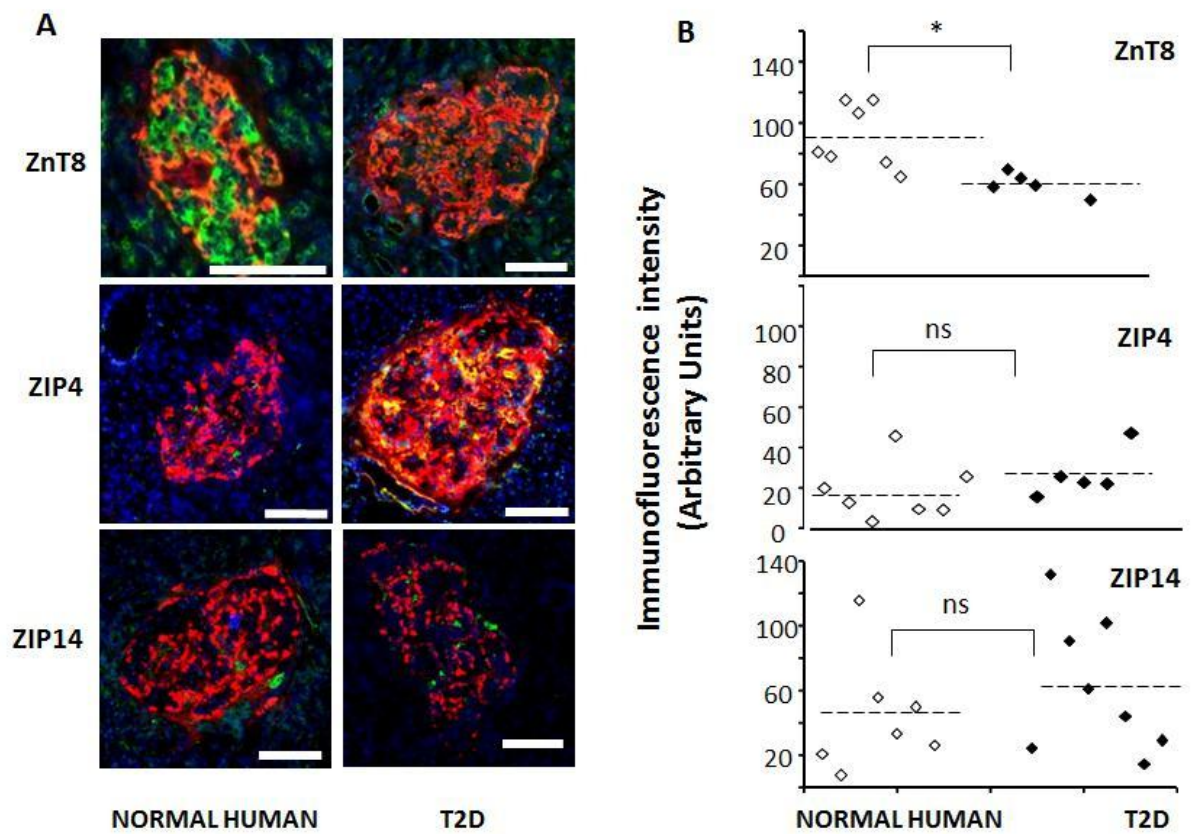

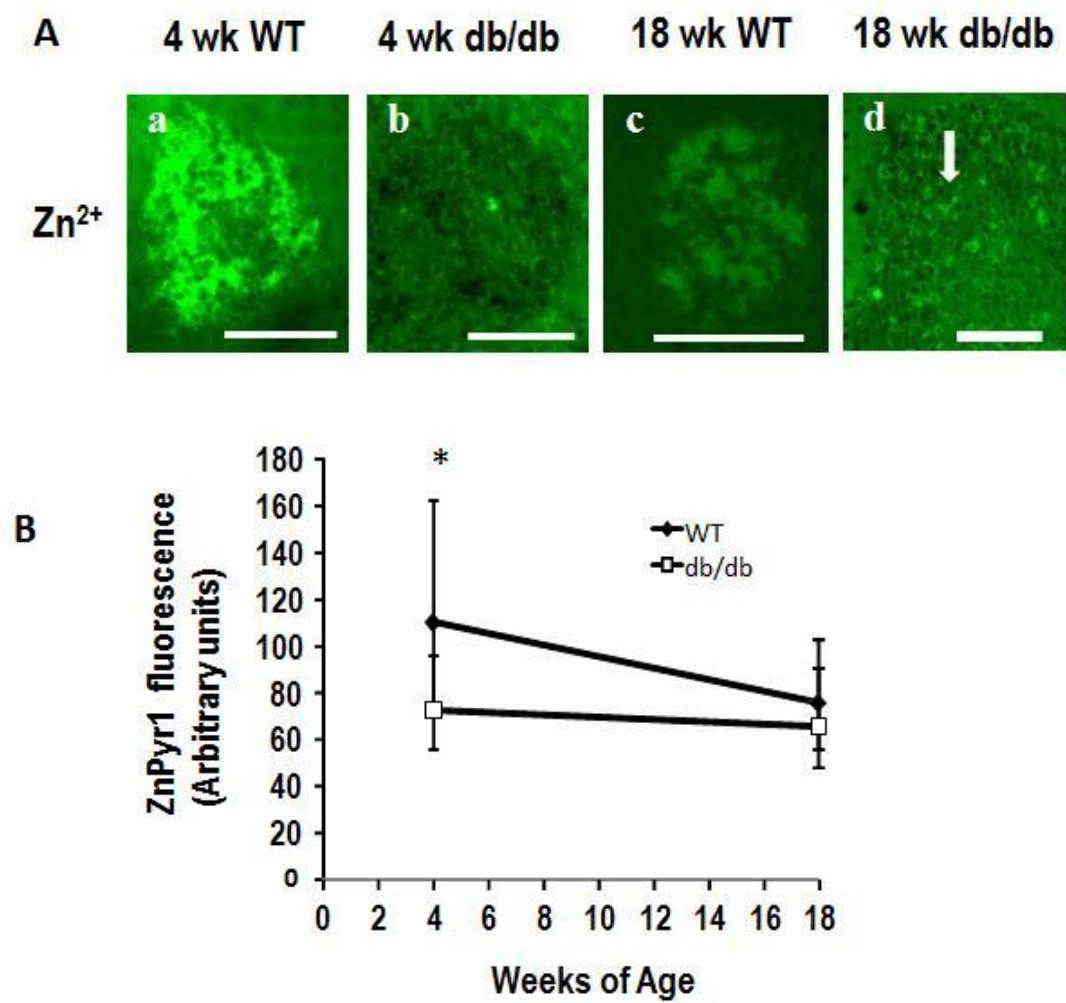
Figure 1 Bosco et al

Figure 2   Bosco et al

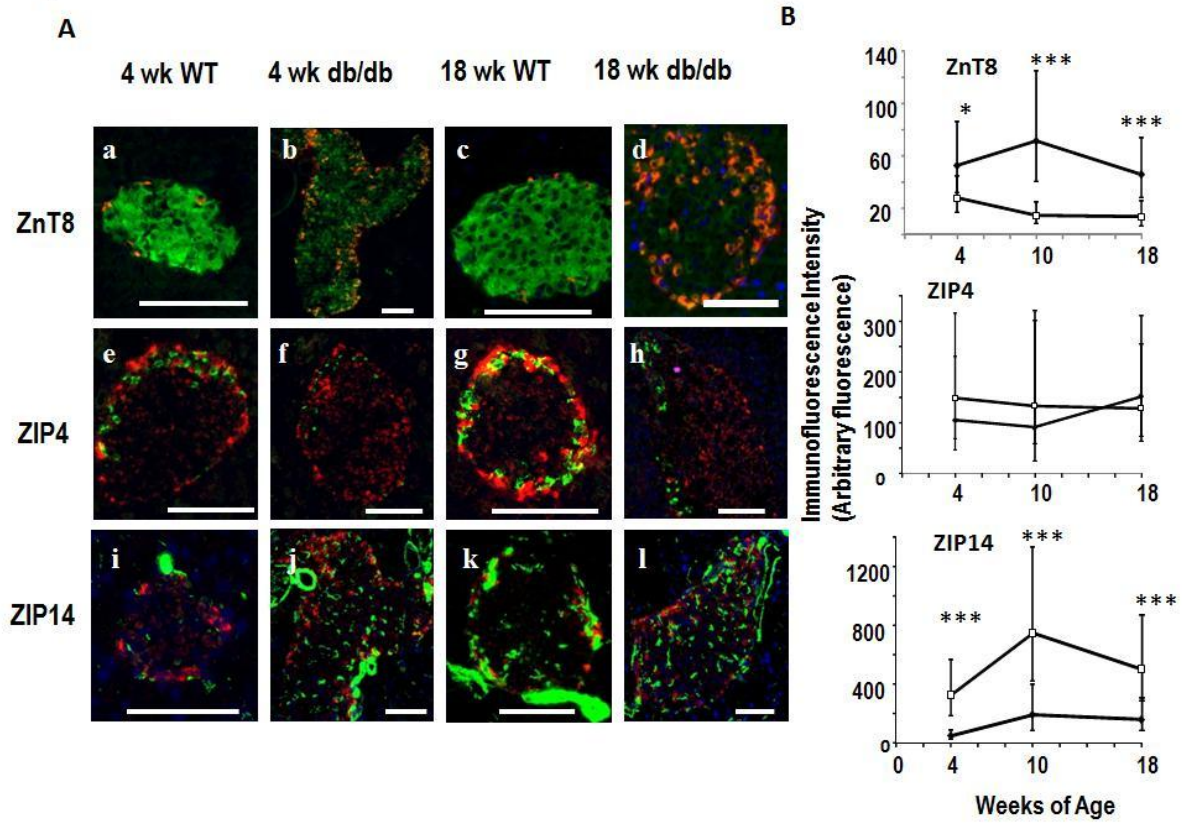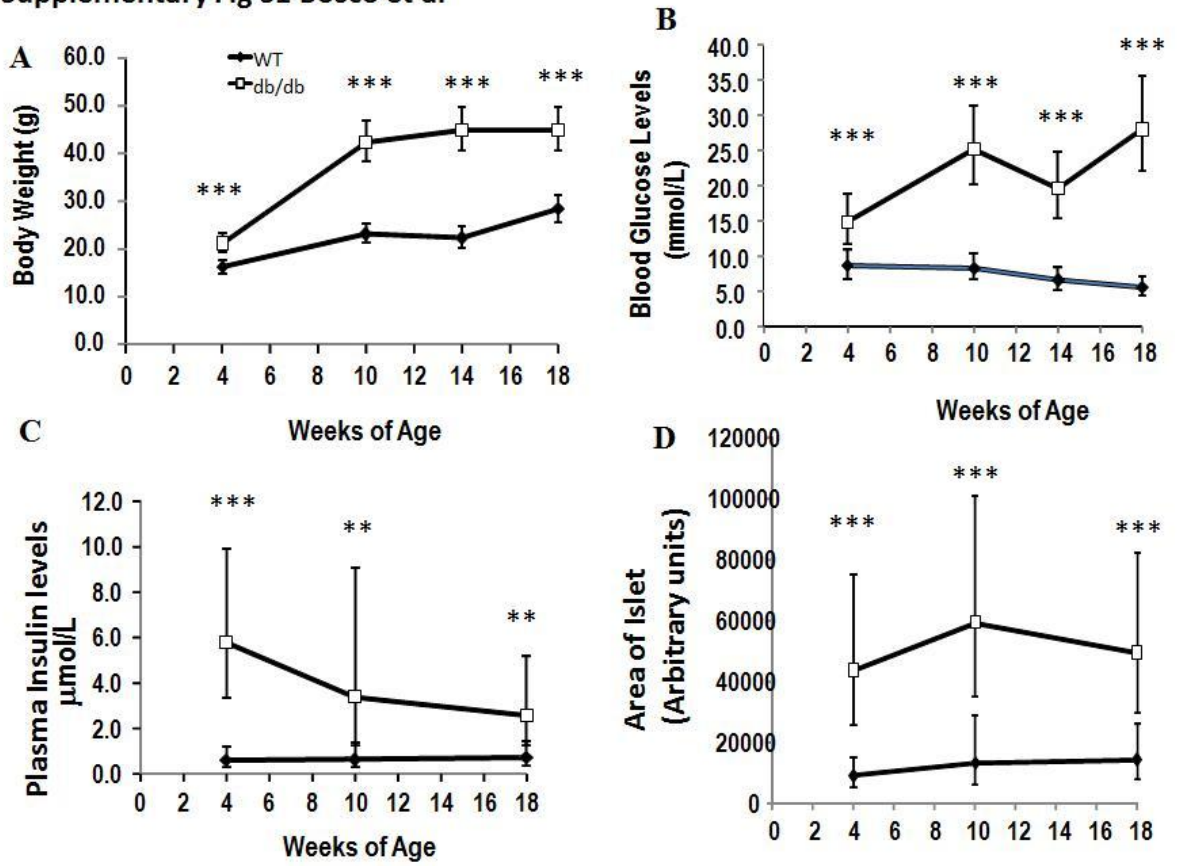A   4 wk WT   4 wk db/db   18 wk WT   18 wk db/db

Zn²⁺

B

Figure 3 Bosco et al

Figure 4 Bosco et al

ZIP4

SMSN

ZIP14

CD68

Supplementary Fig S1 Bosco et al

A – Body Weight (g) vs Weeks of Age; WT and db/db; *** at 4, 10, 14, 18 weeks.

B – Blood Glucose Levels (mmol/L) vs Weeks of Age; *** at 4, 10, 14, 18 weeks.

C – Plasma Insulin levels µmol/L vs Weeks of Age; *** at 4, ** at 10, ** at 18 weeks.

D – Area of Islet (Arbitrary units) vs Weeks of Age; *** at 4, 10, 18 weeks.

Supplementary Fig S2 Bosco et al